Exploration of the possible role of microRNA(s) and small extracellular vesicles in chemotherapy-induced bystander effects.

Arinzechukwu Ekene Ude

A thesis submitted in partial fulfilment of the requirements of the University of the West of England, Bristol for the Degree of Doctor of Philosophy

Faculty of Health and Life Sciences, University of the West of England, Bristol

March 2021

Copyright disclaimer

This copy has been supplied on the understanding that it is copyright material and that no quotation from the thesis may be published without proper acknowledgement.

Acknowledgments

Abstract

Advances in modern chemotherapeutic regimens have led to an increase in the overall survival of leukaemia patients in recent years. However, haematopoietic stem cell transplantation (HSCT) remains the curative option for these patients. In HSCT, high dose chemotherapy is often given pre-transplant to remove the leukaemic stem cells (LSC) within the bone marrow (BM) microenvironment of the patients prior to infusion of donor stem cells to reconstitute haematopoiesis. Despite its success, HSCT can also lead to development of *de novo* primary malignancy as chemotherapy can also exert deleterious effects on actively dividing cells whilst targeting LSC. Donor cell leukaemia (DCL) is a type of *de novo* primary malignancy whereby transplanted stem cells become malignant in the recipient whilst the donor remains healthy. Despite the growing incidence of DCL due to advancement in genetic testing, the aetiology and mechanism of DCL remain unknown. Therefore, using DCL as a pathological pivot, this thesis explored the possible roles of microRNA (miRNAs) and small extracellular vesicles (sEVs) in chemotherapy-induced bystander effects (CIBE). Bystander effect occurs when toxic signals induce biological effects in unexposed cells, which are in close proximity to the directly exposed cells, via intercellular communication. A co-culture bystander model, which promotes cell-to-cell communication between cell compartments *in vitro* was utilised to investigate the concept of CIBE thus mimicking the BM microenvironment. HS-5 stromal cells and TK6 lymphoblast cells were co-cultured using culture inserts, which allowed isolation of bystander TK6 cells to detect cytotoxicity and genotoxicity following indirect exposure to drugs. The drugs used in this study were alkylating agents (chlorambucil and carmustine), and topoisomerase inhibitors (etoposide and mitoxantrone), which have been shown to induce CIBE in a previous study. Microarray analysis was performed using bystander cells' RNA to identify candidate miRNAs that may be involved in CIBE. Drug-treated HS-5 cells were fixed with 2% paraformaldehyde, negatively stained with uranyl acetate and examined by transmission electron microscopy (TEM) to visualise sEVs release. Furthermore, sEVs derived from drug-treated HS-5 cells were isolated, characterised and tracked for uptake and internalization by bystander cells. Expression of candidate miRNAs was validated in treated HS-5 cells, conditioned medium (CM), isolated sEVs and bystander cells by qRT-PCR following sEVs uptake.

All drugs promoted genotoxicity in the bystander cells whilst maintaining good viability. However, only mitoxantrone produced statistically significant cytotoxic and genotoxic events in the bystander cells. These events persisted within the bystander cells over five days thus suggesting that the 'safe period' given to transplant patients to recover from the effects of pre-transplant chemotherapy may not be safe after all. Further examination of the CM illustrated that chemotherapy promotes the release of sEVs into the CM by HS-5 cells in comparison to untreated HS-5 cells. These sEVs were internalized by the bystander cells in a time-dependent manner and once internalized, released their cargo into the cells to elicit bio-molecular effects. Differential miRNA signatures were also found in the treated HS-5 cells and bystander TK6 cells. The expression levels of hsa-miR-146a-5p, hsa-miR-16-5p, hsa-miR-20a-5p, hsa-miR-17-5p were all upregulated in treated HS-5 cells but repressed in bystander TK6 cells. However, the expression level of hsa-miR-30d-5p was repressed in treated HS-5 cells and upregulated in bystander TK6 cells. These candidate miRNA signatures were also found in CM and sEVs. However, only hsa-miR-17-5p was found in treated sEVs thus implying hsa-miR-17-5p may play a crucial role in CIBE. These candidate miRNAs regulate genes involved in cellular signalling pathways, cell division and cell survival. Therefore, these suggest that the miRNAs are selectively sorted and packaged into EVs, and subsequently trafficked to the bystander cells wherein they may determine the fate of these cells. Collectively, these analyses provide a novel finding that soluble factors such as miRNAs and sEVs, released by treated stromal cells within the BM microenvironment may play a vital role in the propagation of CIBE signals to the incoming donor cells thereby eliciting deleterious effects. However, these may not tell the whole story as there may be an interplay between complex signals in CIBE. Thus, further investigation needs to be done to fully understand the mechanisms involved.

Poster and Oral Presentations

- United Kingdom Environmental Mutagen Society (UKEMS) annual conference. Leuven, Belgium. June 2017

- South West RNA UK Club annual Conference. Cardiff. June 2017

- Childhood Cancer annual conference. Newcastle. September 2017

- CRIB annual conference. UWE Bristol. January 2018

- MSc annual conference. UWE Bristol. January 2018

- International Society for Extracellular Vesicles (ISEV) annual conference. Barcelona, Spain. May 2018.

- Advances in cell/tissue culture annual conference. Cardiff. July 2018

- UKEMS annual conference. Oxford. April 2019

- PGR annual conference. UWE Bristol. July 2019

- South West RNA UK Club annual conference. Bath. June 2019

- PhD to Consulting annual conference. London. September 2019

- CRIB monthly lectures. UWE Bristol. November 2019

Publications

- Ude, A., Ladomery, M. and Morse, R. (2018) Role of exosomes in chemotherapy-induced bystander effects. ISEV2018 abstract book, *Journal of Extracellular Vesicles.* 7 (issue suppl.1). Available from: https://doi.org/10.1080/20013078.2018.1461450

- Ude, A., Ladomery, M. and Morse, R. (2019) The role of exosomes in chemotherapy-induced bystander effect. *Mutagenesis.*

Table of Contents

List of Figures

List of Tables

Abbreviations

µg – microgram

µl – microlitre

µM – micromolar

ml - millilitre

nM – nanomolar

ALL- Acute lymphoblastic leukaemia

AML – Acute myeloid leukaemia

ANOVA – Analysis of variance

AO – Acridine orange

ATCC - American Type Culture Collection

BCA - Bicinchoninic acid

BCRP – Breast cancer resistance protein

BE – Bystander effects

BM – Bone marrow

BMSC – Bone marrow mesenchymal stem cells

bp – base pair

CAR – Carmustine

CD – Cluster of differentiation

cDNA – Complimentary DNA

CHL – Chlorambucil

CIBE – Chemotherapy-induced bystander effects

CFU-F - Colony forming unit fibroblasts

CLL – Chronic lymphocytic leukaemia

CM – Conditioned medium

CML – Chronic myeloid leukaemia

Ct – Threshold cycle

DCL –Donor cell leukaemia

DMEM-HG - Dulbecco's modified eagles medium high glucose

DMEM-LG - Dulbecco's modified eagles medium low glucose

DMEM-f12 - Dulbecco's modified eagles medium f12 ham

DMSO - Dimethylsulphoxide

DNA – Deoxyribonucleic acid

EDTA - Ethylenediaminetetraacetic acid

ETO –Etoposide

EUTOS - The European Treatment and Outcome Study

EV –Extracellular vesicles

FAB – French-American-British

FBS – Fetal bovine serum

G-CSF - Granulocyte colony stimulating factor

GO – Gene ontology

GVHD – Graft versus host disease

GVL – Graft versus leukaemia

HLA – Human leucocyte antigen

HRP - Horseradish peroxidase

Hsa – *Homo sapiens*

HSC – Haematopoietic stem cells

HSCT – Haematopoietic stem cells transplantation

HTLV – Human T-Lymphotrophic virus

HUVEC - Human umbilical vein endothelial cells

IMDM – Iscove's modified dulbecco's medium

ISCT – International Society for Cellular Therapy

ISEV - International Society for Extracellular Vesicles

LSC – Leukaemic stem cells

M-CSF - Macrophage colony stimulating factor

MAC - Myeloablative conditioning

MDS – Myelodysplasia

MHC – Major histocompatibility complex

miRNA – MicroRNA

miRTC - Reverse transcription control

MISEV - Minimal information for studies of extracellular vesicles

MLL – Mixed lineage leukaemia

MMC – Mitomycin C

MN – Micronuclei

MRD – Minimal residual disease

MRP – Multi-drug resistance-associated protein

MSC – Mesenchymal stem cells

MTX – Mitoxantrone

MVB - Multivesicular bodies

NER - Nucleotide excision repair

NMAC - Non-myeloablative conditioning

NTA – Nanoparticle tracking analysis

OECD – Organisation for Economic Co-operation and Development

P-gp – P-glycoprotein

PB – Peripheral blood

PBS – Phosphate buffered saline

PBSC – Peripheral blood stem cells

PI – Propidium iodide

PPC - Positive PCR control

PTLD - Post-transplant lymphoproliferative disorder

qRT-PCR - Quantitative real time polymerase chain reaction

RBC – Red blood cell

RFLP -Restriction fragment length polymorphisms

RIBE – Radiation-induced bystander effects

RIC - Reduced intensity conditioning

RISC – RNA-induced Silencing Complex

RNA – Ribonucleic acid

ROS – Reactive oxygen species

RPMI – Roswell Park Memorial Institute

RT – Room temperature

SCE – Sister chromatid exchange

SCF - Stem cell factor

SD – Standard deviation

SDS - Sodium dodecyl sulphate

sEVS – Small extracellular vesicles

SIDP - Short inversion or deletion polymorphisms

SNP - Single nucleotide polymorphisms

STR - Short tandem repeats

TEM – Transmission electron microscope

TNT - Trinitrotoluene

TRM – Therapy-related malignancy

UCB – Umbilical Cord Blood

VEGF - Vascular endothelial growth factor

VNTR - Variable number of tandem repeats

WBC – White blood cell

WHO – World Health Organisation

YCS - Y-specific chromosome sequence

1.0 Introduction

1.1 Leukaemia

1.1.1 Definition

Leukaemia encompasses a wide range of blood cancers that are characterised by the accumulation of abnormal and/or immature white blood cells due to uncontrolled proliferation, lack of differentiation and lack of apoptosis in these cells. Due to heterogeneity of the disease, a complete blood count is always essential whenever leukaemia is suspected however, the hallmark laboratory findings are variable and usually include leucocytosis, anaemia, leukopenia, thrombocytopenia or immunosuppression (Davis *et al.,* 2014; Hijiya *et al.,* 2016; Kumar *et al.,* 2019). Identification of kidney and liver involvement via serum creatinine and electrolyte levels, and liver function tests respectively, may also provide clinicians with relevant information to make initial diagnosis (Hampel *et al.,* 2017; Suzuki *et al.,* 2017; Wancho *et al.,* 2018). This may be due to infiltration of these extramedullary organs by the leukaemia. Nevertheless, leukaemia diagnosis is confirmed by further examination of the bone marrow (BM) or peripheral blood (PB). Symptoms often include weight loss, fatigue, bleeding, abdominal discomfort, splenomegaly, sweats, bone pain and fever, though these symptoms are nonspecific and may not be seen in all patients (Suzuki *et al.,* 2017; Kumar *et al.,* 2019).

1.1.2 Epidemiology

Collectively, leukaemias are the 13th most common cancer in the UK and 11th most common cancer in the world accounting for 2.6% of all cancer incidences worldwide (International Agency for Research on Cancer, 2014; Cancer Research UK, 2016; World Cancer Research Fund, 2018). Leukaemia predominantly affects caucasians, with males more predisposed to the disease than females and increases with age thus leukaemia affects both adults and children. In a recent population-based study conducted on the epidemiological patterns of leukaemia in 184 countries, the highest regional leukaemia rate for men, estimated at 11.3 per 100,000 population for 2012 – was found in Australia and New Zealand, followed by Northern America and western

Europe at 10.5 per 100,000 and 9.6 per 100,000 respectively (Miranda-Filho *et al.,* 2018). For females, Australia and New Zealand, and Northern America had the highest leukaemia incidence rate at 7.2 per 100,000, next was western Europe at 6.0 per 100,000 (Miranda-Filho *et al.,* 2018). In the UK, leukaemia is also more common in men than in women: 20.3 versus 11.4 per 100,000 population for 2016, with about 9,900 new leukaemia cases diagnosed in both sexes every year; a marked increase in incidence rate by 16% since the 1990s (Cancer Research UK, 2016). However, the outlook for patients is much better than two to three decades ago, with better cure rates and longer-term disease free survival. Leukaemia overall survival rate has improved remarkably in the last 40 years worldwide with almost half of the population diagnosed with leukaemia surviving for at least five years or more (Pulte *et al.,* 2013; Cancer Research UK, 2016). This increased survival rate in leukaemia patients has been attributed to advances in the treatment of the disease and improved access to treatment (Viesani *et al.,* 2018).

1.1.3 Aetiology

Aetiology of leukaemia remains unclear and perhaps involves multiple factors. However, increase in age and exposure to chemicals such as benzene are known risk factors (Appelbaum *et al.,* 2006; Khalade *et al.,* 2010). An increased incidence of leukaemia was reported in the inhabitants of Hesse County in Germany due to environmental contamination with benzene derivative trinitrotoluene (TNT), which was used to produce explosives during World War II (Kolb *et al.,* 1993; Kilian *et al.,* 2001).

A higher incidence of leukaemia was found in individuals exposed to ionizing radiation as reported in Hiroshima and Nagasaki registries (Preston *et al.,* 1994; Greaves, 1997). There is also a reported increase in childhood leukaemia in children under 5 years who live within 5 km of nuclear power plants in Germany (Kaatsch *et al.,* 2008; Spix *et al.,* 2008). However, this contradicts the findings of Bithell *et al.,* (2013) who found little evidence of a link between increased leukaemia risk and distance to nuclear power plants in the UK. This may be because nuclear power plants are often installed further away from population centres in the UK compared to Germany (Muirhead *et al.,* 2013).

Although smoking had not been previously reported to be a classic risk factor for leukaemia, evidence from several epidemiological studies indicates an increased risk of leukaemia development of the myeloid form among smokers compared to non-smokers (Bjork *et al.,* 2001; Chelghoum *et al.,* 2002; Moorman *et al.,* 2002; Fircanis *et al.,* 2014). Interestingly, this risk reduced following cessation of smoking (Musselman *et al.,* 2013).

Furthermore, there are well-established studies that suggest family history as a significant risk factor for leukaemia development later in life (Goldin *et al.,* 2004; Segel *et al.,* 2004; Tegg *et al.,* 2010). However, leukaemia in children is not inherited and may be due to environmental exposures in utero. These environmental factors cause chromosomal translocations, functional fusion genes or pre-leukaemic clones thereby leading to development of childhood leukaemia (Mori *et al.,* 2002; Mitchell *et al.,* 2009; Cárceles-Álvarez *et al.,* 2017). Chromosomal abnormalities and acquired genetic abnormalities such as Down's syndrome also increase the risk of leukaemia development by 20-fold (Hasle *et al.,* 2000).

The aetiological relationship between certain viruses and leukaemia has since been established over the years (Almeida *et al.,* 1963; Shafer, 1966; McNally *et al.,* 2013). Some of the viruses that have been linked to progression of leukaemia include cytomegalovirus, Epstein-barr virus, human herpes virus and human T-lymphotrophic virus (HTLV; Bartenhagen *et al.,* 2017). Therapy-related malignancy (TRM) may also arise as a result of long-term complications of chemotherapy and/or radiotherapy for an underlying disorder. This leukaemia type is directly related to therapy received and has been linked to two drug classes, alkylating agents and topoisomerase inhibitors (Joannides and Grimwade, 2010).

1.1.4 Types, prognosis and staging

Accurate classification and diagnosis of leukaemia are important to select the right treatment regimen for the patients, as survivors are predisposed to relapse or development of a second tumour (Bain, 2017). Leukaemia classification depends on the type of blood cell in which the cancer originates, and by the pace of disease progression. Myeloid or myelogenous leukaemias arise in early myeloid cells such as red blood cells (RBC), platelets and white blood cells (WBC) other than lymphocytes, whilst lymphocytic leukaemia emerge in cells that mature into

lymphocytes (Bain, 2017). Leukaemia may also be acute or chronic based on how fast the disease progresses. Acute leukaemias are usually aggressive, often begin abruptly and progress rapidly if untreated due to rapid accumulation of immature cells called blasts in the BM, whereas chronic leukaemias involve maturation arrest at a later stage hence cells grow slowly and the disease progresses gradually (Bain, 2017). Acute leukaemia is diagnosed if at least 30% of the total nucleated cells in the BM are blast cells with predominance of erythroblasts.

As a result, leukaemias are divided into four main types:

- Acute lymphoblastic leukaemia (ALL)
- Chronic lymphocytic leukaemia (CLL)
- Acute myeloid leukaemia (AML)
- Chronic myeloid leukaemia (CML)

Acute lymphoblastic leukaemia (ALL) arises as a result of a defect in clonal proliferation of lymphoid progenitor cells in the BM and sites of extramedullary haematopoiesis, such as spleen and liver. ALL occurs mainly in children however, it can also have a debilitating effect in adults. ALL was initially classified into three different subtypes (L1, L2 and L3) according to the French-American-British (FAB) classification system, which is based on assessment of cytochemical and morphological features such as size, cytoplasm, nucleoli, vacuolation and basophilia (Bennett *et al.,* 1976). It requires the examination of the BM and PB films and differential counts performed on both samples (Bain, 2017).

Over the last two decades, the World Health Organisation (WHO) proposed another classification system, which accounts for clinical features, morphology as well as cytogenetic profiles of the leukaemic blasts. As a result, three subtypes of ALL were initially identified: B lymphoblastic, T lymphoblastic and Burkitt-cell Leukaemia (Bain, 2017). In 2008, the WHO classification system was revised and B-lymphoblastic subtype was divided into B-ALL with recurrent genetic abnormalities and B-ALL not otherwise specified whilst Burkitt-cell leukaemia was adjudged the same entity as Burkitt Lymphoma (Vardiman *et al.,* 2009).

The outcome of ALL differs from patient to patient due to different prognostic factors, including age and white blood cell (WBC) count at the time of diagnosis, cytogenetic abnormalities and response to initial therapy. Age > 60 years, elevated WBC count, presence of Philadelphia chromosome t(9;22), hypodiploidy, complex karyotype, and presence of minimal residual disease (MRD) portend a worsening prognosis (Terwilliger and Abdul-Hay, 2017).

Chronic lymphocytic leukaemia (CLL) is the most prevalent form of adult leukaemia in the western world, and usually affects elderly patients above 65 years of age (O'Reilly *et al.,* 2018; Wancho *et al.,* 2018). CLL is characterised by accumulation of abnormal lymphocytes in the BM, blood, lymph nodes and spleen thereby rendering them unable to fight infections (Ghia *et al.,* 2007). CLL has a heterogeneous course; it can have a fast or slow progression depending on the individual. As a consequence, Rai *et al.* (1975) and Binet *et al.,* (1977) introduced staging systems for CLL to ascertain whether and when to start a treatment.

Many patients, who have the slow progressive form of the disease, do not require treatment at the onset of the disease and by the time they do, the disease has progressed with acquired comorbidities (Wancho *et al.,* 2018). However, other patients require urgent treatment due to fast progression of CLL. Rapidly progressed CLL is more aggressive and indicated by a number of genetic factors such as deletion of the short arm of chromosome 17 [del(17p)], deletion of the long arm of chromosome 11 [del(11q)], and a mutation of the tumour suppressor gene for tumour protein 53 *(TP53)* (O'Reilly *et al.,* 2018).

Other prognostic factors capable of predicting an adverse course of the disease at the time of diagnosis include lymphocyte-doubling time (<6 months), serum beta-2 microglobulin (>3.5 mg/L), cell surface expression of CD38, CD49d and zeta chain-associated protein 70 and presence of immunoglobulin heavy chain variable gene mutation in CLL cells (Ghia *et al.,* 2007; Parikh, 2018). Presence of prolymphocytes (>10%) in the PB, high levels of thymidine-kinase in the serum and soluble CD23 in the serum, and MRD at the end of CLL therapy also correlate with a worse prognosis (Ghia *et al.,* 2007; O'Reilly *et al.,* 2018). Nevertheless, some are associated with better prognosis such as chromosomal abnormalities including del13q and trisomy 12 (Ghia *et al.,* 2007; Wancho *et al.,* 2018).

Acute myeloid leukaemia (AML) is the second most common leukaemia after CLL but accounts for the majority of most leukaemia-related deaths in the world (National Cancer Institute , 2020). AML is characterized by the accumulation of abnormal immature myeloblasts (at least 20%), RBC or platelets in BM or PB due to differentiation block and maturation arrest (Estey, 2019). However, AML progresses rapidly if left untreated and these abnormal cells can spread to other parts of the body such as skin, gums and central nervous system (Estey, 2019).

AML is highly heterogeneous, hence there are different subtypes of AML. Previously, Bennett *et al.,* (1976) classified AML into six subtypes (M1 – M6) based on the FAB classification system however, Bloomfield (1985) and Lee *et al.,* (1987), revised this and two new subtypes, M0 and M7, were added to the list. However, between 2001 and 2016, the WHO classification system was introduced and modified to include all the new approaches in AML diagnosis and management (Arber *et al.,* 2016). Consequently, six major subtypes were defined such as AML with recurrent genetic abnormalities; AML with myelodysplasia-related features; therapy-related AML; AML not otherwise specified; myeloid sarcoma; and myeloid proliferation related to Down syndrome. Furthermore, these subtypes are divided into three risk groups: favourable, intermediate and adverse-risk groups based on cytogenetics. However, prognosis and response to therapy within these groups differ widely, making AML a challenge to treat.

Clinical factors, such as platelet count, serum creatinine or albumin, increased age and performance status of the patient at time of diagnosis constitute prognostic factors for determining the outcome of patients, however cytogenetic abnormalities offer the strongest prognosis in AML (De Kouchkovsky and Abdul-Hay, 2016; Estey, 2018). In addition to cytogenetics, data obtained after commencement of induction therapy are relevant prognostic tools in determining patients' outcomes. Patients who present with MRD, develop a second malignancy in the form of AML with a prior haematological malignancy or show symptoms of TRM following cytotoxic therapy are associated with poor overall survival (Ng *et al.,* 2000; De Kouchkovsky and Abdul-Hay, 2016; Estey, 2018).

Chronic Myeloid Leukaemia (CML) originates in defective pluripotent stem cells in the BM thus leading to accumulation of abnormal progenitors and their precursors in the BM and PB (Elefanty

et al., 1990). It is majorly characterised by a specific cytogenetic abnormality called the Philadelphia chromosome, which arises because of a reciprocal translocation between chromosomes 9 and 22 that disrupts the homeostatic regulation of haematopoiesis in the BM (Davis *et al.,* 2014). This generates *BCR-ABL1* fusion gene by recombination of the tyrosine kinase encoding *c-abl* oncogene on 9q34 and *bcr* gene on 22q11.2 (Elefanty *et al.,* 1990). The *BCR-ABL1* fusion gene encodes the oncoprotein BCR-ABL1 that primarily causes the chronic phase of CML due to its active tyrosine kinase activity (Mughal *et al.,* 2016). Accelerated and blast phases of the disease have also been defined. This is based on the platelet count, percentage of blasts in BM or PB, and or proliferation of blasts in extramedullary sites apart from spleen (Baccarani *et al.,* 2006; Baccarani *et al.,* 2009).

Several advances have been made to set hallmark prognostic tools, in addition to the *BCR-ABL1* fusion gene, for patients with CML. A prognostic scoring system for CML was first introduced in 1984 by Sokal *et al.,* for patients treated with busulfan, followed by Hasford *et al.,* (2008) who introduced the Euro score for patients treated with interferon α. Both scoring systems proved to be useful in the chemotherapy and interferon era. However, the European Treatment and Outcome Study (EUTOS) proposed a simpler scoring system that is specific to imatinib, which impedes the tyrosine kinase activity of *BCR-ABL1* fusion gene (Hasford *et al.,* 2011). Age, response to therapy, presence of comorbidities and phase of disease also offer prognostic information in these patients (Mughal *et al.,* 2016).

1.2 Bone marrow involvement in leukaemia

Haematopoiesis, the process by which blood cells are produced, primarily occurs in the BM. The haematopoietic system is hierarchically organised, with the haematopoietic stem cells (HSC) at the apex, and eventually leads to production of RBC, WBC and platelets (Figure 1.1). HSC possess self-renewal and multi-potential capabilities that enable them to provide a constant output of all blood cell lineages throughout life (Kumar *et al.,* 2018). Consequently, haematopoiesis is strictly regulated by intrinsic and extrinsic factors to maintain homeostasis (Testa, 2004; Hattangandi *et al.,* 2011). The rate of production of new blood cells balances the rate of destruction of aged blood cells via programmed cell death or apoptosis (Paulson *et al.,* 2011). However, stress

triggers increased haematopoiesis leading to resumption of haematopoiesis in extramedullary sites, such as spleen and liver, to restore normalcy (Rivella, 2012).
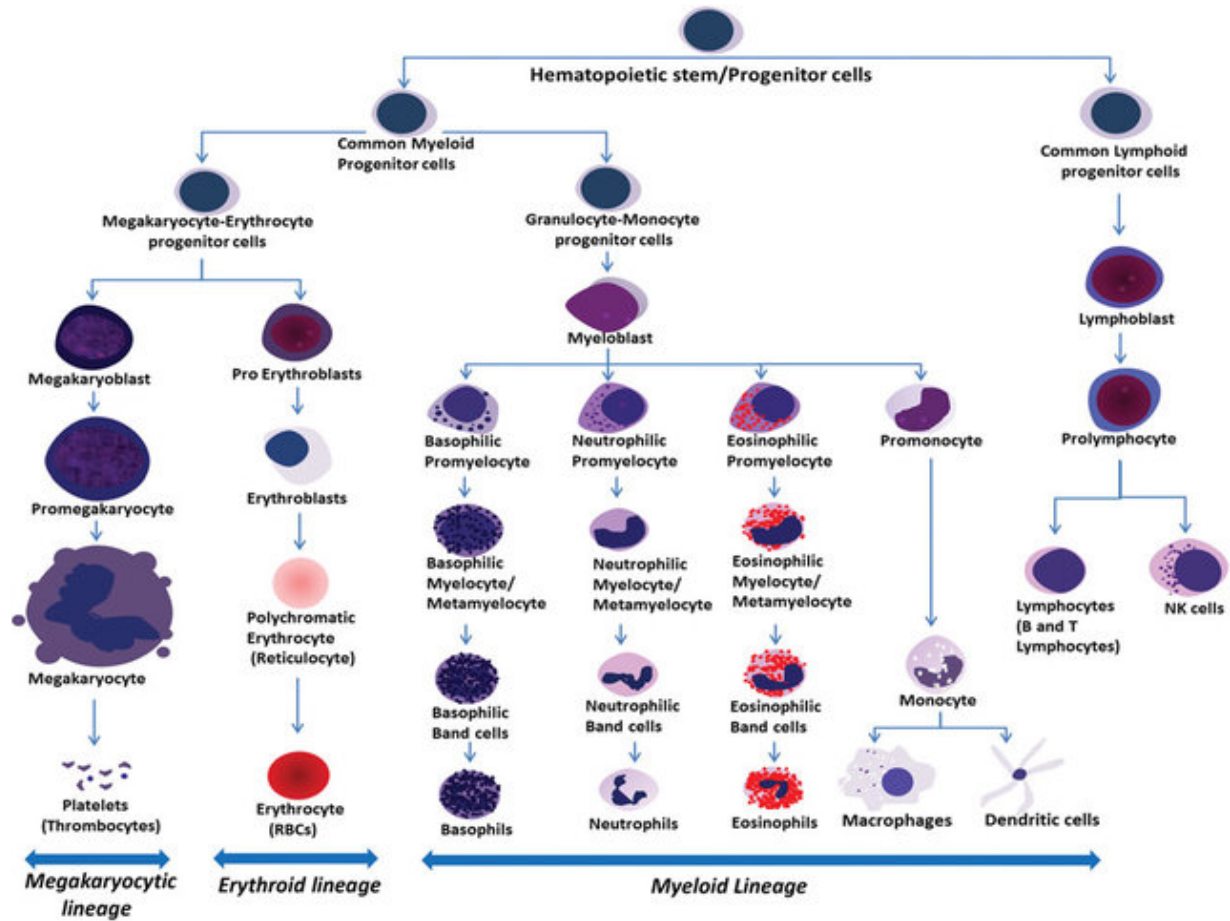
Figure 1.1: Developmental hierarchy of haematopoietic cells. Different blood cell lineages develop from haematopoietic cell precursors to mature blood cells. Haematopoiesis starts in the yolk sac then proceeds to the liver where committed myeloid and lymphoid progenitors are produced. This leads to the production of haematopoietic stem/progenitor cells in the bone marrow, which then undergo self-renewal to constantly produce permanent adult stem cells to maintain the haematopoietic pool throughout life. This figure is credited to Mahalingaiah *et al.,* (2018) with permitted usage under the creative common license.

Furthermore, increased BM activity driven by stress can lead to 'ineffective haematopoiesis' resulting in cytopenia, with anaemia the most frequent (Ginzburg & Rivella, 2011; Davis *et al.,* 2014). This is due to multistep alterations in the normal cell regulatory processes that cause an imbalance in the number of progenitor cells proliferating and number of mature blood cells produced. This misregulation in the haematopoietic process results in the development of varied

pathological conditions including leukaemia (Tsiftsoglou *et al.,* 2009; De Luisi *et al.,* 2013; Karlic *et al.,* 2013).

1.2.1 Bone marrow microenvironment

The BM is a multifunctional soft tissue that consists of a heterogeneous mixture of stem, progenitor and mature cells of different lineages. The parenchyma contains HSC and haematopoietic progenitor cells whereas the stroma consists of non-haematopoietic mesenchymal stem cells (MSC) (Zhao *et al.,* 2012). Similar to HSC, MSC that regulate bone remodelling, are multipotent in nature and have the ability to self-renew and differentiate into varied tissues of mesenchymal origin including adipocytes, osteoblasts, fibroblasts, reticular cells, endothelial cells, tissue macrophages and osteoclasts (Zhao *et al.,* 2012; Raegan & Rosen, 2016).

MSC were initially identified as fibroblastic cells that are capable of adhering to culture flasks and eventually growing into cells of mesenchymal origin, but recent reports suggest that MSC can also differentiate into myocytes, neurons, hepatocytes and cardiomyocytes (Friendenstein *et al.,* 1970; Caplan, 1991; Catacchio *et al.,* 2013). The International Society for Cellular Therapy (ISCT) has since proposed the minimal criteria to define MSC *in vitro*: adherence to a plastic surface, proliferation as colony forming unit fibroblasts (CFU-F), multipotent mesodermal differentiation and characteristic phenotype of surface markers, including CD44, CD90, CD105, CD106, CD166 and Stro-1 (Dominici *et al.,* 2006; Horowitz *et al.,* 2006; Ramakrishnan *et al.,* 2013).

MSC and HSC inhabit a unique hypoxic microenvironment in the BM referred to as the BM niche (Figure 1.2). This BM niche provides autocrine, paracrine and endocrine signalling that maintain and support the properties of regenerative cells (Anthony & Link, 2014; Scadden, 2016). The direct interaction between MSC and HSC in the perivascular space of the BM is critical to the regulation of haematopoiesis. HSC quiescence, a fundamental property of HSC that enables them to protect themselves from functional exhaustion and cellular insults thereby maintaining lifelong production of blood cell lineages, is strongly dependent on the MSC and their derived cells (Nakanmura-Ishizu *et al.,* 2014; Reagan & Rosen, 2016).
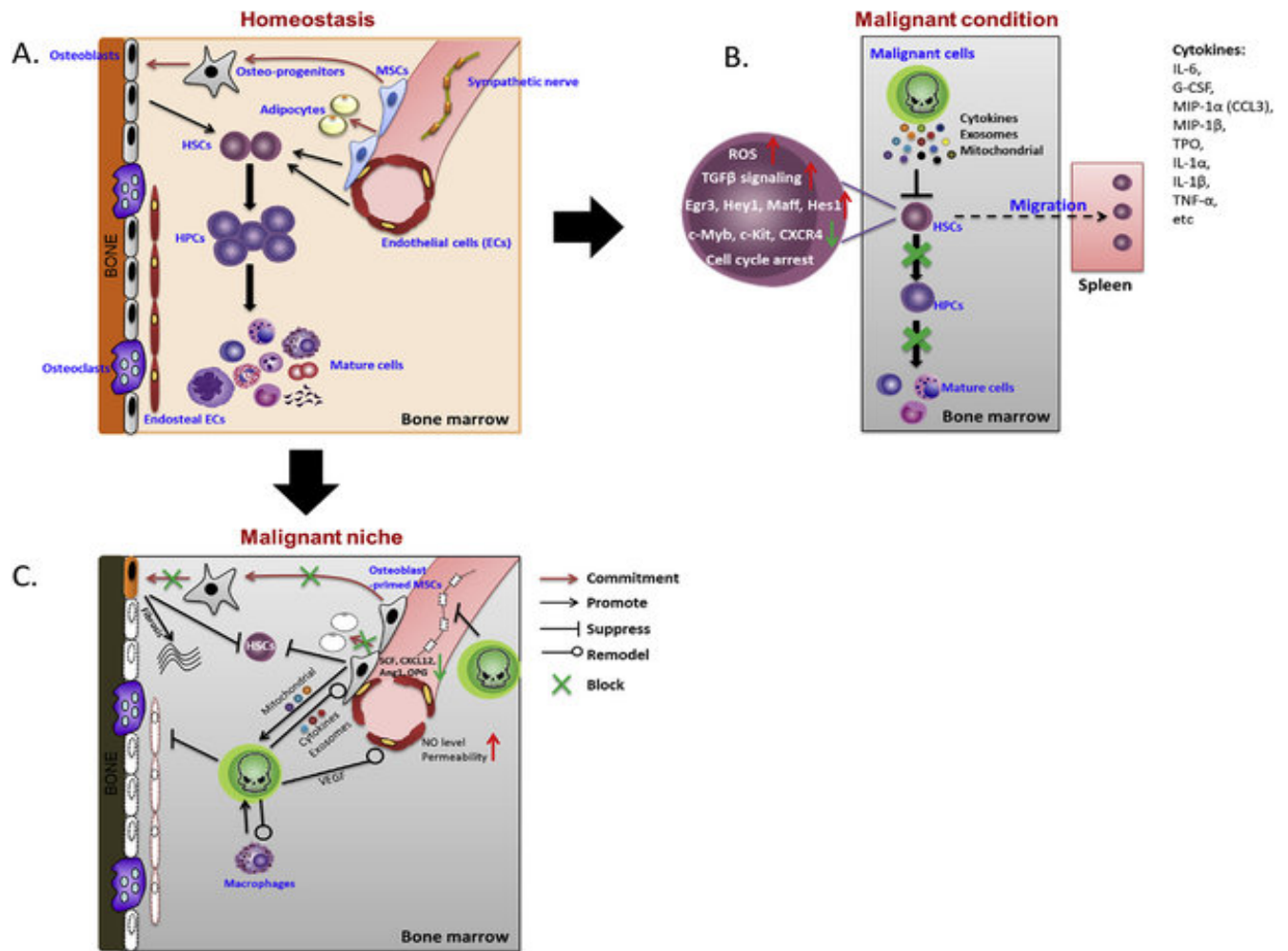
Figure 1.2 Involvement of the BM microenvironment in leukaemia. A. An overview of a normal BM microenvironment in homeostasis. B. This normal BM microenvironment can be altered via invasion of malignant cells, which release soluble factors like exosomes and cytokines to suppress HSC differentiation partially due to several signalling pathways. C. These malignant cells remodel the cells in the niche to create a malignant BM niche thereby suppressing haematopoiesis whilst supporting leukaemic cell growth. This figure is credited to Cheng *et al.,* (2018) with permitted usage under the creative common license.

MSC also secrete growth factors and cytokines involved in anti-apoptosis, angiogenesis and immunoregulation (Gnecchi & Melo, 2009; Gottipamula *et al.,* 2013; Norozi *et al.,* 2016). MSC carry out immunoregulatory functions either through direct intercellular contact with a large number of effector cells, or through secretion and release of soluble factors and extracellular vesicles (EVs) into the extracellular milieu, which are then taken up by these effector cells (Savukinas *et al.,* 2016; Fracchiolla *et al.,* 2017). Consequently, MSC maintain the BM

microenvironment or niche to ensure immune surveillance and homeostasis of haematopoietic activity (Wexler *et al.,* 2003; Chan *et al.,* 2006; Castillo *et al.,* 2007).

However, this intricate balance between HSC and MSC may be disrupted by malignant cell invasion and excessive reactive oxygen species (ROS) production thus altering cellular differentiation within the BM niche (Figure 1.2) and result in malignancy (Reagan & Rosen, 2016; Prieto-Bermejo *et al.,* 2018). Malignant cells accumulate and colonize the BM niche thereby modulating the niche to be pro-inflammatory to support their own expansive growth at the expense of normal cells, marked by cytopenia (Fracchiolla *et al.,* 2017; Kumar *et al.,* 2018). Depending on the type of malignant cells colonizing the BM niche and the extent to which the BM niche has been altered, normal and malignant BM niches differ in varied ways. MSC in the malignant BM niche become abnormal and stimulate evasion of immune surveillance with increased number of regulatory T cells and decreased number of effector T cells that have the ability to kill malignant cells (Chiarini *et al.,* 2016; Fracchiolla *et al.,* 2017). In a recent study by Mansour *et al.* (2016), BM isolated from 20 AML samples had increased levels of regulatory T cells compared to healthy subjects, contributing to an immunosuppressive microenvironment. Also, incorporation of EVs containing proteins and microRNA (miRNA) signatures, derived from CLL patients, into MSC led to the secretion of pro-inflammatory cytokines and other soluble factors by target cells thereby contributing to a malignant BM niche (Paggetti *et al.,* 2015). Furthermore, AML-derived EVs also induced suppression of normal haematopoiesis in mice through the expression of DKK1 whilst blockade of regulator of EVs release, Rab27a, resulted in delayed leukaemia development in these mice (Kumar *et al.,* 2018).

1.3 Treatment of leukaemia

Treatment of leukaemia can be difficult and depends on many factors due to the complexity of the disease. To define treatment, leukaemia patients are usually categorised into different risk groups based on prognostic factors such as age, type of leukaemia and other clinical and laboratory features. Chemotherapy and radiotherapy remain the mainstay treatment for leukaemia however, clinicians also employ monoclonal antibodies (e.g. rituximab for ALL), targeted therapies (e.g. tyrosine kinase inhibitors for CML) and haematopoietic stem cell

transplantation (HSCT) in the treatment of leukaemia (Sacha, 2014; Jabbour *et al.,* 2015). Chemotherapeutic drugs used for leukaemia are administered either alone or as a combination therapy. These include alkylating agents, topoisomerase inhibitors, antimetabolites, plant alkaloids and antibiotics (Figure 1.3). However, the focus will be on the drugs related to the work in this thesis.
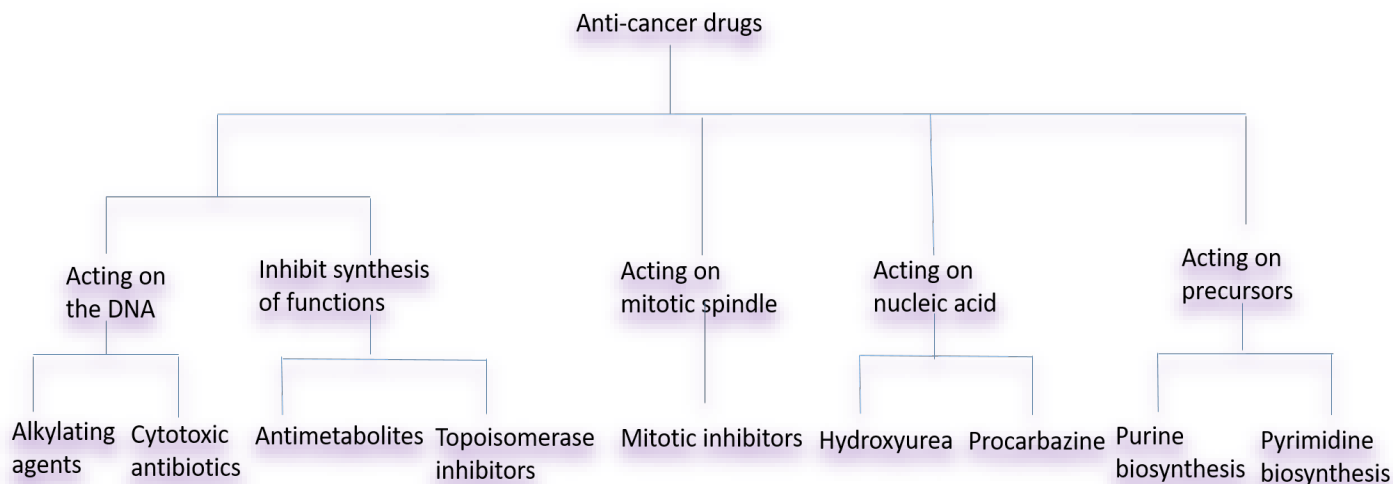
Figure 1.3 Mechanisms of action of anti-cancer drugs. Different drug groups are employed in the treatment of cancer such as alkylating agents, antimetabolites, cytotoxic antibiotics, purine antagonists, pyrimidine antagonists, plant alkaloids, topoisomerase inhibitors, and other unclassified agents. Alkylating agents alter cell function by forming covalent bonds with amino, carboxyl, sulphydryl and phosphate groups in DNA, RNA and proteins of cells. They attach an alkyl group to the nitrogen atom at the 7 position of the purine base guanine in DNA thus resulting in cross-linkage of DNA strands. Topoisomerase inhibitors inhibit the enzymatic activity of DNA topoisomerase II in tumour cells, such as replication and transcription thus exposing them to DNA damage. Alkylating agents and topoisomerase inhibitors are the main drug groups used in this study.

1.3.1 Alkylating agents

Alkylating agents are the oldest class of drugs used in the treatment of leukaemia. They are a diverse family of reactive compounds that covalently bind to electron-rich atoms in biological molecules such as nucleic acids (DNA and RNA) and amino acids thereby interfering with DNA replication and transcription (Colvin, 2003; Fu *et al.,* 2012).

Alkylating agents can inflict cytotoxic DNA damage or mutagenic damage by three different mechanisms. Firstly, they act by transferring their alkyl carbon groups onto the guanine base of the DNA molecule thereby altering the DNA structure and function in the process (Fu *et al.,* 2012). This disrupts the ability of leukaemic stem cells to proliferate and in an attempt by DNA repair enzymes to rectify the damage, the DNA fragments and the cells die.

In the second mechanism, alkylation of the DNA may result in mispairing of the nucleotide bases thus causing mutation (Ralhan and Kaur, 2007; Fu *et al.,* 2012). Lastly, they can induce DNA damage via formation of cross-linkage bonds between atoms in the DNA. Cross-linking of the DNA strands, by bifunctional alkylating agents, blocks the separation of the DNA strands, which is a prerequisite for DNA synthesis during cell division or transcription (Figure 1.4; Clauson *et al.,* 2013; Huang and Li, 2013). However, binding to one strand of the complementary DNA double helix, by monofunctional alkylating agents, does not prevent separation of the DNA strands but hinders the ability of important DNA enzymes – helicase, polymerase and ligase - to access the DNA thereby resulting in cell death (Kondo *et al.,* 2010; Fu *et al.,* 2012).
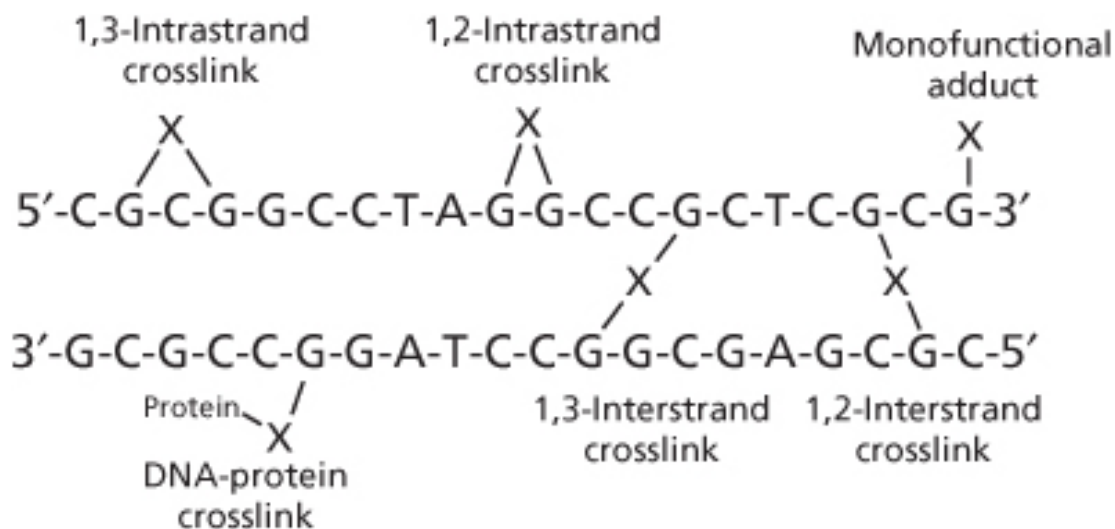
Figure 1.4 Formation of crosslinks by DNA-damaging agents. Bifunctional alkylating agents, chlorambucil and carmustine form bifunctional adducts including interstrand and intrastrand crosslinks between DNA strands. These cause DNA lesions or double strand breaks that require complex repair mechanisms especially nucleotide and/or base excision repairs and if irreparable, may lead to cell death. These drugs can also be metabolised to their intermediates, which could act by forming monofunctional adducts and/or DNA-protein crosslinks thereby causing DNA fragmentation, protein synthesis inhibition and eventually cell death.

Furthermore, there are six classes of drugs that make up this drug group and these include nitrogen mustards derived from mustard gases (e.g. chlorambucil), nitrosoureas (e.g. carmustine), alkyl sulfonates (e.g. busulfan), triazines (e.g. dacarbazine), piperazines and ethyleneimines (e.g. thiotepa) (Colvin, 2003; Ralhan and Kaur, 2007). These drugs are further divided into those that react directly with DNA (e. g. nitrosureas and nitrogen mustards) and those that form a reactive intermediate, which then reacts with the DNA (e.g. alkyl sulfonates).

Following preliminary research findings, which showed that main alkylating agents – chlorambucil and carmustine – caused increased micronuclei formation in a bystander lymphoblast cell line (Okeke, 2019). These drugs were identified as candidate alkylating agents to drive this research forward.

1.3.1.1 Chlorambucil

Chlorambucil is a non cell-cycle specific nitrogen mustard derivative that acts on lymphocytes (IARC, 2012). It is a lipid soluble drug that is rapidly absorbed by cells via passive diffusion, and metabolised, once absorbed, to more toxic phenyl acetic acid mustard thus enhancing its toxic effects (Mclean *et al.,* 1979; Newell *et al.,* 1981). It acts as a bifunctional alkylating agent that can bind to the N^7 position of guanine, N^3 position of adenine and thiol groups of proteins and peptides thereby interfering with DNA, RNA and protein synthesis through the formation of cross-links between two DNA strands (Barnouin *et al.,* 1998; Davies *et al.,* 1999). These crosslinks are either interstrand or intrastrand with the former being stable and irreparable by nucleotide excision repair (NER) enzymes than the latter, thus causing double strand breaks and a block in DNA replication and transcription (Loeber *et al.,* 2008; Di Antonio *et al.,* 2014).
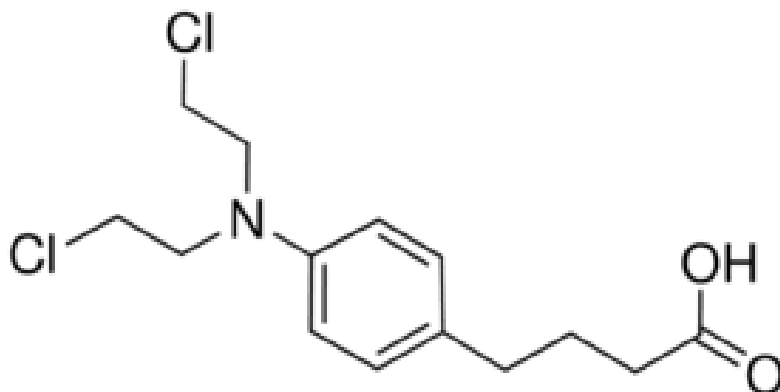
Figure 1.5 Chemical structure of chlorambucil

1.3.1.2 Carmustine

Carmustine, also known as bis-chloroethylnitrosourea or BCNU, belongs to the nitrosoureas family of alkylating agents, which are capable of crossing the blood brain barrier due to their lipophilic nature. Although alkylating agents are generally considered cell cycle phase nonspecific, carmustine causes formation of interstrand cross-links that block DNA replication and transcription, inhibit progression of S phase of cell cycle and subsequently causes cell death in dividing cells (Nikolova *et al.,* 2017). It requires hydrolysis to its active intermediates, in the liver, which act by alkylating the purine bases of DNA thus forming monoadducts and subsequently interstrand crosslinks thus inhibiting DNA, RNA and protein synthesis and causing fragmentation (Colvin, 2003; Bethseda, 2012).
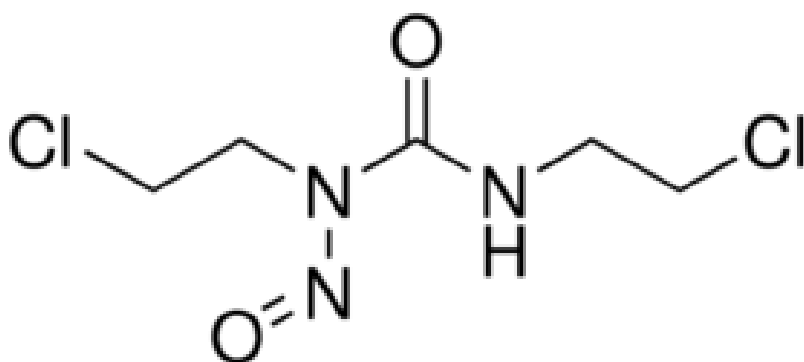
Figure 1.6 Chemical structure of carmustine

1.3.2 Topoisomerase inhibitors

Topoisomerase inhibitors are antineoplastic agents that impair the ability of the nuclear, topoisomerase enzymes, to regulate DNA topology during various genetic processes including DNA transcription and replication (Wilson *et al.,* 2001; Meier *et al.,* 2017). There are two main types of topoisomerase enzymes: topoisomerase I and topoisomerase II, which are present in all cells. Topoisomerase I makes single-strand breaks whilst topoisomerase II makes double-strand breaks to allow the separation and unwinding of the intertwined DNA strands (Hande, 2008; Kathiravan *et al.,* 2013). Similar to alkylating agents, topoisomerase inhibitors are cell cycle non-specific however, they would work most successfully during the ligation step in S-phase of cell cycle thereby causing both single and double strand breaks that affect the genome and thus lead to cell death (Nunhart *et al.,* 2019).

These inhibitors may block the effect of either topoisomerase enzymes however, the two main topoisomerase inhibitors, etoposide and mitoxantrone, chosen for this study target topoisomerase II enzyme. Topoisomerase II inhibitors may be poisons or catalytic inhibitors, and are both capable of inhibiting the enzymatic action of topoisomerase II. However only the poisons cause accumulation of topoisomerase II-linked double strand breaks whilst catalytic inhibitors act on the enzyme prior to formation of DNA breaks (Figure 1.7; Jensen and Sehested, 1997).

1.3.2.1 Etoposide

Etoposide or VP-16 is derived from podophyllotoxin, an anti-microtubule agent, which is extracted from the May apple plant (Kathiravan *et al.,* 2013). Etoposide poisons topoisomerase II and converts it into a potent cellular toxin by stabilizing and interacting with the enzyme's covalently cleaved DNA complexes (Jacob *et al.,* 2011). This inhibits the ability of the enzyme to ligate and repair the DNA thereby causing accumulation of DNA strand breaks. These accumulated breaks cause cell cycle arrest at S and G2/M phases hence preventing transition into the mitotic phase of cell cycle (Smith *et al.,* 1994; Jacob *et al.,* 2011).
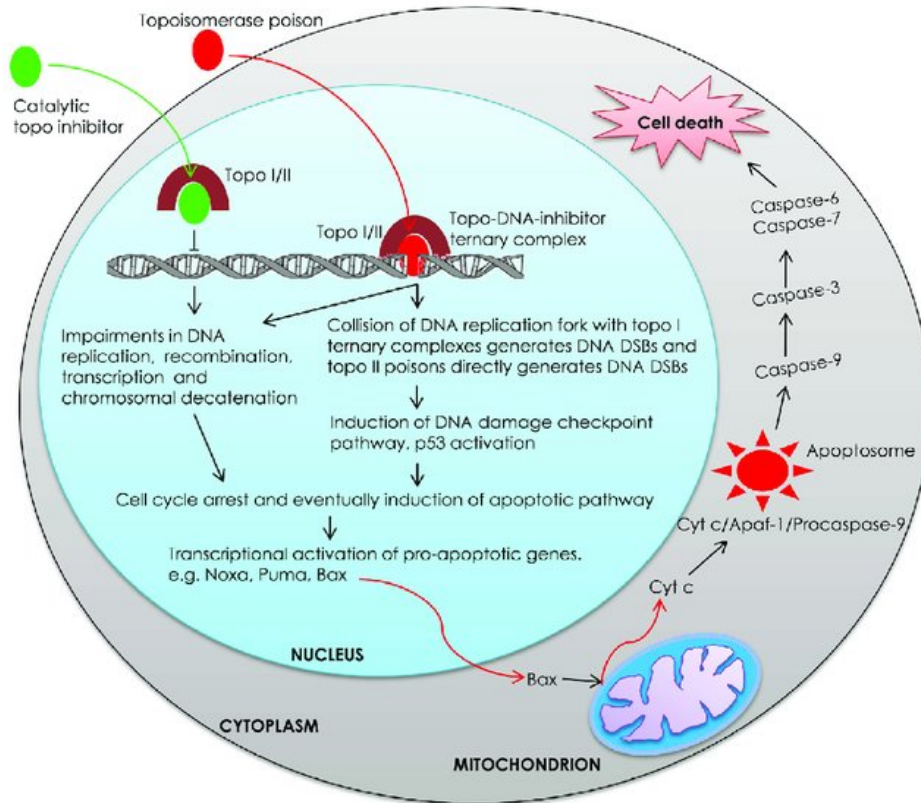
Figure 1.7 Mechanism of action of topoisomerase inhibitors. Topoisomerase inhibitors exert inhibitory effects on DNA topoisomerase enzymes' functions by acting as either catalytic topoisomerase inhibitors or topoisomerase poisons. This impedes DNA replication, recombination, transcription and decatenation thus causing DNA damage. This leads to cellular stress, cell cycle blockade and eventually cell death. This figure is credited to Jain *et al.,* (2017) with permitted usage under the creative common license.

Two known homologous isoforms, alpha (α) and beta (β), of the topoisomerase II enzyme exist. Two separate genes produce these isoforms during cell cycle but they differ in their molecular weight (Boland *et al.,* 2000; Hande, 2008). Etoposide targets the α isoform, which is essential for cell proliferation thereby inducing an anti-tumour effect, however it can also interact with β isoform, which is non-essential for cell growth to induce treatment-associated malignancy (Gatto and Lee, 2003; Asarova *et al.,* 2007). Etoposide is metabolised by cytochrome P450 in the liver, to etoposide catechol, which can be further oxidised to a quinone by cellular oxidases (Jacob *et al.,* 2011). These metabolites are also potent poisons that maintain the disruption of topoisomerase II enzymatic activity.
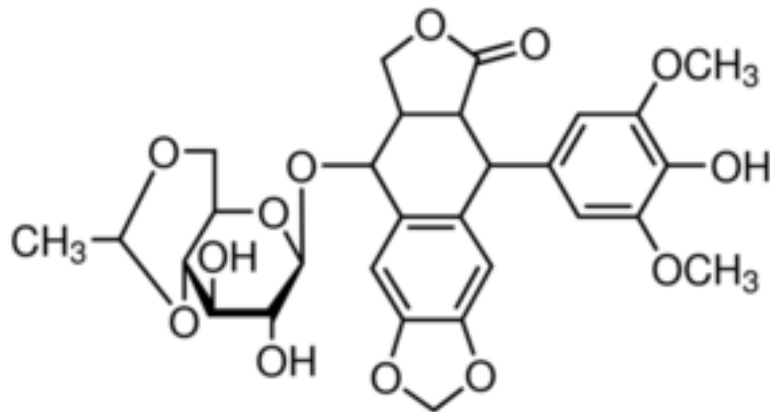
Figure 1.8 Chemical structure of etoposide

1.3.2.2 Mitoxantrone

Mitoxantrone (or novatrone) is a synthetic dihydroxyanthracenedione derivative that modulates the immune system through the interference of topoisomerase II activity to religate DNA strand breaks. It binds to the enzyme and disrupts its catalytic cycle thereby generating free radicals and making the DNA double strand breaks to persist, which may eventually lead to cell death (Faulds *et al.,* 1991; Jacob *et al.,* 2011). However, its cytotoxic effects may also result from aggregation and compaction of DNA, inhibition of microtubule assembly and inhibition of protein kinase C activity (Wiseman and Spencer, 1997). This mitoxantrone-induced DNA damage acts as a stimulus for NF-kappa β activation thereby increasing the secretion of pro-inflammatory genes including cytokines such as tumour necrosis factor alpha (Boland *et al.,* 2000).

Although mitoxantrone is not considered cell cycle specific, it can cause cell cycle arrest, particularly in late S phase (G2/S), by intercalating the DNA thereby causing DNA aggregation and DNA strand breaks (Faulds *et al.,* 1991; Wiseman and Spencer, 1997). Mitoxantrone is rapidly absorbed by tissues, penetrates blood cells and persists in the body for long periods (Faulds *et al.,* 1991). Mitoxantrone is also metabolised and readily oxidised, by cytochrome P450 in the liver, to several metabolites including monocarboxylic and dicarboxylic acid derivatives (Ehninger *et al.,* 1990). Mitoxantrone can also be oxidised by myeloperoxidases to an active metabolite, naphthoquinoxaline, which covalently binds DNA and RNA hence enhancing the cytotoxic effect of the drug (Mewes *et al.,* 1993; Panousis *et al.,* 1995). However, resistance to mitoxantrone has

been identified in leukaemia cell lines due to different mechanisms such as alterations in topoisomerase II activity and/or levels, enhanced DNA repair mechanisms, over-expression of P-glycoprotein, decreased intracellular drug binding and prevention of drug-induced apoptosis (Faulds *et al.,* 1991; Dunn and Goa, 1996).
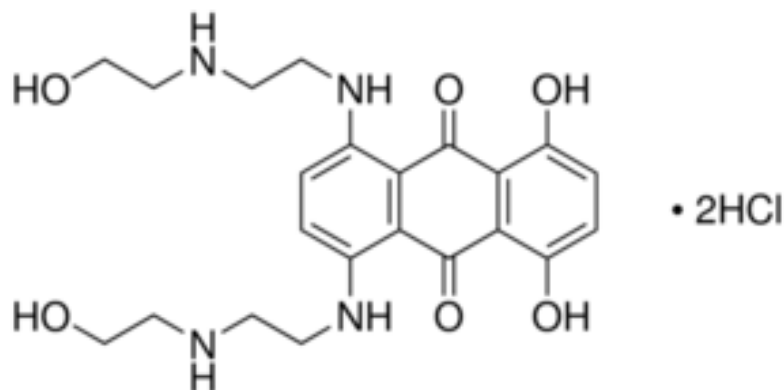
Figure 1.9 Chemical structure of mitoxantrone

1.4 Genotoxicity following chemotherapy

Although these chemotherapeutic agents are crucial in the treatment of leukaemia, they can also exert toxic effects on normal cells that are dividing frequently, particularly those in the BM, gonads and gastrointestinal tract thereby leading to formation of DNA lesions in these cells. As a result, biological response to these drugs is complex due to the diverse cellular repair mechanisms and response pathways that are often elicited. The genotoxicity of these drugs seem to be dependent on impaired DNA replication and transcription (Frei *et al.,* 1992).

1.4.1 Chromosomal/cytogenetic aberrations

Genomic instability via chromosomal or cytogenetic aberrations in cancer cells as well as normal cells often limit the efficacy of these drugs. These drugs may induce clastogenic (chromosomal breakages) or aneugenic (loss of chromosome) effects in cells thereby increasing the frequency of numerical or structural aberrations in the DNA.

Alkylating agents, chosen for this study, are associated with clastogenic effects in cells following treatment. Carmustine induced deletion mutations in mice (Chinnasamy *et al.,* 1997). This was associated with high frequency of micronuclei (MN), a chromosomal instability and/or genotoxicity marker. Chlorambucil induced structural chromosome aberrations and deletion mutations in *Drosophila melanogaster* and spermatogonial stem cells of mice respectively (Russel *et al.,* 1989; Rodriguez-Arnaiz *et al.,* 2004). Chlorambucil also increased the frequency of chromosomal abnormalities such as deletions, translocations and inversions in fibroblasts of patients with hairy cell leukaemia (Haglund *et al.,* 1997).

Similarly, topoisomerase inhibitors, mitoxantrone and etoposide, induced chromosomal breaks and exchanges in Chinese hamster lung fibroblastic cells (Yang and Rafia, 1985; Suzuki and Kane, 1994; Suzuki *et al.,* 1995). This clastogenic effect is linked to their ability to stabilize the cleavage complex of the topoisomerase enzyme. However, etoposide only induced chromatid-type aberrations in mutant KB cell lines that are resistant to etoposide with no accumulation of the cleavage complex (Suzuki *et al.,* 1997).

Furthermore, these drugs can also cause interchromosomal translocations such as *MLL* gene on chromosome 11 band q23 by blocking the G2/M checkpoint during cell cycle (Ohshima *et al.,* 1996; Nakada *et al.,* 2006; Brassesco *et al.,* 2009). This *MLL* gene plays a critical role in mutagenesis through misregulation of gene expression and creation of oncogenic fusion genes. Etoposide-induced partial chromosomal duplications and deletions were also reported in B6C3F1 mice (Marchetti *et al.,* 2001; Marchetti et *al.,* 2006). Consequently, these genetic aberrations enhance the risk of developing a second primary cancer. This risk increases 5 years post-chemotherapy and has been frequently observed in long-term survivors (Hijiya *et al.,* 2009; Bhatia, 2013; Cheung-Ong *et al.,* 2013).

1.4.2 Mutagenicity and apoptosis

Cells respond to DNA damage by DNA repair mechanisms, activating cell cycle checkpoints or trigerring apoptosis, and these processes overlap each other. However, genomic damage in the nucleus can also be signalled to mitochondria tipping the balance in favour of apoptosis rather than repair and survival (Norbury and Zhivotovsky, 2004). Apoptosis is thought to be crucial in

the maintenance of homeostasis through elimination of worn out, aged or dying cells with damaged DNA from the replicating pool, in order to inhibit genomic instability and associated risk of cancer (Meinteres *et al.,* 2001). Therefore, it would be expected that suppression of apoptosis would result in increased survival of mutant cells and thence enhanced mutagenesis.

Several reports revealed that chemotherapeutic drugs at concentrations that induce apoptosis result in mutation with the overexpression of *BCL2*, a proto-oncogene that can block apoptosis induced by these chemotherapeutic drugs. Carmustine-induced apoptosis in isogenic Chinese hamster ovary cell lines was eliminated by expression of *BCL2* and repair mechanism (Meikrantz *et al.,* 1998). However, transfection of mouse B-cells (CH31 clones) with human *BCL2* sense plasmids inhibited etoposide-induced cytotoxicity/apoptosis but had no effect on the production of DNA-protein cross-links and DNA strand breaks (Kamesaki *et al.,* 1993). This shows that *BCL2* can block DNA fragmentation, which is a hallmark of apoptosis, but cannot disrupt initial DNA damage that may possibly lead to mutagenic events. This was supported by the findings of Hashimoto *et al.,* (1995), which revealed that etoposide-cytotoxicity induced DNA recombination and increased mutant frequency in Chinese hamster V79 cells despite suppression of apoptosis in these cells through *BCL2* overexpression. DNA recombination seems to be responsible for the large deletions and rearrangements in the genome. Etoposide-induced cell death has also been reported in HeLa cells through the formation of giant multi-nucleated cells that are characteristic of aberrant mitotic events (Lock and Stribinskiene 1996). Furthermore, formation of micronuclei (MN), a chromosomal instability and/or genotoxicity marker, was evident in CTTL-2 cytotoxic T-cells from mouse strain C57bl/6 that was transfected with *BCL2* plasmids following treatment with etoposide despite a significant reduction in apoptosis (Meintieres *et al.,* 2001). Etoposide and mitoxantrone, even at low levels of toxicity, also induced MN formation despite little or no reduction in cell growth (Stopper *et al.,* 1999). Collectively, these suggest that inhibition of biochemical steps in apoptosis could be accompanied by induction of mutagenic events in cells following exposure to etoposide and mitoxantrone.

Furthermore, the genotoxic effects of drugs could be enhanced by modifying the ability of these drugs to directly target mitochondrial DNA to induce apoptosis and mutagenicity. According to Fonseca *et al.,* (2011), the effect of chlorambucil can be potentiated through

compartmentalisation and activation in the mitochondria thus leading to cell death in patient samples, cancer cell lines and cells with resistance to chlorambucil or inhibited apoptotic signals. Additionally, Milliard *et al.,* (2013) showed that localization of chlorambucil to the mitochondria led to cell cycle arrest and apoptosis in breast and pancreatic cell lines that are resistant to chlorambucil. Resistance to chlorambucil may be due to inhibition of apoptotic signals initiated by the overexpression of genes such as *BCL2* and *p53* hence mitochondrial targeting of chlorambucil could lead to biochemical alterations in the apoptotic pathway and thence cell death.

1.5 Haematopoietic stem cell transplantation

Although chemotherapy and radiotherapy serve as the main approaches, HSCT remains the only curative therapy for leukaemia. HSCT has been employed in the treatment of numerous malignant and non-malignant haematological diseases ever since it was demonstrated over 50 years ago that infused HSC have the ability to reconstitute immuno-haematopoiesis after myeloablative conditioning (MAC) and transplantation (Thomas *et al.,* 1957). Due to a continued improvement in HSCT outcome, indications for HSCT continue to grow across the world, however HSCT does not correct underlying diseases. A recent study by the European Society of Blood and Marrow Transplantation revealed that over 400,000 transplants were done in Europe in 2015 (Passweg *et al.,* 2016). The principle of HSCT involves the reconstitution of BM with donor/harvested cells, following maximal reduction of damaged stem cells with MAC (high dose chemotherapy and/or radiotherapy), and adequate immunosuppression to enhance successful engraftment of 'new' stem cells and destruction of defective cells (Dominquez-Gonzalez & Moore, 2013; Perumbeti *et al.*, 2013).

1.5.1 Types of stem cell transplantation

HSCT may be autologous (using cells from the same person) or allogeneic (another person). Autologous transplantation is not usually indicated in leukaemia due to the high risk of disease relapse in these patients through the infusion of leukaemic stem cells (LSC) which may persist. However, it is used in the treatment of other haematological malignancies such as lymphoma

and multiple myeloma (Passweg *et al.,* 2016). Allogeneic transplantation offers a better disease-free survival in leukaemia due to its ability to create a graft-versus-leukaemia (GVL) effect through reconstitution of immuno-haematopoiesis in the patient.

1.5.2 Sources of stem cells

Choosing the appropriate stem cell source for allogeneic transplantation can be a difficult task for clinicians. There are certain factors to consider and these include the primary disease, stage of the disease, age of the patient, time and urgency of transplantation, human leucocyte antigen (HLA) match between patient and the donor, stem cell quantity and the experience of the transplantation centre (Demiriz *et al.,* 2012).

There are three main sources of stem cells that can be used for HSCT such as BM, PB stem cells (PBSC) and umbilical cord blood (UCB) and each has its own pros and cons that makes it suitable for particular disease settings (Demiriz *et al.,* 2012; Cheuk, 2013). However, these benefits and risks conferred by each stem cell source may alter depending on the conditioning regimen, strategies for prophylaxis and treatment for graft-versus-host-disease (GVHD) and graft manipulation (Cheuk, 2013). Nevertheless, the aim of choosing the right stem cell source is to enhance disease-free survival in the patient through GVL effect at the expense of high risk of graft rejection, disease relapse or GVHD.

1.5.3 Conditioning regimen

The conditioning regimen can be either one or a combination of chemotherapy, radiotherapy or immunotherapy (Gyurkocza and Sandmaier, 2014; Jethava *et al.,* 2017). Some of the chemotherapeutic drugs commonly used in conditioning regimens are alkylating agents and topoisomerase inhibitors. Previously, HSCT was restricted only to young patients in good condition due to toxicity of MAC. MAC requires use of high intensive conditioning, which rids BM of LSC. However, reduced intensity conditioning (RIC) or non-myeloablative conditioning (NMAC) has enabled treatment of the elderly, high-risk patients and patients with comorbidities that make up the major proportion of leukaemic patients (Champlin, 2013; Babushok & Hexner, 2014). The difference between RIC and NMAC regimens is that the former require stem cell

support whilst the latter may result in minimal cytopenias that do not require stem cell support (Sengsayadeth *et al.,* 2015). NMAC entails the induction of mixed chimerism between the host and donor lymphocytes and this genetic mismatch causes an immune reaction that is tipped in favour of cells from the donor through donor lymphocyte infusions in order to elicit GVL effect. However, the risk of graft rejection or disease relapse is higher in these less intensive conditioning regimens compared to MAC due to persistence of LSC in BM. Furthermore, the MSC population remains host-derived following allogeneic transplantation despite sustaining MAC or RIC capable of inducing stromal damage (Spyridonidis *et al.,* 2005; Bartsch *et al.,* 2009). This pre-exposure of MSC to chemotherapy during conditioning cause phenotypic and differentiation alterations that may lead to protection of leukaemic cells during chemotherapy (Kumar *et al.,* 2017; Somaiah *et al.,* 2018).

1.6 Complications after stem cell transplantation

Despite the success recorded with HSCT, it is limited by numerous complications (Table 1.1). These sequelae, most importantly graft rejection and GVHD, may develop early or late following HSCT. GVHD, caused by a HLA mismatch and/or genetic disparity between the donor and recipient, is the major cause of morbidity and mortality following allogeneic HSCT (Hartwig *et al.,* 2007; Atarod and Dickinson, 2013). This disparity leads to the destruction of the host's tissues by the donor lymphocytes. GVHD may be acute or chronic depending on timing and clinical manifestations, and is often treated with corticosteroids. However, some patients do not respond to corticosteroid treatment and are usually treated with different immunosuppressive drugs with varying responses (Przepiorka *et al.,* 2020). Acute GVHD occurs under 100 days of HSCT whereas chronic GVHD manifests after 100 days (Sung and Chao, 2013). Interestingly, GVHD is invariably linked to the beneficial GVL effect hence dissociating GVL from GVHD remains the basis of various transplantation studies.

Furthermore, a relapse, which indicates a return of the original disease, may arise due to intrinsic or acquired resistance of cancer to the drug (Swift *et al.,* 2014; Xu *et al.,* 2014). For example, this may be due to immune evasion, by LSC, through upregulation of CD47, an anti-phagocytic marker, and presentation of MHC class II associated invariant chain derived peptide on their

surfaces (Majeti *et al.,* 2009; van Lujin *et al.,* 2012). Thus, LSC persist in the BM and cause MRD. As a result, leukaemia relapse is a major cause of post-transplant mortality.

Table 1.1 Complications associated with stem cell transplantation

Complication	HSCT type	Reference (s)
Graft-versus-host disease (GVHD)	Allogeneic	Hartwig *et al.,* (2007); Atarod and Dickinson, (2013).
Graft rejection	Allogeneic	Chevallier *et al.,* (2012); Mehta and Faulkner, (2013).
Secondary malignancy	Autologous, allogeneic	La Nasa *et al.,* (2013); Atsuta *et al.,* (2014).
Therapy-related malignancy	Autologous, allogeneic	Bhatia, (2013).
Treatment-related mortality	Autologous, allogeneic	Champlin, (2011); Reisner *et al.,* (2011).
Disease relapse	Autologous, allogeneic	Chevallier *et al.,* (2012); Atarod and Dickinson, (2013); Cheuk, (2013).
Donor cell leukaemia	Allogeneic	Wisemann, (2011); Bobadilla *et al.,* (2015).
Non-relapse mortality	Autologous	McClune *et al.,* (2010).
Post-transplant lymphoproliferative disease (PTLD)	Allogeneic	Kontoyiannis, (2013).
Long-term complications	Allogeneic	Atarod and Dickinson, (2013); Mehta and Faulkner, (2013); Perumbeti *et al.,* (2013).
Autoimmune disease	Autologous, allogeneic	Faraci *et al.,* (2014).

Due to a lack of specificity of chemotherapeutic agents whilst targeting cancer cells, during conditioning, the genotoxic damage may be extended to non-targeted cells thus enhancing the risk of developing a malignancy in these normal cells. This phenomenon of a second primary cancer that develops following treatment for a primary disease is known as TRM. This has been more frequently observed in long-term survivors and this has been linked to alkylating agents and topoisomerase inhibitors (Bhatia, 2013; Cheung-Ong *et al.,* 2013). These different drug

groups induce different types of TRM, which are distinguished by the course of the disease and the time it takes for leukaemia to develop following conditioning.

The first type induced by alkylating agents often presents as a pre-leukemic period of myelodysplasia (MDS) and usually develops after 5-7 years, whilst the topoisomerase inhibitors-induced type is not preceded by MDS and occurs after 2 years (Kröger *et al.,* 2003). However, the prognosis for TRM is poor regardless of the type that develops. This is mainly due to the fact that TRM shares cytogenetic aberrations with *de novo* leukaemia of unknown aetiology, such as monosomy or deletions on chromosomes 5 and/or 7, and *TP53* mutation (Pedersen-Bjegaard *et al.,* 2008; Bhatia, 2013). As a result, TRM may serve as "*in vivo* model" to study the origin of *de novo* leukaemia. Furthermore, recent findings have shown that HSCT can also lead to a new haematological malignancy known as donor cell leukaemia (DCL). Whilst TRM is due to direct exposure of non-target cells to drugs, DCL will be because of indirect exposure to drugs.

1.7 Donor cell leukaemia

DCL is a rare type of leukaemia that develops in a patient following allogeneic HSCT, in which the transformed cells are donor-derived. This can occur as either a very early complication or a late complication. These donor-derived cells have not been exposed to any form of conditioning so it remains unknown why the donor remains healthy but the donor cells become malignant when transplanted in a patient.

1.7.1 Epidemiology

In 1971, Fialkow and colleagues described the case of a female patient who relapsed, under 100 days, after HSCT from her HLA-matched brother for ALL; the leukaemic cells contained a Y chromosome. Due to irregularities in its recognition and in reporting, DCL is not always clear and often confused for relapse. According to Wiseman (2011), DCL might be responsible for 5% of all post-transplant 'relapses'. Consequently, the incidence of DCL remains relatively unknown as the cases were previously reported as relapse, however there has been a massive increase in reported cases in the literature, which suggests that this may be more common than initially expected. It has been reported to be 0.12% by the European Society for Blood and Marrow

Transplantation during a 21-year period (Hertenstein *et al.,* 2005) and 0.84% by the Tokyo Cord Blood Bank (Nagamura-Inoue *et al.,* 2007).

About 75% of DCL cases are different from the original disease and often arise as AML in 53% of cases, 25% as ALL and 20% as MDS (Wisemann, 2011). Most reported cases arise from adult patients however, there are several reported cases of paediatric DCL to date (Stein *et al.,* 1989; Haltrich *et al.,* 2003; Fraser *et al.,* 2005; Cetin *et al.,* 2006; Sevilla *et al.,* 2006; Crow *et al.,* 2010; Wang *et al.,* 2011; Bobadilla-Morales *et al.,* 2015). Most adult DCL cases present as AML or MDS whereas paediatric DCL present as mostly AML and/or ALL (Bobadilla *et al.,* 2015).

However, DCL has a poor prognosis in both groups. The interval between transplant and the occurrence of a second primary cancer is an important parameter for the study of risk, cause and pathogenesis of the disease (Wang *et al.,* 2011). The latency period between allogeneic HSCT and occurrence of DCL covers a range of 1 to 193 months (Hertenstein *et al*., 2005; Wang *et al*., 2011). However, the maximum interval in children who developed DCL was 156 months (median, 23 months).

1.7.2 Aetiology and proposed mechanisms

Understanding the conundrum that surrounds the oncogenic transformation of donor cells in a patient may provide insights in studying leukemogenesis. However, the aetiology is unknown due to difficulty in determining its diagnosis and incidence. As a result, several scientists have proposed different mechanisms, involving interplay between many factors, to explain this anomaly (Figure 1.8). These factors may be extrinsic factors provided by the patient's BM microenvironment or intrinsic factors in the donor (Torra and Loeb, 2011).

1.7.2.1 Extrinsic factors

Due to the lack of leukaemia development in the donors, a number of hypotheses suggest that extrinsic factors, in the patient, contribute to this rare malignant transformation of the incoming cells thus promoting DCL. Such extrinsic factors may include damaged BM microenvironment and impaired immunosurveillance. A growing body of evidence suggests that the homeostatic nature

of the BM microenvironment is altered by the conditioning regimen prior to HSCT. According to Flynn and Kaufman (2007), this alteration reflects the 'seed and soil' hypothesis, whereby the BM microenvironment serves as the soil whilst the donor cells act as the seed.
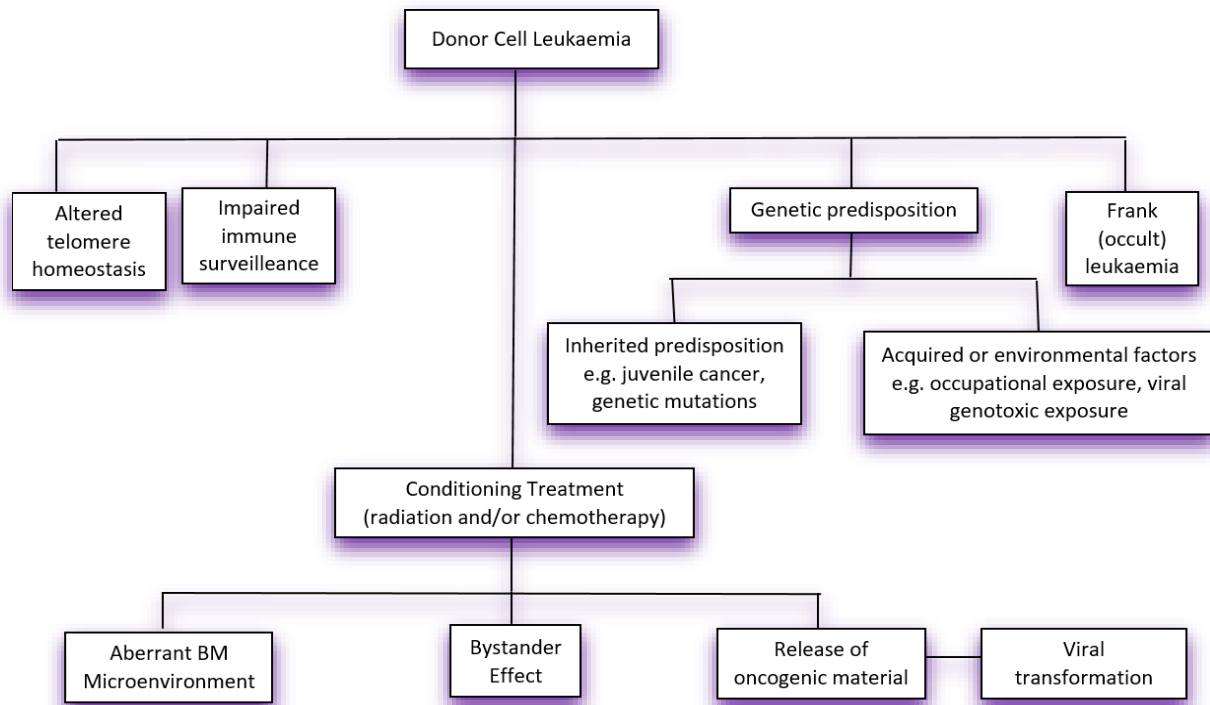
Figure 1.10 Proposed mechanisms of donor cell leukaemia. Different theories have been proposed to explain this phenomenon such as prior genetic predisposition to cancer, altered telomere homeostasis, impaired immune surveillance, occult leukaemia and conditioning treatment, which will further debilitate the BM, cause a bystander effect in non-targeted cells or release oncogenic materials Adapted from Wiseman (2011).

Consequently, this encompasses the dysregulation of genes, cytokine signalling, transcription factors and receptors/ligands involved in intercellular communication. This is due to the residual effects of radiotherapy and/or chemotherapy thereby causing inter-cellular communication between recipient's cells and the transplanted cells from the donor in the BM microenvironment as a consequence of an inflammatory-type response (Ruiz-Arguelles *et al.,* 2007; Wisemann, 2011). Transfer of radiotherapy/chemotherapy-induced residual effects or oncogenic materials present in the BM microenvironment may also occur through a bystander effect or by genomic fusion of the patient's LSC to the donor cells (Wiseman, 2011; Bobadilla-Morales *et al.,* 2015). Furthermore, increased DNA replication/repair errors and mutations may succeed

transplantation due to enhanced proliferative drive in a bid to reconstitute haematopoiesis in the BM (Nagamura-Inuoe *et al.,* 2007; Gustafsson *et al.,* 2012).

Communicable and infectious agents such as Epstein-Barr virus may impair the patient's immune system post-transplantation thus leading to the development of a malignant disorder known as post-transplant lymphoproliferative disorder (PTLD) (Nagamura-Inuoe *et al.,* 2007; Torra and Loeb, 2011). This is often due to dire need to suppress the immune system, to prevent graft rejection, during HSCT thus leading to the depletion of T-cells, which will in turn hamper the ability of T-cells to stimulate B-cells and subsequently alleviate any immune attack. Histocompatibility disparities in the patient may also cause a sustained antigenic stimulation of donor cells as seen in lymphoid DCL (Wang *et al.,* 2011).

1.7.2.2 Intrinsic factors

All these aforementioned extrinsic factors are speculative however, and seem like looking at the far end of a rather complex process, as cells require multiple hits to their DNA, without repair, for cancer to develop. Thus, there may be environmental factors that cause these multiple hits to the DNA and thence induce dysregulation of numerous signalling pathways. This suggests that certain factors may cause these intrinsic changes in the donor and provide the 'first hit' whilst these extrinsic factors in the recipient serve as the 'second hit' thereby leading to oncogenic transformation of these cells and/or their progeny (Flynn and Kaufman (2007).

Donor-derived factors such as genetic predisposition to leukemogenesis or presence of a pre-leukaemic clone may also contribute to the development of DCL especially when the donor is a sibling. The occult leukaemic clone could evolve independently through acquisition of a prerequisite second 'hit' in the damaged BM microenvironment thus causing it to proliferate uncontrollably (Hertenstein *et al.,* 2005).

1.7.3 Diagnosis, prognosis and treatment

Initially, the diagnosis of DCL was based only on morphological differences and this may have contributed to its under-detection, especially in sex-matched cases. However, the advent of new

molecular techniques has led to an improvement in detection and analysis of donor-host chimerism. As a result, the diagnosis of DCL is dependent on accurate identification of the donor origin of the leukaemic cells to rule out any confusion with relapse (McCann and Wright, 2003).

Karyotype analyses or genetic analyses using markers such as variable number of tandem repeats (VNTR) or short tandem repeats (STR) must be carefully performed to obtain accurate results (Wang *et al.,* 2011). The use of karyotype analyses has enabled the identification of abnormal karyotype such as deletions, translocations, whole or partial loss of chromosome 5/7 and rearrangement of the 11q23 locus containing the *MLL* gene that are all frequently found in DCL cases (Ma and Tiu, 2016). However, Spinelli et *al.,* (2000) were the first to illustrate the importance of using microsatellite analysis to identify the donor origin of leukaemia. They reported the presence of an XX clone, found in a male patient, following HSCT from his HLA-identical sister. The XX clone was shown by STR typing to be of patient origin hence suggesting the probable loss of Y chromosome followed by duplication of the X chromosome. Other molecular methods that have been reliably used in the investigation of DCL include fluorescent *in situ* hybridization (FISH), YCS-PCR for detecting Y-specific chromosome sequence (YCS), single nucleotide polymorphisms (SNP), restriction fragment length polymorphisms (RFLP), and short inversion or deletion polymorphisms (SIDP) (Thiede, 2004; Ruiz-Arguelles *et al.,* 2007).

Nevertheless, DCL is very severe largely due to its heterogeneous presentation, however it is only treatable with chemotherapy or HSCT hence the need for further studies (McCann and Wright, 2003). Consequently, there are important factors to consider in order to accurately classify DCL. These include stem cell source, type of conditioning regimen given, age and sex of the patient and donor, histocompatibility differences and family ties between the patient and donor, health status of the donor, types of primary and DCL malignancies, method(s) used for analysis of patient-donor chimerism and confirmation of donor origin of the leukaemia (Wiseman, 2011).

1.8 Bystander effect

Every live cell, whether normal or tumour, inherently responds to threat by sending signals to the surrounding neighbours. The neighbouring cells could respond to these signals immediately

or cause genomic instability in their progeny (Perumal *et al.,* 2017). Bystander effect (BE) refers to the manifestation of treatment-related toxic effects on unexposed cells, which are in close proximity to the directly exposed cells. This BE is well described after radiotherapy.

1.8.1 Radiation-induced bystander effect

Radiation-induced bystander effects (RIBE) was first described in 1992 when it was shown that DNA damage-dependent effects are not restricted to directly targeted cells but these irradiated cells can release signals to unirradiated cells post-treatment (Nagasawa and Little, 1992). About 1% of cells underwent α-particle irradiation, however 30% of cells exhibited increased sister-chromatid exchange (SCE) highlighting possible communication between damaged and normal cells. Ever since then, extensive research has been done in this field confirming the existence of RIBE.

RIBE manifests via a wide range of biological endpoints. These include formation of MN, chromosomal aberrations, apoptosis or cell death, cell cycle deregulation, increased mitochondrial mass, reduced clonogenic survival, inflammation, gene mutation, altered gene expression, SCE, DNA double strand breaks, loss of global DNA methylation, neoplastic transformation, differentiation and proliferation (Kortubash *et al.,* 2007; Najafi *et al.,* 2014; Song *et al.,* 2016). The signals that mediate this RIBE, such as cytokines, reactive oxygen species (ROS), nitric oxide, proteins, RNA, mRNA and miRNAs, can be transferred between cells via gap junctions or the extracellular medium (Prise & O'Sullivan, 2009; Dickey *et al.,* 2011; Sokolov and Neumann, 2018).

These bystander endpoints may be due to molecular changes caused by alterations in the expression of miRNAs. The expression of miRNAs was reportedly altered in a bystander 3-dimensional tissue, which was distinct from the microRNAome changes found in the directly irradiated cells (Kovalchuk *et al.,* 2010). MiRNA profiles were also differentially expressed in irradiated and bystander lymphoblast cells whilst miR-21 was implicated in RIBE in fibroblast cells (Chaudhry and Omaruddin, 2012; Xu *et al.,* 2014).

However, emerging reports support that miRNA, RNA and proteins can be packaged into EVs, including microvesicles, exosomes and apoptotic bodies (from fragmented apoptotic cells), which are taken up by the neighbouring or distant cells (Chen *et al.,* 2012; Lou *et al.,* 2017). According to Al-Mayah *et al.,* (2015), irradiated MCF7 breast epithelial cells released exosomes containing proteins and RNA, which induced DNA damage in unirradiated cells. This BE persisted in the progeny of the bystander cells, which were also found to be capable of inducing BE themselves via exosomes. Furthermore, exosomes isolated from irradiated conditioned medium induced BE through transfer of miR-21 (Xu *et al.,* 2015). Exosomes also propagated RIBE signals via miR-7 thereby inducing autophagy in the lung (Song *et al.,* 2016; Cai *et al.,* 2017). These EV-derived miRNAs can also induce RIBE in the BM and spleen (Szatmari *et al.,* 2017).

Furthermore, the effects of radiation can be delayed and thence appear long periods after exposure, thereby causing genomic instability and enhancing the risk of oncogenic transformation. Radiation also induced telomere shortening and bridge formation *ex vivo,* which are indicative of genomic instability (Gorman *et al.,* 2009). Radiation-induced genomic instability can also manifest as chromosomal alterations, MN, gene amplification, gene mutations, delayed cell killing and cell transformation (Preston, 2005; Perumal *et al.,* 2017).

1.8.2 Chemotherapy-induced bystander effect

Although there is ample evidence of RIBE, BE is not exclusive to radiotherapy but can also be triggered by other forms of cellular stress including genotoxic agents, whether physical or chemical (Figure 1.9). Normal human fibroblasts exhibited high levels of DNA double-strand breaks following exposure to low concentrations of sodium dodecyl sulphate (SDS) via the release of cytokines (Dickey *et al.,* 2009). Therefore, BE is variable and depends on dose, type of radiation/chemical agents, experimental model, and type of donor and recipient cells (Perumal *et al.,* 2017).

The concept of chemotherapy-induced bystander effect (CIBE) has piqued the interest of researchers in recent times ever since it was shown that these chemotherapeutic agents have the ability to exert BE similar to ionizing radiation. In 1990, Moolten and Wells became the first researchers to describe the ability of treated cells to confer chemosensitivity upon their

untreated neighbours. They reported that ganciclovir, a nucleoside analogue specifically activated by herpes simplex virus thymidine kinase (*HSV-TK*) gene, induced CIBE *in vitro.* This was further supported by a report that these HSV-TK expressing cells need to be in contact with the non-transduced cells for this BE to occur (Freeman *et al.,* 1993).

1.8.2.1 Possible mechanisms

The possible mechanisms of CIBE are poorly understood due to limited evidence of CIBE in literature. However, some researchers have implicated conditioned medium (CM) containing soluble factors such as EVs released by the treated cells, and ROS in addition to direct cell contact in the mechanism of CIBE. Cells, in direct contact with each other, can also communicate via gap junctions (Dickey *et al.,* 2011; Sokolov and Neumann, 2018).
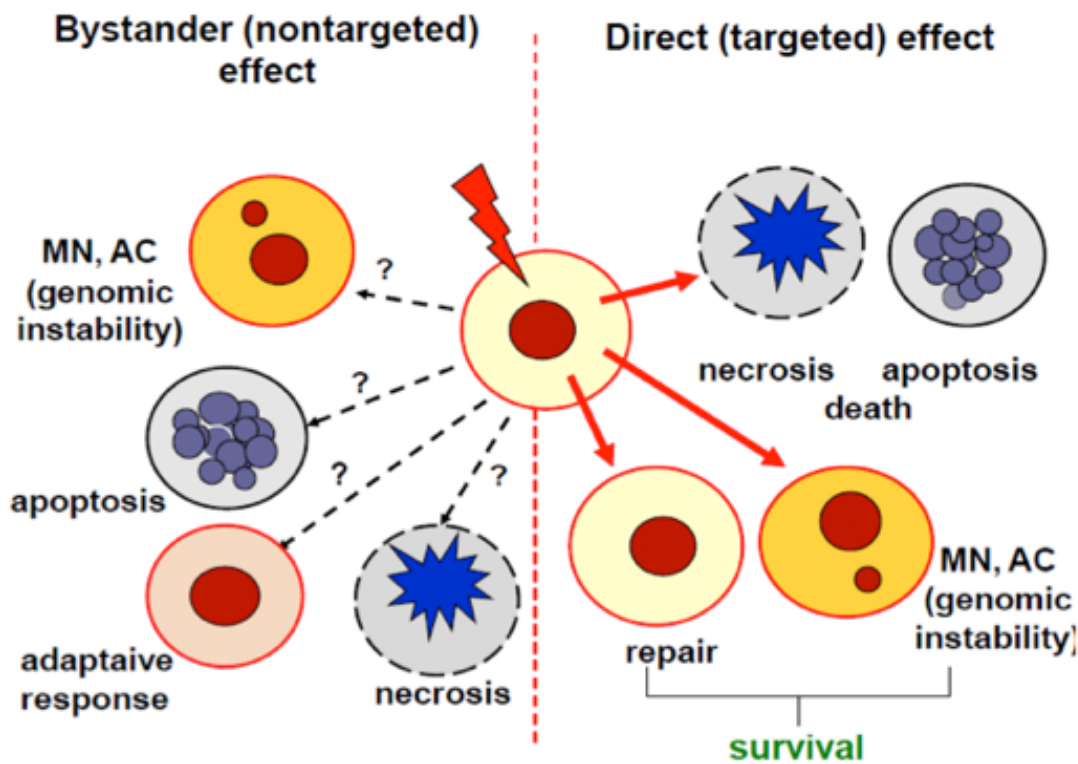
Figure 1.11 Cell-damaging effects in cells exposed and unexposed to therapy. Treatment of cells with radiation and/or chemicals induces different effects such as micronuclei (MN) formation, apoptosis, necrosis and genomic instability. These same effects can also be induced in non-targeted cells in close proximity or far from these treated cells via secretion and release of alterative signals from the treated cells, which are internalised by the untreated cells. AC; chromosomal aberrations. Adapted from Widel (2012).

There is evidence that cells treated with alkylating agents can transfer DNA-damaging effects of these drugs to their untreated neighbours via gap junctions. Cisplatin conferred BE in bystander embryonic fibroblasts by direct cell contact via gap junctions (Jensen and Glazer, 2004; Peterson-Roth *et al.,* 2009). This agrees with the results of Arora *et al.,* (2018), which revealed that bystander lung and ovarian cells also receive cisplatin-induced BE via gap junctions. These suggest that the sensitivity of bystander cells to cisplatin is potentiated via the gap junctions. Mitomycin C (MMC) also induced BE in unexposed bystander cells via gap junctions (Rugo *et al.,* 2005).

Nevertheless, alkylating agents can also induce CIBE via CM, hence it seems that these BE triggered by alkylating agents is dependent on the type of cell used and may involve more than one mechanism. This is in line with the findings of Kumari *et al.,* (2009), which revealed that MMC induced BE in hepatoma cells via CM, but not in cervical cancer cells. In support of these findings, MMC also failed to induce bystander killing in cervical cancer cells following CM transfer and co-culture experiments with macrophages due to proteasomal degradation in the cancer cells (Singh *et al.,* 2015). However, bystander cell death was achieved when these cells were pre-treated with MG132 to inhibit these proteasomes. Furthermore, MMC and phleomycin, caused BE in human B lymphoblastoid cells via release of soluble factors in the CM (Asur *et al.,* 2009).

In addition, chloroethylnitrosourea agents such as fotemustine and cystemustine, unlike carmustine, induced BE in tumour cells via CM containing proteins (Demidem *et al.,* 2006; Merle *et al.,* 2008). This conferred protection to the cells against chemotherapy via growth inhibition and alterations in glutathione. This may explain why carmustine causes TRM. Doxorubicin, an anthracyline antibiotic that also targets topoisomerase enzyme, can also cause BE via CM, however this effect may be dependent on cell type. The work of Di *et al.,* (2008) revealed that doxorubicin, sold as Adriamycin, induced BE in naïve breast cancer cells, but not in naïve colon cancer cells, via CM. Chinese hamster V79 cells treated with another antibiotic, actinomycin D, also relayed treatment signals, via CM containing soluble factors, to the untreated cells (Jin *et al.,* 2011).

However, paclitaxel and vincristine, unlike doxorubicin and 5-fluoracucil, increased the release of ROS thereby inducing BE in breast, lung and leukaemia cells in a co-culture model (Alexandre

et al., 2007). The discrepancy in the ability of doxorubicin to induce BE in breast cancer cells may be due to differences in experimental models and endpoints, chosen by the researchers, to evidence CIBE in these cells. Furthermore, bleomycin and neocarzinostatin induced BE via generation of ROS in lung adenocarcinoma cells, PB lymphocytes and human BMSCs that were grown in co-culture (Chinnadurai *et al.,* 2011). The ability of bleomycin to potentiate BE was further supported by the findings of Chinnadurai *et al.,* (2013), which revealed that this drug could induce BE in lung adenocarcinoma cells grown both in 2D and 3D co-cultures.

Chemotherapy-treated cells can also release EVs into the CM following treatment, which have the ability to trigger phenotypic changes in naïve recipient cells when engulfed by these cells. Ovarian cells, when treated with cisplatin, released EVs that caused BE in non-treated cells (Samuel *et al.,* 2017). This collaborates with the reports of Lin *et al.,* (2017), in which etoposide-treated prostate cancer cells released microvesicles that caused DNA damage, when taken up by bystander cells. Furthermore, MSC treated with paclitaxel released microvesicles that induced growth inhibition in human pancreatic cells (Pascucci *et al.,* 2014).

Regardless of the mechanism of CIBE, the biological endpoints from these studies include cell death or inhibition of cell growth, chromosomal aberrations, DNA damage, MN formation and drug resistance. However, these effects could be delayed thereby inducing genomic instability in the progeny of bystander cells. Bleomycin-induced effect in bystander lung adenocarcinoma cells persisted at delayed times following co-culture (Chinnadurai *et al.,* 2013). This is in line with the reports of Gorman *et al.,* (2009), which showed that the bystander cells had a reduction in telomere length and an increase in bridge formations following exposure to medium from tumour treated with a combination of folinic acid, oxaliplatin and fluorouracil.

1.9 MicroRNAs in response to bystander effects

MiRNAs are single stranded non-coding RNAs that are approximately 19-22 nucleotides in length that repress mRNA translation or inhibit gene expression at the post-transcriptional level by binding to the 3'-untranslated region of specific target mRNAs. These miRNAs are produced in the nucleus and cytoplasm where they undergo successive enzymatic cleavage by RNA

polymerase II, DROSHA and DICER1 from primary transcripts through hairpin precursors miRNA to mature miRNA before integration into the RNA-inducing silencing complex (Gordon *et al.,* 2013). Due to their ability to modulate gene expression, miRNAs play significant roles in the regulation of haematopoiesis by targeting various genes and transcription factors involved in cell proliferation, differentiation and apoptosis (Cammarata *et al.,* 2010).

However, aberrant miRNA expression is also associated with pathogenesis of various diseases, including leukaemia. The linkage between aberrant miRNA expression and leukaemia was first reported in CLL (Cammarata *et al.,* 2010). These miRNAs may act as oncogenes or tumour suppressors. Upregulation of oncogene miRNAs and downregulation of tumour suppressor miRNAs support leukemogenesis (Gordon *et al.,* 2013).

1.9.1 MicroRNAs and extracellular vesicles

Recently, miRNAs have attracted much attention in cell communication and bystander studies. These small RNA molecules were first discovered in *Caenorhabditis elegans* by Lee *et al.,* in 1993 but have since been confirmed to be present in mammals and plants. There are 1917 mature human miRNA sequences in the miRNA registry (miRBase ver. 22;12). However, miRNAs may also circulate in extracellular compartments, including blood (serum/plasma), saliva, milk and urine (Chen *et al.,* 2012).

These extracellular miRNAs are stable, with sufficient integrity, despite high extracellular ribonuclease (RNase) activity, hence suggesting that these extracellular miRNAs are protected from RNAse degradation in some way (Chen *et al.,* 2008). The extracellular miRNAs also remained stable when exposed to different temperatures, pH or freeze-thaw cycles. To explain this phenomenon, it was suggested that these extracellular miRNAs are enclosed in lipid-bilayered vesicles called EVs. This was further supported by the findings of Ge *et al.,* (2014), which revealed that plasma miRNAs enclosed in EVs remained stable at different temperatures and different storage times. These EV miRNAs act as secreted molecules capable of travelling between neighbouring cells to alter the recipient cell's phenotype thus influencing various biological processes (Katsuda *et al.,* 2014).

1.9.2 Extracellular vesicles and cell-to-cell communication

EVs are lipid bilayered membrane vesicles that are naturally released by cells. EVs are grouped into exosomes (≤ 200 nm), microvesicles (≥ 200 nm and ≤ 1000 nm) and apoptotic bodies based on their size, intercellular origin and release mechanisms (Figure 1.10). Exosomes originate from endosomes, formed from inward budding of the plasma membrane into the cytoplasm to form multivesicular bodies (MVB), and are released into the extracellular milieu via the fusion of the MVB with the plasma membrane (Wilms *et al.,* 2014). Microvesicles are derived from plasma membrane and released into the extracellular space by outward budding of the plasma membrane (Wilms *et al.,* 2014). Other sub-types of EVs have also been mentioned in literature such as exomeres, large oncosomes and enveloped viruses (Lou *et al.,* 2017; Zhang *et al.,* 2018). Due to this heterogeneity, detection and classification of these EVs is challenging. Although most researchers use 'exosomes' to describe EVs, EVs will be referred to as small extracellular vesicles (sEVs) within this study. This is in line with the guidelines from the International Society for Extracellular Vesicles (ISEV) for characterising EVs (Thèry *et al*., 2018).

sEVs are produced by different cell types and have different fates and functions. Their function is determinant on cell-to-cell communication via transport of their cargo of proteins, lipids and nucleic acids to recipient cells (Figure 1.11). Recipient cells internalise sEVs by either clathrin-dependent endocytosis or clathrin-independent pathways, such as phagocytosis, macropinocytosis, caveolin-mediated uptake or lipid raft-mediated internalization (Mulcahy *et al.,* 2014; Durak-Kozica *et al.,* 2018). This illustrates that sEVs may gain entry into a cell via different routes.

However, reports by Horibe *et al.,* (2018) revealed that recipient cells take up sEVs via different mechanisms that depend on the recipient cells. sEVs uptake by breast cancer cells (BT-549) was inhibited following the disruption of exosomal lipid rafts whilst annexin involved in cell adhesion and growth were shown to play a role (Koumangoye *et al.,* 2011). Furthermore, proteinase K treatment inhibited sEVs uptake by ovarian cancer cells whilst glycoproteins containing sialic acids were found on the surface of sEVs (Escrevente *et al.,* 2011). These suggest that the uptake mechanism used by sEVs may be determined by factors, such as the surface proteins,

glycolipoproteins and glycoproteins found on both sEVs and recipient cells. However, the mechanism of exosome internalisation remains poorly understood. Following internalization, sEVs may fuse with endosomes and become transcytosed, or mature into lysosomes and become degraded (Zhang *et al.,* 2015). However, EVs can also have an effect on bystander cells without uptake or release of their cargo. A recent study by Salimu *et al.,* (2017) revealed that EVs derived from prostate cancer cells reduced T cells' response and induced immunosuppression without cellular uptake or transfer of their cargo.
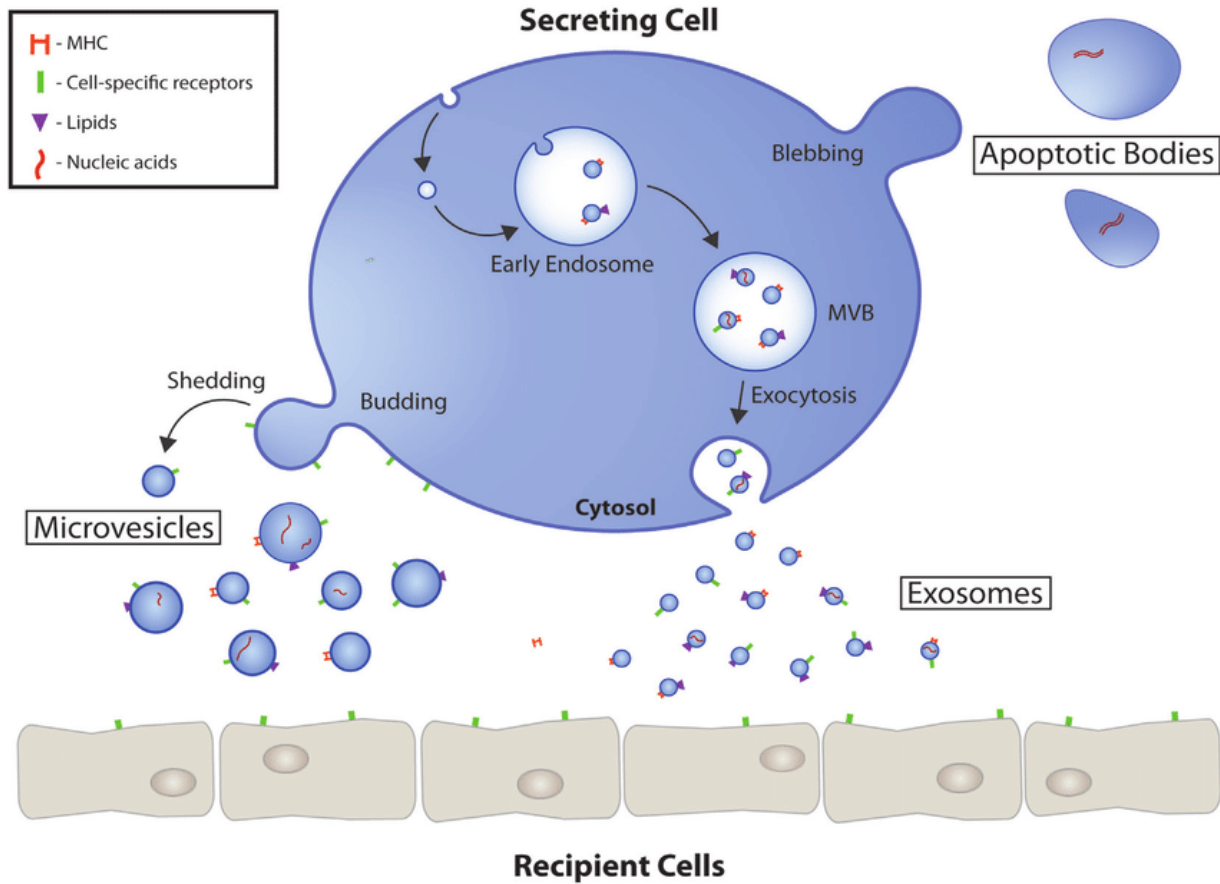
Figure 1.12 Biogenesis and secretion of extracellular vesicles (EVs). Eukaryotic cells release three different types of EVs. First, microvesicles are shed via outward budding of the plasma membrane, which is engineered by redistribution of phospholipids and contraction of cytoskeletal proteins. Secondly, exosomes arise as intraluminal vesicles by inward budding of endosomal membrane to form multivesicular bodies (MVB). MVB fuse with plasma membrane to release their contents into the extracellular milieu. Thirdly, apoptotic bodies are the largest and formed during programmed cell death or apoptosis mediated by membrane blebbing. These EVs have characteristic markers such as proteins, lipids and nucleic acid. This figure is credited to Gustafson *et al.,* (2017) with permitted usage under the creative common license.
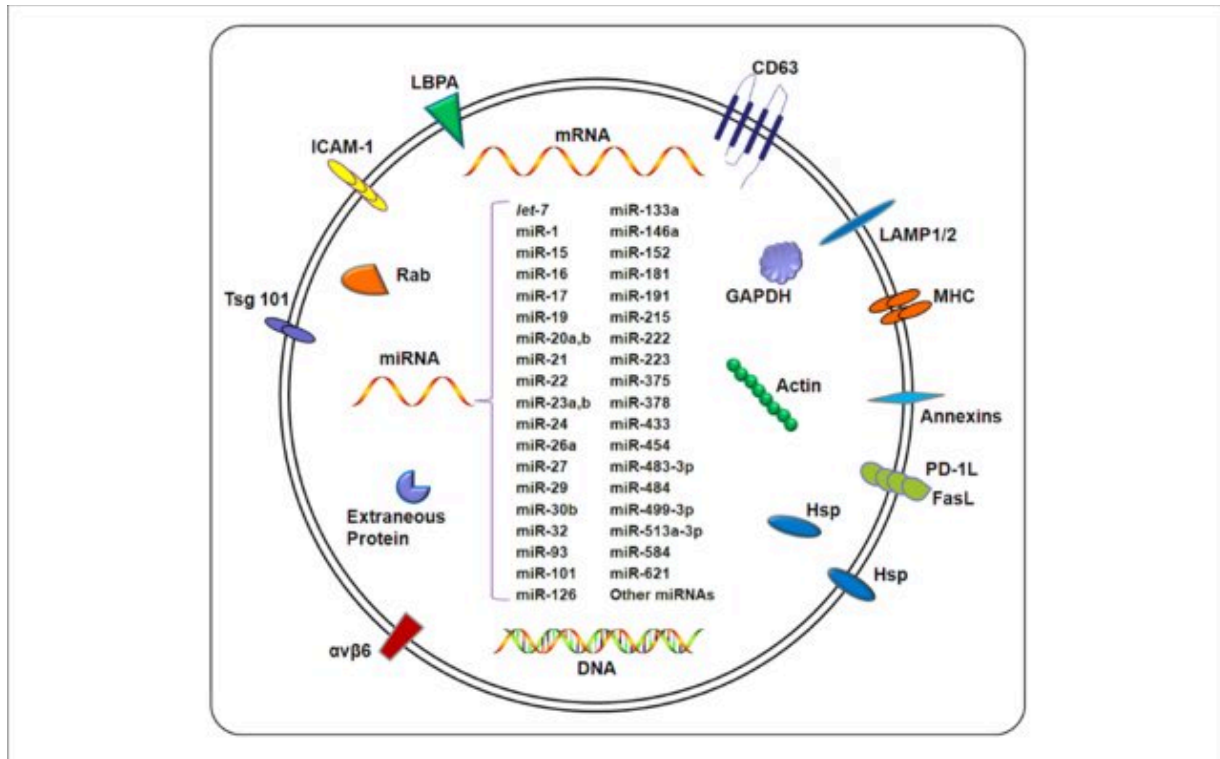
Figure 1.13 The composition of small extracellular vesicles. sEVs carry a wide array of membrane-bound and cytosolic molecular content including DNA, mRNA, miRNA and proteins. This figure is credited to Hu *et al.,* (2012) with permitted usage under the creative common license.

1.9.3 Evidence of EV-microRNAs in bystander effect

In 2007, Varadi *et al.* published the first reported evidence of miRNA transfer between cells via exosomes (cited in Zhang *et al.,* 2015). Since then, there has been a number of publications with similar observations (Kosaka *et al.,* 2010; Kogure *et al.,* 2011; Montecalvo *et al.,* 2012). Once transported, EV-derived miRNAs play different functions, such as characteristic changes in the expression levels of target genes and phenotypic changes in the recipient cell. These functions may depend on the nature of the secreting and recipient cells (Figure 1.12). Cellular stress conditions have been reported to reflect in the RNA content of cell-derived EVs (de Jong *et al.,* 2012).

Exosomes derived from cisplatin-treated A549 lung cancer cells were found to contain miRNAs and mRNA, and conferred chemo-resistance to cisplatin when added to untreated A549 cells (Xiao *et al.,* 2014). This was further supported by the work of Pink *et al.,* (2015), which showed

that exosomes isolated from cisplatin-resistant ovarian cancer cell line, CP70, increased resistance to cisplatin in another ovarian cancer cell line, A2780, however this was independent of miRNAs. Furthermore, exosomal miR-96 from H1299 lung cancer cell line also increased resistance to cisplatin in bystander cells via interaction with LIM-domain only protein 7 (Wu *et al.,* 2017). However, exosomes from A2780 treated with curcumin mediated transfer of miR-214 thus leading to an increase in cisplatin-sensitivity (Zhang *et al.,* 2017). These suggest that curcumin abrogates this chemo-resistance and modulates expression of miRNAs capable of conferring chemo-sensitivity in cells.
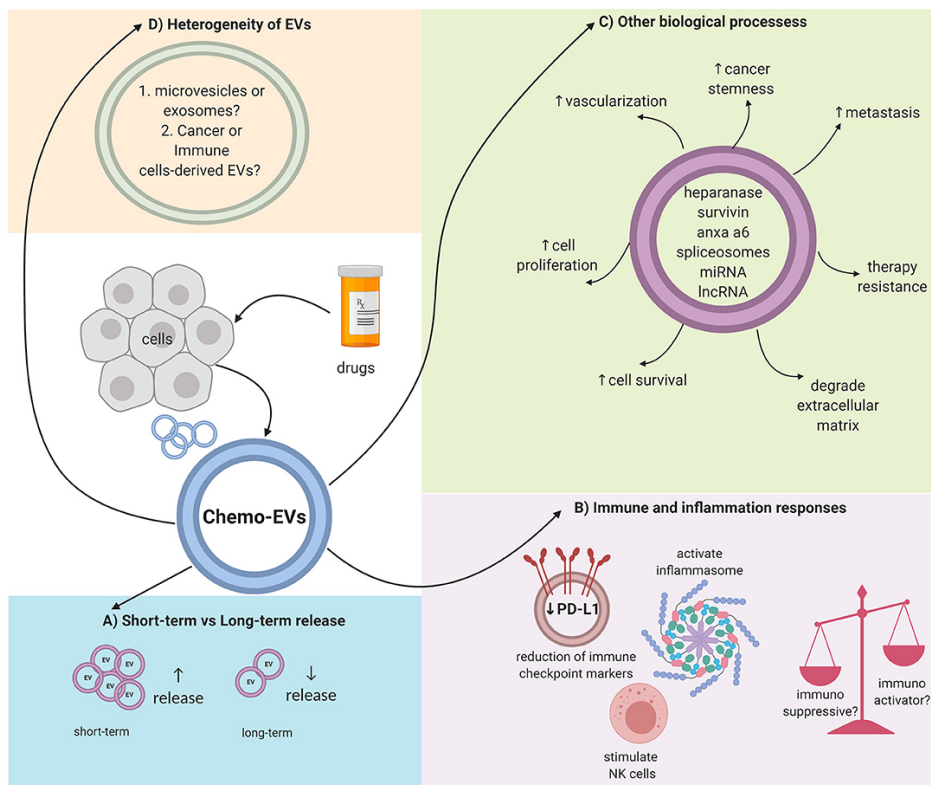
Figure 1.14 Possible effects of chemotherapy-induced extracellular vesicles (EVs). **(A)** The amount of EVs secreted by cells following treatment with chemotherapeutic drugs could depend on the time it takes for the drugs to be absorbed. **(B)** These chemo-EVs could modulate the immune system but whether they lead to immune-suppression or immune-activation remains to be fully investigated. **(C)** Depending on the type and nature of the secreting cell, chemo-EVs may affect different biological processes such as proliferation and cell viability through transport of its cargoes. **(D)** Chemo-EVs could be heterogeneous thereby making it hard to fully understand the role of these chemo-EVs. This figure is credited to Razak *et al.,* (2019) with permitted usage under the creative common license.

Furthermore, chemotherapeutic agents used in the treatment of breast cancer have also been shown to mediate CIBE and modulate gene expression via transfer of exosomal miRNAs. Docetaxel resistance was transported via exosomal miRNA, breast cancer cells to GFP-S cells, which stimulated the alteration of gene expression in GFP-S cells and enhanced the resistance of the cells to docetaxel (Chen *et al.,* 2014). MCF-7 breast cancer cells resistant to tamoxifen relayed BE signals via transfer of exosomal miR-221/222 thereby conferring resistance to tamoxifen in recipient cells by altering the expression of P27 and ERα in these cells (Wei *et al.,* 2014).

Interestingly, MSC can also mediate BE in the BM microenvironment. MSC-derived exosomes conferred sensitivity to temozolomide, an alkylating agent, in glioblastoma cells via transfer of anti-miR-9 thus increasing cell death and caspase activity (Munoz *et al.,* 2013). Furthermore, the expression of vascular endothelial growth factor (VEGF), a potent angiogenic factor, was found to be downregulated in mouse breast cancer line (4TI) both *in vitro* and *in vivo* following internalization of MSC-derived exosomes that contained miR-16 (*Lee et al.,* 2013). Additionally, increased proliferation and metastasis was reported in MCF-7 breast cancer cells following treatment with serum-derived MSC-exosomal miR-21 and miR-34a (Vallabhaneni *et al.,* 2014). Collectively, these suggest a dichotomy in the BE-mediated by MSC-derived EVs within the tumour microenvironment and this may be dependent on the miRNA(s) in the EVs cargo.

Cancer cells may also transfer oncogenic phenotypes to bystander cells via EV-derived miRNAs. Human umbilical vein endothelial cells (HUVEC) internalised K562 leukaemic cells-derived exosomal miR-92a, which triggered an increase in cell migration and tube formation via reduced expression of integrin α5 (Umezu *et al.,* 2012). Exosomes isolated from *MYCN*-amplified neuroblastoma cell lines contained oncogenic miRNAs, which were internalised by recipient cells thus diminishing cell growth (Haug *et al.,* 2015).

Furthermore, EVs can also directly export or sequester anti-cancer drugs. Several reports have shown that chemotherapeutic drugs such as paclitaxel could be loaded onto MSC-derived EVs as well as macrophages-derived EVs and then exported or sequestered to elicit bystander effects in cancer cells (Pessina *et al.,* 2013; Pascucci *et al.,* 2014; Kim *et al.,* 2016). Similar results have also been reported for cancer cells-derived EVs following exposure to chemotherapeutic agents such

as etoposide, mitoxantrone, cisplatin, mitomycin, paclitaxel, doxorubicin, irinotecan, gemcitabine, methotrexate and topotecan (Ifergan *et al.,* 2005; Safaei *et al.,* 2005; Chapuy *et al.,* 2008; Goler-Baron and Assaraf, 2011; Lv *et al.,* 2012; Federici *et al.,* 2014; Aubertin *et al.,* 2016; Koch *et al.,* 2016; Muralidharan-Chari *et al.,* 2016; Goh *et al.,* 2017).

Based on this premise, it is reasonable to acknowledge that CIBE has been established however, the potential mechanism(s) by which this happens remains to be fully elucidated and forms the basis of this research. As new drugs are introduced, at a fast pace, into the market, this poses great clinical implication for improved cancer therapy. Therefore, better understanding of the mechanism of DCL aetiology will help improve patient outcome. Since donor-derived haematopoiesis is supported and maintained by host-derived stromal microenvironment following allogeneic-HSCT through intercellular communication, it is likely that MSC also transfer 'damage' to incoming cells from the donor in the BM microenvironment.

1.10 Hypothesis

Using DCL as the clinical pivot, this research hypothesises that miRNA transferred via EVs are involved in CIBE in the BM microenvironment and can induce toxicity in HSC following exposure of MSC to pre-transplant chemotherapy. Monitoring the secretome of cells and content of MSC-derived EVs following exposure to chemotherapy may identify molecular changes that may have a functional effect in HSCT recipients that could potentially be used to indicate and detect DCL development.

1.11 Aims and Objectives

Since chemotherapy agents have been shown to be able to induce bystander effect from MSCs and EVs released by MSC are known to play an important role as message delivery vehicles, this project aimed:

1. **To develop a co-culture model that will enable the confirmation of CIBE following treatment with alkylating agents and topoisomerase inhibitors**

- Culture conditions of the chosen cell lines, HS-5 and TK6, were optimised to ensure optimum growth of these cells throughout the experiments.
- Optimisation include morphology, cell viability assessments as well as other minimal criteria proposed by the International Society for Cellular Therapy (ISCT) to define MSC *in vitro.*

2. **To evaluate the ability of the chosen alkylating agents and topoisomerase inhibitors to induce CIBE**

   - HS-5 cells were treated with two alkylating agents and two topoisomerase inhibitors for 1 hour and 24 hours to ascertain the ability of these drugs to induce stromal damage.
   - HS-5 cells were treated with these drugs for 24 hours, washed off afterwards and co-cultured, in fresh culture medium, with TK6 cells. CIBE was evaluated by cell viability and genotoxicity in the bystander cells
   - The chosen drugs were chlorambucil and carmustine (alkylating agents) and topoisomerase inhibitors (etoposide and mitoxantrone), which have been implicated in the development of TRM.

3. **To explore the duration of CIBE**

   - HS-5 cells were treated, as above, and conditioned medium harvested after 24 hours. HS-5 conditioned medium was then used to co-culture TK6 over a period of 5 days (duration that is safe for a transplant) with replacement of conditioned medium each day.
   - CIBE was evaluated and determined by cell viability in bystander cells.
   - HS-5 cells were treated with ranging doses of these drugs to determine if the dosage has an effect on the bystander effect.

4. **To evaluate the role of miRNAs and EVs as a mode of action for CIBE**

   - **MiRNAs** – Changes in miRNA expression due to drug exposure were compared between treated HS-5 cells and untreated HS-5 cells using kits available from Qiagen.
   - Changes in miRNA expression were also compared between TK-6 exposed to treated HS-5 cells and TK6 cells exposed to untreated HS-5 cells following co-culture.

- MiRNA expression profiles in HS-5 conditioned medium and serum used in cell culture was also be explored.

- **EVs** - HS-5 cells were found to release EVs hence these EVs were isolated and characterised by electron microscopy and nanoparticle tracking analysis.

- HS-5 cells-derived EVs were co-cultured with TK6 cells to show the internalisation of the EVs by these cells using fluorescent labelling.

- HS-5 cells-derived EVs were also co-cultured with TK6 cells and bystander effects were determined by cell viability and genotoxicity assays.

- Trafficking of these miRNAs in EVs from HS-5 cells to bystander TK6 cells by qRT-PCR was also explored.

2.0 Materials and Methods

All reagents that were used in this research work were purchased from Sigma Aldrich, UK except where otherwise stated.

2.1 Samples

Two human cell lines were chosen to mimic what happens in the BM microenvironment where MSC and HSC in the stroma interact to promote haematopoiesis.

2.1.1 Stromal cell line

HS-5, a human stromal cell line, was purchased from American Type Culture Collection (ATCC through LGC standards, UK). HS-5 is an adherent human (male) fibroblast cell line that was derived from long-term BM culture transformed with amphotrophic retrovirus vector (Roecklein and Torok-Storb, 1995; Torok-Storb *et al.*, 1999). HS-5 cells secrete cytokines, miRNAs, macrophage colony stimulating factor (M-CSF), granulocyte colony stimulating factor (G-CSF) and stem cell factor (SCF; kit ligand), which play a key role in its support for proliferation of progenitor cells (Roecklein and Torok-Storb, 1995; Torok-Storb *et al.,* 1999; Graf *et al.,* 2002; Balakrishnan *et al.,* 2014).

2.1.2 Lymphoblast cell line

TK6, human B-lymphoblastoid suspension cells were supplied by Professor Ann Doherty (AstraZeneca, Cambridge UK). These cells were derived from the spleen from a patient with hereditary spherocytic anaemia (Xu *et al.,* 2017). TK6 possess a number of characteristics, which make them suitable for genetic toxicology studies such as functional p53 protein, heterozygosity at the TK locus, stable genome and stable mutation frequencies (Zhang *et al.,* 1995; Xu *et al.,* 2017).

2.2 Chemotherapeutic agents

Two chemotherapeutic agents were chosen from each of the two drug groups, alkylating agents and topoisomerase inhibitors, which are linked to TRM. For alkylating agents, chlorambucil (CHL; 10 µM, 20 µM, 40 µM) and carmustine (CAR; 1 µg/µl, 5 µg/µl, 10 µg/µl) were used whilst etoposide (ETO; 1 µM, 5 µM, 10 µM) and mitoxantrone (MTX; 100 ng/µl, 250 ng/µl, 500 ng/µl) (both Stratech Scientific, UK) were the topoisomerase inhiitors used. The top dose for each drug is a clinically relevant dose. Stock solutions of all drugs were made in 100% ethanol except etoposide, whose stock was prepared in chloroform/methanol (1:1). All drugs were further diluted in isotonic phosphate buffer saline (PBS), to 100x the final dose concentrations. The dosage range corresponds to the clinically relevant plasma serum concentrations measured in patients receiving these drugs (table 2.1). The levels used correspond to the conditioning doses for these drugs and patient's plasma levels in a HSCT setting. These concentrations were selected in order to determine the maximal tolerable dose relevant to the patient's plasma levels where HS-5 cells were capable of inducing a bystander effect.

Table 2.1: Plasma concentrations of chemotherapeutic agents. Peak plasma concentrations of these agents obtained from literature was used to determine the concentrations used in the present study.

Drugs	Solubility	Plasma Concentration (this study)	Clinical dose	References
Chlorambucil	Ethanol (100%)	40 µM	0.6 mg/kg 0.2 mg/kg (oral)	Hong *et al.,* (2010)
Carmustine	Ethanol (100%)	10 µg/ml	300-750 mg/m^2	Henner *et al.,* (1986)
Etoposide	Ethanol/Chloroform (1:1)	10 µM	100 mg/m^2 (oral)	Clark *et al.,* (1994); Millward *et al.,* (1995)
Mitoxantrone	Ethanol (100%)	500 ng/ml	12 mg/m^2 (IV)	Smyth *et al.,* (1986); van Belle *et al.,* (1986)

2.3 Cell culture

2.3.1 HS-5 stromal cells

HS-5 were cultured in high glucose Dulbecco's Modified Eagles medium (DMEM-HG) supplemented with 10% heat-inactivated foetal bovine serum (FBS), L-glutamine (2 mM), penicillin (100 U/ml) and streptomycin (100 µg/ml) at 37°C in a humidified atmospheric 5% CO_2 air (Heracell CO_2 incubator; Thermofisher Scientific, UK). However, for study of sEVs, HS-5 cells were maintained in a similar fashion with slight modification; exosome-depleted FBS (Systems Biosciences, US) was used instead of heat inactivated FBS. Cells were grown in a 75cm^2 vent cap Corning cell culture flask (Fisher Scientific, UK) by changing the medium every 2-3 days until cells were in log growth phase (concentration of 1 x 10^6 cells). Subsequently, cells were trypsinized (see section 2.5), counted manually by trypan blue dye dilution (see section 2.10) or using the Luna FL automated cell counter (Logos Biosystems, France) and seeded in a 1:3 split at a density of 1 x 10^4 cells/cm^2. Cells in passage 3-9 were used for experiments.

2.3.2 TK6 lymphoblastoid cells

TK6 cells were cultured in RPMI 1640 medium (Gibco Invitrogen, UK) supplemented with heat inactivated FBS (10%), L-glutamine (2 mM), penicillin (100 U/ml) and streptomycin (100 µg/ml) at 37°C in a humidified atmospheric 5% CO_2 air. For sEVs studies, TK6 cells were grown in similar conditions to HS-5 in DMEM-HG supplemented with 10% exosome-depleted FBS, L-glutamine (2 mM), penicillin (100 U/ml) and streptomycin (100 µg/ml). TK6 cells were visualised under the microscope and had a medium change every 1-2 days until they reached 70-80% confluence. Cell pellets were then obtained after centrifugation at 300 g for 10 minutes (Harrier; MSE, UK) re-suspended in fresh medium and counted manually by trypan blue dye dilution or using the Luna FL automated cell counter. Cells were then sub-cultured at a density of 3 x 10^5 cells per ml.

2.4 Thawing of cryopreserved cells

Cells were transferred from liquid nitrogen to an ice box for transport between labs and then thawed in a 37°C water bath (Grant Instruments, UK) by rapid agitation. The vial was then transferred to a biohazard level 2 culture hood (Scanlaf Mars; Labogene, UK) just before the ice completely melts and quickly thawed by adding a wash medium (either RPMI 1640 or DMEM-HG supplemented with 20% FBS) in a dropwise manner to fill the vial. The content of the vial was aliquoted into a 15 ml tube and made up to the 15 ml mark using 1ml aliquots of the wash medium and subsequent mixing over a 10-minute period. HS-5 cells were spun at 230 g for 5 minutes whilst TK6 cells were spun at 300 g for 10 minutes. The washing and centrifugation process were performed quickly as possible to ensure the removal of dimethylsulphoxide (DMSO) from the cells. The supernatants were discarded and the washing process repeated before seeding the cells at the appropriate densities.

2.5 Detachment of adherent cells

HS-5 cells were sub-cultured by trypsinization after attaining 70-80% confluence, using a working solution (1X) containing 0.25% trypsin and 1 mM ethylenediaminetetraacetic acid (EDTA). The culture medium was discarded before washing the cells with 1X PBS. Depending on the surface area of the culture flask used, enough volume of 1X trypsin solution was added to the cells just to cover all the cells and incubated at 37°C. After 3-5 minutes, the culture flask was given a gentle tap to ensure detachment of the cells followed by addition of fresh complete culture medium to deactivate the trypsin effect. Cells were spun at 230 g for 5 minutes, the wash step repeated and then re-suspended in fresh medium. Cells were counted as previously mentioned and re-seeded at the appropriate density.

2.6 Cryopreservation of cells

Cryopreservation of the cell lines was done to ensure that a master stock and a large batch of working stock are preserved in a viable state for future assays at the same passage. This

eliminates the need to maintain cells in culture for a long time, the risk of mutation of cells that leads to a change in their characteristics and the risk of microbial and cross-contamination with other cell lines (Fogh, 1973; Wang *et al.,* 2013).

Both cell lines were frozen using a solution containing 65% culture medium, 25% FBS and 10% DMSO. The DMSO was added to prevent formation of ice crystals during the process; lest the cells will be destroyed. The solution was placed on ice before adding it dropwise into the cells. Cell suspensions were transferred into cryovials at a concentration of 3 x 10^6 cells per ml and 1 x 10^6 cells per ml for TK6 and HS-5 respectively. The cryovials were then placed into a cryovial-holding chamber ('Mr Frosty'), which contains isopropanol and enables gradual freezing at a rate of approximately 1°C per minute, and placed in a -80°C ultra low temperature freezer (New Brunswick Scientific, UK) for 2-3 hours. Afterwards, the cells were transferred to vapour phase liquid nitrogen.

2.7 <u>CFU-F assay</u>

The colony forming capacity of HS-5 cells as MSC was determined and compared in five culture media: DMEM-HG, low glucose DMEM, DMEM-F12 Ham, RPMI 1640 and Iscove's Modified Dulbecco's medium (IMDM) (Gibco Invitrogen, Paisley, UK). All media were supplemented with 10% heat inactivated FBS, 2 mM L-glutamine, penicillin (100 U/ml) and streptomycin (100 µg/ml). Cells were seeded at 10 cells/cm^2, 20 cells/cm^2, 30 cells/cm^2 and 50 cells/cm^2 into a 6-well plate containing 2 ml of medium in a humidified culture chamber with a 5% CO_2 atmosphere. The cells were incubated at 37°C for 14 days, changing the culture medium every 2-3 days. After 14 days, the cells were washed with PBS and colonies were fixed with methanol for 5 minutes. Subsequently, crystal violet solution (0.5%) was used to stain the cells at room temperature (RT) for 10 minutes and later washed thrice with distilled water to remove excess dye. The colonies, which were defined as a group of more than 20 cells, were counted manually by light microscopy using the NIKON Eclipse TE 300 inverted microscope.

2.8 Cell proliferation assay

To determine the optimum medium for the co-culture model, HS-5 cells were seeded at 10,000 cells per cm^2 in three culture media: DMEM-HG, RPMI 1640 and IMDM, in 25cm^2 vent cap Corning cell culture flasks (Fisher Scientific, UK). After approximately 120 hours, the cells looked confluent under the microscope and were trypsinized, centrifuged at 230 g for 5 minutes, harvested and counted as described earlier. In contrast, TK6 cells were seeded at 2.5 x 10^4 cells/ml in three culture media: DMEM-HG supplemented with heat-inactivated FBS or sEVs-depleted FBS, and RPMI 1640, in 25cm^2 vent cap Corning cell culture flasks for 72 hours. Afterwards, cells were centrifuged at 230 g for 5 minutes, harvested and counted as described earlier. For sEVs studies, HS-5 cells were seeded at 10,000 cells per cm^2 respectively in DMEM-HG with sEVs-depleted FBS, DMEM-HG with heat-inactivated FBS and RPMI 1640; in 25cm^2 vent cap Corning cell culture flasks and maintained for 42 hours. As mentioned earlier, cells were then harvested and counted.

2.9 Drug sensitivity measurement

Before drug treatment, HS-5 cells (at 70-80% confluence) were seeded in a 12-well plate at a density of 132,000 cells per cm^2 in 500 µl DMEM-HG (HS-5 complete medium). Cells were allowed to attach overnight at 37°C, treated with increasing doses of the drugs and incubated for 1 hour and 24 hours respectively. Afterwards, cells were washed three times with PBS to remove the drugs and fresh medium added to the wells. Cells were returned to the incubator for a period equivalent to one doubling time (42 hours) for normally dividing HS-5 cells. The percentage of surviving cells relative to untreated controls was determined immediately after drug treatment and 72 hours later to determine the recovery ability of HS-5 following chemotherapy based on the previous work of (Li *et al.,* 2004). Morphology of the cells was observed by light microscopy using the ZEISS Primovert inverted microscope for the duration of the experiment.

2.10 Cell viability assay

2.10.1 Trypan blue exclusion dye assay

This dye exclusion test detects viable cells present in a cell suspension. It is based on the principle that dead cells absorb trypan blue dye due to loss of cell membrane selectivity whereas viable cells, which have intact cell membrane, do not (Tennant, 1964; Strober, 2001). Cell suspensions of HS-5 and TK-6 were harvested and spun at 230 g and 300 g respectively for 5 minutes. The resulting supernatant was discarded and cells re-suspended in complete culture medium. About 10 µl of the cell suspension was aliquoted into a microcentrifuge tube and mixed with an equal volume of 0.45% trypan blue. The mixture was loaded onto a Neubauer haemocytometer and the viable and non-viable cells were counted immediately by light microscopy at low magnification (X10). To calculate the number of viable cells per mL of culture, the formula below was applied.

$$(Number\ of\ viable\ cells\ counted\ \div Number\ of\ grids\ counted) \times Dilution\ factor\ \times 10,000$$

Percentage viability was calculated as: $(Number\ of\ viable\ cells\ \div Number\ of\ total\ cells)\ \times\ 100$

To validate these counts, the number of viable cells and percentage viability were determined using the Luna FL automated cell counter thus minimising possible error from manual cell count.

2.10.2 Acridine orange/propidium iodide assay

Furthermore, cell viability was also determined by acridine orange/propidium iodide (AO/PI) fluorescence assay in order to make these findings robust. It is based on the principle that AO can permeate both live and dead cells, and as such stain all nucleated cells to generate green fluorescence whilst PI stains dead nucleated cells with poor membrane integrity and generates red fluorescence. Cells stained with AO/PI solution (50 µg/ml), in a 1:10 dilution, were counted using the Luna FL automated cell counter. Protocols were set to take cognizance of the ranges of sizes of cells used in this study. The automated counter produced figures for live, dead and total cells, and percentage viability within seconds.

51

2.11 Genotoxicity assay: *in vitro* micronucleus assay

This assay detects genotoxic damage in cells that have undergone cell cycle, through the formation of MN within the cytoplasm of interphase cells. MN may be as a result of loss of either fragments of chromosome or whole chromosomes during nuclear division (Fenech, 2007).

Cell viability was determined in both treated and control cells by trypan blue exclusion or AO/PI assay to ensure that there were enough viable cells (50% viability) to perform the genotoxicity assay (OECD, 2014). Cells (2 x 10^4 per slide) were aliquoted into micro-centrifuge tubes and spun at 200 g in a Micro-centaur Plus micro-centrifuge (Sanyo MSE, UK) for 5 minutes. After decanting the supernatant, the cell pellets were re-suspended in PBS (150 µl) and dispensed into Shandon cytofunnels attached onto a clean grease free microscope slide. The cells were then centrifuged at 300 g for 8 minutes using a Shandon Cytospin 4 (ThermoScientific, UK). Microscope slides were carefully removed from the centrifuge and air-dried. Slides were fixed using 90% methanol for 10 minutes, to avoid detachment of cells from the slides, and air-dried. Slides were dipped in fresh phosphate buffer (0.66% w/v potassium monobasic + 0.32% w/v sodium phosphate dibasic; pH 6.4), and stained with 24mg/200ml AO (w/v in phosphate buffer) for 45 seconds. Slides were then 'washed' twice in fresh phosphate buffer for 10 and 15 minutes respectively, air-dried and stored in the dark at RT to avoid fading.

For analysis, slides were mounted with phosphate buffer, cover slipped with a clean grease-free cover slip and viewed under the microscope (Nikon Eclipse 80i) at x40 magnification using triple band pass (standard excitation and emission wavelength range of 435-660nm for DAPI, FITC and Texas Red filters). Images were visualised with NIS Elements software and captured with a Nikon Digital Sight DSF1 camera (Nikon Instruments, Europe). Aberrant cells were identified through the distinctive properties of AO where the cytoplasm stains orange/red and nuclear material (including MN) appear green. Slides were scored for mononucleated cells (normal), binucleated and multinucleated cells with or without micronuclei, lobed cells, apoptotic and necrotic cells. 1000 cells were scored per culture and 2000 cells scored per treatment.

2.12 HS-5 and TK6 bystander co-culture

A co-culture model has been previously developed by another PhD student (Figure 2.1; Kelechi Okeke, personal communication). HS-5 cells were seeded at a density of 132,000 cells/cm^2 into a 12-well plate containing 1ml of DMEM-HG medium per well and allowed to attach overnight in an incubator at 37°C. This density was sufficient enough to ensure cells were confluent before and during the experiment due to the surface area of the well. HS-5 cells were then treated with clinically relevant doses of chlorambucil, carmustine, etoposide and mitoxantrone (see table 2.1). These treated cells were incubated at 37°C, 5% CO_2 for 24 hours respectively. Cells were washed twice to ensure removal of the drugs and 1 ml of fresh complete DMEM-HG medium was added into the wells. Culture inserts with pore size of 0.4 μm (Millipore, UK) were transferred into the wells using sterile forceps and TK6 cells (5.0 x 10^5/ml) suspended in 1ml of complete medium aliquoted within the culture insert. Cells were allowed to co-culture at 37°C and 5% CO_2 for 24 hours before TK6 cells were harvested, viability assessed and adequate density aliquoted for the MN assay. TK6 cells served as bystander cells in all experiments.
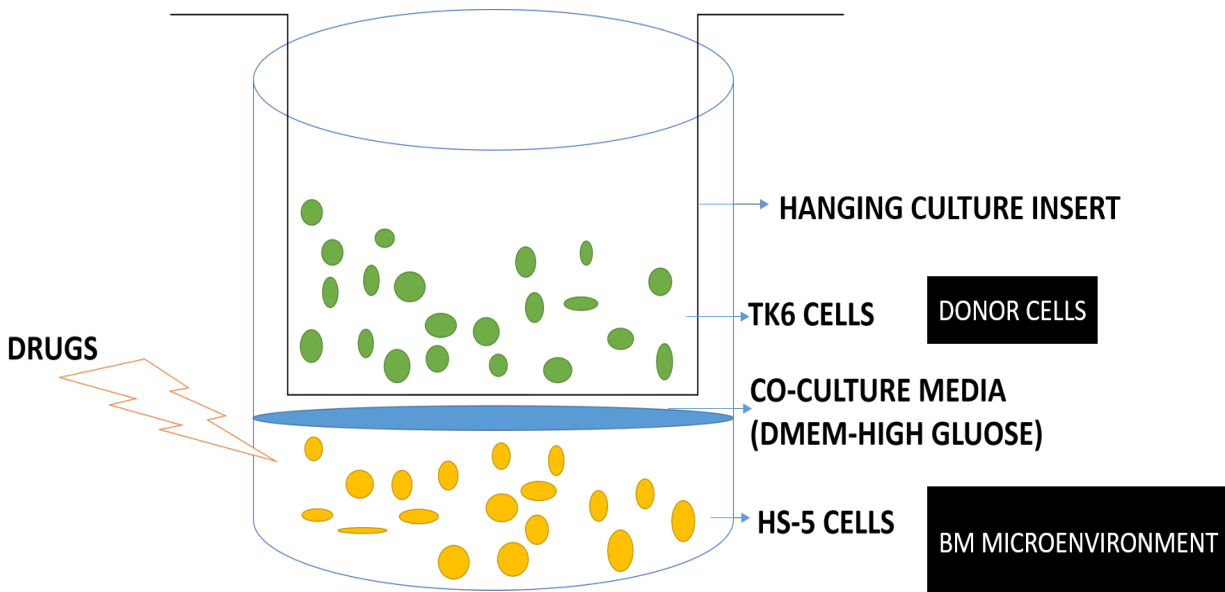
 Figure 2.1 Representation of the co-culture model to determine bystander effect. HS-5 cells were exposed for 1 or 24 hours to drugs, then washed free of drug treatment, followed by addition of TK6 (bystander cells) into the well via a culture insert. Both cell lines were suspended in DMEM-HG medium and incubated at 37^{0}C at 5% CO_2 for 24 hours before assessing the viability and genotoxicity of bystander cells.

2.13 Evaluation of the duration of bystander effect

2.13.1 Collection of conditioned medium

As previously mentioned in section 2.12, HS-5 cells were treated with clinically relevant doses of carmustine, chlorambucil, etoposide and mitoxantrone for 24 hours, washed free of drug and added fresh medium. After 24 hours, CM was collected and centrifuged sequentially for 5 minutes at 1000 g and 10 minutes at 3000 g using Beckman Allegra X-22R centrifuge with SX 4250 rotor (Beckman Instruments, USA) to remove cell debris. The CM was collected and filtered using 0.22 μm filter (Merck Millipore, UK) to remove contaminating apoptotic bodies and cell debris, and stored at -20°C until needed. This was repeated for a period of five days; collecting CM every 24 hours for the duration of the experiment.

2.13.2 Co-culture of TK6 cells with conditioned medium

This was done to ascertain if HS-5 cells release soluble factors into the culture medium following drug treatment, which are capable of mediating a bystander effect in nearby cells, and to determine how long this bystander effect persists in the nearby cells. CM obtained as aforementioned, was used to seed TK6 cells (5 x 10^5 cells/ml) in a 12 well plate and co-cultured over a period of five days. The filtered CM was used to seed a new batch of TK6 cells. This was repeated every 24 hours over a period of five days. The number of viable cells and percentage viability of the cells were assessed every day using the Luna FL automated cell counter.

2.14 Small extracellular vesicles in bystander effect

2.14.1 Transmission electron microscopy (TEM)

HS-5 (1x10^6) cells were treated with clinically relevant doses of carmustine (10 μg/ml), chlorambucil (40 μm), etoposide (10 μm) and mitoxantrone (500 ng/ml) for 24 hours. Afterwards, cells were washed three times with PBS and then fixed in 5% glutaraldehyde (TAAB Laboratories Equipment Ltd, UK) in 0.1M sodium cacodylate (TAAB Laboratories Equipment Ltd, UK) buffer

(pH 7.43). Cells were then washed three times in 0.1M sodium cacodylate buffer and post-fixed in 0.75% osmium tetroxide (TAAB Laboratories Equipment Ltd, UK) containing 1.5% potassium ferrocyanide. The cells were enrobed in low temperature gelling agarose (0.3g in 10ml of distilled water) and gradually dehydrated in ascending concentrations (70%; 90%; 100%) of ethanol, transferred to propylene oxide (TAAB Laboratories Equipment Ltd, UK) and embedded in Taab embedding resin (TAAB Laboratories Equipment Ltd, UK). After embedding, samples were sectioned using a Reichert-Jung Ultracut E ultramicrotome. They were double stained with potassium permanganate (Agar Scientific Ltd) in 0.1M phosphate buffer pH 6.5 and Reynold's lead citrate (1963). Samples were observed using a Phillips CM10 transmission electron microscope with a Gatan Orius SC 100 charge coupled device camera (model 832) operating at 60kV.

2.15 Isolation of small extracellular vesicles

Small extracellular vesicles (sEVs) were isolated by two methods: size exclusion column chromatography (SEC; iZON Science, UK) and ExoQuick Precipitation kit (System Biosciences, US). For SEC, HS-5 cells (13,000 cells per cm^2) were seeded in triplicates in a 75cm^2 vent cap Corning cell culture flask whilst 125,000 cells per cm^2 were seeded in triplicates in a 12-well plate for ExoQuick-based extraction. Both extraction methods employed DMEM-HG medium supplemented with 10% exosome-depleted FBS and glutamine. Cells were treated with clinically relevant dose of mitoxantrone (500 ng/ml) for 24 hours, washed three times with PBS and re-seeded in fresh medium.

2.15.1 ExoQuick precipitation method

About 10ml of CM was obtained as previously described, transferred to a sterile microcentrifuge tube and mixed with 200 μl of ExoQuick TC (System Biosciences, US) and incubated at 4°C for 18-24 hours. The ExoQuick TC-CM mixture was spun at 1500 g for 30 minutes (Beckman Allegra X-22R centrifuge with SX 4250 rotor) to obtain a white pellet. The supernatant was aspirated off whilst the pellet was spun at 1500 g in a microcentaur plus microcentrifuge for 5 minutes to remove residual ExoQuick solution and then resuspended in 250 μl PBS. Microsphere beads

(System Biosciences, US), which were prepared by washing 0.2 unit of beads twice with 80 μl of PBS, were used to purify the isolated sEVs. The beads were mixed with the isolated sEVs, vortexed (Whirlimixer, Laboratory FSA Supplies, UK) for 3 minutes and placed on an Stuart SSL3 gyro-rocker at RT for 35 minutes to ensure complete mixture. The sample was sequentially centrifuged for 3 minutes at 3000 g and 5 minutes at 8000 g. The supernatant, which contains the purified sEVs, was aspirated into sterile micro-centrifuge tubes and stored at -80°C until needed for further analysis.

2.15.2 Size exclusion column chromatography

About 10ml CM obtained from HS-5 cells was concentrated to 500 μl using Amicon Ultra-15 centrifuge tubes (Merck Millipore, UK) by centrifuging them sequentially for 18 minutes at 3900 g (Beckman Allegra X-22R centrifuge with SX 4250 rotor) and 10 minutes at 10,000 g (Beckman Allegra X-30R centrifuge with F2402H rotor) to remove any precipitate that may cause problems during downstream analysis. The qEV columns (iZON Science, UK) were placed in a vertical position using a stand tube clamp (Figure 2.2) and equilibrated by rinsing the column with 10 ml of fresh filtered (0.22 μm) PBS.

The time taken for 5 ml of buffer to flow through the qEV columns was noted (started timing at 2 ml and stopped at 7 ml) in order to detect when to clean the column. The concentrated sample (500 μl) was loaded onto the columns before adding the buffer to aid its movement down the column. The resulting fractions (500 μl) were collected immediately; the first six fractions do not contain vesicles and were collected in one collection (15 ml) tube to save time and avoid measurement error of six individual tubes whilst fractions 7, 8 and 9 were collected separately for sEVs analysis.

Following collection of the vesicles, about 2 ml buffer was added above the top filter of the qEV column to collect the fraction 10, which was discarded. Fractions 7, 8, 9 were stored at -80°C until needed for further analysis. Each qEV column was used just twice before discarding them and was flushed with 10 ml of buffer in order to avoid sample contamination. The time taken for 5 ml of buffer to flow through was also noted, and then stored in 20% ethanol at 4°C.
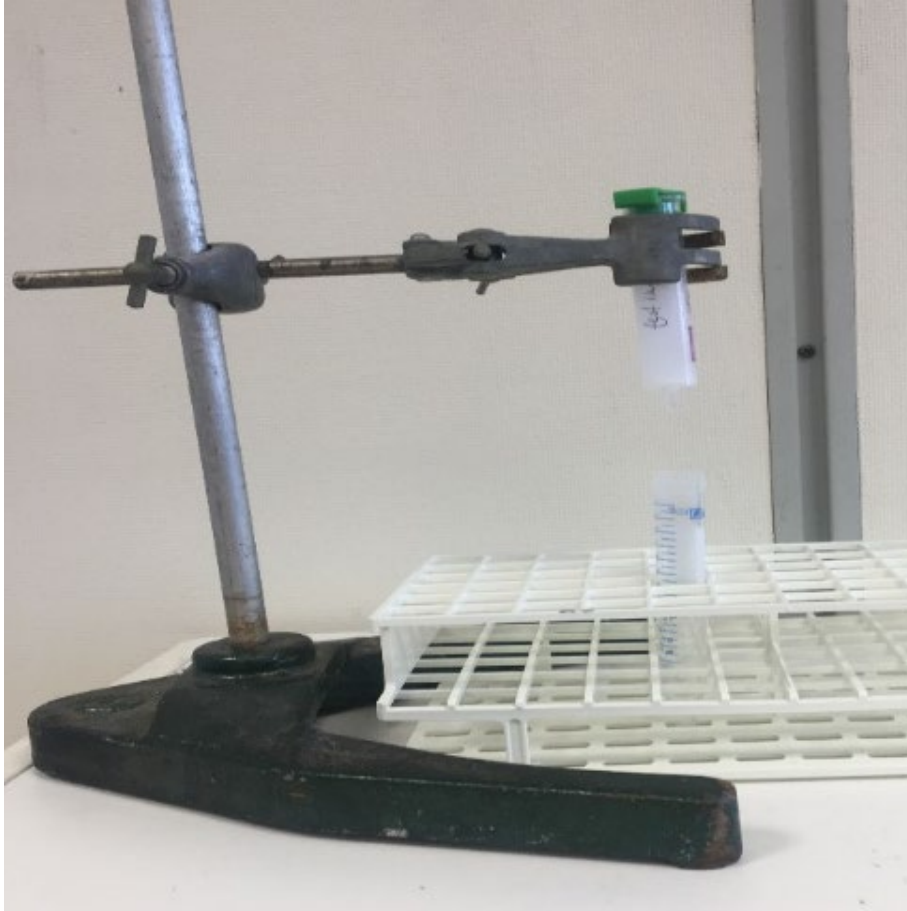
Figure 2.2 Representation of the size exclusion column chromatography model. Samples were passed through the column with the aid of filtered PBS buffer and resulting fractions were collected in 15ml tubes (for fractions 1-6) and/or 1.5ml microtubes (for fractions 7-9).

2.16 Quantification of small extracellular vesicles

There are a number of ways to identify and characterise isolated sEVs. Here, TEM, nanoparticle tracking analysis (NTA) and particle to protein estimation to determine identification and purity of the samples.

2.16.1 Transmission electron microscopy

TEM was performed based on Sohel *et al.,* (2014) with slight modifications. sEV samples (30 µl) were diluted 1:2 in freshly prepared 4% paraformaldehyde (60 µl) and incubated for 15 minutes.

sEV samples were then distributed on parafilm as 10 µl droplets. Carbon formvar coated copper 400 mesh grids (TAAB Laboratories Equipment Ltd, UK) were discharged with 0.01% alcian blue solution (TCS Biosciences Ltd, UK) or bacitracin for 30 seconds, rinsed three times in filtered (0.22 µm) ultra-pure water and dried under a lamp. Grids were then inverted over the sEV sample droplets and incubated at RT for 30 minutes. Excess water was removed by blotting with filter paper in between washes. The grids were then stained with one 20 µl droplet of 2% (w/v) aqueous uranyl acetate for 10 minutes and washed three times with droplets of filtered ultra-pure water. Excess solution was blotted with filter paper. The sample was dried under a lamp for one hour. Grids were visualised under a Phillips CM10 electron microscope with a Gatan Orius SC 100 (model 832) operating at 60kV.

2.16.2 Nanoparticle tracking analysis

The size and concentration of sEVs were measured by NTA using a NanoSight LM10 with a laser wavelength of 642 nm and the NTA 2.3 build 0033 analytical software (Malvern Instruments Ltd, UK). Samples were vortexed to ensure complete mixture and then diluted in Dulbecco's phosphate buffered saline (DPBS; x50 for control; x100 for MTX treated cells). At least five 30 s videos were recorded for each sample and the software was used to estimate concentration (x 10^8/ml) and mean diameter (nanometres) of the sEVs. The recording was monitored manually and performed at RT. Camera gain was 350 and the shutter speed was 14.99 ms. For analysis, the detection threshold was set to 10 and the type to multi. The blur, minimum track length and minimum expected particle size were all set to auto. Calibration was carried out using 100 nm silica beads diluted to a known concentration in PBS.

2.16.3 Protein estimation

Protein concentration in sEV samples was estimated via two different but similar methods: Bradford assay and Bicinchoninic acid (BCA) assay.

2.16.3.1 Bradford assay

To estimate the purity of sEV samples, sEVs were prepared and diluted in PBS (X100 for ExoQuick isolated sEVs; X50 for SEC isolated sEVs) and then compared in triplicates against serially diluted bovine serum albumin (BSA) as standard, with PBS used as a blank. BSA standards (2.5 – 25 µg/ml) were prepared. Each standard or unknown sample (150 µl) was ejected into appropriate wells in a 96-well microplate (Corning, UK) before adding 150 µl of the Coomasie Reagent (Thermofisher Scientific, UK) to each well and left to mix for 30 seconds on a plate orbital shaker. The plate was further incubated for 10 minutes at RT. The absorbance of each standard and unknown sample was then measured at 570 nm on a FLUOstar Omega Microplate Reader (BMG Labtech, UK), which uses the MARS data analysis software to generate values. A standard calibration curve was generated and values for the unknown sEV samples were extrapolated from this standard curve, using a third-order polynomial equation, with $r^2 > 0.98$ for each assay. As described previously by Tang *et al.,* (2017), the ratio of particles to protein was determined using the formula:

Ratio = log [(particles concentration/protein concentration)]

2.16.3.2 Bicinchoninic acid assay

sEV samples isolated by SEC were also compared in triplicates against serially diluted BSA as standard, with PBS used as a blank. Each standard or unknown sample (25 µl) was pipetted into appropriate wells in a 96-well microplate before adding 200 µl of the Working Reagent, prepared by mixing 50 parts of BCA reagent A (Bicinchoninic acid) and 1 part of BCA reagent B (copper sulphate) [Thermofisher Scientific, UK], to each well to ensure that the sample to working reagent ratio is 1:8. The samples were mixed thoroughly on a plate orbital shaker for 30 seconds before incubating at 37°C for 30 minutes. Afterwards, the plate was allowed to cool at RT and then the absorbance of each standard and unknown sample was read at 570 nm on a FLUOstar Omega Microplate Reader. Protein concentrations were calculated using a standard calibration curve generated using BSA standards (5 - 250 µg/ml). The ratio of particles to protein as stated in section 2.16.3.1.

2.17 Cytotoxic effect of GW4689 on HS-5

GW4869 is an inhibitor of sEV biogenesis/release that blocks the ceramide-mediated inward budding of MVB and the release of mature sEVs from MVB (Essandoh *et al.,* 2015). Following the previous work of Essandoh *et al.,* (2015), GW4869 powder (0.2 mg; Sigma Aldrich, UK) was initially dissolved in 1ml of DMSO into a stock solution of 0.346 mM GW4869 before dilution in culture supernatants to achieve 5 µM, 10 µM or 20 µM GW4869 concentration. To determine the possible cytotoxic effect of GW4869, HS-5 cells were seeded in triplicates at a density of 132,000 cells/cm^2 into a 12-well plate containing 1 ml of DMEM-HG medium per well and allowed to attach overnight in an incubator at 37°C. Cells were then treated with increasing doses (5 µM, 10 µM, 20 µM) of GW4869 and 0.01% DMSO for 24 hours. DMSO serves as the vehicle control. Afterwards, cell injury was determined by measuring the number of viable cells and percentage viability using the Luna FL automated cell counter (section 2.10).

2.18 Effect of GW4869 on bystander effect

Using the aforementioned bystander model (Section 2.12), HS-5 cells were seeded at a density of 132,000 cells/cm^2 into a 12-well plate containing 1 ml of DMEM-HG medium per well and allowed to attach overnight in an incubator at 37°C. HS-5 cells were pre-treated with GW4869 (5 µM) for an hour to inhibit the generation of sEV prior to drug treatment of chlorambucil (40 µM), carmustine (10 µg/ml), etoposide (10 µM) and mitoxantrone (500 ng/ml), and incubated at 37°C. Twenty-four hours after commencement of drug treatment, the medium containing these drugs was removed, cells were washed three times with PBS and fresh medium was added. Culture inserts (0.4 µm pore size) was transferred into the wells using sterile forceps and TK6 cells (5 x 10^5 cells/ml) were aliquoted into the culture inserts. Cells were allowed to co-culture at 37°C for 24 hours and harvested afterwards to assess the viability and genotoxicity of these bystander cells (sections 2.10 & 2.11).

2.19 Uptake of sEVs by bystander cells

2.19.1 Labelling of sEVs' membrane

ExoGlow-Membrane EV Labelling Kit (Systems Biosciences, US), which is a red fluorescent dye that labels sEVs with intact lipid membranes, was used according to the manufacturer's instructions with slight modifications. Reaction buffer (12 µl) was initially mixed with 2 µl dye before adding the mixture to 0.2 µg of sEV sample and incubated in the dark at RT for 30 minutes. ExoQuick-TC (10 µl) was added afterwards to the mixture and incubated at 4°C for 30 minutes to remove unlabelled dye. The sample was spun at 10,000 g for 10 minutes to obtain sEV pellets. The supernatant was carefully aspirated from the side of the tube and the sEV pellet was re-suspended in PBS. An aliquot was taken to confirm labelling and then the rest stored at -20°C prior to use. The labelled sEVs were transferred onto a clean, grease free slide and visualised under a Leica confocal microscope TCS SP8. Images were taken with the LAS X software.

2.19.2 Labelling of sEVs' RNA

The RNA of sEVs was labelled using the ExoGlow-RNA EV Labelling Kit (Systems Biosciences, US), a green fluorescent dye that specifically labels sEV RNA cargo, by following the manufacturer's instructions. Each sEV sample (0.2 µg) was initially mixed with 300 µl incubation buffer before adding 5 µM of ExoGlow RNA probe to the mixture. The mixture was then incubated in the dark for an hour at 37°C. An aliquot was taken to confirm labelling and then the rest stored at -20°C prior to use. The labelled sEVs were placed on a clean, grease free slide and visualised under a confocal microscope.

2.19.3 Uptake of sEV by TK6

TK6 cells (1 x10^6 cells) were seeded into a 6-well plate containing 2 ml of serum-free medium or DMEM-HG complete medium. Membrane-labelled sEVs were added to TK6 cells cultured in serum-free medium whilst RNA-labelled sEVs were cultured in DMEM-HG complete medium to

inhibit transfection of free RNA probe into the cells. Cells cultured in both conditions were incubated for 3 hours at 37°C. Afterwards, TK6 cells were stained for 25 minutes with 20 µl/ml of DiO or DiI dye (Thermofisher Scientific, UK) for those cultured with membrane-labelled sEVs and RNA-labelled sEVs respectively. Cells were then washed three times with PBS and resuspended in PBS. Cells were transferred to a clean, grease free slide and visualised under a confocal microscope.

2.19.4 Inhibition of sEV uptake by TK6

As previously described (sections 2.19.1 and 2.19.2), the membrane and/or RNA of sEVs were labelled with dyes before incubating them with heparin (10 µg/ml) or PBS as control at 37°C for 30 minutes. Heparin is an anti-coagulant that delays blood coagulation but also inhibits sEVs' uptake. TK6 cells (1 x10^6 cells) were seeded into a six-well plate in serum-free medium and DMEM-HG medium respectively and co-cultured with the labelled sEVs for 3 hours at 37°C. Following incubation, cells were stained with DiO or DiI dye (20 µl/ml) and incubated at 37°C for 25 minutes. Cells were washed three times with PBS to remove unbound dye and resuspended in PBS. Cells were then transferred to a clean, grease free slide and visualised under a confocal microscope.

2.20 Effect of sEVs on bystander cells

TK6 cells were seeded into 12 well plates (day 0) at 500,000 cells per well. After 24 hours, cells were treated with PBS and sEVs extracted from untreated or MTX-treated HS-5 cells (0.2 µg), and allowed to co-culture for 24 hours at 37°C. On day 2, the number of viable cells and percentage viability were determined using the Luna FL automated cell counter as described in section 2.10. Genotoxicity in these cells were also determined by MN assay (section 2.11).

To inhibit this effect, TK6 cells were seeded on day 0 as previously described. Twenty-four later, cells were pre-treated with 10 µg/ml of heparin for 30 minutes at 37°C prior to treatment with PBS and sEVs extracted from untreated or mitoxantrone-treated HS-5 cells (0.2 µg) for 24 hours. On day 2, cells were further treated with 10 µg/ml of heparin for 30 minutes at 37°C. The number

of viable cells and percentage viability, and genotoxicity were then assessed using the Luna FL automated cell counter and MN assay respectively (sections 2.10; 2.11).

2.21 Effect of sEVs on direct effect of mitoxantrone on bystander cells

TK6 cells were seeded into 12 well plates (day 0) at 500,000 cells per well. After 24 hours, cells were treated with PBS and sEVs extracted from untreated or MTX-treated HS-5 cells (0.2 µg) and allowed to co-culture for 24 hours at 37°C. On day 2, cells were treated with MTX (500 ng/ml) for 24 hours. On day 3, the number of viable cells and percentage viability were determined using the Luna FL automated cell counter as described in section 2.10. Genotoxicity in these cells were also determined by MN assay (section 2.11).

To inhibit this effect, TK6 cells were seeded as initially described and pre-treated with heparin (10 µg/ml) for 30 minutes. Cells were then incubated with sEVs extracted from untreated or MTX-treated HS-5 cells (0.2 µg) in the presence or absence of 10 µg/ml heparin for 24 hours at 37°C. On day 2, heparin treatment (10 µg/ml) was continued for 30 minutes before treating the cells with MTX (500 ng/ml) for 24 hours. On day 3, the number of viable cells and percentage viability were determined using the Luna FL automated cell counter (section 2.10). Genotoxicity in these cells were also determined by MN assay (section 2.11).

2.22 RNA extraction

2.22.1 Cells

RNA from cells (HS-5 and TK6) was isolated using the Absolutely RNA miniprep kit (Agilent Technologies, UK) according to the manufacturer's instructions. HS-5 and TK-6 cells were harvested following 24-hour treatment with mitoxantrone (500 ng/ml) and counted using the Luna FL automated cell counter. The cells were further spun at 230 g (HS-5) and 300 g (TK6) for 5 minutes and 10 minutes respectively to obtain a pellet. The supernatant was completely

removed before adding lysis buffer-β-mercaptoethanol mixture (140:1) to the pellet, then vortexed properly to homogenize the mixture. The homogenate was transferred to a seated prefilter spin cup and spun in a microcentaur plus microcentrifuge at 14,500 g (maximum speed) for 5 minutes. The resulting filtrate was retained and mixed thoroughly with an equal volume of 70% ethanol by vortexing the tube for 5 seconds. The mixture was then transferred to a seated RNA binding spin cup and spun at maximum speed for 60 seconds in a microcentrifuge. Low-salt wash buffer (600 µl; 1X) was added to the spin cup and spun in a microcentrifuge at maximum speed for 60 seconds. The spin cup was placed in a new microcentrifuge tube and spun at maximum speed for 2 minutes. DNase solution, prepared by mixing 50 µl of DNase Digestion Buffer with 5 µl of reconstituted RNase-free DNase I, was added onto the matrix and incubated on a Dri-block DB-2A heat block (Techne, UK) at 37°C for 15 minutes. The matrix was then washed with 600 µl of 1 X High-Salt Wash Buffer and spun in a microcentrifuge at maximum speed for 60 seconds before further washes in 600 µl and 300 µl of 1 X low-salt wash buffer respectively. Elution buffer (30 µl) was then added to the spin cup, placed in a fresh 1.5ml microcentrifuge, and incubated for 10 minutes at RT. The sample was then spun at maximum speed for a minute to obtain purified RNA. The elution process was repeated to obtain RNA with a better concentration. The purified RNA was then stored at -20°C until further use.

2.22.2 Conditioned medium

As previously described in section 2.13.1, CM was obtained and mixed with 10 µl/ml of β-mercaptoethanol and incubated on ice for 15 minutes and then spun at 3000 g for 60 minutes. The resulting supernatant was concentrated down to 200 µl using Amicon ultra-15 tubes (Millipore UK) by spinning the tubes at 3900 g for 85 minutes at 4°C (Beckman Allegra X-22R wit SX4250 rotor). The concentrates were treated as previously described in section 2.22.1 using the Agilent kit in order to extract the RNA. The eluted RNA was also transferred to -20°C refrigerator until further use.

2.22.3 Small extracellular vesicles

Following the manufacturer's instructions with slight modifications, sEVs were lysed with 350 µl of lysis buffer and 2.5 µl of β-mercaptoethanol and vortexed for a few seconds to homogenise the mixture. The homogenate was then treated as previously described in section 2.22.1 using the Agilent kit to isolate the RNA. The isolated RNA was stored at -20°C until further use.

2.23 RNA purity and concentration

The purity and concentration of RNA in all samples was quantitated and measured by spectrophotometry using a Nanodrop one (Thermofisher Scientific, UK). The purity of RNA samples was determined by the 260/280 and 260/230 ratios of absorbance values. A range of ~ 2.0 for 260/280 and a range of 2.0–2.2 (260/230 ratio) was accepted as "pure" for RNA. Lower ratios may indicate the presence of DNA, protein, phenol, EDTA, guanidine or other contaminants that absorb at or near 260, 230 or 280 nm.

2.24 RNA integrity – agarose gel electrophoresis

The integrity of the RNA was determined for all samples using agarose gel electrophoresis. Dry agarose powder (0.5g; Bioline, UK) was mixed in 50 ml of 1X Tris Acetate EDTA (TAE) buffer and heated intermittently for 1.5 minutes in a microwave (SANYO super microwave 900 W) to dissolve the 1% w/v TAE agarose gel until the solution became clear. Ethidium bromide (3 µl at 10 µg/ml) was added to the gel and mixed properly. The gel was then poured into a sealed casting tray with a comb and allowed to cool for 10-15 minutes. The casting tray was assembled in a FHU 10 or FHU6 miniplus submarine gel (Fisher Scientific, UK) containing enough 1X TAE Buffer to cover the gel before removing the comb. The samples and a kilobase (kb) DNA ladder (500 bp to 10kb; New England Bio Labs, UK) were loaded into the wells, and electrophoresed for 30 minutes at 80 V electrophoresis power supply - EPS 601 (Amersham, Biosciences, UK). The gel product was visualised using a MiniBIS UV illuminator (DNR Bio-imaging System, Israel).

2.25 Complimentary DNA (cDNA) synthesis

RNA from cells, conditioned medium and sEVs were converted to complimentary DNA (cDNA) using the miScript II RT kit (Qiagen, UK) based on the manufacturer's instructions. Reverse transcriptase master mix was prepared by mixing 2 µl of 10 X miScript Nucleic mix, 4 µl of 5X miScript Hi Spec Buffer, 2µl of miScript Reverse Transcriptase mix and variable amount of RNAse free water. The template RNA was mixed with the reverse transcriptase master mix bringing the volume to 20 µl and incubated sequentially for 60 minutes at 37°C and 5 minutes at 95°C (Scotlab Dri-block DB-1, Techne, UK). The reverse transcription reaction was then diluted in 200 µl RNAse free water and stored in 110 µl aliquots at -80°C ultra low temperature freezer (New Brunswick Scientific, UK) until needed.

2.26 qRT-PCR array analysis of bystander cells RNA

The reverse transcription reaction was performed as previously described in section 2.27 using about 250 ng of RNA sample to synthesize cDNA from TK6 cells. The synthesized cDNA was diluted with 200 µl RNAse-free water (Qiagen, UK). For microarray analysis, miScript SYBR Green PCR kit and pathway-focused miScript miRNA PCR Arrays (both Qiagen, UK) were used according to the manufacturer's instructions. Diluted cDNA (200 µl) was mixed thoroughly but gently with RNAse free water (1000 µl), 10X miScript Universal primer (275 µl) and 2X Quantitect SYBR Green PCR master mix (1375 µl) to obtain a final volume of 2750 µl. Thus, this ensured that each well contained about 0.5-1.0 ng cDNA. Reaction mix (25 µl) was added to each well in a 96-well miScript miRNA PCR Array containing forward primers for 84 human miRNAs and tightly sealed with an optical adhesive film. The PCR array was centrifuged at RT for a minute at 1000 g (Beckman Allegra X-22R centrifuge with S2096 rotor) to remove bubbles. The PCR array plate was placed in a thermal cycler (Applied Biosystems Step One Plus, Thermofisher Scientific, UK) and run for 40 cycles with the thermal cycler conditions indicated in table 2.2.

Unknown miRNAs were quantitated by SYBR green-based quantitative real time polymerase chain reaction (qRT-PCR). Dissociation (melting) curve analyses of the PCR products was

performed to verify the specificity and identity of the generated amplicons. The Ct value or threshold cycle, which indicates the number of cycles required for the fluorescent signal of the reaction to cross a threshold, was generated. The Ct value is inversely proportional to the amount of the target cDNA in the sample. Using the Ct value, the positive PCR control (PPC) and reverse transcription control (miRTC) served as quality control at every step of the process. The difference between the Ct values of PPC and miRTC were used to determine the success of the reverse transcription reaction whilst a Ct value of 19 ± 2 (PPC) was used to identify high quality RNA, correctly run cycling program and correctly defined thresholds.

Table 2.2 qRT-PCR cycling conditions. Denaturation, annealing and extension steps were cycled.

Step	Time	Temperature	Remarks
Initial activation step	15 minutes	95°C	HotStar Taq DNA Polymerase was activated by this step
Denaturation	15 s	94°C	
Annealing	30 s	55°C	
Extension	30 s	70°C	Fluorescence data was collected
Hold		4°C	
Number of cycles	40	-	-

The expression of 84 miRNAs was normalized with the average Ct value of six small nuclear RNAs – SNORD61, SNORD68, SNORD72, SNORD95, SNORD96A and RNU6B/RNU6-2. The array also contained non-human miRNA, cel-miR-39-3p, from *Caenorhabditis elegans* that could be used as an alternative normalizer. Fold changes in the level of each miRNA was relatively quantified using the comparative CT ($2^{-\Delta\Delta CT}$) method as described by Rao *et al.,* (2013). The array was repeated three times for the both batches of cells – control and test.

2.27 Bioinformatics: miRNA target genes prediction

To predict miRNA targets, target prediction programs such as Target Scan Human (http://targetscan.org), miRBase (http://mirbase.org), miRDB (http://mirdb.org) and TargetLink (https://ccb-web.cs.uni-saarland.de/mirtargetlink/) were used. These target prediction programs contain human miRNA targets and also offer information on human miRNA-miRNA interactions. The predicted miRNA target genes were identified and analysed by using Functional Enrichment analysis tool (http://www.funrich.org/). FunRich (Version 3.1.3) is a stand-alone software that can leverage the Gene Ontology (GO) to identify and determine the biological, molecular and cellular processes represented in the gene profile.

2.28 Quantitative real time polymerase chain reaction (qRT-PCR)

To validate the PCR array, quantifications were performed using the SYBR green qRT-PCR assay (Qiagen, UK) with a two-step reaction process of the following miRNAs: miR-146a-5p, miR-30d-5p, miR-16-5p, miR-17-5p, miR-20a-5p, and miR-200c-3p. In the first step, reverse transcription was performed as previously described in section 2.27 using about 125 ng (CM and sEVs) or 250 ng (HS-5 and TK6) of RNA by incubating for 60 minutes at 37°C followed by heat inactivation for 5 minutes at 95°C. The newly synthesized cDNA was diluted with 200 µl of RNAse free water to ensure at least 50 pg – 3 ng of cDNA per PCR. Each sample was run in duplicate for analysis using the same cycling conditions as previously mentioned in section 2.26. At the end of the PCR cycles, dissociation (melting) curve analyses were performed to validate the specificity and identity of the generated PCR products. The Ct value of each miRNA was normalised using small nuclear RNAs (SNORD61 and RNU6B/RNU6-2) as internal controls for cells whilst miR-150-5p was used as a negative control. As previously described by St Pierre *et al.,* (2017), the small nuclear RNAs were deemed appropriate for data normalization by BestKeeper, GeNorm and NormFinder. The NormFinder (version 0.953) algorithm was used as an Excel add-in and as an R-script (NormFinder for R version 2015-01-25; available at http://moma.dk/normfinder-software). The qbase+

software (version 3.1) was used to perform data normalisation using GeNorm algorithm; available at https://genorm.cmgg.be/) whilst BestKeeper software tool (version 8.1) available at https://www.gene-quantification.de/bestkeeper.html was also used to perform data normalization. These software pacgkages compute variations of different reference small nuclear RNAs indicating the two that are suitable for qRT-PCR data normalisation in this study. Refinder (https://www.heartcure.com.au/reffinder/?type=reference) was then used to integrate the data from these computational software tools to compare and rank the tested candidate normalizers. Fold changes in the level of each miRNA was relatively quantified using the comparative Ct ($2^{-\Delta\Delta CT}$) method except where the Ct values were too low to be considered. A schematic illustration of the bioinformatics workflow, which illustrates the tools and databases employed to uncover the interactions in the miRNA-based regulatory networks is shown in figure 2.3.

Microarray datasets	→	Data processing and analysis	→	Data integration	→	Network analysis
Qiagen miScript PCR array		$2^{-\Delta\Delta CT}$ method		TargetScan miRBase miRDB TargetLink		FUNRICH
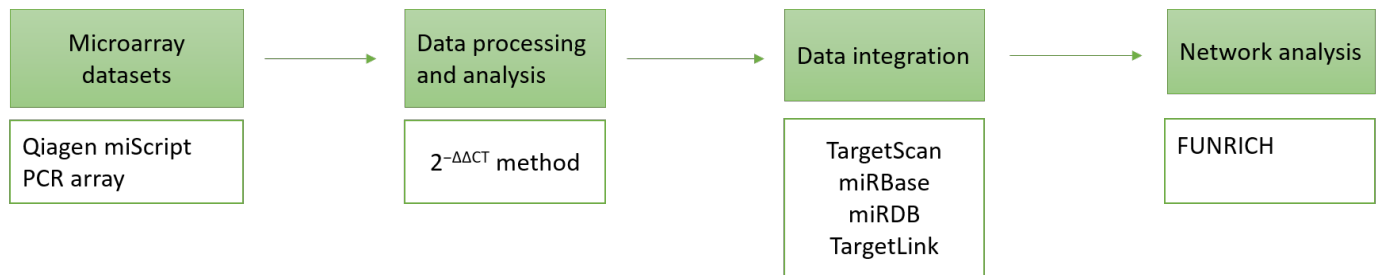
Figure 2.3 Schematic illustration of miRNA bioinformatics workflow. PCR microarray was performed to identify possible candidate miRNAs involved in chemotherapy-induced bystander effects. The fold changes in these candidates were analysed using the $2^{-\Delta\Delta CT}$ method. Predictions of the target genes of these microRNAs were mapped out using various target prediction programs. The predicted target genes were further analysed by using the FUNRICH software.

2.29 Cell cycle analysis

TK6 cells were seeded into 12 well plates (day 0) at 500,000 cells per well. After 24 hours, cells were treated with PBS and sEVs extracted from untreated or mitoxantrone-treated HS-5 cells (0.2µg), and allowed to co-culture for 24 hours at 37°C. On day 2, the number of viable cells and percentage viability were determined using the Luna FL automated cell counter (section 2.10). About 200,000 cells were taken from each treatment and transferred into a 15 ml falcon tube. The samples were centrifuged at 400 g for 5 minutes at 4°C. About 200 µl of cold PBS was added

to each tube and kept on ice. Samples were vortexed to minimise cell aggregation before adding 1 ml 80% ice-cold ethanol. Samples were transferred to a 4°C refrigerator for 24 hours. After 24 hours, samples were left on the bench to warm to RT before adding 2 ml of RT PBS. Samples were pelleted at 600 g for 5 minutes and then resuspended in 480 µl PBS-RNase A mixture (478.5 µl of PBS and 1.5 µl of 10 mg/ml RNase A). The samples were transferred to 1.5 ml microcentrifuge tube and incubated at RT for an hour. About 20 µl PI (1 mg/ml stock, final concentration 40 µg/ml) was added to each sample and analysed with the flow cytometer. Cells treated with mitoxantrone was used as a positive control. Gating (see appendix) was done to exclude debris and collect cell cycle data. Flow cytometry data analysis was performed using FCS Express flow cytometry software (version 7.04.0014).

2.30 Statistics

All graphs were made and statistical analyses performed, using GraphPad Prism version 8.2.1 except where otherwise stated. D'Agostino-Pearson omnibus and Shapiro-Wilk normality test were used to test for normality. All experiments were done a minimum of three biological repeats unless otherwise stated. The unpaired Student t-test was used to determine direct significance between treated and untreated (control) samples, while one-way or two-way ANOVA was used for group comparisons followed by a Tukey or Dunnett posthoc multiple comparison test. Data are expressed either as mean ± standard deviation (SD) of replicates. Statistical significance of the presented graphs were identified as * $p<0.5$, ** $p<0.01$, *** $p<0.001$ **** $p<0.0001$.

3.0 Cell line characterization

3.1 Introduction

Several physiological and biological processes in the body such as cell differentiation, migration, and growth require *in vivo* research, which is not always attainable, and thus, we are restricted to experimentation of animal models or human samples *ex vivo.* However, *ex vivo* culture conditions are not physiological in its entirety and may influence the biological properties of cells (Drela *et al.,* 2018). Furthermore, these samples are not readily available, as they require ethical clearance to obtain them. Therefore, a cost-effective alternative, an appropriate *in vitro* model, needed to be developed to enable the study of cells, at a cellular and molecular level, in a controlled environment. Such models have enabled scientists to have an advanced perception and understanding of the mechanisms that underlie cell behaviour *in vivo* thus inferring their function during health and disease (Duval *et al.,* 2017). As a result, cell cultures are prerequisite *in vitro* tools for the study of cell and tissue physiology and pathophysiology.

Furthermore, mammalian cell culture systems have also been widely applied in life sciences and medicine for drug and vaccine discovery, and development and determination of drug efficacy and toxicity. These cell culture systems may either be primary cell culture or cell line culture; each with its own pros and cons (Silicka, 2017). However, these culture systems are usually single cellular entities that ignore cellular crosstalk, which is relevant to the current study. The efficacy of these culture systems is also limited by growth conditions, which do not give a true representation of the natural cellular microenvironment. Misrepresentation of the natural microenvironment has led to persistent problems encountered in interpreting *in vitro* data (Huh *et al.,* 2011; Yao and Asayama, 2017). The cellular microenvironment is biochemical in nature and heavily influenced by the way cells interact with each other as well as their functionality. The proliferation of cells depends on growth factors, cytokines and integrins, which are surface receptors that ensure that the position of the cells is correctly situated within the tissue thereby activating varied signalling cascades (Guadamillas *et al.,* 2011). These factors also influence cell responses to other stimuli.

Although CIBE studies initially employed *in vivo* mice models (Demidem *et al.,* 2006; Merle *et al.,* 2008), others have since turned to *in vitro* models by culturing the cells separately in monolayers and transferring the CM to the bystander cells (Di *et al.,* 2008; Jin *et al.,* 2011). However, CIBE has also been shown in a co-culture system (Jensen & Glazer, 2004; Alexandre *et al.,* 2007; Arora *et al.,* 2018). As a result, co-cultures have generated more interest in recent times to potentiate drug research. A co-culture entails culturing two distinct cell populations in such a way that there is communication between them. Co-cultures provide information on cell-to-cell communication and may serve as a good *in vivo* model representative. Due to its robustness, predictability and scalability compared with monocultures, the current model has enabled comprehensive testing and monitoring of drug effects on cell-to-cell interactions. This intercellular interaction is dependent on soluble factors released into the extracellular environment, which is determined by the experimental set up (Goers *et al.,* 2014). However, these co-cultures require *in vitro* characterization and optimisation of culture conditions, which can be labour intensive.

Therefore, it is pertinent to ensure that cell culture conditions are optimised for cellular growth and to enhance reproducibility of experimental data. In order to better mimic cell and tissue physiology, cells require certain prerequisites such as adequate growth medium, substrates that enable cell attachment, a temperature control system, and an incubator that provides the optimum osmolality and pH for these cells. However, the choice of a quality culture medium is the most essential aspect of cell culture as this can affect the quality of the cells and cause experimental variation thereby affecting the general research outcome (Arora, 2013; Yao and Asayama, 2017). It is important to mention that there is no evidence of *in vitro* co-culture medium in support of miRNA involvement in CIBE. Kelechi Okeke (personal communication) first established an *in vitro* transwell co-culture model using HS-5 stromal cells and TK6 cells within our research group. Although these cell lines have been previously characterised separately, her study first explored the functionality of these cells as a co-culture in DMEM-HG supplemented with FBS, 2mM L-glutamine and antibiotics. Both cell lines of choice are of human origin and were chosen to represent the heterogeneity of the BM microenvironment and to provide the optimum standard culture conditions. TK6 cells is a human B lymphoblastoid cell line that is commonly used in genotoxicity studies because they are p53 proficient and karyotypically stable (Lorge *et*

al, 2016). Peforming genotoxicity studies in TK6 cells eliminates donor availability seen in human peripheral blood lymphocytes and reduces the percentage of non-relevant positive results compared to p53-mutated cell lines (Smart *et al,* 2020).

Additionally, culture medium is usually supplemented with serum, glucose, antibiotics and growth factors that can cause alterations in the production and composition of EVs. In order to avoid the co-isolation of exogenous EVs, EVs are usually isolated from culture medium conditioned by cells in serum with depleted exosome, serum from other species, or serum-free culture medium (Pachler *et al.,* 2017; Saury *et al.,* 2018). Nevertheless, the need to deplete EVs in the serum depends on the downstream use of the isolated EVs. Culture medium supplemented with FBS may contain abundant nucleic acids that can interfere with the cell-culture derived extracellular nucleic acids (Wei *et al.,* 2016). However, commercially available exosome-depleted sera are rarely devoid of xenogeneic substances such as recombinant growth factors whilst serum-free culture medium can affect the proliferation and differentiation of MSCs *in vitro* (Pachler *et al.,* 2017). Therefore, there is need to optimise the choice of culture medium and equipment, and other experimental conditions to ensure that robust data is generated.

3.2 Methods

3.2.1 CFU-F Assay

The colony forming capacity of HS-5 cells as MSC was determined and compared in five culture media: DMEM-HG, DMEM-LG, DMEM-f12, RPMI 1640 and Iscove's Modified Dulbecco's medium (IMDM) (Gibco Invitrogen, Paisley, UK) as described in section 2.7. All cell culture procedures were performed as described in section 2.3. The colonies were counted manually by light microscopy using the NIKON Eclipse TE 300 inverted microscope.

3.2.2 Cell culture medium optimization

To determine the optimum medium for the co-culture model, HS-5 cells were seeded at 10,000 cells per cm^2 in three culture media: DMEM-HG, RPMI 1640 and IMDM, in $25cm^2$ vent cap Corning

cell culture flasks. TK6 cells were seeded at 2.5 x 10^4 cells/ml (low density) and 3.0 x 10^5 cells/ml (high density) in three culture media: DMEM-HG supplemented with FBS or sEVs-depleted FBS and RPMI 1640 as described in section 2.8. All cell culture procedures were performed as discussed in section 2.3. Cell viability assessment in different media was determined by the trypan blue exclusion assay and acridine orange/propidium iodide assay using the LUNA counter as discussed in section 2.10.

3.2.3 Serum optimization for extracellular vesicular studies

HS-5 cells were seeded at 10,000 cells per cm^2 in DMEM-HG with sEVs-depleted FBS, DMEM-HG with heat-inactivated FBS and serum-free DMEM-HG; in $25cm^2$ vent cap Corning cell culture flasks and maintained for 42 hours as described in section 2.8. All cell culture procedures were performed as discussed in section 2.3. Cell viability assessment in different media was determined by the trypan blue exclusion assay and acridine orange/propidium iodide assay using the LUNA counter as discussed in section 2.10.

3.3 Results

3.3.1 Morphology and growth of cells

First, the morphologies and growth potentials of the cells used in this study were investigated to ascertain the alternative growth conditions for these cells. A number of commercially available culture medium was explored to choose the most appropriate culture medium for maintaining good functionality of the cells but in a co-culture environment. MSC are anchorage-dependent cells that require a culture surface to proliferate whilst HSC do not need any surface for growth and can grow optimally in suspension (Merten, 2015).

3.3.1.1 Functionality and quality of HS-5 cells

MSC form colonies and grow as CFU-F over time, and the efficiency with which they form colonies is an important assay for determining the functionality and quality of cell preparations (Kuznetsova *et al.,* 2009). According to ISCT, MSC must have the ability to adhere to culture plate,

generate density-independent CFU-F colonies and differentiate into osteoblasts, adipocytes and chondrocytes. To satisfy this aspect of the ISCT criteria, cells were seeded at varying low densities in five media (DMEM-HG, DMEM-LG, IMDM, RPMI 1640 and DMEM-f12) supplemented as previously described in Chapter 2.7 and incubated for 14 days. A colony was described as a group of more than 20 cells. It is noteworthy that this batch of HS-5 cells has been previously shown to be capable of differentiating within this lab (Saeed Kabrah, personal communication).

Colonies were observed 6-8 days after initial plating. These resultant colonies contained a subpopulation of cells capable of generating new fibroblast colonies from single cells. The cells were of different sizes and shapes, which might be representative of cell function as shown in figure 3.1. The CFU-F count was significantly higher at 50 cells/cm^2 therefore the use of this seeding cell density might prove to be the most advantageous condition. The basal medium for HS-5 cells is DMEM-HG however; RPMI 1640 and IMDM produced more colonies than other medium used, including DMEM-HG (Figure 3.2). The cells produced the most colonies in RPMI 1640, followed by IMDM and DMEM-HG. Whilst the difference between the number of colonies observed in RPMI 1640 and IMDM at 10 cells/cm^2 (p = 0.9999) and 20 cells/cm^2 (p = 0.5773) was not statistically significant, the difference between colonies observed in these media was statistically significant when the cells were seeded at 30 cells/cm^2 (p = 0.0442) and 50 cells/cm^2 (p = 0.009). Similarly, DMEM-LG produced more colonies than DMEM-HG at 10 cells/cm^2 and 20 cells/cm^2 whilst DMEM-HG produced more colonies than DMEM-LG when seeded at a higher density (30 cells/cm^2 and 50 cells/cm^2). However, these differences in the number of the colonies were not statistically significant regardless of the seeding density. Furthermore, there was a statistically significant difference in the colonies produced in DMEM-HG and DMEM-LG media compared to RPMI 1640 and IMDM at all cell seeding densities. DMEM-f12 produced no colony regardless of the density the cells were seeded. Collectively, these suggest that there is a correlation between the number of cells plated and the number of CFU-F counted when analyzing the effect of densities. In addition, it can also be inferred that all these medium, except DMEM-f12, can support the colony formation or the funcationality of HS-5 cells. RPMI 1640 is the best for growth of HS-5 cells and the morphology of the cells most closely matches primary MSC (personal communication).

| | 10cells/cm^2 | 20cells/cm^2 | 30cells/cm^2 | 50cells/cm^2 |
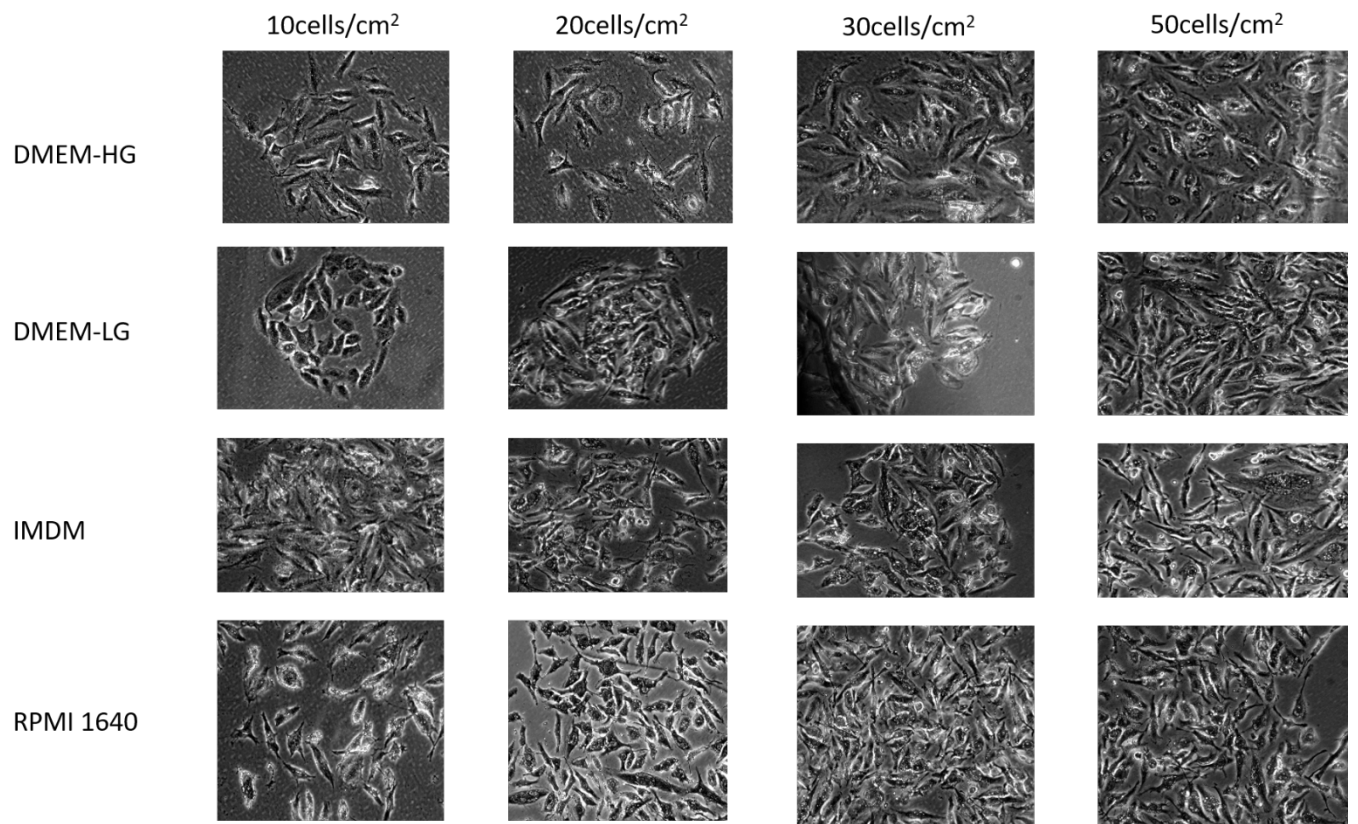
Figure 3.1 HS-5 cells form colonies and grow as colony forming unit-fibroblasts (CFU-Fs) over time. Cells were seeded at 10 cells/cm^2, 20 cells/cm^2, 30 cells/cm^2 and 50 cells/cm^2 in a 6-well plate and incubated for 14 days. The plates were visualized under an inverted phase-contrast microscope at x10 magnification. (Scale bar = 30µm)
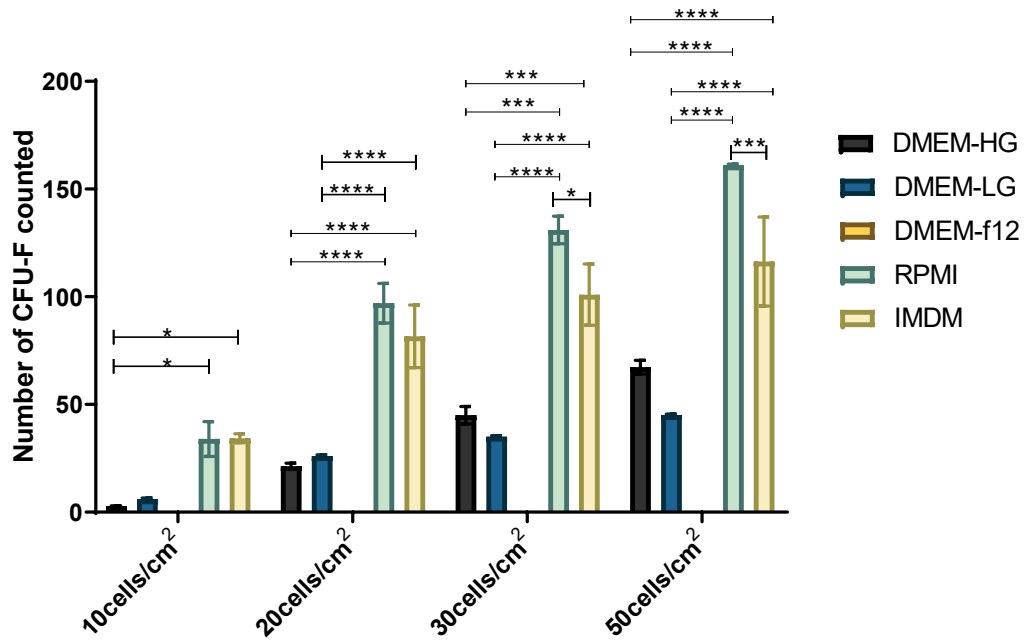
Figure 3.2 HS-5 cells produce colonies when seeded at low densities. Cells were seeded at 10 cells/cm^2, 20 cells/cm^2, 30 cells/cm^2 and 50 cells/cm^2 with 2 ml of medium in a 6-well plate and incubated for 14 days. Number of colonies produced by these cells were counted using the inverted phase contrast light microscope. Histogram shows that HS-5 produce more colonies in RPMI and IMDM than other medium especially DMEM-HG, which is the recommended medium for these cells. Error bars show mean ± standard deviation. Statistical significance was done using the ANOVA for two-way factorial design (n=3; * $p<0.05$, ***$p<0.001$, ****$p< 0.0001$).

However, when the seeding density of the cells was increased to 1000 cells/cm^2, 2000 cells/cm^2, 3000 cells/cm^2 and 5000 cells/cm^2, uncountable colonies were observed in cells that were cultured in DMEM-HG, RPMI 1640 and IMDM but not in DMEM-LG as depicted in figure 3.3. The rationale here is that cell seeding density is an important transplantation variable and these cells are usually cultured at high densities. These results suggest that DMEM-LG may not be a good culture medium option for these cells at high density. In addition, the cells looked confluent and a bit detached from the plastic surface. It can be inferred that the reason for this is that the cells, at confluency or high-cell density, undergo contact inhibition of proliferation, which is a fundamental property whereby normal cells cease proliferation and cell division. Anchorage-dependent cells are known to undergo cell-detachment-induced cell death (anoikis) once confluent. The well plates used in the experiment can be seen in figure 3.4.

77
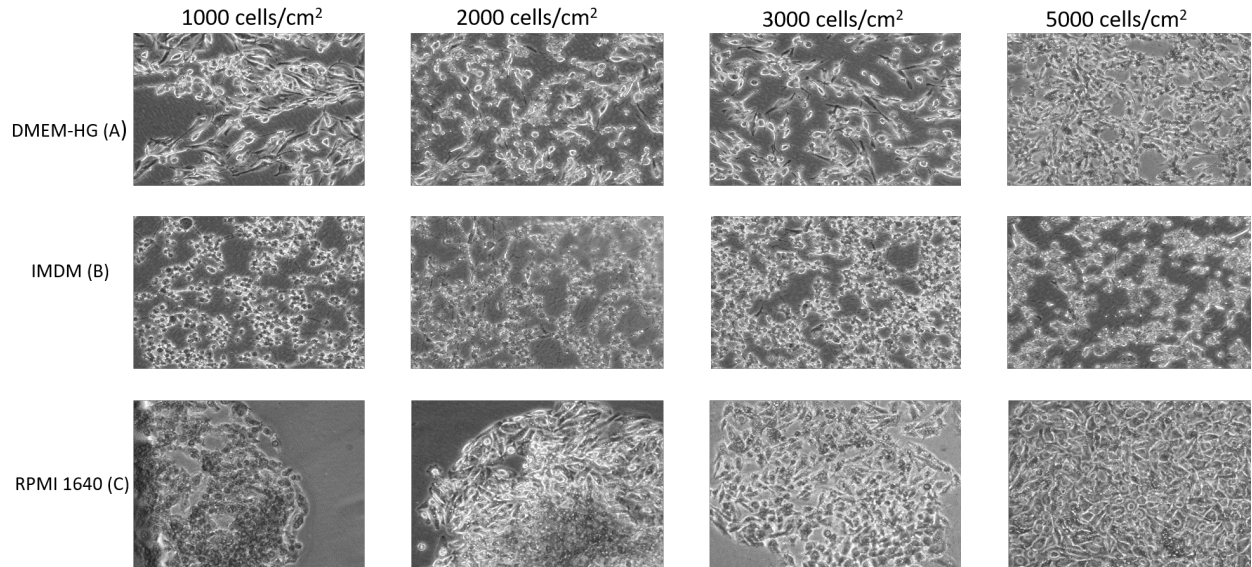
Figure 3.3 HS-5 cells produce colonies when seeded at high densities. Cells were seeded at 1000 cells/cm^2 , 2000 cells/cm^2, 3000 cells/cm^2 and 5000 cells/cm^2 with 2 ml of medium in a 6-well plate and incubated for 14 days. Number of colonies produced by these cells were assessed under an inverted phase contrast light microscope x10 magnification). Cells produced numerous colonies in DMEM-HG, RPMI and IMDM showing that these media are suitable for their growth (Scale bar = 30μm).
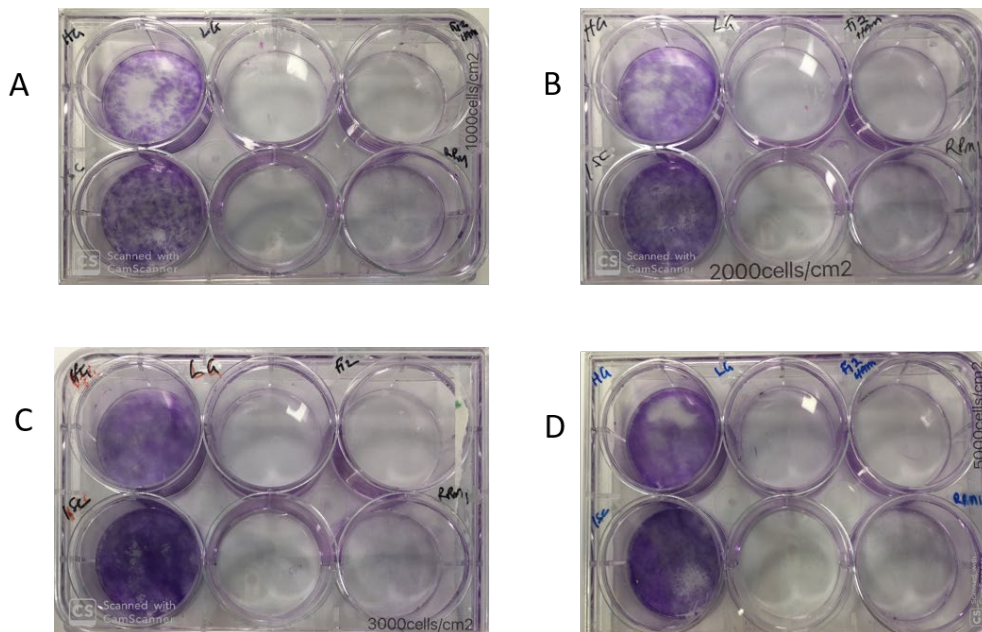
Figure 3.4 Representative colony formation assay plates after seeding HS-5 cells at high densities. Cells were seeded at (A) 1000 cells/cm^2, (B) 2000 cells/cm^2, (C) 3000 cells/cm^2 and (D) 5000 cells/cm^2 with 2 ml of medium in a 6-well plate and incubated for 14 days. Afterwards, cells were fixed with methanol and stained with crystal violet.

Number of colonies produced by these cells were assessed under an inverted phase contrast light microscope. Representative colony formation assay plates

3.3.1.2 HS-5 cells grow in different media

Following the previous observations that HS-5 cells can adhere to cell culture surfaces and grow in colonies with a fibroblast-like morphology as MSCs do in culture, cells were seeded in three chosen culture media – (DMEM-HG, RPMI 1640 and IMDM) – all supplemented with 10% FBS for 120 hours to determine the proliferation rate of these cells as discussed in section 2.8. Light micrographs of the HS-5 cells were taken every 24 hours for the duration of the experiment. Cell proliferation rate and percentage viability for these cells were determined every day for a total of 120 hours. Cells were seeded in triplicates for each 24 hours count.

Cells appeared singly, exhibited a spheroid shape and adhered to the culture flask within 24 hours after commencement of culture in all media used. However, the cells reverted to their characteristic fibroblast-like morphology in all media used after 48 hours. This may be due to the fact that these cells grow by forming colonies, which they seem to have formed after 48 hours. The cells' morphologies appeared to be similar in all media used however; fibroblastic projections of the cells in RPMI 1640 appeared to be highly elongated when compared to DMEM-HG and IMDM after 96 hours. A morphologically homogenous population of fibroblastic cells with 90% confluence was seen after 120 hours (Figure 3.5).

All the media used produced viable cells of over 90% (Figure 3.6A); DMEM-HG had the highest with 97% whilst RPMI 1640 had the least with 93% despite the morphological advantage it seems to confer on these cells. About 96% of the cells in IMDM were viable. However, there is no significant difference between the viability of the cells in these media. Furthermore, cells that were cultured in DMEM-HG had the highest cell count after 120 hours (Figure 3.6B) with a six-fold expansion rate (Figure 3.6C) and a doubling time of just over 41 hours (Figure 3.6D). This may be because DMEM-HG, as the recommended medium for these cells, provides the optimum culture conditions. RPMI 1640 produced similar results to DMEM-HG; with doubling time of 47 hours and four-fold expansion rate. IMDM had the least cell growth with a 3-fold expansion rate and doubling time of 54 hours. However, there was no statistical significant difference between

the rate of growth of HS-5 cells in these three media. Due to this reason, DMEM-HG was chosen as the culture medium for the growth of HS-5 cells throughout this study.
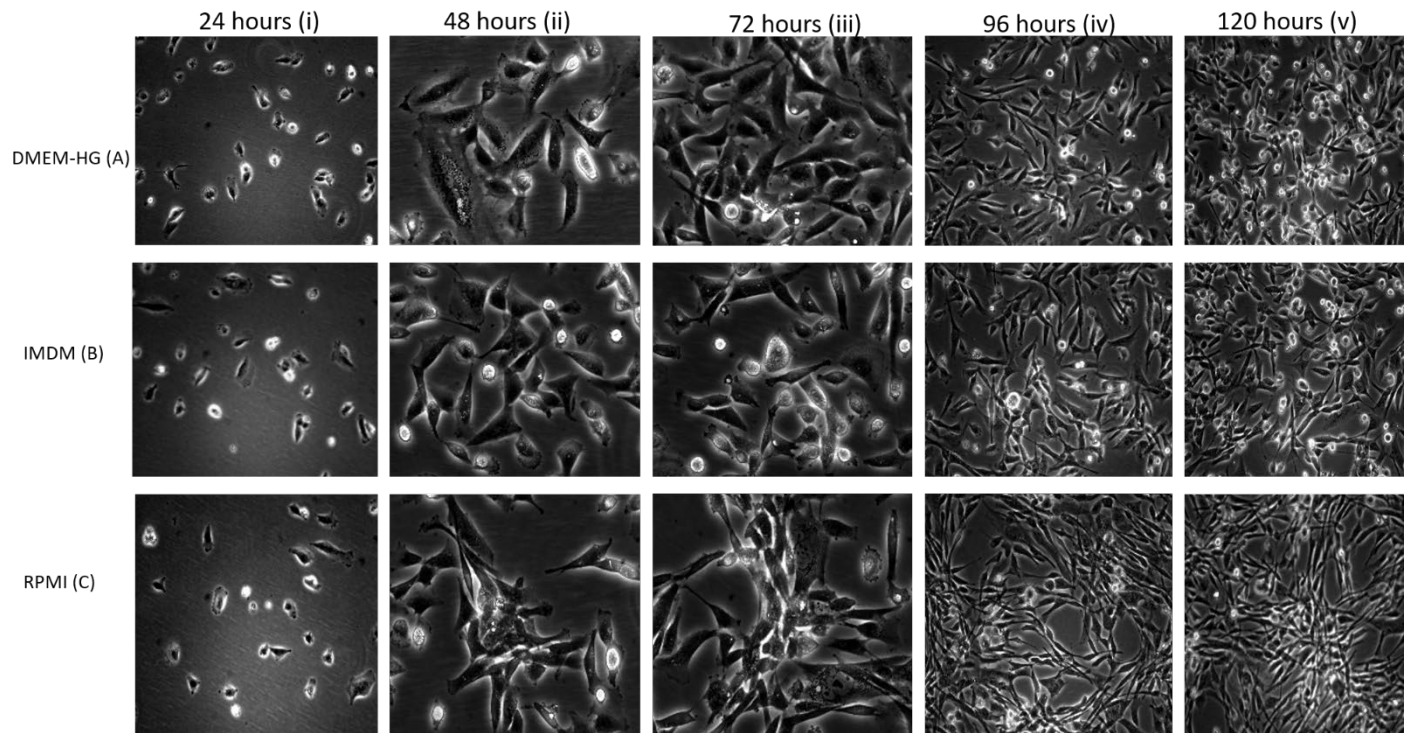
Figure 3.5 Morphology of HS-5 in different culture media. Photomicrographs were taken every 24 hours for five consecutive days when HS-5 were cultured in complete DMEM-HG (A), IMDM (B) and RPMI 1640 media (C). The fibroblastic morphology of HS-5 cells is observed in all media used. Cells were seeded at 10,000cells/cm^2 in a 25cm^2 culture flask with 5ml of medium. Representative results from 3 experiments are shown. Scale bar, 30μm.

A

Cell Viability after 120 hours

B

Cell Count HS-5 after 120 hours

C

Doubling Time

D
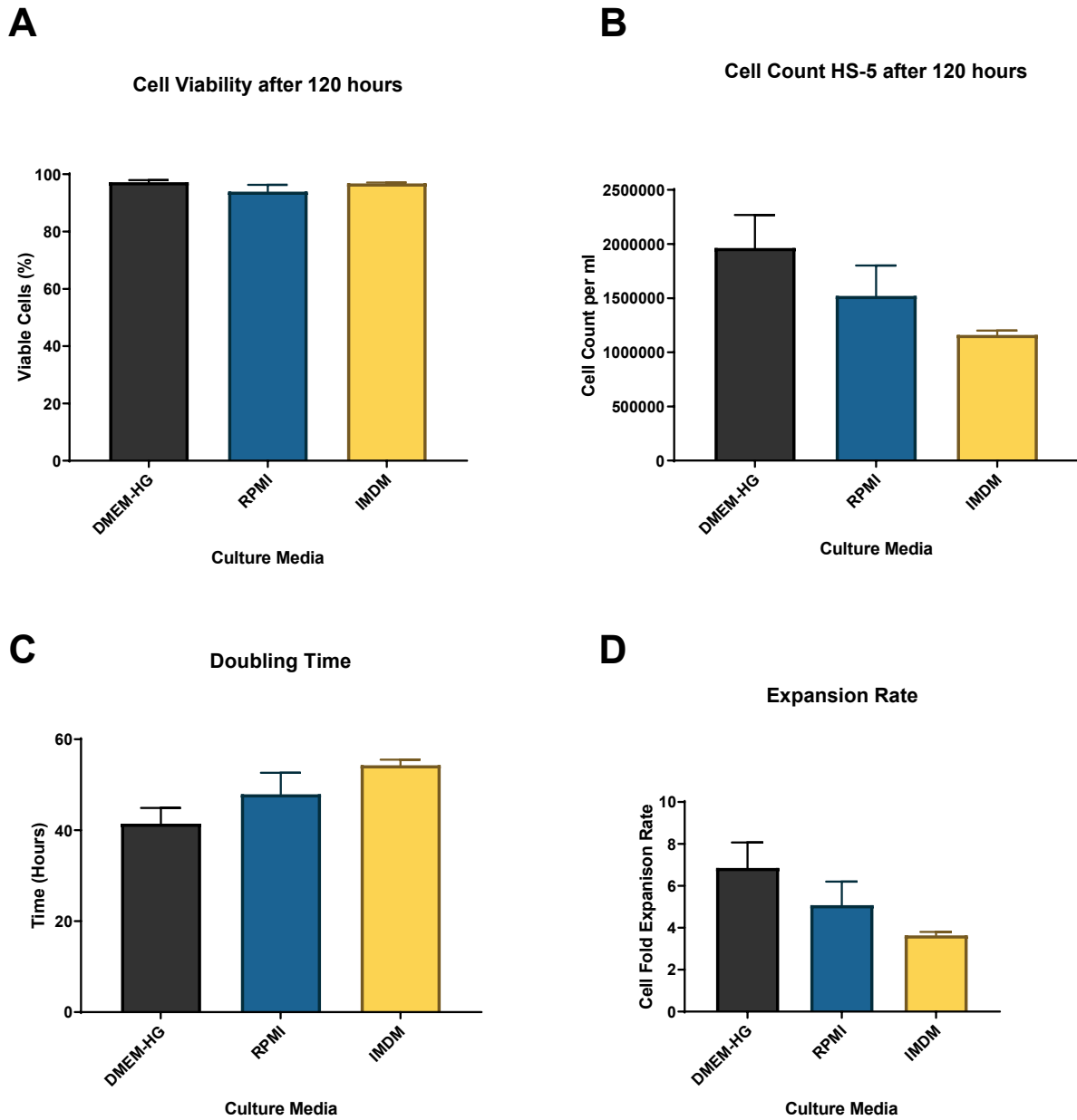
Expansion Rate

Figure 3.6 Proliferation of HS-5 cells. Cells were seeded at 10,000 cells/cm^2 in a 25cm^2 culture flask with 5ml medium and counted every day for 5 days. The cell viability (A), total live cells (B), doubling time (C) and fold expansion rate (D) of these cells in different media are shown here. The fold expansion rate shows how much the cells grew from their initial seeding density to the final count. Error bars show the mean ± SD (n=3). Statistical significance was done using the ANOVA for one-way factorial design.

3.3.1.3 HS-5 cells grow in medium supplemented with sEVs-depleted serum

Since DMEM-HG has been chosen as the appropriate medium for HS-5 cells to grow, different serum supplementation of DMEM-HG was tested inorder to ascertain the appropriate for vesicular studies. FBS used in cell culture may contain exogenous sEVS that may contaminate the endogenous sEVs isolated from cells. In order to eliminate this problem downstream, cells were grown in DMEM-HG supplemented with no FBS (serum-free medium), 10% FBS and commercially obtained exosome-depleted serum as previously described in section 2.8 to determine the growth potential of HS-5 in these media. This was to choose the appropriate medium for assessing sEVs involvement in CIBE. This is in reference to the minimal information for studies of extracellular vesicles (MISEV) guidelines proposed by the International Society for Extracellular Vesicles (ISEV) in 2018 (Thèry *et al.,* 2018). Percentage viability of the cells was determined after 41 hours, which has been previously ascertained as the doubling time for these cells in DMEM-HG.

Here, a similar rate in proliferation of cells was observed in these media. However, cells that were cultured in DMEM-HG with FBS had the highest cell count (8.89 x 10^5 cells/ml; Figure 3.7) as expected. This was followed by cells grown in DMEM-HG with exosome-depleted FBS with a cell count of 7.74 x 10^5 cells/ml. Less growth was seen in cells that were seeded in serum-free medium but the differences were not statistically significant for any of the culture conditions. Therefore, the results suggest that the reproducibility of cellular values is better for both FBS and exosome-depleted medium but more inconsistent for serum-free medium. As a result, DMEM-HG with exosome-depleted medium was confirmed as a suitable choice for culture and would be less likely to interfere with downstream analyses of sEVs and miRNA due to CIBE.
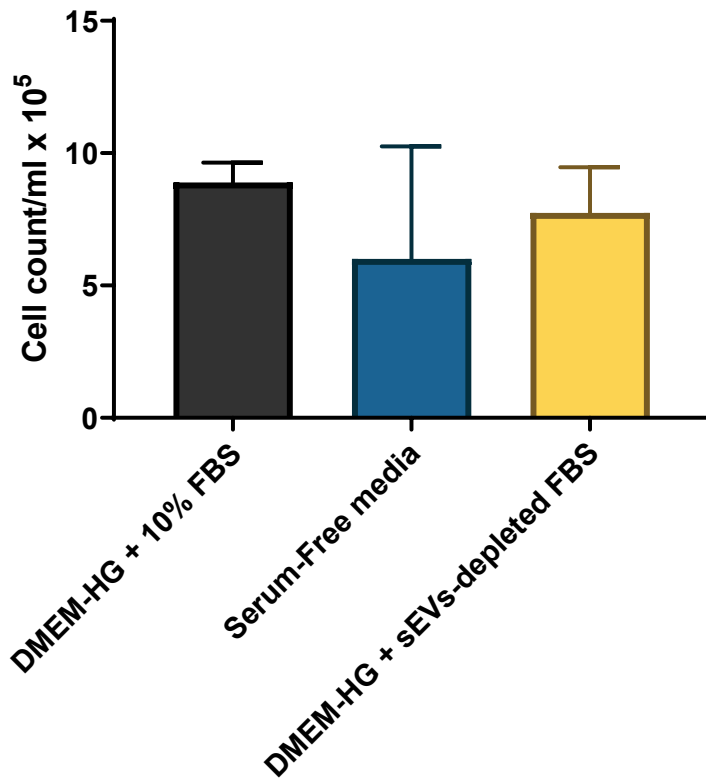
Figure 3.7 HS-5 cells can grow in DMEM-HG made-up with different serum supplements. Cells were seeded at 10,000 cells/cm^2 with 5 ml of medium in a T-25 culture flask and incubated for 42 hours. Percentage viability of the cells were determined. Error bars depict the mean ± SD (n=3). There was no statistically significant difference between the three media. Statistical significance was done using the ANOVA for one-way factorial design.

3.3.1.4 TK6 cells grow in different media

Following the previous observations that HS-5 cells can grow in DMEM-HG supplemented with FBS or sEVs-depleted FBS and RPMI 1640, TK6 cells were seeded in these three culture media to determine the proliferation of these cells as discussed in section 2.8. Cell proliferation rate and percentage viability for these cells was determined every day for a total of 72 hours. Cells were seeded in triplicates for each 24 hours count.

The growth rate curve of the cells in all media used is shown in figure 3.8A and illustrates that cells grow faster in RPMI 1640 compared to DMEM-HG. This may be because RPMI 1640 is the recommended medium for these cells that provides the appropriate environment for these cells

to grow optimally under standard conditions. However, there was no statistical difference between the growth rates of the cells in these media. Interestingly, the cells seeded in DMEM-HG grew at the same rate regardless of the serum supplement. Furthermore, the viability of the cells in all media was over 90% (figure 3.8B); DMEM-HG with FBS had the highest with 94.9% whilst RPMI 1640 had the least with 93.7% despite the growth advantage it seems to confer on the cells. About 94.8% of the cells in DMEM-HG with sEVs-depleted FBS were viable. However, there is no significant difference between the viability of the cells in these media.

In addition, the cells grown in RMPI 1640 had a four-fold expansion rate (figure 3.8C) and a doubling time of 16 hours (figure 3.8D). DMEM-HG produced similar results to RPMI 1640 irrespective of the serum supplement. DMEM-HG with FBS had a doubling time of 19 hours and a 3.82-fold expansion rate whilst cells grown in DMEM-HG with sEVs-depleted FBS had a 3.93-fold expansion rate and doubled within 18.3 hours. However, there was no statistical significant difference between the media. Since the cells have shown to be able to grow in all three media, RPMI 1640 was chosen to monoculture the cells whilst DMEM-HG with FBS was chosen for co-culture with HS-5 cells. DMEM-HG with sEVs-depleted FBS was used to grow the cells for vesicular studies.

Furthermore, when these cells were grown at a higher density (3×10^5 cells/ml) for 72 hours, the cells grew exponentially in all media (figure 3.9A) however the growth of the cells in RPMI 1640 slowed down after 48 hours, indicating that the cells grow at a higher rate in RPMI 1640 than in DMEM-HG with different serum supplements. This is further supported by the viability of the cells after 72 hours (figure 3.9B), which showed that the viability of the cells in RPMI 1640 dropped down to 87% compared to 91% and 93% in DMEM-HG with FBS and DMEM-HG with sEVs-depleted FBS respectively. This difference in viability in different media was statistically significant (RPMI 1640 vs DMEM-HG with FBS, p = 0.0030; RPMI 1640 vs DMEM-HG with sEVs-depleted FBS, p = 0.0002; DMEM-HG with FBS vs DMEM-HG with sEVs-depleted FBS, p = 0.0170). This suggests that the growth of cells in RPMI 1640 when maintained in an over-dense environment may have resulted in nutrient depletion, an accumulation of waste products, hypoxia or a combination of these events.

A TK6 Growth Curve
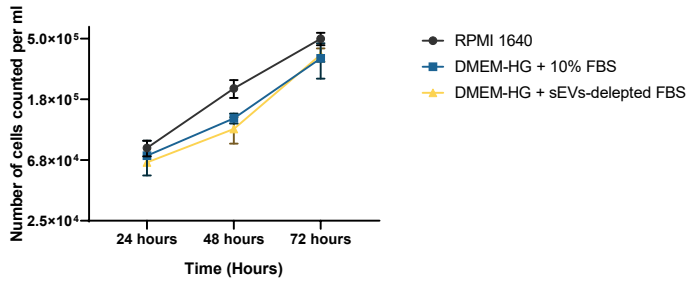
B TK6 cells viability after 72 hours
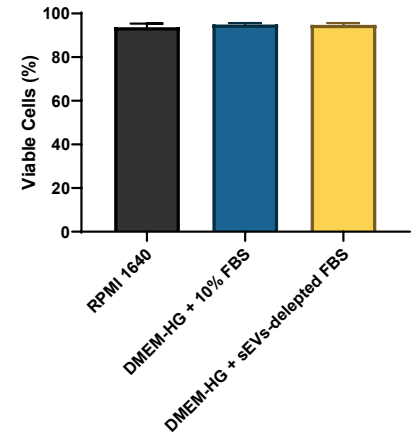
C TK6 cells Expansion Rate
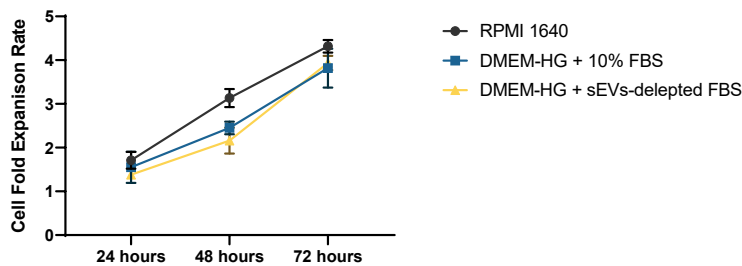
D TK6 cells doubling time
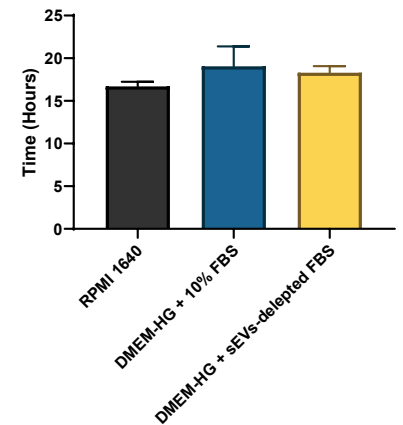
Figure 3.8 Proliferation of TK6 cells when seeded at low density. Cells were seeded at 2.5 x 10^4 cells/ml in a $25cm^2$ culture flask with 10ml medium and counted every day for 72 hours. The growth rate (A), total live cells (B), fold expansion rate (C) and doubling time (D) of these cells in different media are shown here. The growth rate curve shows how these cells grow exponentially in different media whilst this exponential growth from the initial seeding density to the final count is exhibited as the fold expansion rate. Error bars show the mean ± SD (n=3). Statistical significance was done using the ANOVA for one-way factorial design.

A
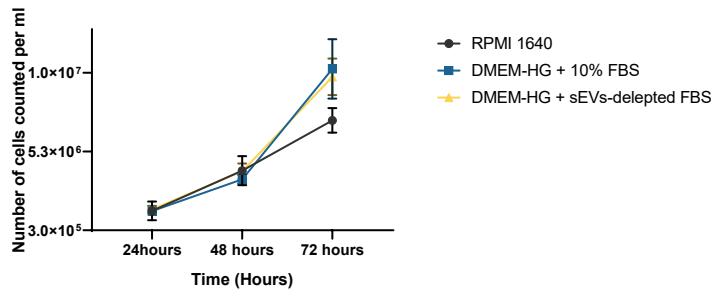
B
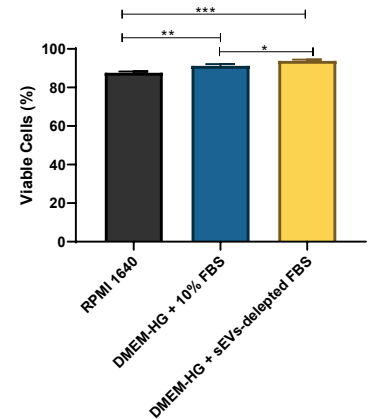
Figure 3.9 Proliferation of TK6 cells when seeded at high density. Cells were seeded at 3.0×10^5 cells/ml in a 25cm^2 culture flask with 10ml medium and counted every day for 72 hours. The growth rate (A) and total live cells (B) of these cells in different media are shown here. Cells grow exponentially in different media however the growth of cells in RPMI 1640 appears to be slow down after 48 hours. Error bars show the mean $\pm$ SD (n=3). Statistical significance was done using the ANOVA for one-way factorial design test (*$p<0.05$, **$p<0.01$, ***$p<0.001$).

3.4 Discussion

Cell culture conditions are crucial to the overall outcome of the study. A current survey in Nature by Baker (2016) revealed that many scientists fail to reproduce their own experiments. Therefore, it was important to set the suitable culture conditions for the cell lines to grow in order to ensure accuracy, reliability and reproducibility of assay outcomes. It is important to note that the co-culture model had been previously set up within the research group and described by Kelechi Okeke (personal communication). The two cell lines that were used were HS-5 stromal cells and TK6 lymphoblast cells, which were grown in DMEM-HG supplemented with FBS, 2mM L-glutamine and antibiotics. HS-5 is widely used as a model bone marrow niche cell line to understand the functionality of MSC (Weisberg *et al.,* 2008; Vangapandu *et al.,* 2017). TK6 lymphoblast cells was also chosen as the ideal cell line for this genototxicity study due to: (a) widely accepted status by the OECD for use in *in vitro* mammalian genetic toxicology studies (OECD, 2012). (b) Chromosomal stability and proficiency in cellular defence mechanisms (Lorge

et al., 2016. (c) Rich supply of benchmark data from key genetic toxicology labroatories around the world (Lorge *et al.,* 2016; Detringer *et al.,* 2017; Bryce *et al.,* 2017; Bryce *et al.,* 2018; Smart *et al.,* 2020).

Whilst the HS-5 cells and TK6 cells were separately grown in DMEM-HG and RPMI 1640 respectively, DMEM-HG was chosen as the appropriate medium for these cells to grow in co-culture. HS-5 and TK6 cell lines have also been utilized in co-culture systems. The results, supported by evidence in literature, suggest that these cells are quite flexible in which media they can grow in and can grow competently in several conditions. Recently, conditioned serum-free αMEM medium from HS-5 cells was used to co-culture NB4, an AML-derived cell line (Chen *et al.,* 2015). In another study, HS-5 cells was separately grown in DMEM-HG medium prior to co-culture, in RPMI 1640 medium supplemented with 10% FBS, with an AML cell line, HL-60 (Guan *et al.,* 2018). Furthermore, flow cytometry was used to study the live characteristic parameters of HS-5 cells in a hypoxic co-culture model with different AML cell lines (Podszywalow-Bartnicka *et al.,* 2018). Their cells were cultured in RPMI 1640 medium supplemented with 10% FBS whilst HS-5 cells was seeded on a collagen precoated glass bottom dish unlike in this study in which culture inserts were used to separate the cell lines. In addition, TK6 was also used to co-culture Caco-2 intestinal cells in RPMI 1640 with glutamax and supplemented with 5% FBS (Le Hègarat *et al.,* 2012) whereas in another study, TK6 was co-cultured with RAW264.7 macrophage cells in a modified transwell system containing DMEM-HG medium supplemented with 10% FBS (Kim *et al.,* 2016). In the Kim *et al.,* (2016) paper, the genotoxicity of the cells was measured following exposure to nitric oxide and ROS.

In this chapter, three approaches were taken to ascertain and confirm the suitable culture conditions for the stromal cell line, HS-5. In the first approach, the ability of the cells to form colonies or grow as CFU-F in five different culture media was investigated whilst in the second approach, the growth rate of the cells in three different culture media, chosen from the first approach, was calculated. Lastly, the suitable cell culture conditions to prevent contamination and/or enable optimal isolation of sEVs from the cells was also determined. Afterwards, the suitable culture conditions for TK6 cells was determined by growing the cells in different culture media. Sterile culture technique was employed whilst culture medium was replaced with fresh

medium every three days. Cell morphology and cell growth were monitored microscopically. CFU-F was also counted microscopically whilst cell viability was determined by trypan blue exclusion assay and AO/PI viability assay.

3.4.1 Cell culture medium: CFU-F colony formation

HS-5 cells were seeded at 'high' densities that correspond to normal culture conditions and at low densities, in five conventional cell culture media; DMEM-HG, DMEM-LG, DMEM-f12, IMDM and RPMI 1640 supplemented with 10% FBS. This is to fulfil one of ISCT criteria of confirming the functionality of stromal cells, which is the ability to adherently grow as CFU-F. This is also indicative of the proliferative and migratory abilities of MSC (Mareschi *et al.,* 2012). When cultured at low densities, the HS-5 cells formed colonies after 6-8 days and this is in line with the findings of Dexheimer *et al.,* (2011) who showed that MSC formed colonies within 7 days of culture. The colonies were also of varying sizes depicting the heterogeneous nature of HS-5 cells as MSC. These results herein are also similar to the reports of Mareschi *et al.,* (2012), which revealed that MSC colonies appear heterogeneous however; they considered clusters of 50 cells as colonies in contrast to this study in which 20 cells were considered. Twenty (20) cells is a reasonable cut-off to eliminate colonies that are actually growing from smaller 'clusters' of cells with ceased proliferation. Although DMEM-HG is usually the preferred medium of choice for MSC culture (Dexheimer *et al.,* 2011) however the medium that proved to be the most suitable for these cells to form colonies was RPMI 1640, followed by IMDM and then DMEM-HG. The cells produced more colonies in RPMI 1640 and IMDM compared to DMEM-HG. Culture conditions such as choice of culture media, supplements and serum compositions have been shown to have an effect on the phenotypes of MSC colonies and also cause a variation in CFU-F yield and number (Lapi *et al.,* 2008).

In addition, there seems to be a direct correlation between the number of cells seeded and the number of CFU-F colonies counted as the number of colonies increased in accordance with the number of cells. This is supported by a 2008 study, Neuhuber *et al.,* which revealed that MSC grow as very dense colonies at low plating density but spread evenly across the plates at high density. However, these findings are in contrast to the findings of Mareschi *et al.,* (2012), which

showed no direct correlation between the parameters. Nevertheless, in their study, when the cells were seeded at high densities between 1000 cells/cm^2 and 5000 cells/cm^2, cells formed colonies rapidly. The colonies were too large and overlapping to count in DMEM-HG, RPMI 1640 and IMDM but not in DMEM-LG unlike in the reports of Delk and Farasch-Carson (2012), which showed that HS-5 cells grow well in DMEM-LG supplemented with 10% FBS.

The results from this study suggest that the cells have spread evenly across the plates thus reaching confluency within 14 days of culture. As a result, the cells looked stressed and detached from the plastic surface. It took BM MSC (1000 cells) grown in T25 or T75 flasks to reach confluence within 16 days (Mareschi *et al.,* 2012). Confluence has been shown to affect MSC colony formation, particularly for 100% confluent cells. BM-MSC were able to form colonies as the confluence of the cells increased until reaching 80% followed by a decrease (Abo-Aziza and Zaki, 2016). In another study, cells seeded at high densities became overpopulated at the colony center and this led to the inhibition of cell growth at the colony center because of contact inhibition (Neuhuber *et al.,* 2008). The median number of colonies formed, in BM MSC extracted from donors, dropped from 62.5 at 10,000 cells/cm^2 to 11.3 at 100,000 cells/cm^2 (Mareschi *et al.,* 2012).

Therefore, these suggest that the stressed morphology of the cells seen in this study is typical of anchorage-dependent cells detaching from their surrounding extracellular matrix. Since HS-5 cells are anchorage-dependent cells that require adherence to plastic surface to proliferate, inability of the cells to adhere to the plastic surface may lead to growth arrest and induction of cell death (Merten, 2015).

3.4.2 Cell culture medium: Growth rate

To determine the growth rate of HS-5 cells, cells were grown in three culture media - IMDM, RPMI 1640 and DMEM-HG. The cells exhibited a fibroblastic-like morphology in all media used after just 48 hours. This is characteristic of all MSCs as previously reported by the ISCT (Ramakrishnan *et al.,* 2013). The fibroblastic projections of the cells were more elongated in RPMI 1640 than other culture medium. This is similar to the in-house findings of Kelechi Okeke (personal communication), which showed that the elongated projections found in RPMI 1640

89

were similar to those found in primary MSC. The morphologies of HS-5 in these media could be further explained by the possibility of these stromal cells differentiating into osteoblasts, adipocytes and chondrocytes (Nombela-Arrieta *et al.,* 2012). The ability of HS-5 to differentiate *in vitro* had been established within the research group.

However, the cells grew best in DMEM-HG after 120 hours, with a six-fold expansion rate in a doubling time of 41 hours. This is in line with the reported findings of Kabrah *et al.,* (2015) however they used DMEM-HG medium supplemented with 11% FBS and 2mM L-glutamine. Several researchers have also shown that HS-5 cells are capable of growing in DMEM-HG medium (Furukawa *et al.,* 2016; Wasnik *et al.,* 2016, Liao and Sharma, 2016; Sane *et al.,* 2018; Deynoux *et al.,* 2019). Nevertheless, the viability of the cells in these three media was above 90% thus highlighting the capability of these media in promoting optimum growth of these cells. Similarity in the results reported in DMEM-HG and RPMI 1640 may be due to flexibility of these cells to thrive in different culture conditions. In 2015, Chen *et al.,* reported that HS-5 cells are capable of growing in RPMI 1640 medium supplemented with 10% FBS. Also, Roecklein *et al.,* (1998) revealed that HS-5 cells can grow in RPMI 1640 medium containing 5% FBS as well as serum-deprived IMDM. However, it is important to mention that the later experiments do not go on for 120 hours but for 24 hours. Therefore, DMEM-HG was chosen as the appropriate medium to grow HS-5 cells in this study. The rationale is that although the cells can thrive in different culture conditions, growth rate and expansion rate of the cells was best in DMEM-HG.

The TK6 cells used in this study was also grown in DMEM-HG supplemented with heat-inactivated serum or sEVs-depleted serum, and RPMI 1640. The growth rate curves indicated that the cells grew exponentially in all media. This is similar to the previous report by Lorge *et al.,* (2016) that revealed that RPMI 1640 provides the optimum culture conditions for TK6 cells to grow. In another study, Chyall *et al.,* (2006) also revealed that TK6 cells grown in RPMI 1640 grow exponentially when diluted to optimal concentrations. Their cells doubled within 15 hours, which is similar to the results in this study that revealed a doubling time of 16 hours for these cells in RPMI 1640. In contrast to this study, Ngo *et al.,* (2019) illustrated that TK6 cells doubled within 20 hours in RPMI 1640. Furthermore, Kelechi Okeke (personal communication) also revealed that

TK6 cells are capable of proliferating optimally in DMEM-HG and RPMI 1640. The results herein suggest that TK6 cells can thrive in different culture conditions.

In addition, when the cells were seeded at a high density in these three media, the growth of the cells in RPMI 1640 slowed down after 48 hours thus suggesting that the cells may have become over-confluent thereby leading to nutrient depletion and starvation, accumulation of waste products, hypoxia or a combination of these events. This highlights the need to subculture and passage these cells atleast twice a week to ensure that the nutrients required for their growth are preserved and maintained. This is supported by the findings of Lorge *et al.,* (2016) that revealed that growth of TK6 cells was slower and the cell counts were lower in heavily confluent cultures in relation to exponentially growing subconfluent cells after 48 hours. Similarly, Chyall *et al.,* (2006) also illustrated that TK6 cells maintained at a higher density grow at a slower rate. They showed that the growth of TK6 cells slowed down when the cells were diluted to 3.1×10^5 cells/ml after 72 hours compared to cells that were diluted to 4.04×10^4 cells/ml.

Therefore, it is important that cells seeded from healthy exponentially growing cultures be used in genotoxicity studies. Over-confluent cultures may affect the growth of the cells thence making them to grow slowly, which may be detrimental to the outcome of the experiments. It has been previously reported that seeding of cells from over-confluent cultures leads to misleading genotoxicity data (Lorge *et al.,* 2016). However, it is important to mention that the later experiments such as genotoxicity assay (MN assay) last for 24 hours and not 72 hours (Chapter 4). Nevertheless, the ability of HS-5 cells and TK6 cells to grow in DMEM-HG medium with different serum supplements means that this medium can serve as the medium of choice for the co-culture of these cells in this study.

3.4.3 Cell culture medium: sEVs isolation

The composition of the cell culture medium used in the recovery of sEVs is a key factor in the production of sEVs. This is because these components are capable of influencing the production and/or composition of sEVs hence it is important to choose the right components and report them accordingly as directed in the ISEV guidelines (Thèry *et al.,* 2018). Different parameters of

cell culture such as glucose level, antibiotics and FBS can drastically alter the yield and cargo of sEVs. FBS contains sEVs, proteins and nucleic acids that may be co-isolated thus leading to interference in downstream *in vitro* studies (Wei *et al.,* 2016; Ludwig *et al.,* 2019). The commercially purchased FBS used in this study was depleted of exosome. The exosome-depleted serum was purchased in batches and the same one was used throughout the study to exclude any variations from that.

As a result, the cargo or purity of sEVs and their intended use downstream have to be taken into consideration during medium composition. This highlights the importance of ensuring that the medium that best aid the growth of HS-5 cells and yield sEVs with a stable cargo was selected and consistently used for cell culture. However, the compromise between optimal conditions for cell growth and those for sEVs production has made determining the optimal conditions for sEVs production a challenge. Some researchers opt to use commercial exosome-depleted FBS whilst others choose to use different in-house approaches to deplete the EVs in FBS as there is no standardized protocol for depletion of EVs in FBS (Samuel *et al.,* 2017; Panigrahi *et al.,* 2018; Lee *et al.,* 2019). Alternatively, many researchers choose to culture cells in serum-free medium during the period of EVs production (Haraszti *et al.,* 2019; Mannerstrom *et al.,* 2019).

Here, HS-5 cells were grown in DMEM-HG supplemented with no FBS (serum-free medium), 10% FBS and commercially obtained exosome-depleted FBS to determine the optimal conditions for cell growth and EVs production (chapter 5). The rationale here is that cells produce and release EVs continuously as a means of cellular communication but may be slightly increased or decreased in response to chemotherapy. Therefore, growing HS-5 cells in DMEM-HG with different serum supplements was important to ascertain the appropriate culture conditions that would not interfere with the composition of the vesicles produced and released by these cells following exposure to chemotherapeutic agents. Interestingly, HS-5 cells grew in all medium most especially in DMEM-HG with FBS. The growth rate in commercial exosome-depleted FBS was similar to that found in DMEM-HG with FBS. However, the manufacturer failed to describe the method used for EV depletion. The most common protocols for EV depletion in serum are ultracentrifugation and filtration, and these may result in loss of growth factors in FBS that may impede growth of cells (Ludwig *et al.,* 2019). In 2014, Eitan *et al.,* showed that EV-depleted FBS

obtained by ultracentrifugation has limited capacity to promote cell growth. This was later supported by the findings of Aswad *et al.,* (2016), which revealed that culture of skeletal muscle cells in EV-depleted FBS, obtained by ultracentrifugation, led to altered proliferation and differentiation of the cells. Nevertheless, this contrasts the findings in this study, which showed that commercial EV-depleted FBS has the capacity to support cell growth. This suggests that there are components in commercial EV-depleted FBS that may be absent in EV-depleted FBS by ultracentrifugation. These may be xenogeneic substances such as recombinant growth factors, which give the cells a proliferative advantage (Pachler *et al.,* 2017). It is noteworthy to mention that a full depletion of EVs may not be possible hence ISEV guidelines recommend the use of fresh medium not cultured with cells as controls in downstream EV assays (Thèry *et al.,* 2018), which can be seen in Chapter 5.

Furthermore, cell growth in serum-free medium was reduced compared to other medium used. This may be explained by extensive starvation of the cells, caused by lack of serum, thus changing cellular morphology and behaviour (Ludwig *et al.,* 2019). The number and content of released EVs can also be affected by serum conditions. Serum-free culture led to alterations in the quantity and protein composition of EVs derived from neuroblastoma cells (Li *et al.,* 2014). This is similar to the findings of Haraszti *et al.,* (2019), which revealed that serum-deprivation of MSC led to increased EV production and modification of its lipid and protein composition. However, it is important to mention that comparison of the production of EV by these cells in DMEM-HG with different serum supplements was not done as this isn't within the cope of this study.

3.5 Summary

This chapter has shed some light on the importance of optimization of cell culture conditions in order to produce reliable and reproducible data. The *in vitro* bystander co-culture model had been developed within the research group using HS-5 stromal cell line and TK6 lymphoblast cell line. Here, the functionality and characterization of HS-5 as MSC was identified via their ability to produce CFU-F in different culture medium such as DMEM-HG, DMEM-LG, RPMI 1640 and IMDM when seeded at low and high densities. The colonies were formed within days and the cells exhibited detachment from the plates when seeded at high densities.

HS-5 cells also showed that they could proliferate and differentiate in these media, with DMEM-HG chosen as the appropriate culture medium to drive this study forward. Following 120-hour culture, cells grew exponentially in six folds in under 41 hours. The other media, RPMI 1640 and IMDM, also proved to be good alternatives, with the cells doubling within 47 and 54 hours respectively. However, due to presence of EVs and other xenogeneic substances in serum that may hinder EV production and content, the optimal condition that would allow cell growth for downstream EV production was determined. Cells grew in all three media used, which were serum-free medium, DMEM-HG with FBS and DMEM-HG with exosome-depleted FBS. However, the latter was chosen as the medium to conduct all experiments as it showed that cells can grow in this growth medium. Exosome-depleted FBS also posed the least danger, from the literature, to contaminate the number and content of EV produced by these cells. Therefore, it was important to illustrate that TK6 cells were capable of growing in different media such as RPMI 1640, which is the recommended medium for these cells and DMEM-HG supplemented with FBS and exosome-depleted FBS. Although RPMI 1640 seemed to confer proliferative advantages to these cells, the cells grew exponentially in all growth media when seeded at a low density. However, the growth of cells in RPMI 1640 slowed down when seeded at a high density thus suggesting that this proliferative advantage conferred by RPMI 1640 may cause cells to grow at a faster rate and become over-confluent within a short period. As a result, DMEM-HG supplemented FBS was chosen as the medium for co-culture of HS-5 cells and TK6 cells in this study.

4.0 Evidence of chemotherapy-induced bystander effect

4.1 Introduction

Chemotherapy and radiotherapy can cause DNA damage by targeting the genome of actively dividing cells and thence result in genomic instability. The survival of an organism depends on the maintenance and stability of its genome and as a result, genomic instability can lead to the development and progression of leukaemia if the cell is a HSC. Leukaemia is characterised by DNA mutations such as DNA strand breaks (clastogenicity), point mutations and loss or gain of chromosomes (aneugenicity) caused by uncontrolled cell division (McCann and Wright, 2003). Furthermore, *de novo* primary malignancy such as DCL can also arise following chemotherapy and radiotherapy. This may be due to the transfer of residual chemotherapeutic effects from the exposed cells to their neighbouring cells through various signalling molecules, including cytokines and EV.

Intercellular communication can be propagated by live cells, both normal and tumour, in diverse ways through gap junctions and release of soluble factors into the extracellular fluid. These cells release autocrine and paracrine signals for normal cellular processes and in response to an impending threat or insult on their DNA. The recipient cell can either respond to these signals immediately or transfer these signals to their progenies however, the signals induced by genomic insult may cause genomic instability in the progenies (Perumal *et al.,* 2017). These signal-induced effects that manifest in the recipient cells that had not been initially exposed to direct genomic insult are known as BE. As previously described in section 1.8, these BE could equally manifest as cell death or formation of MN, which is one of characteristics of DNA damage.

It has been established that BE occurs following radiotherapy however there is evidence that other physical and chemical forms of cellular stress can also trigger BE. The BE triggered by these forms vary and depend on the dose, type of radiation/chemical agents, experimental model, and type of donor and recipient cells (Perumal *et al.,* 2017). Moolten and Wells first described the concept of CIBE in 1990, when they revealed that drug-treated cells can transfer treatment

signals to the untreated neighbouring cells thereby resulting in chemosesnsitivity. Since then, CIBE has become an area of interest for many researchers. There is evidence that alkylating agents such as cisplatin and MMC can induce CIBE via gap junctions or release of soluble factors into the CM (Jensen and Glazer, 2004; Rugo *et al.,* 2005; Asur *et al.,* 2009; Peterson-Roth *et al.,* 2009; Kumari *et al.,* 2009; Samuel *et al.,* 2017; Arora *et al.,* 2018). In addition, other alkylating agents such as fotemustine and cystemustine, which are chloroethylnitrosourea agents, have also been implicated in CIBE via release of proteins into the CM (Demidem *et al.,* 2006; Merle *et al.,* 2008). However, there is no evidence in literature that carmustine and chlorambucil, alkylating agents of interest in this study, can cause CIBE. The only evidence that these drugs can induce CIBE comes from an in-house study by Kelechi Okeke (personal communication), which revealed that these drugs transfer treatment signals to the neighbouring cells thus resulting in the formation of MN in the untreated cells.

Furthermore, topoisomerase inhibitors such as etoposide have been shown to induce CIBE. Prostate cancer cells, treated with etoposide, released microvesicles that induced DNA damage in the untreated cells upon uptake (Lin *et al.,* 2017). Although there is no evidence of mitoxantrone-induced CIBE in literature, the study by Kelechi Okeke (personal communication) also revealed that mitoxantrone caused formation of MN in the neighbouring cells. In addition, other antitumour antibiotics such as bleomycin and doxorubixin induced CIBE in cancer cells, PB lymphocytes and BMSC (Di *et al.,* 2008; Chinnadurai *et al.,* 2011; Chinnadurai *et al.,* 2013). Regardless of the drug employed in these studies, the biological endpoints of CIBE were cell death or inhibition of cell growth, chromosomal aberrations, DNA damage, MN formation and drug resistance. However, these effects could be delayed thereby inducing genomic instability in the progeny of bystander cells. Bleomycin-induced effect in bystander lung adenocarcinoma cells persisted at delayed times following co-culture (Chinnadurai *et al.,* 2013).

Whilst chemotherapy targets haematopoietic cell compartment in the BM microenvironment during pre-transplant conditioning, the MSC in the tumour microenvironment also undergo persistent damage from high-dose chemotherapy thereby resulting in phenotypic and functional abberations that may render them chemo-resistant (Kumar *et al.,* 2018). In addition, leukaemia

can alter and transform the MSC in the tumour microenvironment to differentiate into tumour-associated fibroblasts, which play crucial roles in chemo-resistance and tumour progression (Chan *et al.,* 2006; Castillo *et al.,* 2007). This may explain why MSC are capable of withstanding and resisting the cytotoxic and genotoxic effects of several drugs such as cisplatin, vincristine, paclitaxel, etoposide and camptothecin (Li *et al.,* 2006; Mueller *et al.,* 2006; Liang *et al.,* 2011; Bosco *et al.,* 2015; Bellagamba *et al.,* 2016). However, the pattern of MSC response to chemotherapy varies and depends on the drug; for example, drugs like busulfan, cyclophosphamide and methotrexate have reportedly failed to induce cell death in these cells. Regardless of the conflicting reports, the consensus is that the microenvironment remains of the host origin despite the damage incurred.

Therefore, it is important to understand the possible effects of the chosen drugs – chlorambucil, carmustine, etoposide and mitoxantrone – on HS-5 stromal cells and explore the potential transfer of the residual effects of chemotherapy to the bystander cells as the stroma remains host-origin following HSCT (Spyridonidis *et al.,* 2005; Bartsch *et al.,* 2009). In this chapter, an *in vitro* co-culture model was modified based on the previous work of Kelechi Okeke (personal communication) to represent the BM microenvironment and possibly show the interaction of the cells, caused by soluble factors released into the extracellular environment, leading to CIBE. Using HS-5 and TK6 as the model cell lines, separated by a culture insert, to mimic the BM microenvironment, cell death and DNA damage were assessed as bystander endpoints. DNA damage was assessed using the MN assay whilst cell death was measured based on the trypan blue exclusion dye assay. Longevity of the drug-induced bystander effects was also explored. Lastly, the mechanism of CIBE was explored by assessing differential miRNA expression profiles in the HS-5 and bystander TK6 cells.

4.2 Methods

4.2.1 The effect of chemotherapeutic drugs on HS-5 cells

HS-5 stromal cells were were seeded in a 12-well plate at a density of 132,000 cells per cm^2 in 500 μl DMEM-HG medium supplemented with 10% FBS and treated with different chemotherapeutic drugs: chlorambucil, carmustine, etoposide and mitoxantrone as described in section 2.9. All cell culture procedures were performed as discussed in section 2.3. Cell viability after drug treatment was determined by trypan blue assay and acridine orange/propidium iodide assay using the LUNA FL automated cell counter as described in section 2.10.

4.2.2 Recovery ability of HS-5 cells from chemotherapeutic effects

HS-5 stromal cells were treated with different chemotherapeutic agents for 1 hour and 24 hours respectively as described in section 2.9. Afterwards, the cells were washed with fresh medium and re-seeded in fresh DMEM-HG medium and allowed to grow for 72 hours to determine if the cells would recover from these chemotherapeutic effects. All cell culture procedures were performed as discussed in section 2.3. Cell viability after drug treatment was determined by trypan blue assay and acridine orange/propidium iodide assay using LUNA FL automated cell counter as described in section 2.10.

4.2.3 Bystander Effects

The *in vitro* co-culture bystander model was described in section 2.12. HS-5 stromal cells were treated with different chemotherapeutic agents for 1 hour and 24 hours respectively as described in section 2.9. Afterwards, the treated HS-5 cells were co-cultured, separated by a culture insert, with TK6 cells. After 24 hours, TK6 cells were harvested and cell viability was performed by trypan blue assay and acridine orange/propidium iodide assay using the LUNA FL automated cell counter counter as described in section 2.10. Genotoxicity was also assessed in the cells as described in section 2.11.

4.2.4 Bystander duration study

Conditioned medium from HS-5 cells was harvested as described in section 2.13.1 following exposure to chemotherapeutic agents for 24 hours. The conditioned medium was filtered with 0.22 μm filters to remove any cell debris before co-culture with TK6 cells (5×10^5 cells/ml) in a 12 well plate as described in section 2.13.2 over a period of five days. Filtered conditioned medium from treated HS-5 cells was used to seed fresh batches of TK6 cells every 24 hours and was repeated over a period of 5 days. Cell viability was performed by trypan blue assay and acridine orange/propidium iodide assay using the LUNA FL automated cell counter counter as described in section 2.10.

4.2.5 qRT-PCR array analysis in bystander TK6 cells

Following co-culture of TK6 cells with treated HS-5 cells as previously described in section 2.12, RNA from TK6 cells was extracted as illustrated in section 2.22.1. The purity and concentration (section 2.23) and integrity (section 2.24) of the RNA were determined, and converted to cDNA (section 2.25). The resultant cDNA was then used to perform microarray RNA analysis as described in section 2.26. Unknown miRNAs were quantitated by SYBR green based qRT-PCR (Section 2.28). Using the Ct value, the positive PCR control (PPC) and reverse transcription control (miRTC) served as quality control at every step of the process. The difference between the Ct values of PPC and miRTC were used to determine the success of the reverse transcription reaction whilst a Ct value of 19 ± 2 (PPC) was used to identify high quality RNA. The expression of 84 miRNAs was normalized with the average Ct value of six small nuclear RNAs – SNORD61, SNORD68, SNORD72, SNORD95, SNORD96A and RNU6B/RNU6-2. Fold changes in the level of each miRNA was relatively quantified using the comparative CT ($2^{-\Delta\Delta CT}$) method.

4.2.6 MicroRNA profiling and bioinformatics

Five upregulated miRNAs (miR-146a-5p, miR-30d-5p, miR-16-5p, miR-17-5p and miR-20a-5p) and one downregulated miRNA (miR-200c-3p) were chosen as candidates in this study. To predict the target genes of these miRNAs, different target prediction programs that offer information on human miRNA-miRNA interaction were used as described in section 2.7. The genes chosen by

these different target prediction programs were collated together and functional enrichment analysis was performed as described in section 2.7. The FunRich software produces data on the biological processes the predicted target genes of these miRNAs are involved in.

4.2.7 Validation of miRNA in HS-5 and bystander TK6 cells

The expression of the candidate miRNAs (miR-146a-5p, miR-30d-5p, miR-16-5p, miR-17-5p, miR-20a-5p, and miR-200c-3p) was validated in the treated HS-5 cells and the bystander TK6 cells by qRT-PCR as described in section 2.28. The RNA from the cells were extracted (section 2.22.1), purity (section 2.2.3) and integrity (section 2.24) measured before converting the RNA to cDNA (section 2.25). The newly synthesized cDNA was diluted with 200 µl of RNAse free water to ensure at least 50 pg – 3 ng of cDNA per PCR. Each sample was run in duplicate for analysis using the same cycling conditions as previously mentioned in section 2.26. The Ct value of each microRNA was normalised using small nuclear RNAs (SNORD61 and RNU6B/RNU6-2) as internal controls for cells whilst miR-150-5p was used as a negative control. GeNorm and NormFinder softwares were used to analyse the small nuclear RNAs to ascertain those that were appropriate for data normalization. Fold changes in the level of each microRNA was relatively quantified using the comparative CT ($2^{-\Delta\Delta CT}$) method.

4.3 Results

4.3.1 Chemotherapeutic drugs induce cytotoxic effects on HS-5 cells

4.3.1.1 Cytotoxicity effect of chemotherapy on HS-5 cells

To determine the effect of chemotherapeutic drugs employed in pre-transplant conditioning on MSC, cells were seeded in duplicate at 132,000 cells per cm^2 with 500 µl of medium in a 24 well plate and treated with increasing doses of the 4 drugs for an hour and 24 hours. The highest dose of each drug represents the clinically relevant dose used in transplantation settings. Thus, these doses were not exceeded because higher doses would not be used *in vivo.* Each drug group produced a cytotoxic effect on the cells after 1 hour and 24 hours (Figure 4.1).

A

1-hour drug treatment

B

24-hour drug treatment
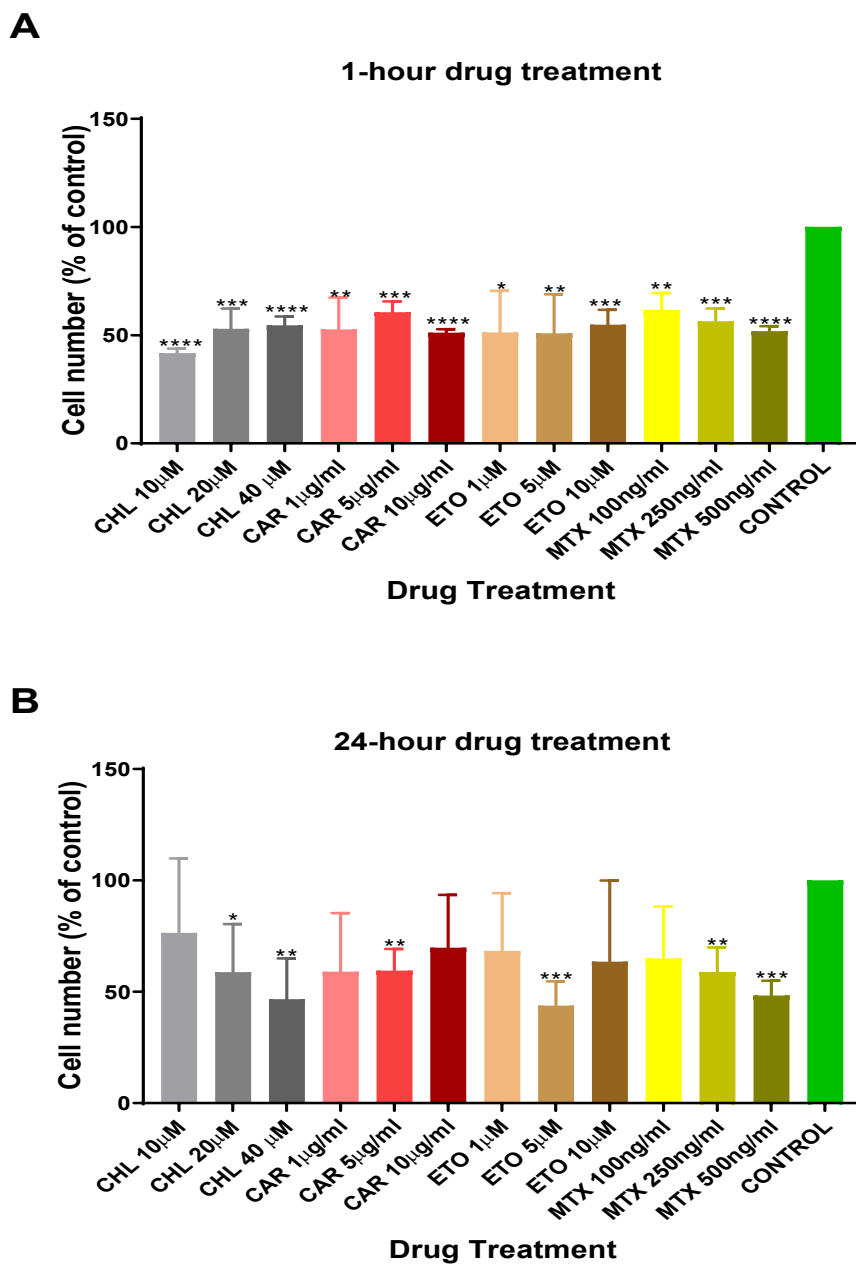
Figure 4.1 The effect of chemotherapy on HS-5. Cells were incubated with increasing doses of alkylating agents (chlorambucil [CHL], carmustine [CAR]) and topoisomerase inhibitors (mitoxantrone [MTX] and etoposide [ETO]) for an hour (A) and 24 hours (B). The drugs are colour coded as increasing shades of the same colour. Data shows the mean ± SD (n=3) and represent the percentage of live cells relative to the untreated control. Statistical significance was done using unpaired student t-test (*$p<0.05$, **$p<0.01$, ***$p<0.001$, ****$p<0.0001$).

However, the drugs were more toxic to the HS-5 cells after an hour than 24 hours. This suggests that drugs are capable of inducing cytotoxic effects in the cells after just an hour but upon longer

exposure, the cells may undergo signal transduction that ultimately results in a cellular response that aids them withstand these chemotherapeutic effects. Nevertheless, mitoxantrone exhibited a dose-dependent cell death at both time points. Although chlorambucil also produced a similar effect after 24 hours, it induced more cell death at low doses (41.7% and 52.9%) when compared to the clinically relevant dose (54.5%) after an hour. These suggest that chlorambucil rapidly exerts its effects on the cells at all doses but upon longer exposure, the cells evade cell cycle checkpoints thereby undergoing incomplete cell death activation and survival of cells at low dose. Etoposide also exhibited an increase in cell death at 5 µM at both time points compared to the clinically relevant dose of 10 µM, which appeared to be less toxic to the cells. Carmustine produced the highest level of cell death at its clinically relevant dose (10 µg/ml) after an hour however, an increase in cell survival was achieved after 24 hours compared to its low doses (1 µg/ml & 5 µg/ml). The reason why these drugs are more toxic at low concentrations than at high concentrations may be due to signal transduction that results in non-specific binding of the drugs to their targets on the cells at high concentrations thus causing the drugs to bind to unintended targets and perhaps survival of the cells. Nevertheless, these results suggest that these drugs may damage the BM microenvironment and attention should be paid to the marrow stromal damage induced by these chemotherapeutic drugs as these agents are widely used in clinical settings during HSCT.

4.3.1.2 The rate of recovery of HS-5 cells from chemotherapy varies and depends on the drug

Since the microenvironment remains of host origin after chemotherapy, it was important to see if this is similar in the current model cell line. Following the induction of cell death in HS-5 cells by chemotherapy, the cells were monitored and assessed afterwards to see if they can recover from the cytotoxic damage induced by these drugs. Chemotherapy-treated cells (for 1 hour and 24 hours) were washed free of drugs, re-suspended in fresh medium and allowed to grow for three days. It is important to mention that the seeding density of the cells was not re-adjusted after treatment; only what was left after treatment was re-seeded. The rationale behind this is that although the cells reduced in number after chemotherapy as seen in figure 4.1, the cell

numbers did not go below 40% of the control cells hence the seeding density is enough to support the proliferation of the cells. For full recovery, the cells would need to overcome drug-induced cell death and proliferate at a similar rate as the control. In the cells treated for an hour, HS-5 cells showed improved recovery of proliferaton when the alkylating agents: chlorambucil and carmustine were removed (figure 4.2).

However, the cell number was still lower than the control at their clinically relevant doses (68.4%, CHL; 65%, CAR). This further suggests that cells treated at a lower dose of these chemotherapeutic drugs may survive with genomic damage despite the therapeutic insult. In contrast, cells treated with chlorambucil after 24 hours showed sustained suppression of proliferation at 20 μM (27.6 %) and 40 μM (9.22%). It is possible that upon longer exposure, chlorambucil undergoes metabolism to its active metabolite phenylacetic mustard, which also has cytotoxic and anti-proliferative effects thus explaining the reduced cell numbers compared to the control at these doses. As a consequence, the cells appear to have evaded the repair mechanisms to undergo cell death.

Interestingly, mitoxantrone sustained its cytotoxic effect even after 72 hours when compared to the same time-point controls. Etoposide also revealed sustained proliferation in cells that were exposed to drugs for 24 hours. Since all four drugs produced similar toxic effects at both timepoints, these results suggest that these topoisomerase inhibitors induce DNA-damaging effects that may be persistent in the cells thus disrupting the growth of the cells during recovery. These also highlight the existence of drug/target interactions even at low drug concentrations, which may be enough to induce persistent alteration in cellular processes.

A

Cell Survival after 72hrs (1-hour treated cells)
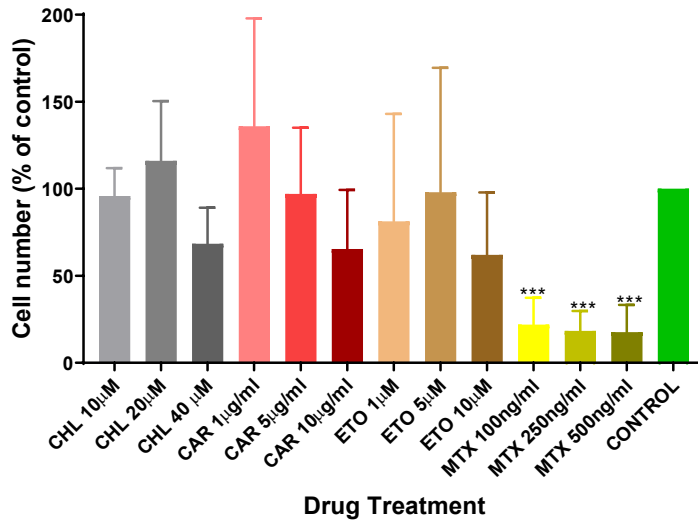
B

Cell Survival after 72hrs (24-hour treated cells)
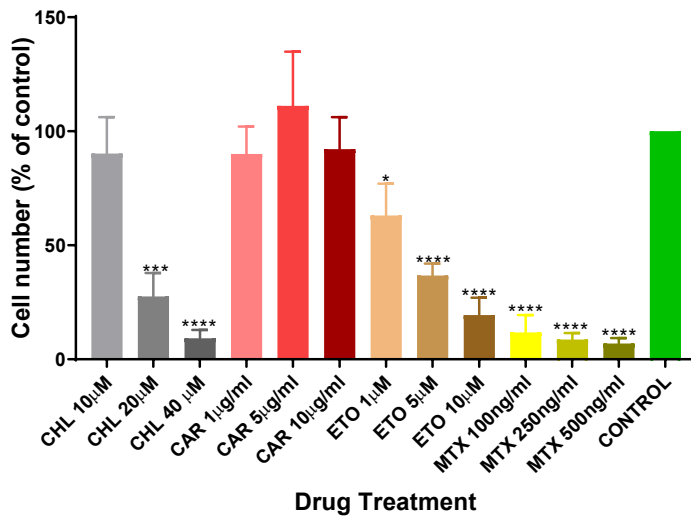
Figure 4.2 Recovery of HS-5 following exposure to chemotherapy. Cells were incubated with increasing doses of chemotherapeutic agents (chlorambucil [CHL], carmustine [CAR], mitoxantrone [MTX] and etoposide [ETO]) for 1 hour (A) and 24 hours (B), washed with PBS and then cultured in complete medium for another 72 hours. Data shows the mean ± SD (n = 3) and represent the percentage of live cells relative to the untreated control. Statistical significance was done using unpaired student t-test (*$p<0.05$, **$p<0.01$, ***$p<0.001$, ****$p<0.001$).

4.3.2 Chemotherapy-induced bystander effect

4.3.2.1 Bystander cytotoxic effects are induced in TK6 cells co-cultured with chemotherapy-treated HS-5 cells

To ascertain if MSCs can transfer the cytotoxic effects of chemotherapy to a neighbouring cell, HS-5 cells were cultured with clinically relevant doses of chlorambucil, carmustine, etoposide and mitoxantrone for 1 hour and 24 hours, washed free of drug with PBS and then co-cultured with TK6 using 0.4 µm pore size culture insert in a 12 well plate. The cells were co-cultured for 24 hours. Interestingly, mitoxantrone-treated HS-5 cells induced a decrease in cell number relative to the control in the bystander TK6 cells [1 hour (74% p = 0.0030) vs 24 hours (79% p =0.04)] at both time points (Figure 4.3). This suggests that the persistent cytotoxicity seen in HS-5 cells following mitoxantrone treatment could be transferred to the bystander TK6 cells thereby inducing cytotoxic effects in these cells. This also highlights the possibility that HS-5 cells release signalling molecules capable of migrating via medium to the bystander cells to induce a cellular response.

TK6 cells following 24-hour co-culture with drug-treated HS-5 cells (1 hour)

A
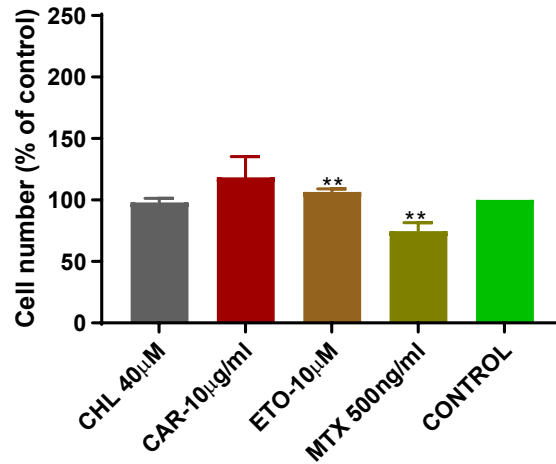
TK6 cells following 24-hour co-culture with drug-treated HS-5 cells (24 hours)

B
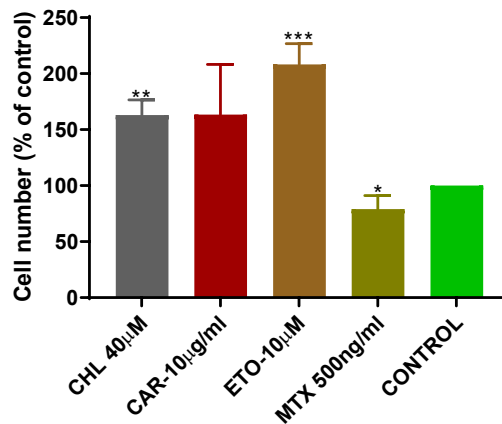
Figure 4.3 Chemotherapy induces varied bystander effects in TK6 cells depending on the drug. HS-5 cells were treated with clinical doses of drugs and washed with PBS before co-culturing them with TK6 cells using a cell culture insert. Data show mean ± SD (n=3) of percentage total cells relative to the untreated control. Statistical significance was done using the unpaired student t-test (* $p<0.05$, ** $p<0.01$, *** $p<0.001$).

In contrast, the TK6 cells exhibited an increase in cell number following exposure to HS-5 cells treated with chlorambucil, carmustine and etoposide. The cells proliferated at an abnormal rate compared to the controls at both time points. Carmustine produced the highest increase in cell

number after 1-hour treatment (118.5%) whereas etoposide did the same after 24 hours (208.1%) however; the reason for this is unclear. It can be inferred that the HS-5 cells may accumulate genetic damage and may aim to 'protect' the bystander cells by promoting their proliferation to replace any lost cells via the signalling molecules released into the medium by HS-5 cells. If this is the case then an increase in proliferation of the bystander TK6 cells may have more devastating effects than a decrease in cell proliferation longterm. An increased proliferation of the cells along with evasion of the cell cycle checkpoints due to increased cell division may suggest that the bystander cells might become cancerous in future.

4.3.2.2 TK6 cells exhibit bystander genotoxic damage following exposure to drug-treated HS-5 cells

The induction of MN formation in TK6 cells was also assessed following co-culture with chemotherapy-treated HS-5 cells to ascertain the level of genotoxic damage in the bystander cells. As shown in figure 4.4, mitoxantrone induced MN formation in the bystander cells, which was statistically significant at both time points [1 hour (118 MN scored p = 0.0004) vs 24 hours (92.3 MN scored p = 0.0025)]. The manual scoring system remains an important source of variability notwithstanding that the criteria for scoring have been standardized inorder to minimise analysis error. Nevertheless, the cells must be atleast 50% viable following exposure to a genotoxic agent for genotoxicity data to be valid. In addition to its induction of MN formation, mitoxantrone induced decreased cell proliferation to 74.7% and 79.1% at both time points (figure 4.3). Therefore, it can be inferred that mitoxantrone gives the strongest bystander effects.

However, etoposide, carmustine and chlorambucil, which induced an increased proliferation in the bystander cells, also induced MN formation in these cells at both time points but none of the drugs showed a statistically significant difference between the drug group and the control. Collectively, these infer that a genotoxic bystander effect from chemotherapy treatment exists. Etoposide induced the highest increase in bystander cell proliferation and produced high MN induction in the bystander cells however, it is inconsistent when compared to mitoxantrone. These further suggest that despite the survival of the bystander cells, these cells accumulate

genomic damage perhaps because of increased cell division, which may have adverse effects longterm.

MN induction in TK6 cells following expsoure to drug-treated HS-5 cells (1 hour)

MN induction in TK6 cells following expsoure to drug-treated HS-5 cells (24 hours)
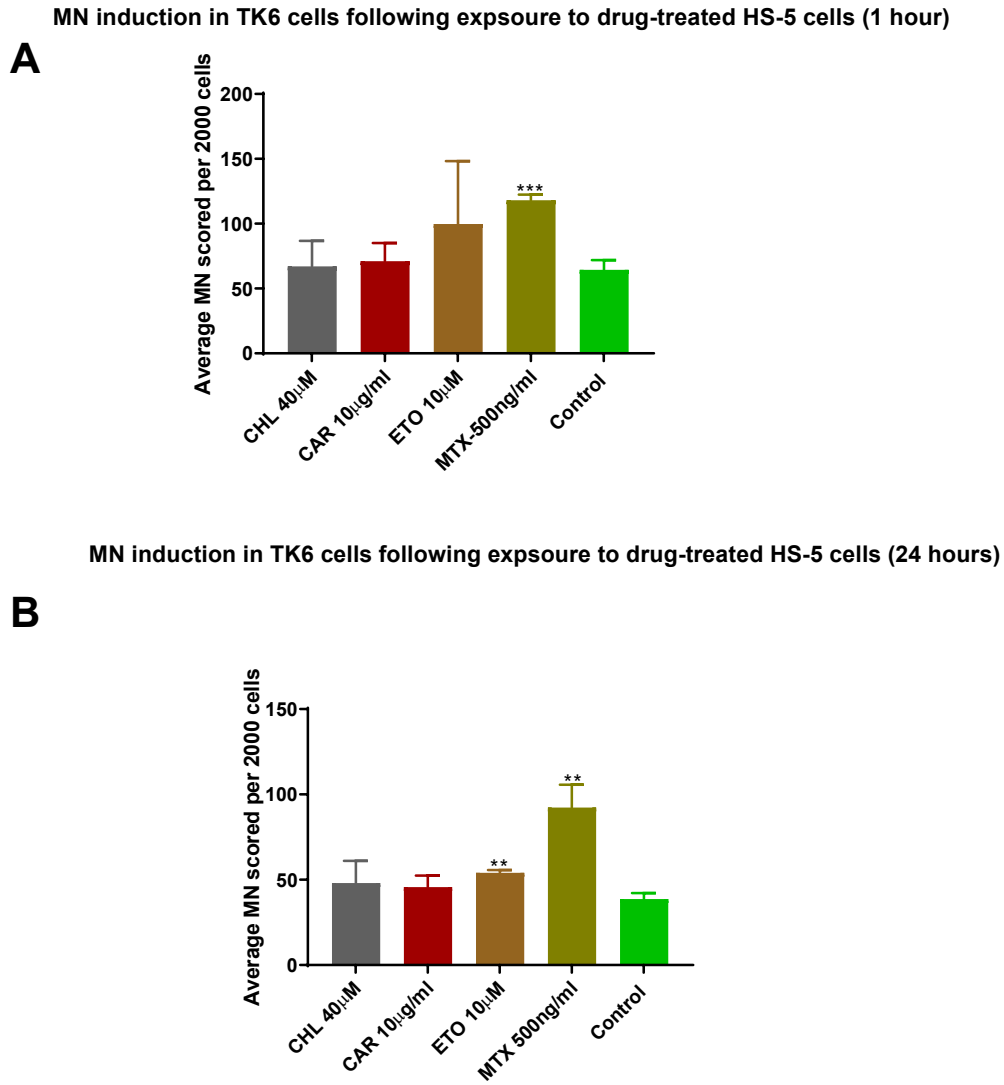
Figure 4.4 Chemotherapeutic drugs induce MN formation in bystander TK6 cells. 24-hour co-culture of TK6 cells with HS-5 cells that were treated with drugs for an hour (A) and 24 hours (B) resulted in the formation of MN in these cells at different time points. Data show mean ± SD (n=3) of average MN scored per 2000 cells. Statistical significance was done using the unpaired student t-test (**$p<0.01$; ***$p<0.001$).

4.3.2.3 Bystander damage induced in TK6 cells by chemotherapy lasts over 5 days

The duration of BE was investigated over five days to ascertain if these effects are maintained for that period. The five-day gap was chosen in order to correspond to the total gap in time, which a patient is allowed to recover from the effects of pre-transplant conditioning prior to infusion of stem cells. As previously described in section 2.13.2, HS-5 cells were conditioned for 24 hours with clinically relevant doses of chlorambucil, carmustine, mitoxantrone and etoposide before harvesting the conditioned medium, which was then used to seed TK6 cells for 24 hours. Afterwards, the lymphoblastic cells were harvested and assessed for viability. This process was repeated for 5 days as the conditioned medium was double filtered with a 0.22 µm filter every day to remove cellular debris and then used to co-culture a new batch of lymhoblastic cells seeded at 2.5 x 10^5 cells/ml.

As shown in figure 4.5, alkylating agents (chlorambucil and carmustine) induced little or no reduction in cell numbers rather chlorambucil increased the proliferation of the cells after day 1 (103%) in comparison to the control but this was not significant. This is similar to the bystander cytotoxicity data presented in figure 4.3, which resulted in an abnormal increase in bystander cell proliferation after 24-hour co-culture with drug-treated HS-5 cells. The number of the cells seeded in chlorambucil-treated CM in relation to the control ranged from 93.9% to 113.5%, with the latter the highest cell number recorded on day 3. These suggest that chlorambucil promotes variable proliferative effects in the bystander cells. Similarly, the viability of cells exposed to carmustine-treated CM changed from 98.1% (day 1) to 114.2% (day 3) over 3 days relevant to the control. However, the viability slightly reduced to 98.2% on day 4 and maintained a similar count (98.9%) after day 5. This indicates that carmustine promotes increased bystander cell proliferation up to 3 days but then confers bystander cytotoxicity from day 4 to 5. In addition, this contradicts the bystander cytotoxicity data that revealed an increase in cell numbers to 163% compared to the control. Nevertheless, it is clear that the bystander cells survive despite exposure to HS-5 cells treated with alkylating agents and medium conditioned by these drug-treated HS-5 cells.
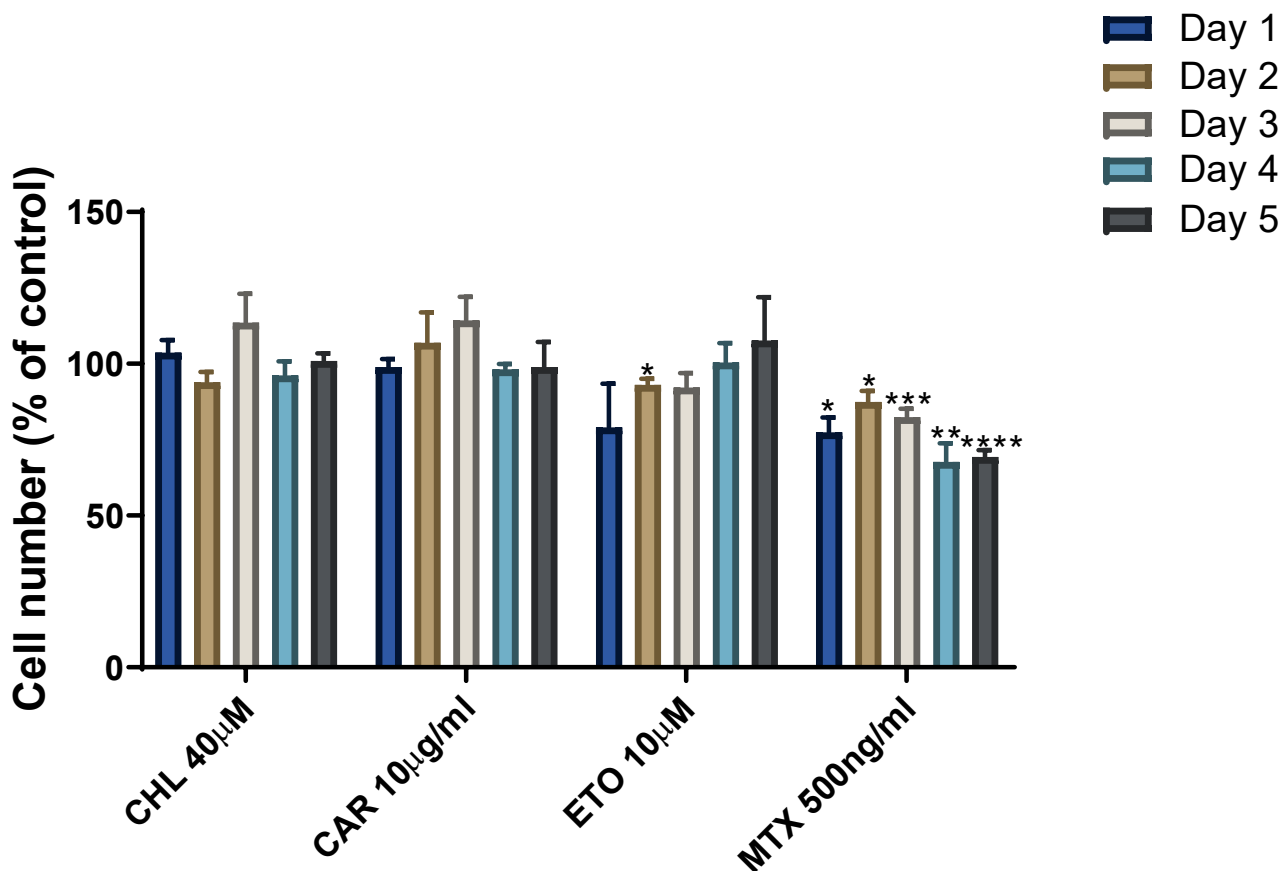
Figure 4.5 Chemotherapy-induced BE can last over five days. Seeding TK6 lymphoblast cells in medium conditioned with chemotherapy led to differential effects on the viability of the cells depending on the drug involved. Data show mean ± SEM (n=3) of percentage total cells relative to the untreated control. Statistical significance was done using the two-way ANOVA (* $p<0.05$, **$p<0.01$, ***$p<0.001$, ****$p<0.001$).

Contrastingly, topoisomerase inhibitors (ETO and MTX) reduced the number of cells in relation to control to 79% and 77% respectively on day 1. MTX maintained this effect over the five day period with the lowest reduction in the number of cells recorded on day 4 (67.7%) followed by day 5 (69.3%). All these were still above the 50% threshold recommended by OECD in its guidelines. Therefore, results suggest that mitoxantrone is the most toxic to the cells similarly as was shown in the co-culture experiment using culture inserts (section 2.12). The bystander cytotoxicity data revealed that bystander cell number percentage reduced to 79.1% relative to the control. In contrast, the cells recovered from the toxic effects of ETO and gradually increased

its viability to 93.1%, 92.2%, 100.4% and 107.6% respectively from day 2 to day 5. Thus, this suggests that ETO continues to promote bystander cell proliferation over 5 days at a rate that is higher than the control because the cell number percentage appears to be increasing. This corresponds to the data from the bystander cytotoxicity data, which exhibited that ETO causes a marked increase in bystander cell proliferation. Nevertheless, it is noteworthy that these bystander cells showed good viability in response to the drugs and this could be highly relevant if it is associated with increased genotoxic events and may lead to mutagenic events *in vivo.*

4.3.3 Differential miRNA expression profiles in cells

Leukaemia treatment is often performed in cycles and any change in gene expression profiles of the MSC could lead to resistance to chemotherapy and progression of leukaemia. As a result, the miRNA signature profiles of HS-5 cells and bystander TK6 cells were examined to determine if these drug-induced effects could alter the expression of miRNA by these cells. Since a relay of damaging effects can cause bystander effects as previously shown in section 4.22, the rationale here is that miRNA control gene expression at the post-transcriptional level hence any deregulation of miRNA expression in the cells may have important biological implications. Mitoxantrone was chosen as the main drug of interest due to consistency in its ability to transfer both cytotoxic and genotoxic effects to the bystander cells.

4.3.3.1 qRT-PCR array analysis of miRNA expression in bystander TK6 cells

Firstly, microarray analysis of TK6 bystander cells was assessed by qRT-PCR in order to choose candidate miRNAs in the microRNAome of the bystander cells that could be involved in this CIBE. The rationale here is that if miRNAs were transferred from HS-5 cells to TK6 cells then a candidate miRNA has to be upregulated in the bystander cells to effect CIBE. By identifying these upregulated miRNA candidates in the bystander cells, their expression levels can then be explored in drug-treated HS-5 cells to see if they had been transferred via the CM.

As described in section 2.28, RNA from these bystander cells, obtained following co-culture with treated HS-5 cells, were converted to cDNA and used to profile the expression of 84 human miRNA signatures. Ct values were obtained and normalised using six small nuclear RNAs. Ct values are inversely proportional to the amount of miRNAs in the sample. The lower Ct values (below 30 cycles) indicate high amount of the miRNA target sequence whilst the higher Ct values (above 35 cycles) reveal low amount of the miRNA target sequence but can also reveal problems with the target or the experimental set up. Fold changes in the level of each miRNA was relatively analysed by comparing with the untreated control and quantified using the comparative $2^{-\Delta\Delta CT}$ method.

Whilst choosing the candidate miRNAs, it is noteworthy to mention that only miRNAs with Ct values below 30 were considered for analysis inorder to be accurate and minimise analysis error. In addition, the fold change cut-off was set at ≥1.5 whilst statistical significance *p*-values of ≤0.05 was considered as the cut-off inorder to eliminate any cofounding effects that may skew data analysis and interpretation. Where a miRNA is increased by ≥1.5 folds without statistical significance, miRNAs close to the statistical significant *p*-value cut-off was chosen. Table 4.1 shows the miRNAs that had Ct values of less than 30 and were upregulated in bystander cells. The most upregulated miRNA in these cells was hsa-miR-30d-5p (1.89), followed by hsa-miR-155-5p (1.82) and hsa-miR-146a-5p (1.78) respectively. However, none of these was statistically significant. Similarly, miRNAs that had Ct values of less than 30 and were downregulated in bystander cells are shown in table 4.2. The most downregulated miRNA in these cells was hsa-miR-200c-3p (-6.20) followed by hsa-miR-92a-3p (-1.71). However, none of these was statistically significant. Although one of the rules set above for choosing a candidate miRNA include upregulation of the miRNA, hsa-miR-200c-3p was chosen as the only downregulated candidate miRNA given its large change here. A loss of signal could affect the viability and functionality of cells if an essential message was silenced hence for this purpose, it was relevant to follow up on such a large loss of signal.

Table 4.1 List of upregulated miRNAs that are in bystander TK6 cells with Ct values less than 30.

MiRNA(s)	Control (Average Ct value)	Treatment (Average Ct value)	Fold change	Fold Regulation	95% CI	*P*-value
hsa-miR-30d-5p	29.17	29.27	1.89	1.89	0.00001, 3.99	0.339
hsa-miR-155-5p	24.22	24.37	1.82	1.82	0.00001, 5.88	0.407
hsa-miR-146a-5p	28.06	28.25	1.78	1.78	1.00, 2.57	0.076
hsa-miR-30e-5p	29.99	30.21	1.74	1.74	0.00001, 5.08	0.422
hsa-miR-103a-3p	28.82	29.06	1.73	1.73	0.51, 2.94	0.261
hsa-miR-20a-5p	27.14	27.34	1.71	1.71	0.77, 2.65	0.125
hsa-miR-29a-3p	27.87	28.12	1.71	1.71	0.00001, 4.83	0.424
hsa-miR-16-5p	27.7	28.04	1.61	1.61	0.56, 2.66	0.218
hsa-miR-21-5p	27.31	27.71	1.54	1.54	0.00001, 5.08	0.444
hsa-miR-320a-5p	27.69	28.04	1.54	1.54	0.00001, 4.53	0.436
hsa-miR-17-5p	28.16	28.6	1.50	1.50	0.84, 2.15	0.162
hsa-miR-181a-5p	29.48	29.96	1.45	1.45	0.49, 2.41	0.339
hsa-miR-29c-3p	28.21	27.39	1.45	1.45	0.00001, 3.54	0.462
hsa-miR-106b-5p	28.41	28.9	1.45	1.45	0.81, 2.09	0.122
hsa-miR-30a-5p	29.1	29.73	1.31	1.31	0.47, 2.16	0.419
hsa-miR-24-3p	30.14	30.56	1.30	1.30	0.59, 2.01	0.362
hsa-miR-181b-5p	28.18	28.85	1.28	1.28	0.00001, 2.75	0.501
hsa-miR-93-5p	27.97	28.65	1.27	1.27	0.02, 2.52	0.523
hsa-miR-let 7f-5p	29.84	30.55	1.24	1.24	0.26, 2.23	0.525
hsa-miR-195-5p	27.83	28.54	1.23	1.23	0.82, 1.65	0.249
hsa-miR-30c-5p	28.12	28.93	1.15	1.15	0.53, 1.78	0.697
hsa-miR-let 7a-5p	27.69	28.52	1.14	1.14	0.27, 2.02	0.604
hsa-miR-23a-3p	25.79	26.63	1.13	1.13	0.00001, 2.57	0.65
hsa-miR-15b-5p	25.1	26.01	1.07	1.07	0.00001, 2.47	0.656
hsa-miR-23b-3p	28.66	29.58	1.07	1.07	0.13, 2.00	0.698

Relative expression levels of the upregulated miRNAs are shown. Student *t*-test of the replicate normalized miRNA expression values was performed for each miRNA in the control and treatment groups. Red colour indicates the candidate miRNAs that were chosen for further tests and validation. Fold change values greater than one indicate an upregulation whilst fold regulation represents the negative inverse of the fold change hence the fold regulation is equal to the fold change.

Table 4.2 List of downregulated miRNAs that are in bystander TK6 cells with Ct values less than 30.

MiRNA(s)	Control (Average Ct value)	Treatment (Average Ct value)	Fold change	Fold Regulation	95% CI	P-value
hsa-miR-200c-3p	28.95	32.61	0.16	-6.20	0.00001, 2.47	0.383
hsa-miR-92a-3p	23.26	25.05	0.58	-1.71	0.18, 0.99	0.202
hsa-miR-191-5p	26.49	27.79	0.82	-1.21	0.44, 1.20	0.417
hsa-miR-25-3p	26.39	27.69	0.83	-1.20	0.18, 1.47	0.797
hsa-miR-222-3p	27.66	28.85	0.89	-1.12	0.59, 1.19	0.499
hsa-miR-26b-5p	28.28	29.45	0.90	-1.11	0.20, 1.60	0.926
hsa-miR-423-5p	27.69	28.53	0.92	-1.08	0.47, 1.38	0.878
hsa-miR-26a-5p	28.15	29.23	0.96	-1.04	0.43, 1.49	0.921

Relative expression levels of the downregulated miRNAs are shown. Student t-test of the replicate normalized miRNA expression values was performed for each miRNA in the control and treatment groups. Red colour indicates the candidate miRNA(s) that was chosen for further tests and validation. Fold change values less than one indicate a negative or down-regulation, and the fold-regulation is the negative inverse of the fold-change. Since the control is assumed to be '1', when divided by the fold change yields the fold regulation.

Furthermore, miRNAs that had Ct values above 30 in the control and treatment groups are also shown in Table 4.3. Interestingly, these miRNAs had a fold change of more than 1.9 folds however; none of these was statistically significant. The miRNAs that had the highest fold changes were hsa-miR-424-5p (5.62), hsa-miR-194-5p (4.27) and hsa-miR-374-5p (4.17). Higher fold changes observed here are because the amount of miRNA goes from nothing to something thus such inconsistency can cause false elevated fold changes. However, it is important to highlight that microarray only determines a relative change and not an absolute amount. Furthermore, other miRNAs had Ct values of more than 35 and were assumed to be either less expressed or not expressed in these cells. These include hsa-miR-150-5p, hsa-miR-32-5p, hsa-miR-101-3p, hsa-miR-302b-3p, hsa-miR-376c-3p, hsa-miR-144-3p and hsa-miR-122-5p (data shown in appendix).

Table 4.3 List of differentially expressed miRNAs in bystander TK6 cells with Ct values more than 30.

MiRNA(s)	Control (Average Ct value)	Treatment (Average Ct value)	Fold change	Fold Regulation	95% CI	P-value
hsa-miR-194-5p	32.4	31.32	4.27	4.27	0.00001, 11.61	0.209
hsa-miR-19a-3p	31.98	31.43	2.96	2.96	0.00001, 7.14	0.302
hsa-miR-99a-5p	32.52	31.61	3.81	3.81	0.00001, 9.47	0.310
hsa-miR-125b-5p	31.14	30.96	2.29	2.29	0.00001, 4.81	0.313
hsa-miR-151-5p	31.12	31.02	2.18	2.18	0.00001, 4.46	0.316
hsa-miR-19b-3p	31.89	31.52	2.62	2.62	0.00001, 6.47	0.328
hsa-miR-128-3p	31.44	31.2	2.35	2.35	0.00001, 5.11	0.331
hsa-miR-186-5p	32.63	31.86	3.48	3.48	0.00001, 9.05	0.336
hsa-miR-374-5p	33.51	32.47	4.17	4.17	0.00001, 12.90	0.358
hsa-miR-18a-5p	31.71	31.56	2.25	2.25	0.00001, 5.42	0.363
hsa-miR-185-5p	32.96	32.32	3.16	3.16	0.00001, 9.31	0.364
hsa-miR-15a-5p	33.59	32.65	3.89	3.89	0.00001, 12.46	0.366
hsa-miR-424-5p	34.71	33.24	5.62	5.62	0.00001, 22.09	0.373
hsa-miR-142-3p	32.5	32.14	2.60	2.60	0.00001, 7.51	0.377
hsa-miR-29b-3p	33.74	33.18	2.98	2.98	0.00001, 10.53	0.384
hsa-miR-100-5p	34.81	34.2	3.09	3.09	0.00001, 13.73	0.390
hsa-miR-let7i-5p	32.7	32.62	2.15	2.15	0.00001, 6.66	0.393
hsa-miR-96-5p	35	34.95	2.10	2.10	0.00001, 10.45	0.394
hsa-miR-210-3p	33.2	33.27	2.07	2.07	0.00001, 7.64	0.394
hsa-miR-130a-3p	34.99	35	2.11	2.11	0.00001, 10.11	0.395
hsa-miR-27a-3p	31.1	31.17	1.93	1.93	0.00001, 4.81	0.429

4.3.3.2 MiRNA profiling and bioinformatics target analysis

Following the results from the microarray analysis of bystander TK6 cells, six miRNAs were chosen for further analysis. Despite none of the miRNAs being statistically significant, the miRNAs were chosen based on two main parameters: fold change ≥1.5 folds and proximity to statistical significance. Thus, five upregulated miRNAs - hsa-miR-146a-5p, hsa-miR-30d-5p, hsa-miR-20a-5p, hsa-miR-17-5p, hsa-miR-16-5p and one downregulated miRNA - hsa-miR-200c-3p - were chosen for further analysis. To act as a negative control, one of the miRNAs, hsa-miR-150-5p, that had average Ct values of 35 and above was chosen. The programs geNorm and NormFinder were

also used to evaluate the small nuclear RNAs. The algorithm recommended the combination of SNORD61 and RNU6B/RNU6-2 for data normalization (data shown in appendix).

As previously mentioned in section 2.27, the miRNAs were then put through different target prediction programs to predict their targets and get further insight on the miRNA-miRNA interactions in humans. It is of particular interest to reliably predict potential miRNA targets as both the deregulation of genes controlled by miRNAs and altered miRNA expression have been linked to cancer and other disorders. However, it is important to mention that the interaction between these miRNAs is complex due to numerous putative miRNA recognition sites in mRNAs. Due to this relative heterogeneity and complexity, no single target prediction program would depict all miRNA-miRNA interactions thus this is why the miRNAs were put through different target prediction programs inorder to make the data robust.

Using the TargetLink software, 47 different targets of these miRNAs were identified. The interactions between these miRNAs and their predicted target genes are illustrated in figure 4.6. There seems to be many interactions between hsa-miR-20a-5p and hsa-miR-17-5p compared to other miRNA-miRNA interactions, with about 32 target genes shared between them. This infers that these miRNAs may control similar cellular and biological processes. Some of their predicted target genes such as *CCDN2, STAT3, MYC, MAP3K, PTEN* and *RUNX1* further suggest that these miRNAs may be involved in bystander effects (Concepcion *et al.,* 2012; Lovat *et al.,* 2015; Fischer *et al.,* 2015; Chakraborty *et al.,* 2016). *STAT3* controls the expression of genes in response to cell stimuli and play a key role in apoptosis and cell growth. *MAP3K* and *MYC* are also involved in the control of cell proliferation, differentiation and survival whilst *CCDN2* and *PTEN* are involved in the regulation of cell cycle thus implying that these genes may be deregulated in CIBE.

The least miRNA-miRNA interaction was found to involve hsa-miR-30d-5p, which had just one interaction with hsa-miR-16-5p and hsa-miR-200c-3p respectively but no further interaction with the other miRNAs. However, it is of interest to mention that this little interaction may be important in CIBE as the genes implicated here, *TP53* and *NOTCH1,* are involved in the control of cell cycle and intercellular signalling pathway respectively thus controlling bystander cell fate decisions. As a 'decision maker' of DNA repair versus apoptosis, the interaction with p53 tumour

suppressor protein is an important one if the cell survives or not which could be important for bystander and DCL.

Furthermore, when the miRNAs were analysed with TargetScan, miRBase and miRDB, 132 different targets of hsa-miR-16-5p were identified. Three miRNAs, hsa-miR-200c-3p (69), hsa-miR-17-5p (66) and hsa-miR-20a-5p (54) had a similar number of predicted target genes identified. Only 17 target genes were identified for hsa-miR-30d-5p. The interaction between these miRNAs via targets genes are illustrated in figure 4.7. The number of interactions between these miRNAs is given whilst colour codes were used to depict most and least interactions. The most interactions were found between hsa-miR-20a-5p and hsa-miR-17-5p compared to other miRNA-miRNA interactions, with about 32 target genes shared between them (36.4%). This agrees with the previous data in figure 4.6 thus further supporting the possible involvement of these miRNAs and their predicted genes in CIBE.
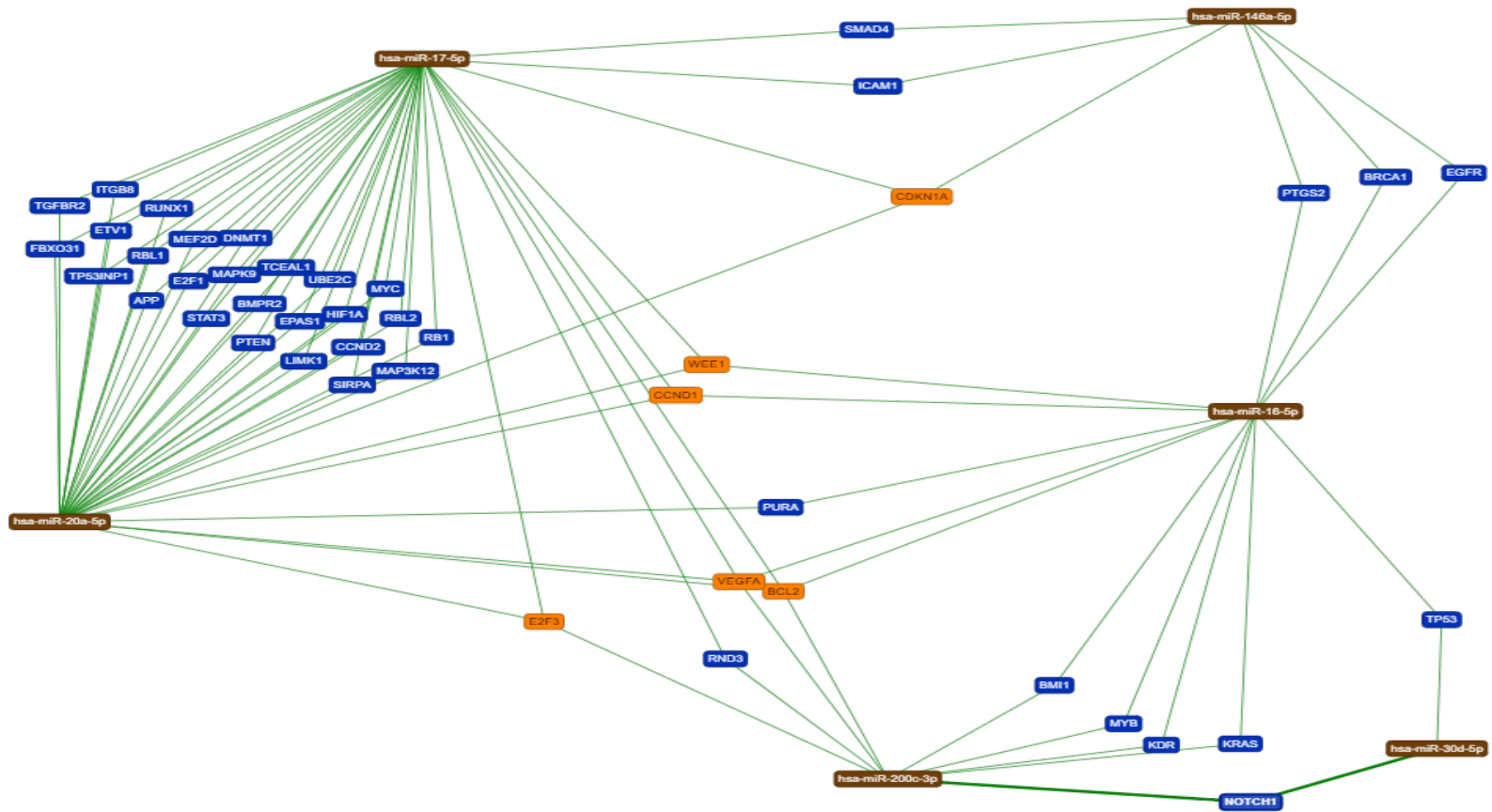
Figure 4.6 MiRNA gene target predictions and the interaction between these miRNAs via their targets. As predicted by TargetLink, the candidate miRNAs interact and share about 47 genes between them. Hsa-miR-17-5p and hsa-miR-20a-5p had the most interactions with 25 genes shared between them.

	hsa-miR-146a-5p	hsa-miR-16-5p	hsa-miR-17-5p	hsa-miR-200c-3p	hsa-miR-20a-5p	hsa-miR-30d-5p
hsa-miR-146a-5p						
hsa-miR-16-5p	2 (1.2%)					
hsa-miR-17-5p	2 (2.0%)	3 (1.5%)				
hsa-miR-200c-3p	0 (0.0%)	5 (2.6%)	3 (2.3%)			
hsa-miR-20a-5p	1 (1.1%)	4 (2.2%)	32 (36.4%)	2 (1.7%)		
hsa-miR-30d-5p	0 (0.0%)	1 (0.7%)	0 (0.0%)	1 (1.2%)	0 (0.0%)	
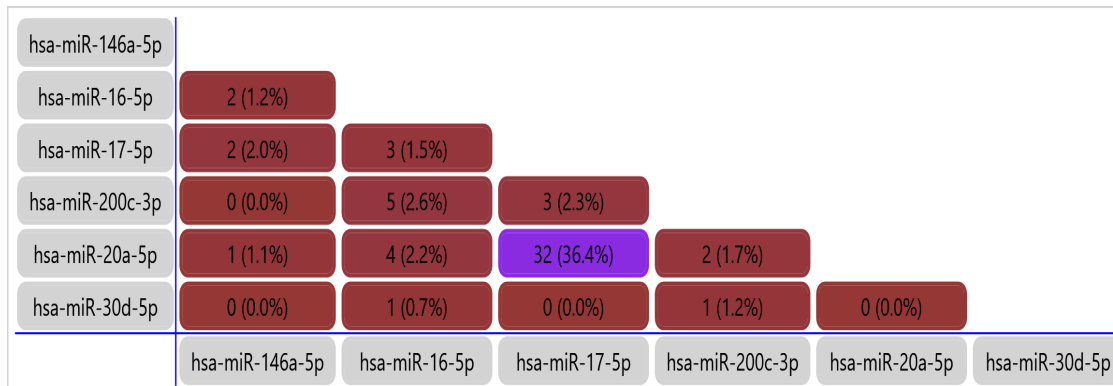
Figure 4.7 Interaction between these miRNAs via their targets. When the miRNAs were further analysed with TargetScan, miRBase and miRDB software, about 54 gene target predictions were identified. The most interaction between miRNAs is depicted in purple whilst the least interaction is depicted in brown. These genes were then analysed with FUNRICH software to understand the interactions between these miRNAs and their target genes.

4.3.3.3 MiRNA functional enrichment analysis

Since the miRNAs control gene expression at the post-transcriptional level, the predicted target genes for each miRNA were then further analysed using the FUNRICH program to identify the functional categories including biological processes these genes regulate. Where mentioned, it is important to note that positive regulation means that the upregulated or downregulated expression of a miRNA results in an increase in the frequency, rate or extent of that particular biological process. In contrast, a negative regulation means an upregulated or downregulated expression of a miRNA would result in a decrease in the frequency, rate or extent of a particular biological process. The biological processes linked to hsa-miR-146a-5p-regulated genes are shown in figure 4.8. Positive regulation of transcription (27.3% p = 0.007), negative regulation of apoptotic pathway (24.2% p = 0.027) and positive regulation of NF-kappa β activity (21.2% p < 0.001) were the most enriched biological pathways for the target genes of hsa-miR-146a-5p. Other signalling pathways such as toll-like receptor signalling pathway (15.25 p < 0.01) and nitric oxidase synthase biosynthetic process (9.1% p = 0.02). Taken together, these suggest that the retention of different signalling molecules and transcription factors may be important intercellular cues in determining bystander cell fate in CIBE. If these transcription factors can

move between the two cell models therefore it can be inferred that the movement of RNA molecules may be one of the intercellular cues behind the short-distance signals seen in CIBE.

Biological process for hsa-miR-146a-5p
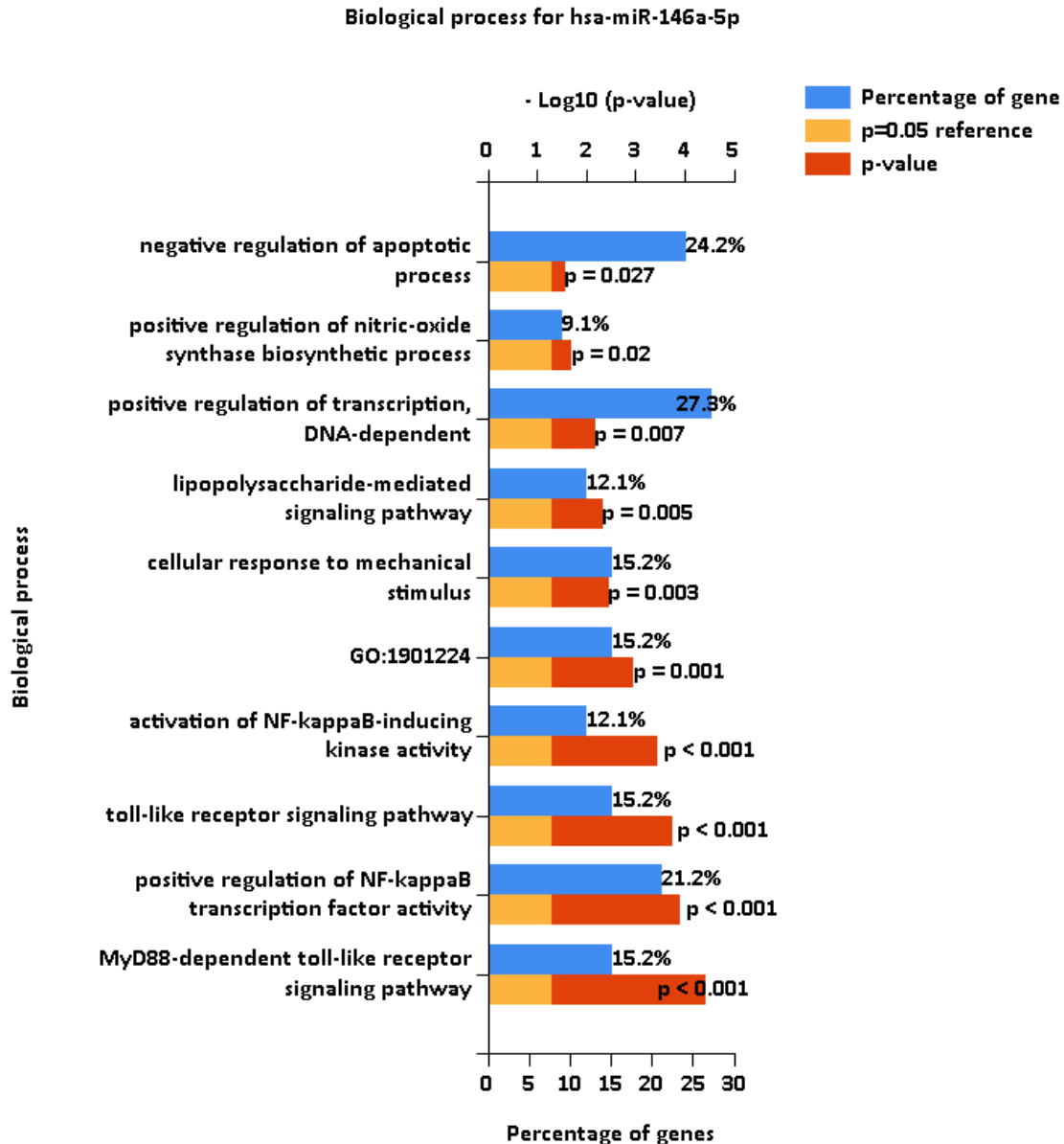
Figure 4.8 Enriched biological processes linked to the predicted target genes of hsa-miR-146a-5p. The bar graphs represent the $-\log$ (p value) for each biological process against the percentage of genes from the data set to the total number of genes involved in respective biological process. Statistical analysis was performed within the software by hypergeometric test, Benjamini-Hochberg and Bonferroni correction test.

For hsa-miR-16-5p (figure 4.9), the most enriched biological processes controlled by its predicted target genes were negative regulation of apoptosis (14.5% $p < 0.001$), protein phosphorylation (12.9% $p < 0.003$) and positive regulation of cell proliferation (12.1% $p = 0.033$), which were statistically significant. This is interesting as one of the regulatory roles that protein phosphorylation plays is the p53 tumour suppressor protein, whose activation can lead to cell cycle arrest or apoptotic cell death thereby suggesting an important role for *TP53* gene in CIBE. However, for hsa-miR-17-5p (figure 4.10) and hsa-miR-20a-5p (figure 4.11), which showed the most miRNA-miRNA interactions, there was an overlap of the biological processes regulated by their predicted target genes. The most enriched biological processes were positive and negative regulation of transcription, positive and negative regulation of transcription from RNA polymerase II promoter and cytokine-mediated signalling pathway. Furthermore, their predicted genes also show these miRNAs negatively control the G1/S phase of the mitotic cell cycle in a statistically significant manner ($p < 0.001$). These further support the idea that cell cycle arrest, signalling molecules, transcription factors and RNA molecules may play important roles in transferring chemotherapeutic effects to the bystander cells.
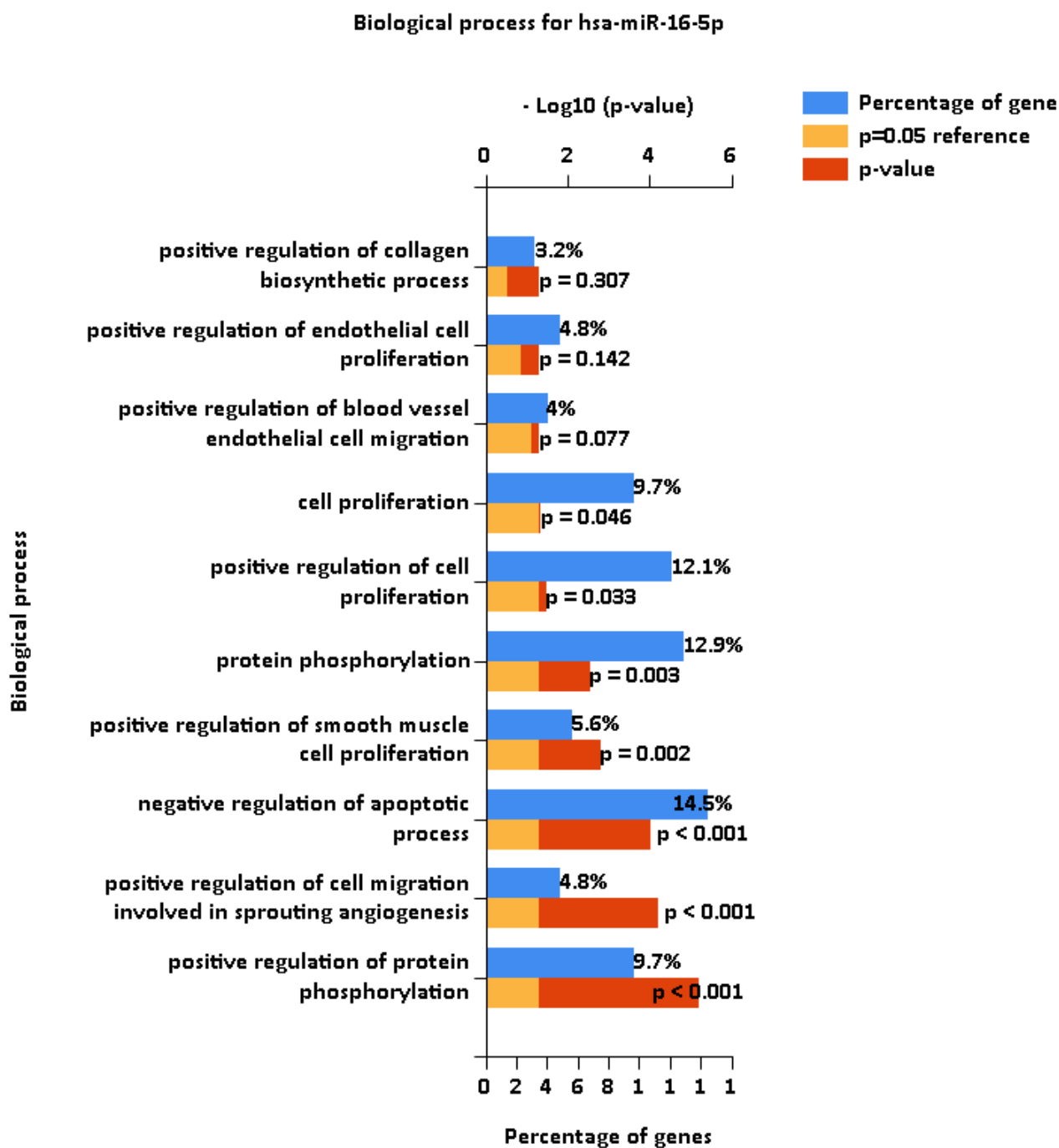
Figure 4.9 Biological pathways predicted to be targeted by genes controlled by hsa-miR-16-5p. The bar graphs represent the − log (*p* value) for each biological process against the percentage of genes from the data set to the total number of genes involved in respective biological process. Statistical analysis was performed within the software by hypergeometric test, Benjamini-Hochberg and Bonferroni correction test.
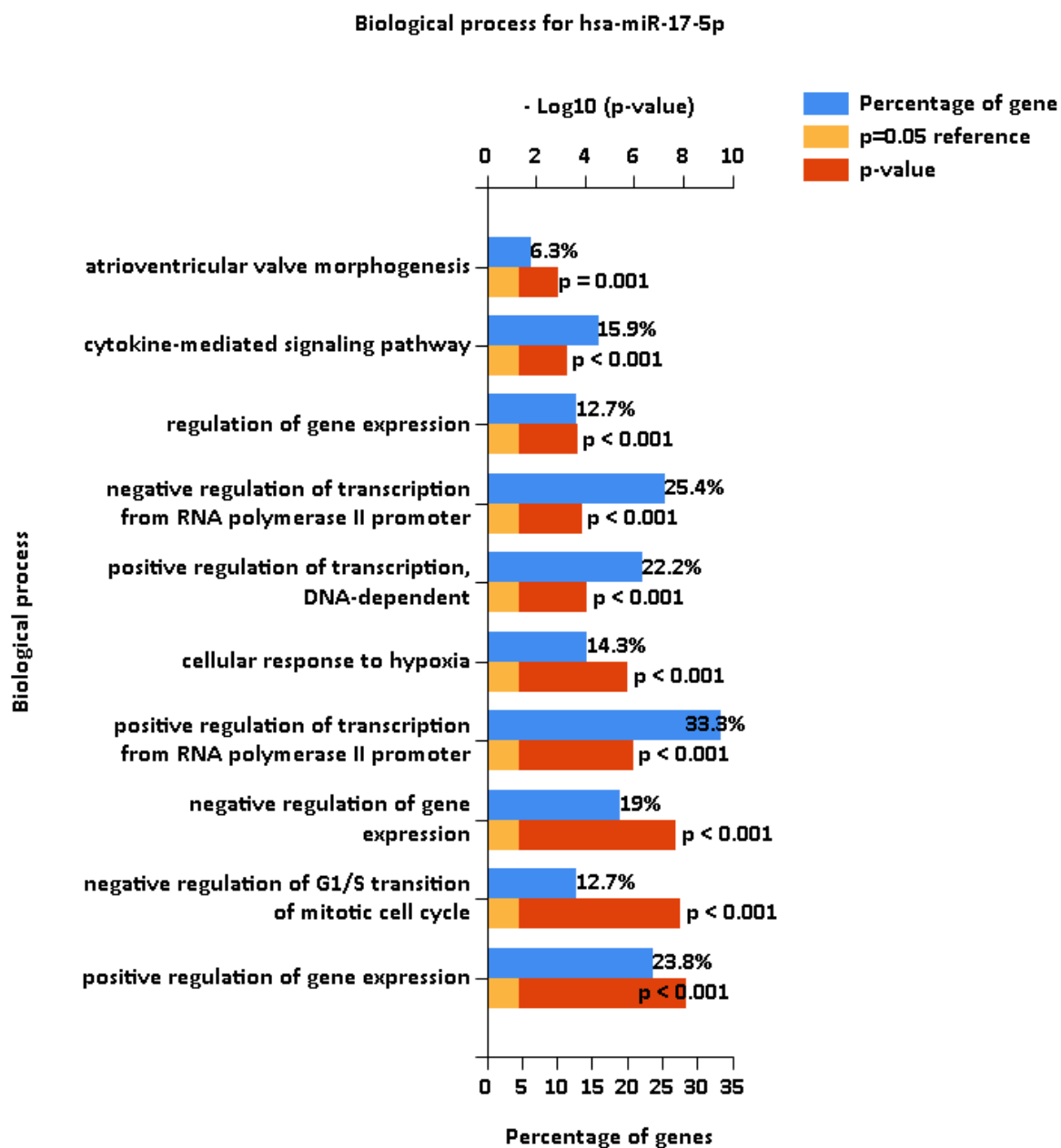
Figure 4.10 Biological pathways predicted to be targeted by genes controlled by hsa-miR-17-5p. The bar graphs represent the – log (*p* value) for each biological process against the percentage of genes from the data set to the total number of genes involved in respective biological process.
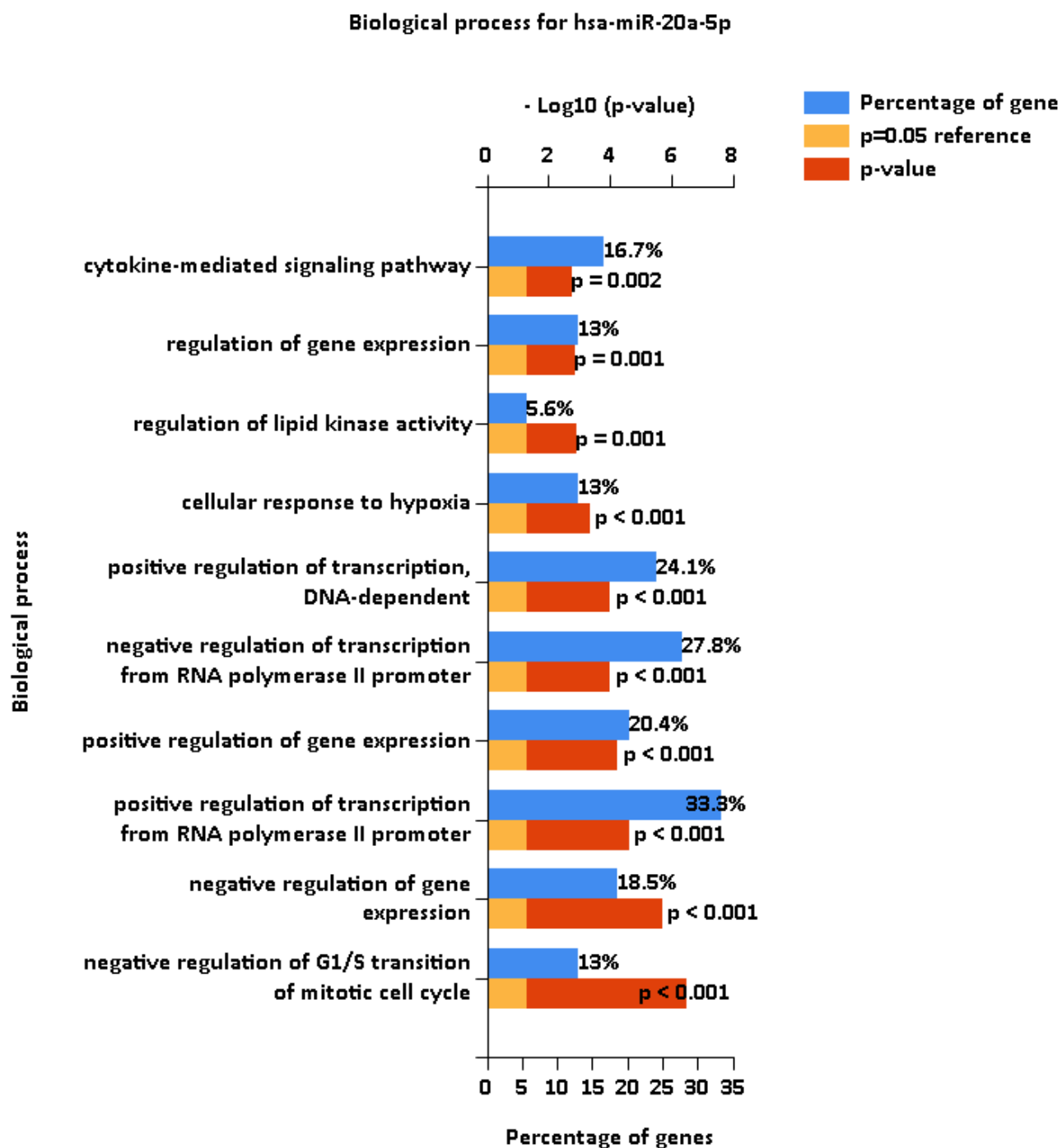
Figure 4.11 Biological pathways predicted to be targeted by genes controlled by hsa-miR-20a-5p. The bar graphs represent the − log (*p* value) for each biological process against the percentage of genes from the data set to the total number of genes involved in respective biological process. Statistical analysis was performed within the software by hypergeometric test, Benjamini-Hochberg and Bonferroni correction test.

However, the biological processes controlled by hsa-miR-30d-5p target genes (figure 4.12) were mostly related to cell death such as degradation of mitochondria (23.5% $p < 0.001$), assembly of the autophagy vacuole (23.5% $p = 0.003$) and negative regulation of cell death (17.6%). However, its negative regulation of cell death is not statistically significant ($p = 0.249$). This suggests that bystander cell death may be as a result of apoptosis and/or autophagy. This also implies that chemotherapy can be the induction stimuli for these outcomes in bystander cells.

Furthermore, the downregulated hsa-miR-200c-3p was also linked to negative regulation of transcription from RNA polymerase II promoter (23.4% $p = 0.001$), positive regulation of cell proliferation (21.9% $p < 0.001$) and positive regulation of gene expression (17.2% $p < 0.001$) as shown in figure 4.13. Other biological pathways identified were positive regulation of the MAPK signalling pathway (12.5% $p < 0.001$) and positive regulation of protein phosphorylation (10.9% $p = 0.012$). These suggest that the downregulation of this miRNA may lead to a decrease in DNA transcription but an increase in cell proliferation and cell signalling, which contradicts the effects of hsa-miR-17-5p and hsa-miR-20a-5p. In addition, hsa-miR-200c-3p was also found to control sprouting angiogenesis (6.3% $p = 0.054$) and cellular response to VEGF stimulus (6.3% $p = 0.03$). These further suggest that there may be complex intercellular cues involving signalling molecules, proteins, angiogenic and transcription factors as well as RNA molecules in CIBE.
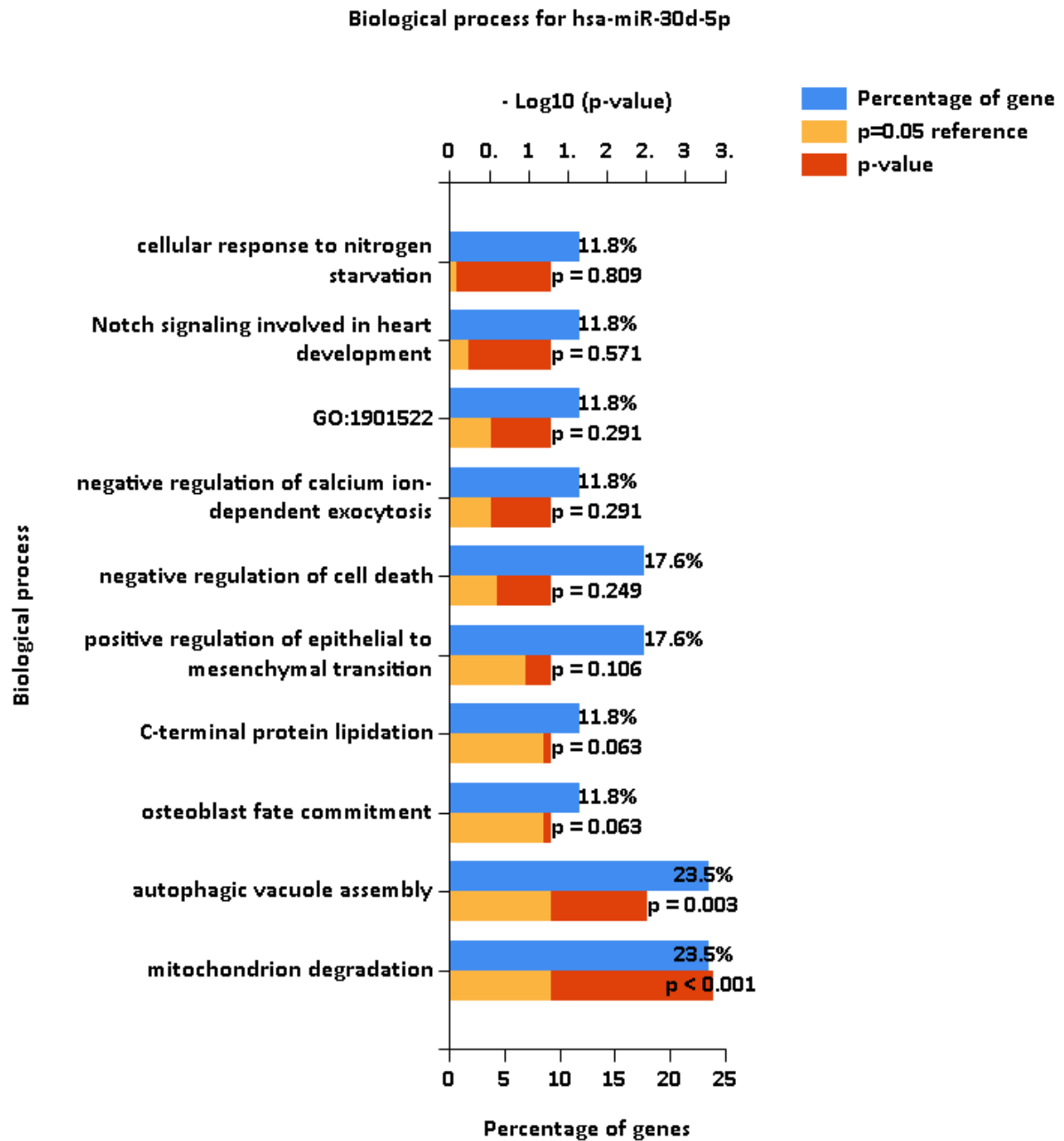
Figure 4.12 Biological pathways predicted to be targeted by genes controlled by hsa-miR-30d-5p. The bar graphs represent the – log (*p* value) for each biological process against the percentage of genes from the data set to the total number of genes involved in respective biological process. Statistical analysis was performed within the software by hypergeometric test, Benjamini-Hochberg and Bonferroni correction test.
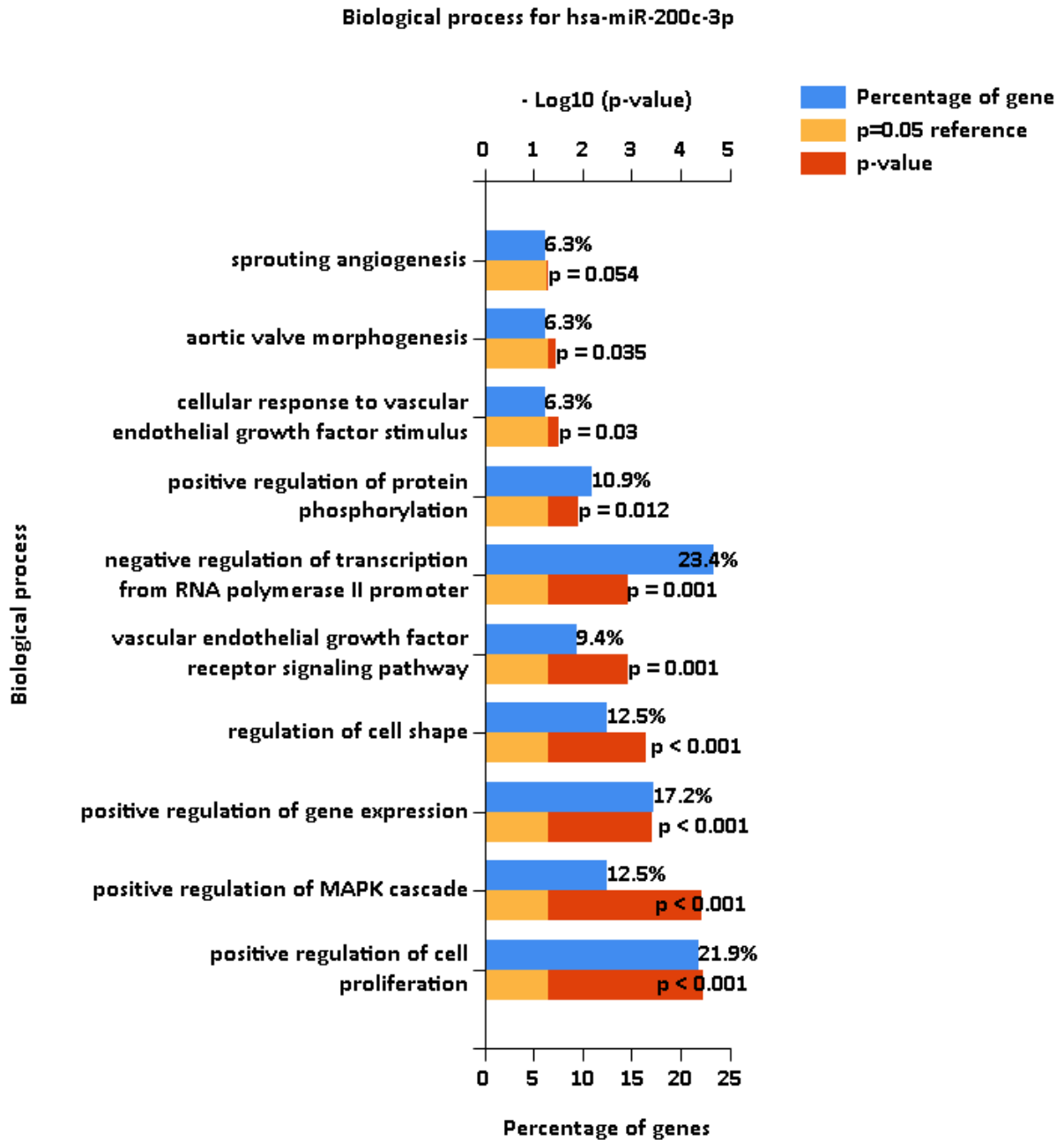
Figure 4.13 Biological pathways predicted to be targeted by genes controlled by hsa-miR-200c-3p. The bar graphs represent the – log (*p* value) for each biological process against the percentage of genes from the data set to the total number of genes involved in respective biological process. Statistical analysis was performed within the software by hypergeometric test, Benjamini-Hochberg and Bonferroni correction test.

4.3.3.4 Validation of selected miRNAs in HS-5 and bystander cells

The change in expression of these candidate miRNAs in HS-5 cells as well as bystander TK6 cells was further explored by qRT-PCR following bioinformatics. HS-5 cells were treated with MTX (500 ng/ml) for 24 hours. After 24 hours, the drugs were removed by washing the cells three times with PBS. Fresh medium was added to the cells and then using a culture insert, bystander TK6 cells were co-cultured with the drug-treated HS-5 cells. After 24 hours, both cells in the upper compartment (bystander TK6 cells) and lower compartment (HS-5 cells) were harvested and their RNA extracted as previously discussed in section 2.22.1. The RNA was converted to cDNA as previously illustrated in section 2.25 before using the cDNA obtained to perform qRT-PCR as described in section 2.28. Ct values of the individual miRNAs in both cell lines were obtained and normalised using SNORD61 and RNU6B/RNU6-2 whilst hsa-miR-150-5p was used as a negative control. Fold changes in the level of each miRNA was analysed using the comparative Ct ($2^{-\Delta\Delta CT}$) method.

As shown in figure 4.14, the expression of the miRNAs was contrastingly distinct in both cell lines. If a miRNA was highly expressed in one cell line, it was less expressed in the other cell line and vice versa. It is of interest to mention that this difference in miRNA expression in both cells was statistically significant ($p < 0.001$). The most expressed miRNA in HS-5 cells was hsa-miR-16-5p, which increased over 3.99 folds but was decreased by 0.62 folds in bystander TK6 cells. This contradicts the microarray data in which hsa-miR-16-5p was upregulated by 1.61 folds in the bystander cells (table 4.1). High expression of this miRNA in the treated HS-5 cells suggests that chemotherapy modulates proliferation, protein phosphorylation and angiogenesis in these cells thereby deciding their fate.

The miRNAs, hsa-miR-17-5p and hsa-miR-20a-5p, which shared the most interactions also showed similar expression levels in both cell lines. In HS-5 cells, the expression levels of hsa-miR-17-5p and hsa-miR-20a-5p increased by 2.61 and 2.32 folds respectively compared to 0.58 and 0.59 folds in bystander TK6 cells. This increase suggests that altered expression of these miRNAs in the treated stromal cells may result in cellular response to hypoxia, cell cycle control and DNA

transcription. However, these results contradict the microarray data that revealed 1.5 (hsa-miR-17-5p) and 1.71 (hsa-miR-20a-5p) fold increase in the bystander cells (table 4.1).

However, the expression of hsa-miR-30d-5p was higher in bystander TK6 cells (1.15 folds) than HS-5 cells (0.85 folds); in similar fashion to the microarray data that showed 1.89-fold increase in the bystander TK6 cells. These suggest that autophagy may be involved in bystander chemotherapeutic effects but not direct chemotherapeutic effects. Interestingly, the only miRNA that showed similar expression levels in both the microarray (table 4.2) and qRT-PCR data in the bystander TK6 cells was hsa-miR-200c-3p however it was also downregulated by 0.14 folds in HS-5 cells. This indicates that angiogenesis, cell signalling and cell proliferation may be involved in deciding the fate of the treated stromal cells and the bystander cells.
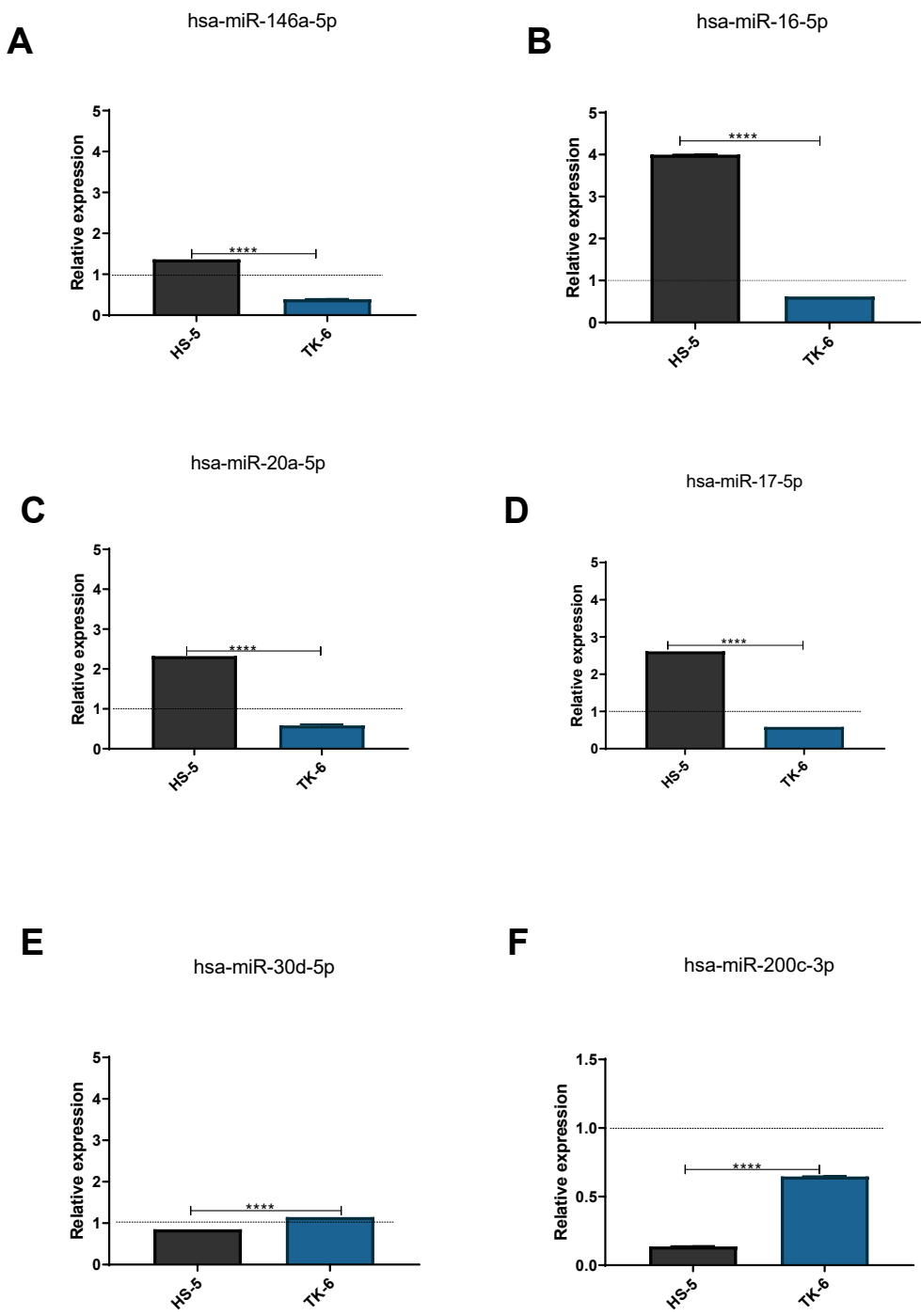
Figure 4.14 Validation of expression levels of miRNAs in HS-5 and bystander TK6 cells. The expression of the candidate microRNAs – (a) hsa-miR-146a-5p (b) hsa-miR-16-5p (c) hsa-miR-20a-5p (d) hsa-miR-17-5p (e) hsa-miR-30d-5p (f) hsa-miR-200c-3p – were validated in HS-5 cells and bystander TK6 cells following 24-hour co-culture. Statistical significance was done using the student t-test (****p<0.001).

4.4 Discussion

The maintenance of haematopoiesis in the BM largely depends upon the interactions between MSC and HSC, and their progeny. MSC play important roles in the maintenance of homeostasis of an organism through cell-to-cell contact and the modulation of cytokine secretion and other signalling molecules involved in intercellular communication in the BM microenvironment (Reagan & Rosen, 2016). However, MSC can turn 'rogue' during tumorigenesis and unintentionally stimulate tumour progression through paracrine factors, suppression of the immune system, migration to the tumour site or differentiation into tumour-associated fibroblasts (Fracchiolla *et al.,* 2017). These tumour-associated fibroblasts are also involved in chemo-resistance. Furthermore, chemotherapy, particularly high-dose chemotherapy administered during conditioning, can also induce morphological and functional damages in MSC thereby causing proliferative problems that will promote chemo-resistance (Shipounova *et al.,* 2017). This study also revealed that there were alterations in the gene expression levels of these drug-treated MSC, which lasted for a year. As a result, a damaged stromal microenvironment may lead to impaired haematopoiesis in patients following HSCT (Storek *et al.,* 2008; Bemark *et al.,* 2012). Dysregulation of haematopoiesis is associated with the development of leukaemia. Therefore, these suggest that a damaged microenvironment and dysregulated haematopoiesis may lead to the development of *de novo* primary malignancy such as donor cell leukaemia.

Herein, the hypothesis is that MSC persist in the BM microenvironment following pre-transplant conditioning during HSCT. As a result, different approaches were taken to ascertain and confirm a possible BE role for MSC. First, HS-5 cells were treated with two different drugs from two drug groups: alkylating agents and topoisomerase inhibitors. Secondly, since MSC can develop functional and morphological damage following chemotherapy, the ability of HS-5 cells to recover from the effects of chemotherapy was determined. Thirdly, the ability of HS-5 cells to transfer these chemotherapy-induced effects to bystander TK6 cells was explored. The duration of these CIBE was also explored over a five-day period. Lastly, the changes in miRNAs expression in both HS-5 cells and bystander TK6 cells were explored to ascertain if these changes under the direct and indirect influence of chemotherapy. Cell viability was determined by trypan blue exclusion

assay and AO/PI viability assay whilst DNA damage was ascertained by MN assay. Changes in miRNA expression was quantified by microarray analysis and validated by qRT-PCR.

4.4.1 Cytotoxicity effect of chemotherapy on HS-5 cells

Chemotherapy damages the BM microenvironment during HSCT and this has been a challenge in the treatment of leukaemia. High-dose chemotherapy has been reported to cause disruption of the marrow architecture and loss of stromal compartments (Kemp *et al.,* 2011). Although a combination of drugs is used during pre-transplant conditioning, understanding the effects of individual drug at clinically relevant dose is important. This study characterizes the effects of chemotherapeutic agents used clinically during HSCT on HS-5 stromal cells.

Firstly, it was demonstrated that all drugs used (chlorambucil, carmustine, etoposide and mitoxantrone) induced stromal cell death after an hour and 24 hours respectively. However, the cells remained viable and proliferated at a reasonable rate thus suggesting chemotherapy did not abrograte their proliferative potential. Several researchers have shown that chemotherapy administered to MSC *in vitro* induce heterogeneous effects on MSC and stromal elements that may affect their functionality (Liang *et al.,* 2011; Oliveira *et al.,* 2014; Bosco *et al.,* 2015; Nicolay *et al.,* 2016; Bellagamba *et al.,* 2016; Somaiah *et al.,* 2018; Wenk *et al.,* 2018). Although there is little or no evidence in literature about the direct effects of carmustine and chlorambucil on MSC, heterogeneous effects of topoisomerase inhibitors on MSC have been reported. Human MSC were relatively sensitive to etoposide following 72-hour treatment (Li *et al.,* 2004) whilst MSC derived from human adipose tissue was resistant to etoposide (10 µM) after 24-hour treatment (Rylova *et al.,* 2012). In addition, BM-derived MSC was resistant to the effects of etoposide whilst mitoxantrone was shown not to have an effect on MSC (Mallam *et al.,* 2010; Nicolay *et al.,* 2016). Another published report revealed that the resistance to etoposide under clinically relevant conditions (0.01 – 100 µM) after 72-hour treatment is associated with an increased level of p53 expression and unaltered phenotype and differentiation potential in MSC *in vitro* (Mueller *et al.,* 2006).

Secondly, mitoxantrone was the only drug to achieve this apoptotic effect in a dose-dependent manner at both time points. Similar effects were found in dental pulp stem cells, which are a valuable source of MSC. Exposure of the cells to lower and higher concentrations of mitoxantrone resulted in premature senescence and caspase-mediated apoptosis respectively (Seifrtova *et al.,* 2013). In addition, Mergenthaler *et al.,* (1987) also revealed that mitoxantrone induce stem cell toxicity at low doses (0.075-20 ng/ml) whilst Chow *et al.,* (2002) also exhbitied a dose-effect of mitoxantrone (0.05 – 0.50 µg/ml) on stem cells after 24 hours. This further suggests that a dose-effect relationship in mitoxantrone-induced toxicities may be more damaging to MSC during pre-transplant conditioning.

Taken together, these results suggest that MSC respond to a variety of chemotherapeutic drugs used in pre-transplant conditioning in different ways. Furthermore, the effects of these chemotherapeutic drugs on MSC vary in severity, and may depend on the dosage of the drugs used. Nevertheless, the cells remained viable thus suggesting that these cells survive despite high-dose chemotherapeutic insult. Although the cellular mechanisms that govern the injured state of these stromal cells are not elucidated in this study, it is likely that MSC have the capacity to survive and maintain their stem cell character in response to these chemotherapeutic agents. Thus, this highlights the importance of assessing the state of the BM microenvironment post-chemotherapy prior to transplantation.

4.4.2 The rate of recovery of HS-5 cells from chemotherapy varies and depends on the drug

The intrinsic recovery of a damaged BM microenvironment is dependent on the stem cell pool, which are normally maintained in a quiescent state but are induced into cell cycle to re-establish the depleted marrow cavity. Upon depletion, BM partially recover at a fast rate due to MSC that undergo differentiation thus enabling them to regenerate or proliferate and self-renew (Georgiou *et al.,* 2010). However, severe damage to MSC may be irreversible especially if effected at the DNA level, with the ability to re-constitute haematopoiesis being completely recoverable in children under the age of four (Galotto *et al.,* 1999; Le Blanc and Ringden, 2005). To recover from the effects of chemotherapy, cells have to grow and overturn toxicity of chemotherapeutic

agents. Cells, treated for an hour, recovered from the effects of chlorambucil, carmustine and etoposide, with at least 60% cell percentage at doses other than the clinically relevant doses. However, the recovery was stunted in cells treated with these drugs after 24 hours, with cell percentage ≤ 50%.

Mitoxantrone was the only drug that maintained its cytotoxic effects at both time points. The reason for this is not clear but reports have shown that mitoxantrone is easily absorbed within minutes however its distribution half-life is between 0.3 and 50 hours, and its terminal half-life varies between 8.9 hours and 9 days (Ehninger *et al.,* 1989; Richard *et al.,* 1992; Canal *et al.,* 1993). Hence, its stability is probably more of an issue and/or the capacity of HS-5 cells to metabolise it, possibly into more metabolites that are toxic.

Mitoxantrone is activated by hepatic microsomal enzyme, P450 mixed-function oxidase to several metabolites, including naphthoquinoxaline that enhance its cytotoxic effect (Mewes *et al.,* 1993; Panousis *et al.,* 1995). Interestingly, MSC are metabolically competent and express cytochrome P450 enzymes and glutathione transferase enzymes both *in vitro* and *in vivo* (Esmaeli *et al.,* 2012; Alonso *et al.,* 2015; Larsen *et al.,* 2020). In addition, HS-5 stromal cells are also metabolically competent and rely on both glycolysis and mitochondrial phosphorylation for their energy supply to modulate the metabolic status of co-cultured cancer cells (Cavnar *et al.,* 2016; Vangapandu *et al.,* 2017). These infer that HS-5 cells may have the capacity to metabolise mitoxantrone to its metabolites thereby enhancing its effects.

The results from mitoxantrone in this study correspond to the previous findings of May *et al.,* (2018), which revealed that HS-5 cells were sensitive to cyclophosphamide-induced DNA damage and this damage persisted in the cells after treatment withdrawal. However, the cells were grown in fresh medium and allowed to recover from cyclophosphamide-induced damage for 48 hours unlike in this study whereby the cells were allowed to recover for 72 hours. Although cyclophosphamide is a bi-functional DNA alkylating agent, it is also a pro-drug just like mitoxantrone. Cyclophosphamide can be metabolised by hepatic p450 enzymes to its active and inactive compounds (Pinto *et al.,* 2009; Veal *et al.,* 2016). These further infer and support the notion that the persistence of the mitoxantrone-induced effects in the stromal cells may be due

to presence of metabolic enzymes in the stromal cells, which metabolises mitoxantrone to its active metabolites.

Furthermore, etoposide can also be metabolised by cell oxidases to metabolites such as etoposide catechol and quinone (Jacob *et al.,* 2011). These metabolites also enhance the toxicity of etoposide thus; this may explain the sustained cytotoxic effect in cells following 24-hour treatment with etoposide in this study. These correspond to the previous reports in literature, which revealed that human MSC that had been exposed to etoposide, paclitaxel and cytarabine *in vitro* for 72 days failed to recover from drug-induced effects after 9 days (Li *et al.,* 2004). However, it is important to note that the dose for etoposide used in this human study (10 mol/L) was well in excess of those used in this study (1 µM, 5 µM, 10 µM), with the latter the clinically relevant dose. It has also been reported that etoposide can easily be absorbed and distributed throughout the body with an elimination half-life of 20 hours to 2 days (Hande *et al.,* 1984; Holthuis *et al.,* 1986; Slevin, 1991). These further suggest that these topoisomerase inhibitors may persist in the cells thereby sustaining their cytotoxic effects in the HS-5 stromal cells.

Nevertheless, HS-5 cells recovered from the cytotoxic effects of carmustine in this study at both time points. Stability studies of carmustine reveal a very short half-life of about 70 minutes, with majority of its metabolites eliminated within 24 hours hence carmustine is often combined with other drugs with prolonged elimination half-life such as vincristine to intensify the chemotherapeutics effects of carmustine (Kyle *et al.,* 2009; Gerson *et al.,* 2018).

In this study, HS-5 stromal cells recovered from the effects of low-dose chlorambucil but did not recover from the effects of high-dose chlorambucil. Although there is little or no data to support the effects of chlorambucil on MSC, chlorambucil that can be metabolised to its active metabolite, phenylacetic acid mustard. However, the elimination of half-lives of chlorambucil and its metabolite are reported to be 1.5 hours and 2.5 hours respectively (Silvennoinen *et al.,* 2000; Gerson *et al.,* 2018). This further suggests that the stability of each drug and metabolism may play a huge role in the recovery of the stromal cells to these chemotherapeutic effects. This is supported by the report that it took 14 days for MSC to achieve full recovery from the cytotoxic effects of cisplatin *in vitro* (Liang *et al.,* 2011). Cisplatin is a cross-linking agent but degrades in a

biphasic manner, with an initial half-life of 25–49 minutes and a terminal half-life of 58–73 hours thereby accumulating in tissues, with the drug detected up to 6 months after dosage (Gerson *et al.,* 2018).

Therefore, the recovery of HS-5 cells from chemotherapeutic effects may be differential and depends on time, stabiliy of each drug and the metabolic properties of these stromal cells thus suggesting that MSC uptake drugs and may release them in a time-dependent manner. There is good evidence that MSC are capable of releasing drugs in a time-dependent manner *in vitro* (Pessina *et al.,* 2011; Bonomi *et al.,* 2013; Bonomi *et al.,* 2015; Clavreul *et al.,* 2017; Coccè *et al.,* 2017). The results of this present study suggest that mitoxantrone, etoposide and chlorambucil significantly reduced the proliferative potential of MSC following 24-hour treatment and this persisted over 3 days. This process may also involve deregulation of gene expression involved in the regulation and maintenance of haematopoiesis in the BM microenvironment. The alteration of gene expression levels in MSC persisted for a year in AML patients following exposure to pre-transplant conditioning (Shipounova *et al.,* 2016). As a result, it is reasonable to think that chemotherapy treatment could affect the functionality of MSC hence this is a great concern during pre-transplant conditioning as these effects may persist in the BM microenvironment and subsequently cause irreversible damage that may lead to the development of *de novo* primary malignancy. Nevertheless, it is important to note that the response of HS-5 stromal cells *in vitro* may not be a true representation of their behaviour *in vivo* and as a consequence, the results inferred from this study may be limited.

4.4.3 Bystander cells are induced in TK6 cells co-cultured with chemotherapy-treated HS-5 cells

Although the co-injection of donor MSC with HSC enhances the engraftment of HSC in patients, haematopoietic recovery and functioning is dependent on the host MSC post-transplantation (Ball *et al.,* 2007; Jaganathan *et al.,* 2010). However, the mechanism by which the host MSC engineer repopulation and reconstitution of the recipient haematopoietic system post-transplantation is yet to be understood. Whilst the direct effects of chemotherapeutic agents on MSC have been described above, there is a paucity of information about their ability to transfer

these chemotherapeutic effects to HSC in bystander co-culture settings. Existing data infer conflicting effects of MSC, pre-exposed to chemotherapy, on the response of cancer cells to chemotherapy. Various studies have reported the ability of chemotherapy-treated MSC to confer protection, from chemotherapy, to leukaemic cells following co-culture via direct cell-cell contact and release of soluble factors (Roodhart *et al.,* 2011; Skolekova *et al.,* 2016; Somaiah *et al.,* 2018). In contrast, co-culture of cancer cells with MSC primed with chemotherapeutic drugs or their conditioned medium enhanced the sensitivity of these cancer cells to chemotherapy (Pessina *et al.,* 2011; Bonomi *et al.,* 2015). Both protection and sensitisation to chemotherapy are bystander effects as there is communication between the treated cells and neighbouring cells that have not been exposed to chemotherapy. The drugs that have been implicated in these effects include vincristine, gemcitabine, paclitaxel, cytarabine, daunorubicin, cisplatin and other platinum agents such as oxaliplatin and carboplatin. These suggest that the MSC contains cells that may play a dual role in controlling drug toxicity in patients' BM microenvironment. The reason for this remains unclear as these studies showed that MSC primed with drugs like paclitaxel, induced both increased and decreased drug sensitivity in leukaemia cells. However, it is clear that MSC can uptake and release a drug in a timely manner via communication with the neighbouring cells that have been unexposed to chemotherapy. Therefore, an important aspect of this study was to determine and understand if HS-5 stromal cells exposed to chemotherapeutic drugs could transmit toxic signals capable of inducing mutagenic events to bystander TK6 cells.

Several researchers have reported evidence of CIBE in cells other than MSC such as hepatoma carcinoma cells, prostate cancer cells and lung adenocarcinoma cells using drugs such as MMC, etoposide, bleomycin, doxorubicin, phleomycin and nitrosureas (Di *et al.,* 2008; Asur *et al.,* 2009; Kumari *et al.,* 2009; Chinnadurai *et al.,* 2013; Lin *et al.,* 2017). Traditionally, bystander effects had been defined as damage in cells that have not been directly exposed to toxic insult however, bystander effects manifested as a wide range of biological endpoints including DNA damage, cell death, proliferation and differentiation in these studies.

Here, the bystander TK6 cells co-cultured with HS-5 cells pre-treated with chlorambucil, etoposide and carmustine exhibited an increase in cell number in relation to the control cells at

both time points whilst those exposed to HS-5 cells pre-treated with mitoxantrone recorded a decrease in cell number. The reason for this variation in CIBE biological endpoints is unknown but may depend on the drug properties that contribute to its mechanism of action or MSC responses, which may differ and be specific to each drug. The results here are similar to the findings of Kumar *et al.,* (2009), which revealed that hepatoma cells treated with mitomycin C transferred cellular signals to the naïve hepatoma cells when co-cultured together, thereby inducing cell death in a dose-dependent manner by propagation of death ligands such as Fas ligand (FasL) and TRAIL. However, mitomycin C-treated cervical cancer cells failed to induce bystander killing in naïve cervical cancer cells when co-cultured together instead the cells proliferated at a similar rate as the control. This infers that the bystander outcome may be linked to intrinsic factors within the bystander cells thus suggesting that these bystander cells may play an important role in CIBE.

Furthermore, the treatment of B16 melanoma cells, from C57BL6/6J mice, with cystemustine and fotemustine induced bystander killing in untreated B16 melanoma cells, unlike in cells pre-treated with carmustine (Merle *et al.,* 2008). The untreated B16 melanoma cells exposed to cells pre-treated with carmustine proliferated at a rate similar to the control, which is similar to the findings in this study. The reason for this is unknown but it favours the idea that the drug properties may contribute to CIBE outcomes. These drugs belong to the same family, as chloroethylnitrosourea whose cellular effects are dependent on DNA alkylation by carbocation (chloroethyldiazohydroxide group) and protein carbamylation by the isocyanate group (Merle *et al.,* 2008). Carmustine contains two carbocation groups (as seen in figure 1.5) compared to the other nitrosourea drugs, which have only one.

In another study within the research group, carmustine, chlorambucil and etoposide also failed to induce bystander killing in AHH-1 lymphoblast cells; mitoxantrone was the only drug to achieve bystander killing in these cells, however all four drugs induced bystander killing in TK6 lymphoblast cells (Kelechi Okeke, personal communication). The reason for this discrepancy in the data from this study and theirs could be due to interindividual differences such as consistency in pipetting and cell counting. In addition, experimental differences such as duration of cell culture and treatment may have played a role. In their study, the stromal cells were treated for

an hour and co-cultured with the bystander cells for 24 hours whilst the stromal cells were treated for 24 hours and co-cultured with the bystander cells for 24 hours in this study. Nevertheless, overall survival is better than for direct treatment in both studies thus suggesting that if this is translated to an *in vivo* setting, most of the cells are surviving whilst showing a bystander effect. Several researchers have shown that direct exposure to chemotherapy leads to higher cell death compared to bystander cell death (Alexandre *et al.,* 2007; Di *et al.,* 2008; Asur *et al.,* 2009; Chinnadurai *et al.,* 2011; Singh *et al.,* 2015; Arora *et al.,* 2018). These also suggest that bystander killing depends on the drug and cell type used in the experiment. The differential response in the bystander TK6 cells observed with these drugs in this study also suggests that the damage to HS-5 cells does not dominantly explain the mechanism at the origin of CIBE.

The evaluation of cytotoxic as well as genotoxic effects of a chemotherapeutic agent occur concomitantly; its cytotoxic evaluation gives information on its lethal and tolerable dose whilst the genotoxic evaluation measures a drug's capacity to induce DNA damage (Shi *et al.,* 2010). In this study, the cell viability did not go below 70% in the bystander TK6 cells, which is enough for genotoxic assessment according to the OECD guideline (OE CD, 2012), which states that cell viability must be at least 50% (± 5%) prior to genotoxic assessment. The good viability in these cells infers that the genotoxic events measured in the bystander TK6 cells are real and of great concern. Mutagenic events can only be manifested in live cells, so good viability following bystander suggests a mechanism by which toxicity of chemotherapeutic agents can be potentiated. TK6 cells have been widely used in genotoxicity testing with reported advantages such as presence of an active tumour protein (p53) involved in cell cycle regulation (Fowler *et al.,* 2012; Lorge *et al.,* 2016). This protein acts as a decision maker in recruiting DNA repair proteins in genotoxic environments as well as apoptosis in high toxicity. Thus, this explains why TK6 was chosen as the bystander cells of choice in this study.

Genotoxic damage was measured by the MN assay, a standard technique used in genetic toxicology studies that is usually reported as the number of cells containing MN per total cells counted. MN arise in the cell cytoplasm because of clastogenic (fragmentation or breakage of chromosomes or chromatids) or aneugenic (abnormal number of chromosomes) events in cells

that fail to be included in the daughter nuclei at the completion of telophase during mitosis (Fenech *et al.,* 2011). Data from this study revealed that all drugs induced MN formation in the bystander TK6 cells above the untreated control however; mitoxantrone was the only drug that caused a significant increase in MN frequency at both time points. Increased MN frequency is often evident in cells following exposure to a toxic substance long before clinical symptoms appear and is associated with increased risk of cancer development (Pardini *et al.,* 2017; Podrimaj-Bytyqi *et al.,* 2018).

The results from this study are in agreement with the findings of Asur *et al.,* (2009) who were the first researchers to use MN frequency as a CIBE endpoint. Naïve human B lymphoblastoid cells (GM15036 and GM15510) exposed to medium conditioned by lymphoblastoid cells cultured in MMC and phleomycin had 3-4 fold increase in MN frequency hence suggesting that the treated cells release soluble factors in the medium capable of inducing bystander effects in the naïve cells. In contrast to their model, an *in vitro* bystander co-culture model was adopted in investigating CIBE in bystander TK6 cells in this study. A porous membrane (pore size 0.4 µm) separated the cell populations thus allowing the study of cell interaction through direct signalling whilst maintaining proper growth and identity of cell types. Similarly, BM MSC, lung adenocarcinoma cells, peripheral blood lymphocytes and normal lung fibroblasts co-cultured for 24 hours with their equivalent cell type that were pre-treated with bleomycin and neocarzinostatin for an hour exhibited an increase in MN frequency (Chinnadurai *et al.,* 2011). However, a higher magnitude of MN frequency was found in peripheral blood lymphocytes and BM MSC. This infers that the MSC and HSC are more susceptible to bystander damage than other types of cells. Thus, it is likely that treated stromal compartment in a patient may transfer chemotherapeutic effects to incoming cells from a donor following HSCT.

Furthermore, it is important to note that increased MN frequency can also arise because of long-term cell culture (Falck *et al.,* 1997). Since the cells were in co-culture for just 24 hours, which is enough time for the dividing cells to undergo cell cycle, it negates the idea that the increased MN frequency found in this study is because of prolonged cell culture but a true representation of the genotoxic effects of the drugs in the bystander cells. It is also negated by comparison with untreated controls of the same culture longevity. This further suggests that the genotoxic effects

in the bystander TK6 cells may be more deleterious than direct exposure thereby causing genomic instability in the progeny, as the cells seem to be viable despite the toxic insult.

4.4.4 Damage induced by chemotherapy lasts over 5 days

Following identification of CIBE with cytotoxic and genotoxic endpoints in the cells by all chemotherapeutic agents via co-culture, it became apparent to understand the duration and mechanism (section 4.4.5) of CIBE in these cells. Whilst a co-culture system was used to study bystander killing and genotoxic events as aforementioend, medium conditioned by treated HS-5 cells was used to assess the duration of these CIBE. This involves transfer of medium, which contains soluble factors released by treated or untreated cells, to bystander cells thereby inducing various biological effects such as DNA damage, cell death, proliferation and differentiation (Asur *et al.,* 2009; Skolekova *et al.,* 2016). Previously, it has been shown that medium conditioned by untreated HS-5 cells was capable of inducing resistance to chemotherapeutic agents, in cancer cells (Weisberg *et al.,* 2008; Zhang *et al.,* 2010; Furukwa *et al.,* 2017; Huang *et al.,* 2017).

Therefore, medium conditioned by HS-5 cells treated with the four chemotherapeutic agents was used to culture bystander TK6 cells for 24 hours and this process was repeated for 5 days to assess any cellular changes. Patients are usually given 2-3 days to recover from the therapeutic effects of pre-transplant conditioning prior to HSCT, however 5 days was chosen for this experiment as this is suggested to be the maximum time that patients could safely be without a transplant. It has been argued that washing of cells after drug exposure is unlikely to remove drug completely from the medium and vital components such as serum, glutamine and glucose may be depleted in conditioned medium. As a result, the conditioned medium was filtered twice with 0.22 µm filters in order to remove any cell debris and remnant of the drugs. It has been previously suggested that the filter material, filter pore size and filter surface area can affect drug clearance (Monaghan and Acierno, 2011).

Interestingly, mitoxantrone was the only drug that maintained its cytotoxic effects in the bystander TK6 cells from day 1-5 whilst etoposide initially reduced the viability of the bystander

TK6 cells on day 1 but recovered on day 2 and maintained this viability for the remainder of the study. However, these results (section 4.3.2.3) are similar to the results observed herein in the bystander *in vitro* co-culture model in which fresh medium was used to culture the cells following drug exposure. This further agrees with the findings of Kelechi Okeke (personal communication), which showed that increased MN frequency was similarly recorded in the bystander TK6 cells following co-culture and conditioned medium experiments with treated HS-5 cells. Collectively, the results herein support the idea that drug-treated HS-5 cells retain the effects of the chemotherapeutic agents and subsequently release bystander signals in the medium that are capable of inducing cellular changes in the bystander TK6 cells. This infers that the bystander signals released by the treated cells into the conditioned medium is stable over a period of five days.

However, it is important to note that there are little data available on the longevity of CIBE. In fact, the longevity of CIBE has only been explored within our research group. The first evidence of CIBE longevity experiments used cell number and MN as cytotoxic and genotoxic endpoints respectively (Kelechi Okeke, personal communication). Data from their study revealed that HS-5 cells treated with chlorambucil, carmustine, etoposide and mitoxantrone induced an increase in MN frequency in bystander TK6 cells over 5 days. Furthermore, the cell number of the bystander cells relative to the control was also reduced to 60% over a five-day period in all drugs used. In this study, only cytotoxic endpoint (cell number) was explored in the longevity study. The cytotoxicity results with mitoxantrone are similar to the findings from the previous report; mitoxantrone-induced bystander killing herein also lasted for five days. However, their findings with the other drugs contradict the results in this study; the bystander cells exposed to medium conditioned by HS-5 cells treated with chlorambucil, carmustine and etoposide proliferated at a similar rate to the control cells. The reason for this discrepancy could be due to differences in experimental factors as the methods from both studies differ. The longevity experiment herein was done using conditioned medium from treated HS-5 cells whilst theirs was performed in a co-culture system. This suggests that CM produces less of a CIBE and that a short-lived signal or messenger is released from the cells, which may have been lost when the CM was harvested after 24 hours however in their study, the bystander cells were constantly exposed to this signal thus

explaining why there was a higher bystander killing in their study. The propagation of bystander signals has also been reported to be dependent on the number of cells present at the time of exposure (Lyng *et al.,* 2002). However, the number of HS-5 cells (1 x 10^5 cells/cm^2) and TK-6 cells (5 x 10^5 cells/ml) used in this study corresponds to the same number used in their study as well. This further infers that the stability of the released factors is the main issue.

Furthermore, previous duration studies have been focused on the propagation of RIBE signals. In 1997, normal human lung fibroblasts treated with low irradiation α-particles induced SCE that persisted in bystander cells. The conditioned medium from normal human lung fibroblasts treated with low irradiation α-particles was frozen at − 20°C for 16 hours, then thawed and transferred onto unirradiated cells and incubated for an additional 24 hours (Lehnert and Godwin, 1997). This suggests that these bystander signals are stable at low temperature, can survive freeze-thaw and is heat-labile. In a similar fashion, fractionated irradiation induced DNA hypomethylation in bystander spleen *in vivo,* which lasted for 14 days however this prolonged signal transduction was not recorded with acute radiation instead DNA hypomethylation was found in bystander spleen up to 6 hours (Baskur, 2010). These support the previous findings in the 70s, which revealed that plasma of atomic bomb victims induced chromosomal breaks in their normal leukocyte cultures 31 years later (Pant and Kamada, 1977). These explain why it has been proposed that RIBE signals are capable of inducing genomic instability that persists from generation to generation. It also supports the fact that it is not just about mutated stem cells in exposed individuals – the affected progeny can induce bystander effects as well.

However, the mechanisms of RIBE and CIBE may differ so care should be taken whilst comparing data from these studies. Variation in the response to chemotherapeutic drugs by HS-5 cells and bystander TK6 cells suggests that CIBE is dependent on the chemotherapeutic agent used and the nature of the cells involved. Furthermore, the persistence of CIBE over five days negates the idea that the suggested 5-day 'recovery' period possible in clinical settings during HSCT is actually a safe window. However, further studies need to be developed and performed to fully understand if the viability of the cells coincides with the genotoxic effects in the bystander cells over a long period. Where genotoxic events persist, the functionality/viability of the cells should also be assessed longterm. The drugs used in this study are part of intensive chemotherapy

regimens used clinically in the treatment of leukaemia and lymphoma (Hecker *et al.,* 2018; Wang *et al.,* 2018; Okay *et al.,* 2019). These cancers have since been linked to the development of DCL in patients months or years after undergoing HSCT (Shiozaki *et al.,* 2014; Bobadilla-Morales *et al.,* 2015; Gabay *et al.,* 2020). Therefore, the limited evidence from this data should be further explored, and with a bigger range of drugs to show which may be or are not safe during pre-transplant conditioning. This should help clinicians to make an informed decision about the therapies given to patients during pre-transplant conditioning thus ensuring preference is given to drugs that can induce little or no CIBE in order to reduce the risk of patients developing a second malignancy.

4.4.5 Differential miRNA expression in HS-5 and TK6 cells

In this study, it has been shown that CIBE signalling can be propagated via two distinct systems involving the use of culture medium: co-culture and medium transfer so it is suggestive that these bystander signals are medium-borne however direct cell-cell signalling whilst in contact cannot be ruled out. These medium-borne bystander signals may be soluble signalling molecules such as cytokines, which have previously been implicated in CIBE (Demidem *et al.,* 2006; Asur *et al.,* 2009; Pessina *et al.,* 2013; Skolekova *et al.,* 2016; Somaiah *et al.,* 2018). Interestingly, this increased expression of cytokines in MSC following chemotherapy coincided with altered expression of different genes including *VEGFA, BRCA1, MYC, NOTCH* and *NME1* that have been implicated in the development and progression of cancers (Devereux *et al.,* 1999; Zhang *et al.,* 2018). In addition, a recent review by Garavelli *et al.,* (2018) illustrated that there appears to be a bidirectional relationship between cytokines and miRNAs.

Therefore, this evidence suggests that CIBE may be epigenetically mediated. Epigenetic changes are alterations in gene expression that include RNA-associated silencing, DNA methylation and histone modification. To investigate the possibility that CIBE is epigenetically mediated, the differential expression of miRNAs in the treated HS-5 cells as well as bystander TK6 cells was explored. However, the microarray experiment of miRNAs expression in bystander TK6 cells after exposure to treated HS-5 cells was first investigated to identify candidate miRNA(s) of interest as this is the first time the possibility of involvement of miRNA in CIBE has been explored. Whilst we

might infer that upregulation of miRNAs that might then be transported to the bystander cells seems like a reasonable premise for CIBE, observations from literature (Chaudhry and Omaruddin, 2011; Xu *et al.,* 2014) showed that simply being vastly upregulated in the treated cells does not guarantee transfer via medium – instead the transport appears to be selective. Thus, in order not to miss a possible candidate for bystander by only focusing on those highly upregulated in HS-5 cells, instead candidates were looked for as upregulated miRNAs in bystander cells, assuming that an increase may result from trafficked signalling molecules.

Previously, a range of investigations have revealed the involvement of miRNAs in the propagation of RIBE signals via medium to bystander cells. Kortubash *et al.,* (2007), who reported deregulation of miR-194 in the bystander spleen, did the first study involving miRNAs in RIBE. There were also alterations in the microRNAome in bystander spleen following exposure to irradiated cells (Kortubash *et al.,* 2008; Kortubash *et al.,* 2010). However, the most common miRNA that has been reported in RIBE studies is miR-21; its deregulated expression coincided with the deregulation of tumour growth factor beta (TGF-β) and release of ROS (Chaudhry and Omaruddin, 2011; Xu *et al.,* 2014; Jiang *et al.,* 2014; Yin *et al.,* 2015). In addition, increased expression of miR-663 led to the downregulation of TGF-β in bystander HeLa cells (Hu *et al.,* 2015).

In the current study, microarray analysis of miRNA expression revealed that hsa-miR-21 was also upregulated in bystander TK6 cells by 1.54 folds. Of the total 84 miRNAs in the PCR array, nine other highly expressed miRNAs that were upregulated by at least 1.50 folds were hsa-miR-155-5p, hsa-miR-30d-5p, hsa-miR-20a-5p, hsa-miR-16-5p, hsa-miR-17-5p, hsa-miR-30e-5p, hsa-miR-103a-5p, hsa-miR-29a-3p, and hsa-miR-320a-5p. However, their expressions were not statistically significant. Furthermore, the expression of hsa-miR-200c-3p was downregulated by (-6.20 folds) in this study but its expression was also statistically insignificant. These contrast the findings of Chaudhry and Omaruddin (2011), which revealed that the expression of hsa-miR-155-5p and hsa-miR-16-5p were downregulated in bystander non-irradiated cervical cancer cells whilst hsa-miR-17-5p was only upregulated for a short period.

In practice, many researchers use array experiments as an indicator and then confirm with qRT-PCR however, these were repeated three times and the data from various arrays integrated to ensure more robust data or outcome. Whilst microarrays are the most logical method for identifying which miRNAs are being expressed, qRT-PCR is often used to validate those results (Camarillo *et al.,* 2011). Therefore, in order to validate this result, miRNAs that were upregulated by at least 1.50 folds were compared against their respective *p*-values to identify those that were close to statistical significance. The rationale behind this is that one would expect that CIBE signals to be propagated by miRNAs that are upregulated rather than downregulated in the treated stromal cells and transferred to the bystander cells. However, a large downregulation of hsa-miR-200c-3p does beg the question that removal of a miRNA could equally change the bystander cell's functionality. As a result, hsa-miR-30d-5p, hsa-miR-20a-5p, hsa-miR-146a-5p, hsa-miR-16-5p, hsa-miR-17-5p and hsa-miR-20a-5p were chosen as upregulated candidates, whereas hsa-miR-200c-3p was chosen as the only downregulated miRNA. However, further differential expression of miRNAs in the treated HS-5 cells and bystander TK6 cells revealed that hsa-miR-146a-5p, hsa-miR-16-5p, hsa-miR-20a-5p and hsa-miR-17-5p were all upregulated in the treated cells but repressed in the bystander cells. This infers that the modulation of these miRNAs might have a role in the response of bystander cells after chemotherapy. These results are similar to the findings of Chaudhry and Omaruddin (2011), which revealed that miRNAs that were upregulated in irradiated TK6 cells were downregulated in non-irradiated TK6 cells. These further highlight that there may be selectivity in the trafficking of miRNAs from cell to cell irrespective of the amount produced. This is supported by recent findings by Skopelitis *et al.,* (2018), which revealed that the trafficking of miRNAs from cell to cell is a regulated process via a gating mechanism polarised at defined cell-to-cell interfaces, and these gatekeepers generate selectivity in long distance trafficking. Furthermore, the differential miRNA expression in the bystander cells could be due to several possible reasons such as increase in the activity of transcription factors, cytokine signalling pathways or induction of ROS from the medium.

Since there's limited data about CIBE, the mechanisms of RIBE and CIBE may differ, however, the results herein imply that cellular modulation of miRNA expression occur following exposure to chemotherapeutic agents, and could be responsible for large-scale gene expression alterations

thereby highlighting a role in regulating drug response. There is a consensus that miRNAs play an important role in pharmacogenomics through the regulation of specific genes that many drugs require to function (Hummel *et al.,* 2010; Rukov *et al.,* 2013; Kortubash *et al.,* 2015; Awan *et al.,* 2017; Han *et al.,* 2017). As a result, these differential changes in the miRNA profiles may mediate regulatory changes leading to the induction of non-targeted cellular effects in the bystander cells that may cause them to transit from healthy cell to disease cell.

Furthermore, the reason for the discrepancy in the microarray qRT-PCR data and differential miRNA qRT-PCR data is unknown however this may be due to lower expression (<2 folds) of these miRNAs in the bystander cells thus suggesting the greater sensitivity of qRT-PCR in identifiying these miRNAs at lower expression levels. There is evidence in literature that there is considerable variability between the two assay platforms at lower expression levels of miRNAs (Ach *et al.,* 2008; Chen *et al.,* 2009; Camarillo *et al.,* 2011). Nevertheless, these miRNAs may be involved in the intercellular signalling pathway between treated HS-5 cells and bystander TK6 cells. In order to evaluate the potential role of these differentially expressed miRNAs, their target genes were predicted bioinformatically and their biological functions and gene ontology were determined. Results from the bioinformatics study herein revealed that pathways involved in various signal transductions such as VEGF signalling pathway, MAPK signalling pathway, NF-Kβ signalling pathway, cytokine-mediated signalling pathway, protein phosphorylation, myD88 signalling pathway and toll like receptor signalling pathway were all enriched pathways for the target genes of the differentially expressed miRNAs. All these pathways are known to be involved in cellular communication and immunomodulatory processes (Osaki and Gama, 2013; Deguine and Barton, 2014; Wu *et al.,* 2018). Alterations of these signalling pathways have also been associated with carcinogenesis (Sever and Brugge, 2015; Wu *et al.,* 2018). Mutations of the MAPK and myD88 signalling pathway genes are found in leukaemia cases whilst leukaemia patients have been shown to have a significantly higher level of VEGF, an important mediator of angiogenesis, in their blood (Pasmat *et al.,* 2015; Improgo *et al.,* 2018; Song *et al.,* 2020). myD88 is crucial in innate immunity especially in toll like receptor signalling and interleukin-1 signalling (Improgo *et al.,* 2018). In addititon, interleukin-21 activates the Raf-ERK-MAPK and Jak/STAT signalling pathways and promotes apoptosis and chemotaxis in leukaemia cells by promoting differential expression

of many cytokines (Faqua *et al.,* 2020). Furthermore, NF-κB controls different biological processes by switching on and off genes; however its activity in AML is altered thus enabling leukaemia cells to proliferate and evade apoptosis (Zhou *et al.,* 2015).

Furthermore, other dominant categories enriched by predicted genes were related to cell division and survival such as transcription factors, cell cycle, cell proliferation, mitochondria degradation, autophagy, cell shape and cellular response to hypoxia and mechanical stress. These infer that genes belonging to signalling pathways associated with cell cycle, DNA damage and DNA repair may be potentiated by CIBE and may have a driving effect on the cells thereby determining their fate (Koussounadis *et al.,* 2014; Foukakis *et al.,* 2018). Therefore, these immune-related and cell-survival signalling factors may predict the development of a second malignancy in the bystander cells following CIBE.

Alterations in the expression of these miRNAs have also been associated with leukaemia. The miR-17-92 cluster (hsa-miR-17-5p & hsa-miR-20-5p) are well known proto-oncogenes that regulate different cellular processes that promote carcingogenesis (Fang *et al.,* 2017). The miR-17-92 cluster has been reported to be involved in CLL, MLL, philadelphia-positive leukaemia and diffuse large B-cell lymphoma (Bo *et al.,* 2015; Mian and Zeleznik-Le, 2016; Spagnuolo *et al.,* 2019). In contrast, hsa-miR-16-5p and hsa-miR-200c-3p both act as tumour suppressor genes that affect cell proliferation, division and apoptosis, and are commonly downregulated in leukaemia cases (Filip *et al.,* 2017; Sun *et al.,* 2019; Casabonne *et al.,* 2020). The expression of hsa-miR-146a-5p and hsa-miR-30d-5p, which are regulated by the NF-κB pathway and c-Myc transcription factors, is also downregulated in leukaemia and lymphoma respectively (Carvalho de Oliveira *et al.,* 2018; Zhou *et al.,* 2018).

Collectively, these results suggest that miRNA profiles in treated and bystander cells are altered and may have a role in regulating their response to chemotherapy. However, if these miRNAs are released into the medium by treated HS-5 cells then there must be a transport pathway for these miRNAs to be internalized by the bystander cells. It is noteworthy to mention that this is the first exploration of miRNA involvement in CIBE so this may serve as an insight into this field. This may

be a complex process hence there is need to develop and perform more studies to further elucidate a detailed understanding of miRNAs function in the mechanism of CIBE.

4.5 Summary

This chapter has focused on the chemotherapeutic effects of drugs used in pre-transplant conditioning on HS-5 cells and the ability of these treated HS-5 cells to transfer these drug-induced effects to the bystander TK6 cells. The BM microenvironment is extraordinarily heterogeneous and the cells that inhabit the BM microenvironment are expected to experience an array of microenvironmental cues following pre-transplant conditioning, which may in turn translate to several genotypic and physiological manifestations in these cells. There is a great deal of evidence that points to MSC as a major regulator of tumour development and progression, are exposed to pre-transplant conditioning during HSCT. Here, the HS-5 cells revealed a variation in response to some of the chemotherapeutic agents used during pre-transplant conditioning. Although HS-5 cells recovered from the chemotherapeutic effects of some of the drugs, the effects of mitoxantrone persisted in the HS-5 cells even after 72 hours. The results herein show that MSC are exposed to what is happening around in the BM microenvironment and are bathed in chemotherapy thus these drugs may compromise their functionality. In addition, MSC may also influence incoming cells from the donor, which have not been exposed to these chemotherapeutic effects, the way we haven't expected by releasing bystander signals that may cause cell death or genotoxic events in these incoming cells upon uptake. Therefore, it is important for clinicians to evaluate these chemotherapeutic agents whilst deciding the appropriate therapy for patients. Since not all patients develop DCL, it is also important for clinicians to review patient/donor-derived issues for influences on response to chemotherapy and/or CIBE.

Following exposure to chemotherapeutic drugs, the profile of HS-5 cells secretome influenced cytotoxic, proliferative and genotoxic changes in the bystander TK6 cells with mitoxantrone having the biggest cytotoxic and genotoxic effects in the bystander cells over five days. Therefore, these suggest that the profile of HS-5 secretome changes following chemotherapy and may be released into the medium to cause these CIBE in bystander TK6 cells following uptake. These

medium-borne factors could be chemokines or cytokines that coincide with dysregulation of miRNA expression profiles in the treated HS-5 cells and bystander TK6 cells. Differential expression of miRNAs, RNA-associated molecules that induce epigenetic changes, in the treated HS-5 cells and bystander TK6 cells revealed that upregulated miRNAs in the treated cells such as hsa-miR-146a-5p, hsa-miR-16-5p, hsa-miR-30d-5p and hsa-miR-17-5p were repressed in the bystander cells. Whilst hsa-miR-17-5p acts as proto-oncogene, other miRNAs act as tumour suppressors in leukaemia and control target genes that are involved in different cellular processes such as apoptosis, proliferation, differentiation and cell division. In addition, the predicted target genes of these miRNAs were genes of different signalling pathways thus suggesting that these miRNAs may control the fate of these cells. Therefore, it can be suggested that if these miRNAs are differentially expressed in these cells hence there may be a vehicle, via medium, for these miRNAs to be transported to the bystander cells. Further investigation and profiling of the HS-5 secretome (Chapter 5) released into the medium during co-culture with bystander TK6 cells has to be done to fully understand the extent of miRNA involvement in the mechanism of CIBE.

5.0 The possible role of sEVs in chemotherapy-induced bystander effect

5.1 Introduction

Cells can communicate with each other through the transfer of a range of molecules including cytokines, chemokines, miRNA, mRNA and proteins that are released into extracellular compartments such as serum, plasma, saliva, milk and urine. These molecules are usually packaged into lipid-bilayered EVs, which renders them more stable at different pH and temperature, and protect them from RNAse degradation (Chen *et al.,* 2008).

It has been established that radiotherapy induces cells to release EVs into the extracellular milieu both *in vivo* and *in vitro* following treatment (Song *et al.,* 2016; Cai *et al.,* 2017; Szatmari *et al.,* 2017; Schoefinius *et al.,* 2017). However, there is limited evidence of the ability of chemotherapeutic drugs to induce EVs secretion and release by cells *in vivo* and *in vitro* (Pascucci *et al.,* 2014; Lin *et al.,* 2017; Samuel *et al.,* 2017; Bandari *et al.,* 2018; Keklikoglou *et al.,* 2019). Some of the drugs that have been able to induce this biological effect include cisplatin, etoposide, and paclitaxel with varying phenotypic changes and altered biological processes in the bystander cells when these EVs are engulfed by these cells. However, EVs produced by cells differ and depend on the secreting cell, hence the fate and functions of these EVs are different. Their function depends on their cargo of nucleic acids, proteins and lipids, which may or may not reflect the composition of the secreting cells and the molecular processes taking place inside these cells (Ludwig *et al.,* 2019; Ortega *et al.,* 2019). Nevertheless, EVs must be taken up by the recipient cells to carry out their functions. However, there is selectivity in uptake of these EVs' contents by the recipient cells *in vitro* (Qiu *et al.,* 2018; Sancho-Alberto *et al.,* 2019; Zhang *et al.,* 2019). The recipient cells internalise these EVs via different pathways such as endocytosis and fusion however, the mechanism of uptake is unclear and usually depends on the recipient cells (Horibe *et al.,* 2018; Durak-Kozica *et al.,* 2018).

Recently, EVs have been shown to be important bioactive components of the MSC secretome. However, the secretion of EVs by MSC *in vitro* depends on cell culture parameters such as cell passage number and cell seeding density (Patel *et al.,* 2017). MSC-derived EVs can induce biological effects including adipogenesis, angiogenesis, apoptosis and proteolysis in recipient cells (Chulpanova *et al.,* 2018). MSC-derived EVs also induce HSC development, BM microenvironment and immune system functions (Cominal *et al.,* 2019). However, the effects of MSC-derived EVs depend on their miRNA signature profiles, which regulate the expression of different target genes and influence various cell-signalling processes. In 2016, De Luca *et al.,* showed that BM-MSC and UBC CD34+ stem cells can communicate via EVs-derived miRNAs during HSCT thereby modifying gene expression and altering biological functions of the recipient cells. These predicted target genes participate in the regulation of haematopoiesis and are associated with the inhibition of the Wnt/*β*-catenin signalling pathway (Xie *et al.,* 2016).

Therefore, MSC-EVs-mediated transfer of miRNAs is an area of active research. Several research studies have reported that MSC-EVs possess the ability to induce therapeutic effects in the heart, liver and brain via the transfer of miRNAs (Wang *et al.,* 2015; Xin *et al.,* 2017; Chen *et al.,* 2018). However, there is a lack of consensus miRNA profile on MSC-EVs and their principal target genes due to heterogeneity in culture conditions, cell status, cell origin and methodology (Qiu *et al.,* 2018). Nevertheless, this may suggest that individual miRNAs combine synergistically to induce the effects of MSC-EVs.

Consequently, it is important to understand the crosstalk between HS-5 cells and bystander TK6 cells as a model of HSCT, and explore if the CIBE is mediated by HS-5 cells-derived EVs as it has been shown that MSC and HSC can communicate via EVs-derived miRNAs during HSCT. This may explain why differential miRNA profile signatures were found in HS-5 cells and bystander TK6 cells (section 4.3.3.4). This chapter explored the release of EVs by HS-5 cells and the investigation of the cargo of these EVs to check if they contain miRNAs that are capable of inducing CIBE in the bystander TK6 cells. In addition, the ability of the bystander TK6 cells to internalise these HS-5-derived EVs as well as the effects of HS-5-derived EVs on bystander TK6 cells were further assessed. Cell death and DNA damage were also assessed as bystander endpoints. DNA damage

was assessed using the MN assay whilst cell death was measured based on the trypan blue exclusion dye assay.

5.2 Methods

5.2.1 Release of sEVs following chemotherapy

HS-5 ($1x10^6$) cells were treated with clinically relevant doses of carmustine, chlorambucil, etoposide and mitoxantrone for an hour. Afterwards, cells were treated as described in section 2.14 and stained with potassium permanganate in 0.1M phosphate buffer pH 6.5 and Reynold's lead citrate (1963). Samples were observed using a Phillips CM10 transmission electron microscope with a Gatan Orius SC 100 charge coupled device camera (model 832) operating at 60kV.

5.2.2 Isolation of sEVs

HS-5 cells were treated with mitoxantrone for 24 hours. Afterwards, CM from the treated cells were prepared and collected as discussed in section 2.13.1. CM was then used as the starting material to isolate sEVs by two methods (ExoQuick precipitation method and SEC) discussed in section 2.15. Following successful isolation of these vesicles, the vesicles were characterised by TEM and NTA as illustrated in section 2.16. The protein levels in the vesicles were estimated by BCA and/or Bradford assay as illustrated in section 2.16.3.

5.2.3 Uptake of sEVs

The vesicles isolated from treated HS-5 cells were labelled with two separate dyes, Exo-Glow-Membrane and Exo-Glow-RNA that specifically label the membrane and RNA of these vesicles as mentioned in section 2.19. Inhibition of the uptake of these sEVs was also done using heparin as described in section 2.19.4. Afterwards, the cells were analysed under a confocal microscope as described in section 2.19.3.

5.2.4 The effect of GW4869 on HS-5 cells and CIBE

HS-5 cells were treated with increasing doses of GW4869 (5μ, 10μ, 20μ) dissolved in DMSO as discussed in section 2.17 to determine if GW4869 has any anti-growth effect on these cells. DMSO was used as the vehicle control. Afterwards, cells were pre-treated with GW4869 before exposure to drugs for 24 hours as described in section 2.18. These treated HS-5 cells were then co-cultured with TK6 cells as discussed in section 2.12, the TK6 cells were harvested 24 hours later and the cell viability and genotoxicity determined as illustrated in sections 2.10 and 2.11 respectivley.

5.2.5 The effect of sEVs on TK6 cells

sEVs isolated from treated HS-5 cells (section 2.15) were used to co-culture TK6 cells in the presence or absence of heparin as described in section 2.20 to determine if this inhibitor will ameliorate any vesicular effect on the cells. TK6 cells were then harvested and analysed for cell viability (section 2.10) and genotoxicity (section 2.11).

5.2.6 The effect of sEVs on mitoxantrone-induced cytotoxicity

As described in section 2.21, TK6 cells were pre-treated with sEVs isolated from treated HS-5 cells prior to exposure to mitoxantrone 24 hours later to determine if sEVs will have any effect on mitoxantrone-induced cytotoxicity in these cells. At the same time, heparin was used to inhibit sEVs uptake by the cells before exposure to mitoxantrone for 24 hours. Cell viability was determined by Trypan Blue assay (section 2.10) whilst genotoxicity was determined by MN assay (section 2.11).

5.2.7 The effect of sEVs on cell cycle

As previously discussed in section 2.29, TK6 cells were exposed to sEVs from treated HS-5 cells in the presence or absence of heparin. Next, the cells were either treated with mitoxantrone (as discussed in section 2.21) or left untreated. The cells were harvested a day later and cell cycle was determined by flow cytometry (section 2.29). TK6 cells exposed to mitoxantrone were used

as positive control whilst TK6 cells treated with PBS and untreated cells were used as negative controls.

5.2.8 Extraction of RNA from extracellular components

The extracellular components in this study, CM and sEVs were collected as previously described in sections 2.13.1 and 2.15 respectively. RNA was collected from these extracellular components and sEVs-depleted FBS, which served as the negative control as described in section 2.22. The purity and integrity of these RNA molecules were determined as described in sections 2.23 and 2.24 respectively.

5.2.9 Detection of miRNAs in extracellular components

The RNA from these extracellular components were converted to cDNA as discussed in section 2.25. The cDNA was then used to determine the levels of the candidate miRNAs previously mentioned in section 4.3.3, by qRT-PCR discussed in section 2.28. Small nuclear RNAs, SNORD61 and RNU6B/RNU6-2 were used as endogenous controls whilst miR-cel-39 was used as a spike-in control.

5.3 <u>Results</u>

5.3.1 HS-5 cells release small extracellular vesicles following chemotherapy

The role of EVs in intercellular communication between HS-5 cells and bystander TK6 cells was assessed. As previously described in section 2.14, HS-5 cells were treated with drugs for an hour, washed and appropriately prepared for observation under the transmission electron microscope. Untreated HS-5 cells shed small extracellular vesicles (sEVs), which appeared to be in clusters (figure 5.1) however, the vesicles seemed low in number. In addition, the sizes of the sEVs appeared to be uniform in contrast to the sEVs released by the cells following treatment with alkylating agents (figure 5.2). Vesicles released by chlorambucil-treated HS-5 cells were packaged

in a sac-like body whilst vesicles released by carmustine-treated HS-5 cells were of varying sizes, which highlights the heterogeneous nature of EVs. This suggests that these vesicles may be exosomes (≤ 200 nm) and microvesicles (≤ 500 nm). Similarly, cells treated with topoisomerase inhibitors, etoposide and mitoxantrone shed many sEVs in cocoon-like and arm-like structures respectively (figure 5.3). Nevertheless, there are clear protruberances from each of the drug treated but not the untreated cells. In addition, the cells seem to release more sEVs under drug-induced stress in comparison to the untreated cells. The sEVs released by alkylating agents also appear to be smaller structures compared to those released by topoisomerase inhibitors.
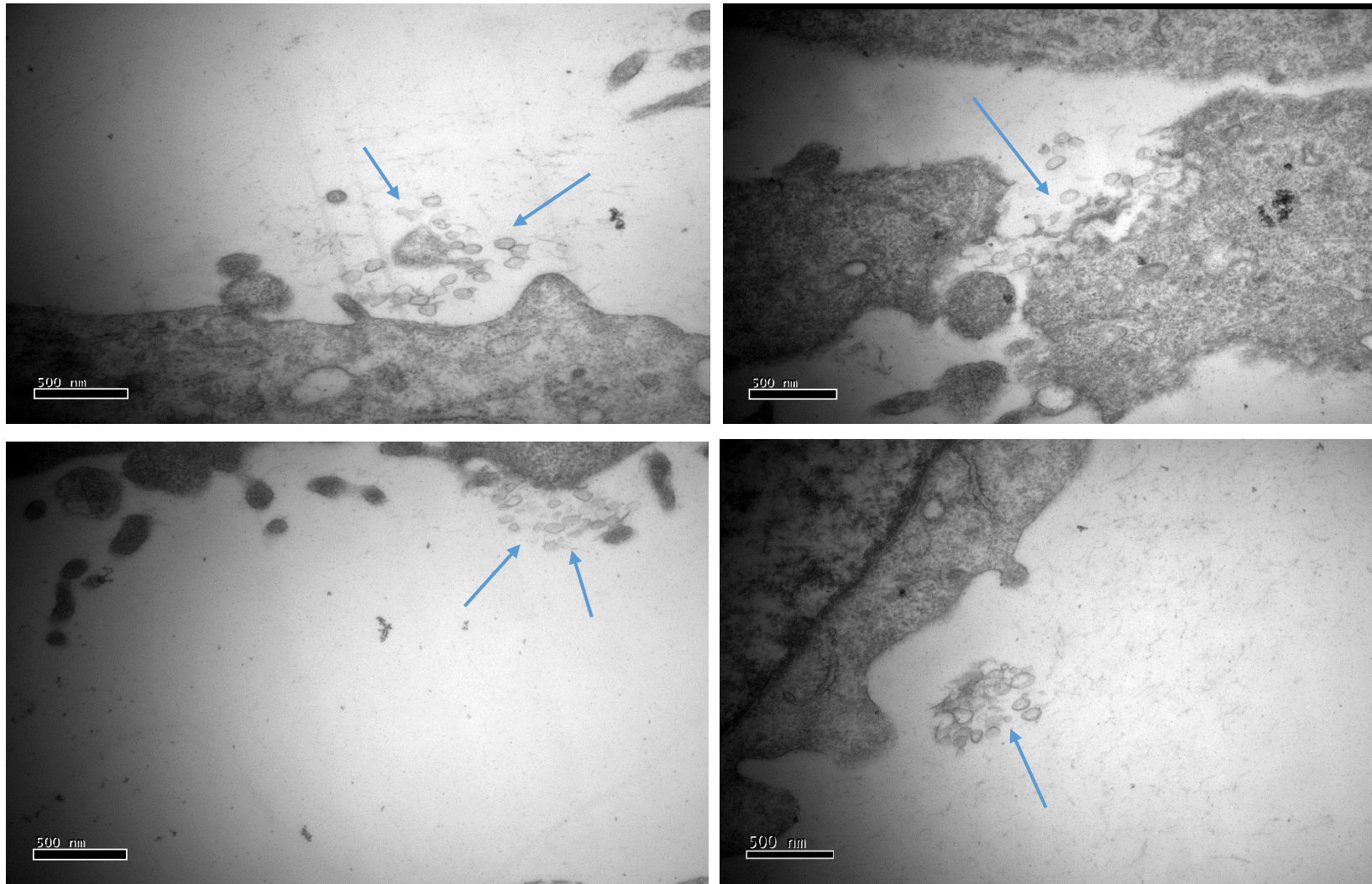
Figure 5.1 HS-5 cells release small extracellular vesicles without induction of chemotherapy. Vesiculation (indicted by blue arrow) was observed in cells before treatment with drugs but they were not in abundance. Scale bar, 500 nm.
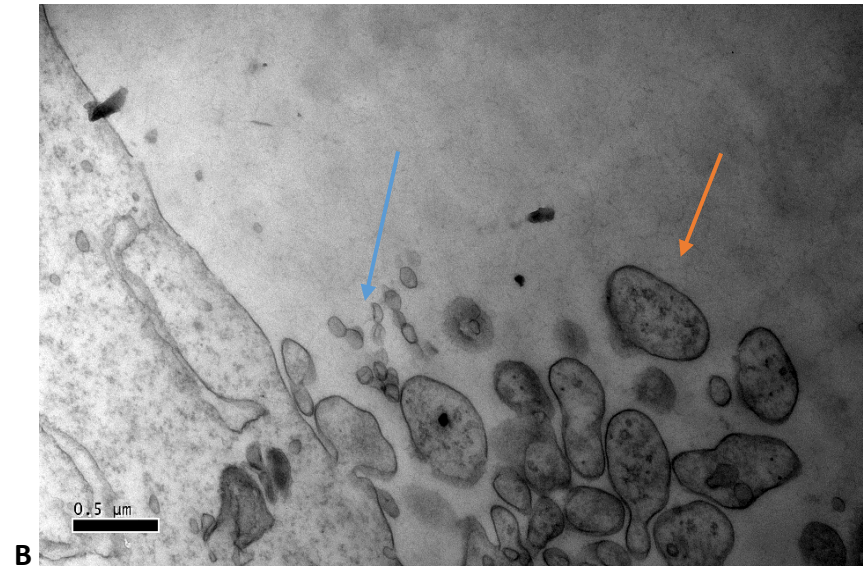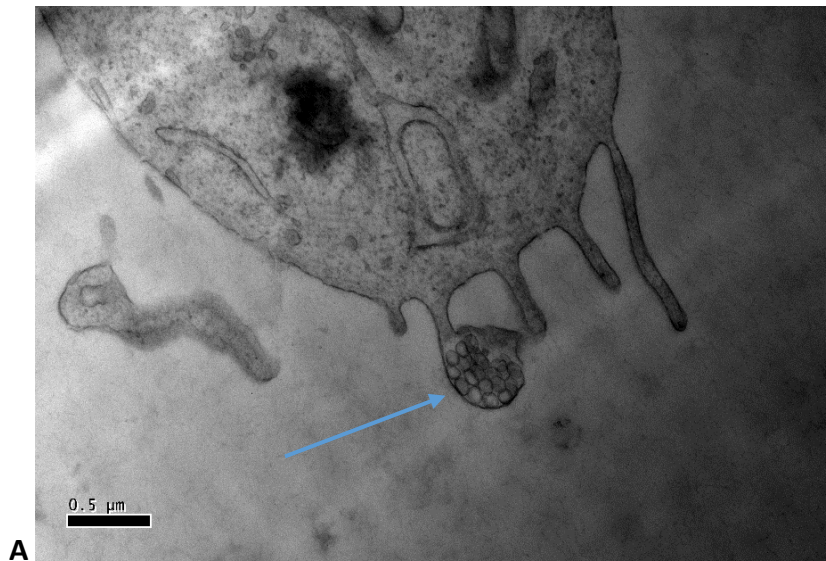
Figure 5.2 HS-5 cells release small extracellular vesicles following treatment with alkylating agents. (A) Transmission electron micrographs of cells exposed to chlorambucil (40 µM) after exposure for an hour. The small extracellular vesicles are packaged in a sac-like body (indicated by blue arrow) awaiting release to the extracellular milieu following fusion of the multivesicular body and the plasma membrane. (B) Transmission electron micrographs of cells treated with carmustine (10 µg/ml) after exposure for an hour. Intense shedding of extracellular vesicles of varying sizes (indicated by blue and orange arrows) occurred after an hour exposure to carmustine. Scale bar, 500 nm.
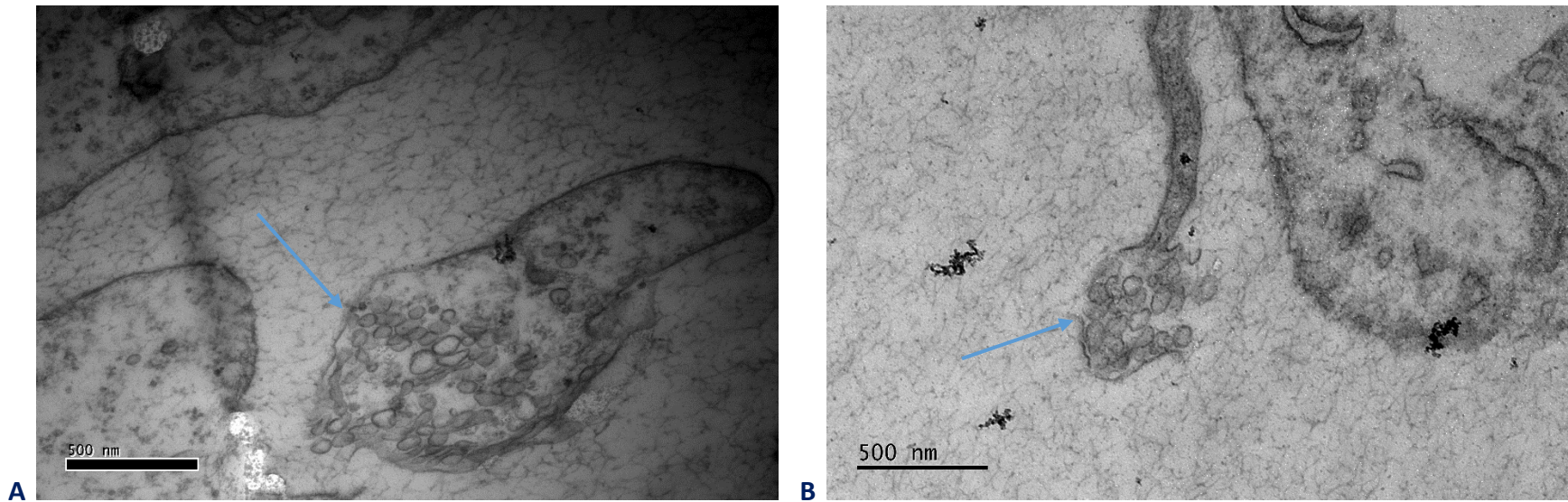
Figure 5.3 HS-5 cells release small extracellular vesicles following treatment with topoisomerase inhibitors. (A) Transmission electron micrographs of cells treated with etoposide (10 μM) after exposure for an hour. The small extracellular vesicles are released into the extracellular milieu in a cocoon-like structure (indicated by blue arrow). (B) Transmission electron micrographs of cells exposed to mitoxantrone (500 ng/ml) after exposure for an hour. Vesicles (indicated by blue arrow) are shed in an arm-like structure. Scale bar, 500 nm.

5.3.2 Characterization of sEVs released by HS-5 cells

5.3.2.1 Transmission electron microscopy

Next, vesicles were isolated from HS-5 cells with and without mitoxantrone treatment by SEC and ExoQuick precipitation methods as described in section 2.15. Transmission electron micrographs of sEVs from untreated and treated cells are shown in figure 5.4 and figure 5.5 respectively. There was no difference in the appearance of the vesicles isolated from the untreated and treated cells. The morphology and structure of the vesicles were consistent with the particulate structure proposed by ISEV. From the figures, it can be seen that the vesicles have a spherical shape. All vesicular particles had a bilayer structure and were around 30 – 100 nm in diameter, which is the typical size range for exosomes. Larger vesicles (> 100 nm) could also be detected (see appendix). This supports the data in figures 5.2 and 5.3 above, which revealed heterogeneity in the sizes of vesicles released by treated cells. Size distribution of these vesicles was determined and confirmed by NTA (section 5.4.2). Based on the different isolation procedures employed in this study and the vesicle characteristics, the vesicles used for subsequent analyses were termed sEVs although the preparation also contained larger vesicles.
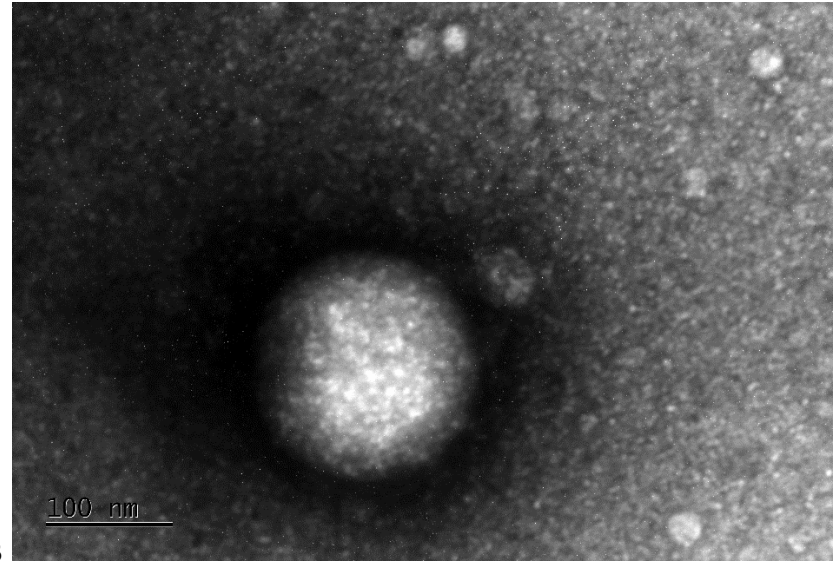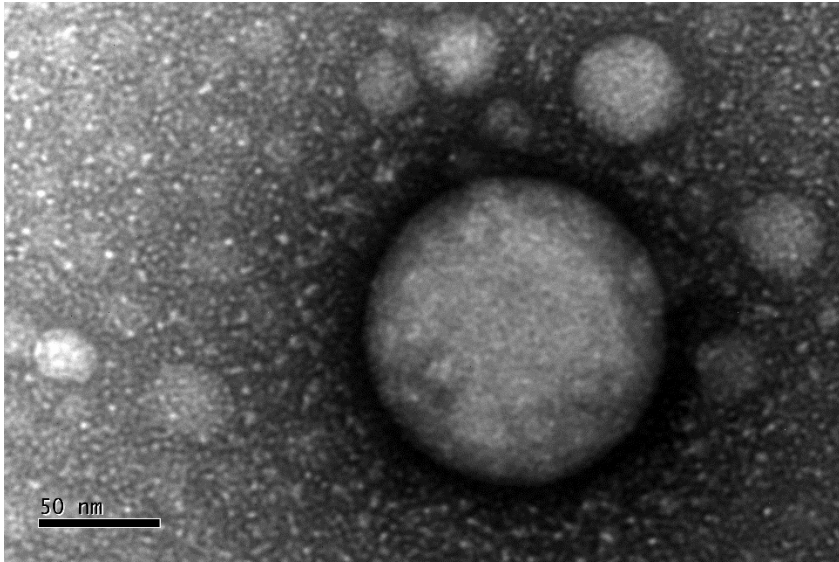
Figure 5.4 Transmission electron micrographs of sEVs isolated from untreated HS-5 cells. sEVs isolated from untreated HS-5 cells by size exclusion column chromatography (A) and ExoQuick Precipitation kit (B) are exhibited. Particles with bilayer structure and of the correct size (30 -100 nm) were observed. Scale bars: 50 nm (A); 100 nm (B).
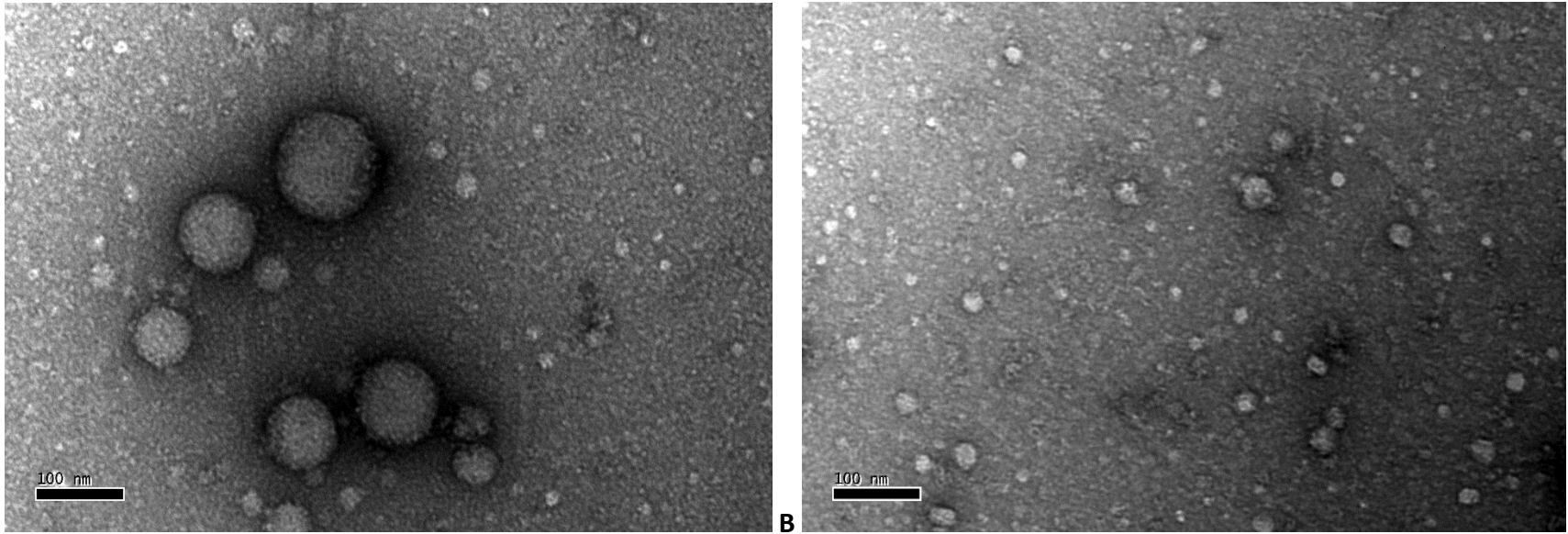
Figure 5.5 Transmission electron micrographs of sEVs isolated from mitoxantrone-treated HS-5 cells. sEVs isolated from untreated HS-5 cells by size exclusion column chromatography (A) and ExoQuick Precipitation kit (B) are exhibited. Heterogeneity in the size of the sEVs (30 -100 nm) was observed. Scale bar, 100 nm.

5.3.2.2 Sizing and quantification of sEVs

Sizing and quantification of the sEVs were performed with the NanoSight LM10 instrument and analysed with NTA as previously described in section 2.16. The results are shown in figures 5.6A (size distribution) and 5.6B (particle concentration) respectively. All sEVs recovered by both isolation protocols were smaller than 300 nm, most of them being in the range of 120 – 250 nm. This agrees with what can be seen visually in figures 5.1 – 5.5 thus suggesting that the size of sEVs released by both untreated and treated HS-5 cells was ≤ 500 nm. However, when the sizes of the sEVs were compared between the isolation protocols, the vesicles isolated with ExoQuick reagent were smaller than those isolated with SEC and this was statistically significant (control: 128 nm vs 205 nm $p < 0.0001$; treated: 129 nm vs 221 nm $p < 0.0001$).

In addition, both protocols ensured that a significant number of sEVs was recovered however, the ExoQuick reagent method recovered more sEVs in higher yields compared to SEC (control: 6.01 x 10^9 vs 1.89 x 10^9 $p = 0.0015$; treated: 7.41 x 10^9 vs 0.8 x 10^9 $p < 0.0001$). Interestingly, more sEVs were recovered from the treated cells via the reagent method in comparison to the untreated cells. This is in line with the data from the transmission electron micrographs, which seemed that cells release more vesicles under drug-induced stress. However, it is in contrast to results from the SEC method in which more vesicles were recovered from untreated cells than treated cells. The reason for this discrepancy in vesicle yield between these two isolation methods may also be due to the co-isolation of non-vesicular aggregates of the same size.

The quantification of sEVs is commonly done using particle concentration and protein concentration. In the SEC method, vesicle recovery is done in fractions 1-9 however, fractions 1-6 often contain contaminants that may skew further experiments. Therefore, only contents of fractions 7-9 were quantified to determine the fraction that produced the most significant number of sEVs (figure 5.6C) and how pure these sEVs were (figure 5.6D). The data show that fraction 8 produced the most abundant sEVs in the untreated cells (3.47 x 10^9) followed by fraction 9 (1.32 x 10^9). This difference in particle yield in the untreated cells was statistically significant (fraction 8 v fraction 7 $p = 0.0035$; fraction 8 vs fraction 9 $p = 0.0122$). However, there was no difference in particle yield between the fractions in treated cells. Furthermore, when the

fractions of the untreated cells was compared to the fractions of the treated cells, only fraction 8 proved to be statistically significant (untreated vs treated p = 0.0043).

The protein concentrations in these fractions were quantified to ensure accurate sEVs quantification as soluble proteins could be co-isolated with sEVs and thence interfere with downstream experiments. In the control cohort, fractions 7 and 9 contained about 7.83 μg/ml and 7.94 μg/ml of protein respectively compared to fraction 8 that was found to have about 4.87 μg/ml of protein. However, when the treated cohort was assessed, fraction 8 had the highest amount of proteins in the sEVs yield (5.26 μg/ml) followed by fraction 9 (3.90 μg/ml) and fraction 7 (1.06 μg/ml). Interestingly, there was no statistical significant difference found between these fractions in the control and treated cohorts due to high variability in outcomes as evidenced by the error bars.

Furthermore, the ratio of particle to protein concentration can also be used to assess the co-isolation of protein contaminants and thence determine the purity of sEVs. Overall, significant differences in this ratio was found between the two sEVs isolation methods (ExoQuick and SEC) in both the untreated (P = 0.0177) and treated cells (P = 0.0318) (figure 5.7). SEC-isolated sEVs showed a higher ratio than those from ExoQuick (control - SEC vs ExoQuick: 8.63 vs. 7.34; Treated - SEC vs ExoQuick: 8.44 vs. 7.48) indicating the less soluble protein contaminants and highest purity. This also suggests that large number of protein aggregates may contribute to the high sEVs counts in ExoQuick-isolated sEVs particles. Therefore, the SEC-isolated sEVs were used in downstream assays to ensure that experimental data was not skewed.
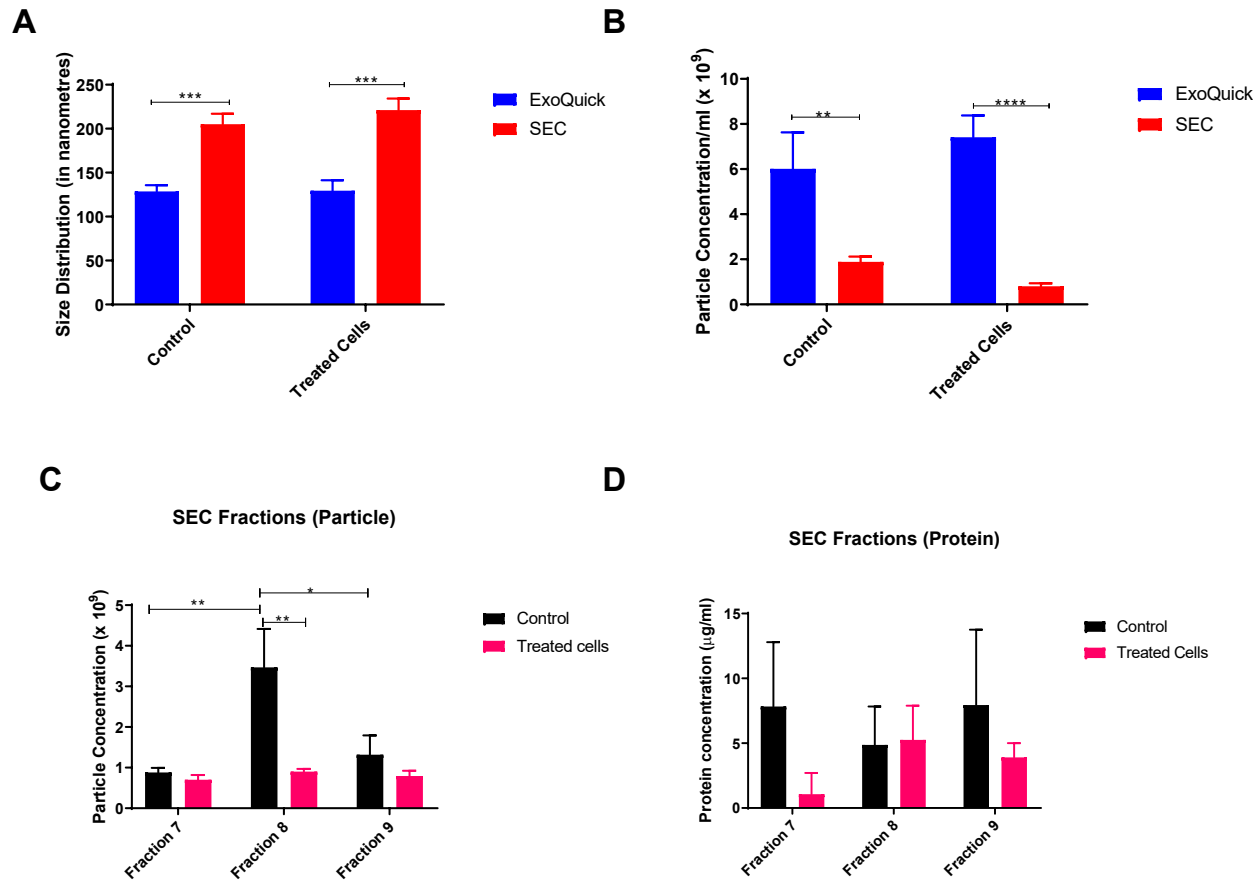
Figure 5.6 Quantification of sEVs by nanoparticle tracking analysis (NTA). (A) Size distribution of sEVs isolated from untreated and mitoxantrone-treated HS-5 cells by size exclusion column chromatography (SEC) and ExoQuick Precipitation kit. SEC-isolated sEVs were larger in size than the ExoQuick-isolated sEVs. (B) Particle concentration of sEVs isolated from untreated and mitoxantrone-treated HS-5 cells by SEC and ExoQuick. Vesicles release was more abundant using ExoQuick than SEC. (C) Particle concentration of SEC fractions. Fraction 8 produced more abundant sEVs than the other fractions. (D) Protein concentration of SEC fractions. Fractions 7 and 9 elutes had more proteins compared to fraction 8. Statistical significance was done using the student t-test (A and B) and two-way ANOVA (C and D) (* $p<0.05$ ** $p<0.01$; *** $p<0.001$ ****$p<0.0001$).
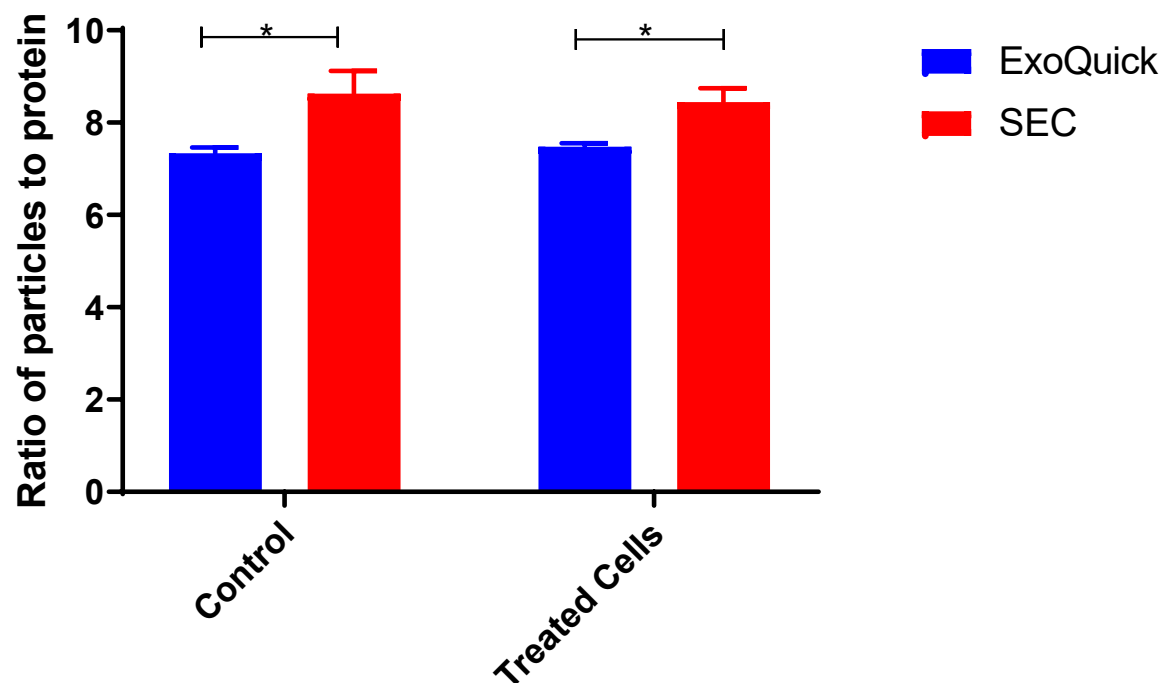
Figure 5.7 Purity of sEVs isolated by SEC and ExoQuick methods. The ratio of particles to protein [log (particles/protein)] was significantly higher for SEC than for ExoQuick. Statistical significance was done using the Student t-test (* $p<0.05$).

5.3.3 Bystander TK6 cells uptake HS-5-derived sEVs

Following the isolation and characterization of sEVs, the ability of the bystander cells to uptake these sEVs was investigated as illustrated in section 2.19. The fluorescent dyes used to track sEVs were Exo-Glow-membrane and Exo-Glow-RNA, red and green fluorescent dyes that are commercially available and specifically label SEVs with intact membranes and RNA cargo respectively. The labelled sEVs were incubated with the bystander cells and following incubation, the bystander cells were stained with a fluorescent dye, DiO (green) or DiL (red), that stain the phospholipids on the membrane of the cells.

After 3 hours, there was evidence of sEVs' uptake by the cells as visualised by confocal microscopy. The sEVs' membrane (red) can be seen on the membrane of the cells (green) as illustrated in figure 5.8. However, it wasn't clear if the sEVs expel their contents into the cells following adherence to the cell membrane. As a result, a time lapse experiment was done over 12 hours to investigate the fate of the sEVs following fusion to the membrane of the bystander cells. As shown in figure 5.9, the fusion of the sEVs to the membrane of the cells was evident after 1 hour whilst internalization of the sEVs seems to have taken place after 3 hours. The internalization process seems to be complete within 6-12 hours of incubation. This indicates that sEV uptake may be a time-dependent process and may involve interaction between substances found on the surface of the membrane of the bystander cells and sEVs.

To confirm that sEVs release their contents into the bystander cells following uptake, the cells were incubated with sEVs' with labelled RNA for 3 hours. The results show that sEVs' RNA are endocytosed into the cells. This indicates that the sEVs are internalised into the cells and once internalised, sEVs release their cargo into the cells (figure 5.10). It is important to mention that unbound dye label was removed to ensure that the fluorescence of cells and sEVs seen in this study was specific to the cells and sEVs and not due to the incorporation of free dye into the cells or sEVs.
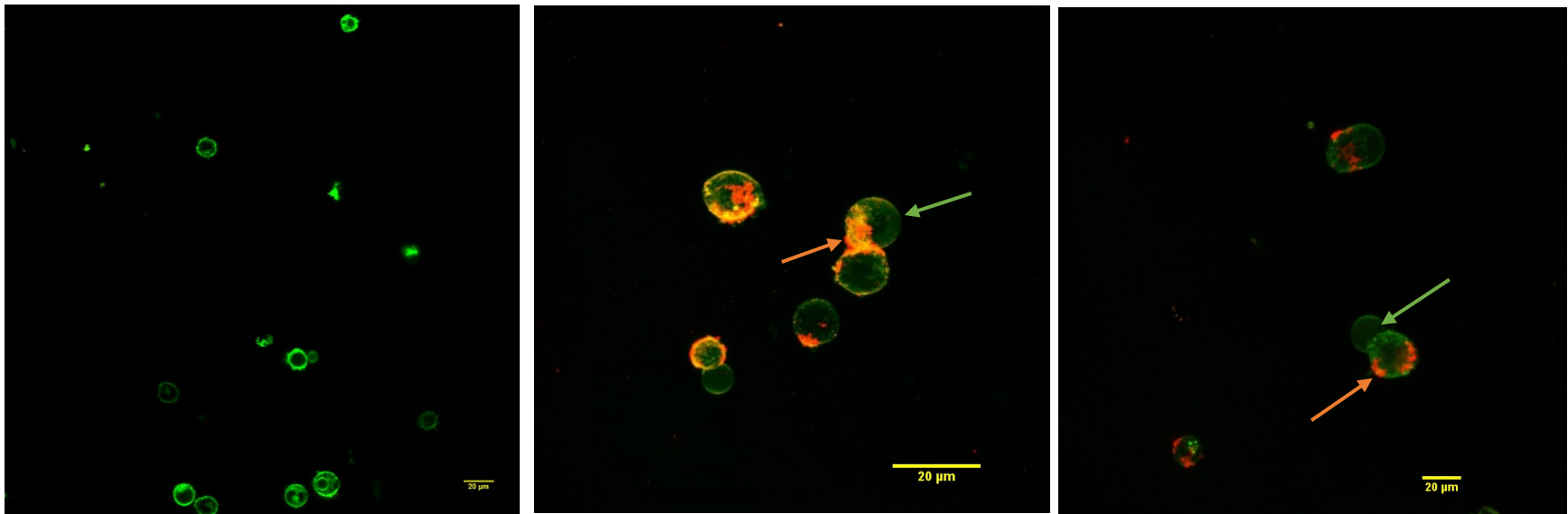
Figure 5.8 Confocal images showing that SEVs' (orange arrow) fuse to the DiO-labelled membrane of the bystander cells (green arrow) via substances found on their membranes. Control contains cells only. Magnification, 20X. Scale bar, 20 μm.
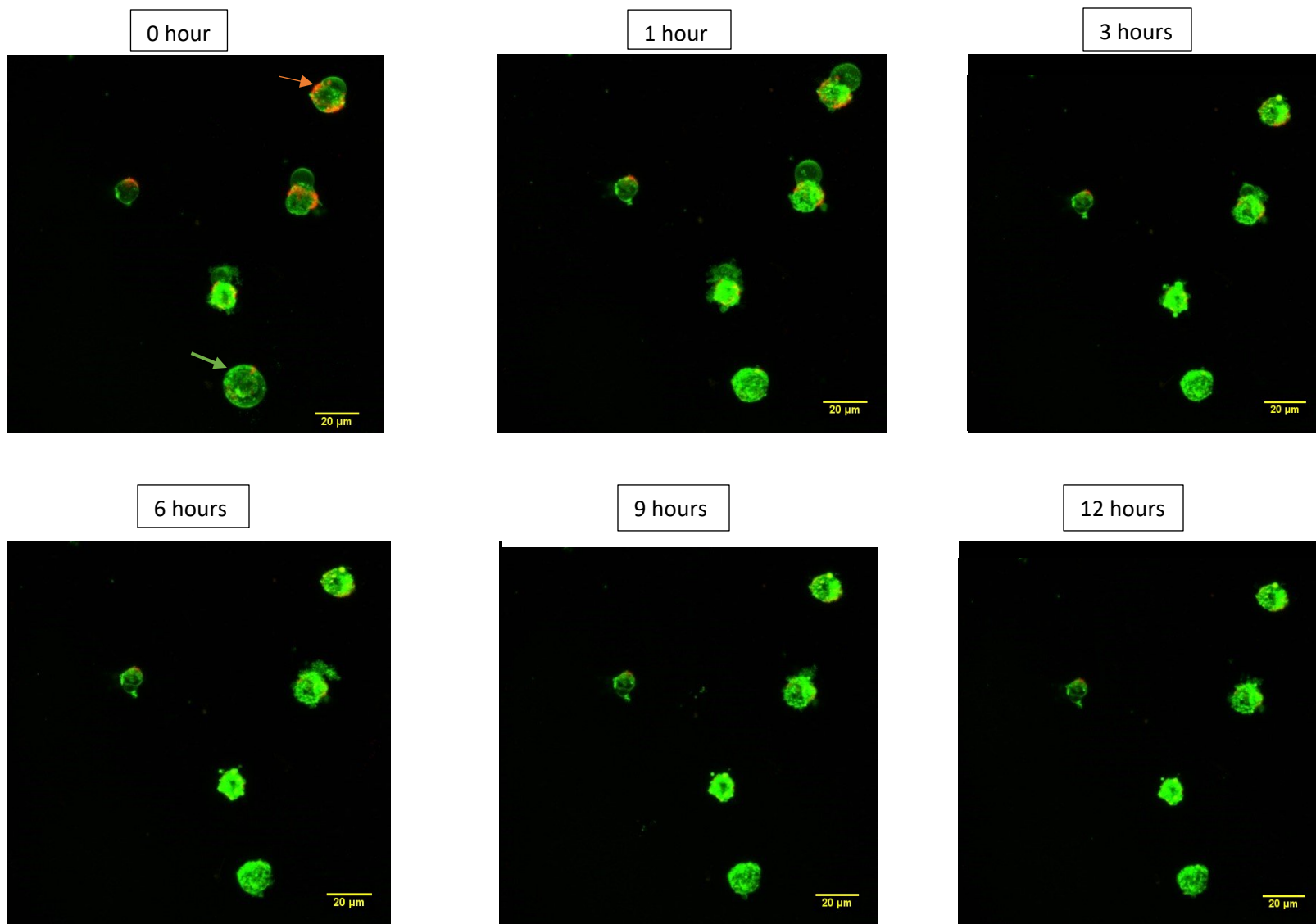
Figure 5.9 Confocal microscopy uptake analysis of sEVs. DiO-labelled bystander cells (green arrow) were incubated in the presence of Exo-Glow membrane labelled sEVs (orange arrow) for 12 hours. Confocal images were taken at 0-12 hours at magnification 20X. Scale bar, 20 μm.
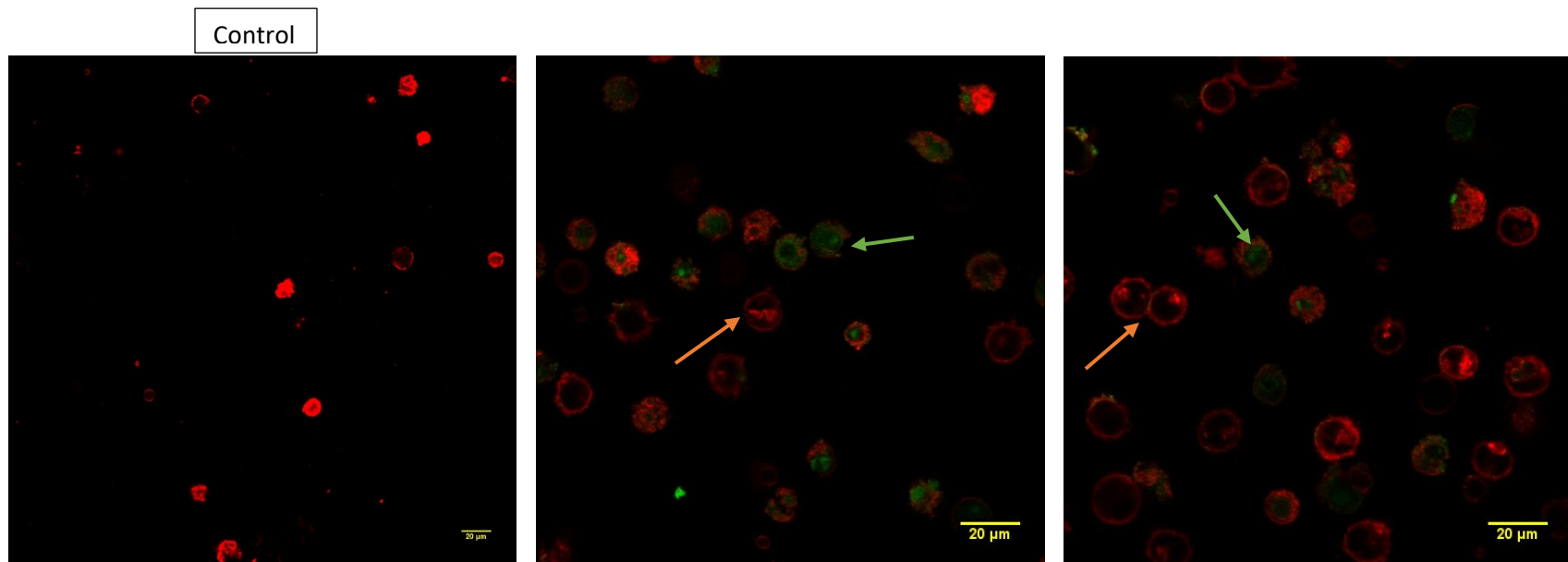
Figure 5.10 Confocal microscopy of the release of RNA cargo of sEVs following uptake by bystander cells. Representative micrographs of the labelled RNA of sEVs (green arrow) inside the cells (orange arrow). Control contains cells only. Original magnification, 20X. Scale bar, 20 μm.

Next, the ability of heparin to inhibit this uptake of sEVs by TK6 bystander cells was investigated. Heparin is an anti-coagulant that prevents the formation of blood clots. As described in section 2.19.4, sEVs were labelled and incubated with heparin for 30 minutes prior to co-culture with bystander cells for 3 hours. Results show that heparin inhibited the fusion of the sEVs, via their membrane, to the cells (figure 5.11A/B) and this resulted in the inability of the sEVs to release their RNA cargo into the cells (figure 5.11C/D). This further suggests that incorporation of sEVs and the release of their cargo into the recipient cells may depend on the successful fusion of these vesicles to the membrane of the recipient cells.
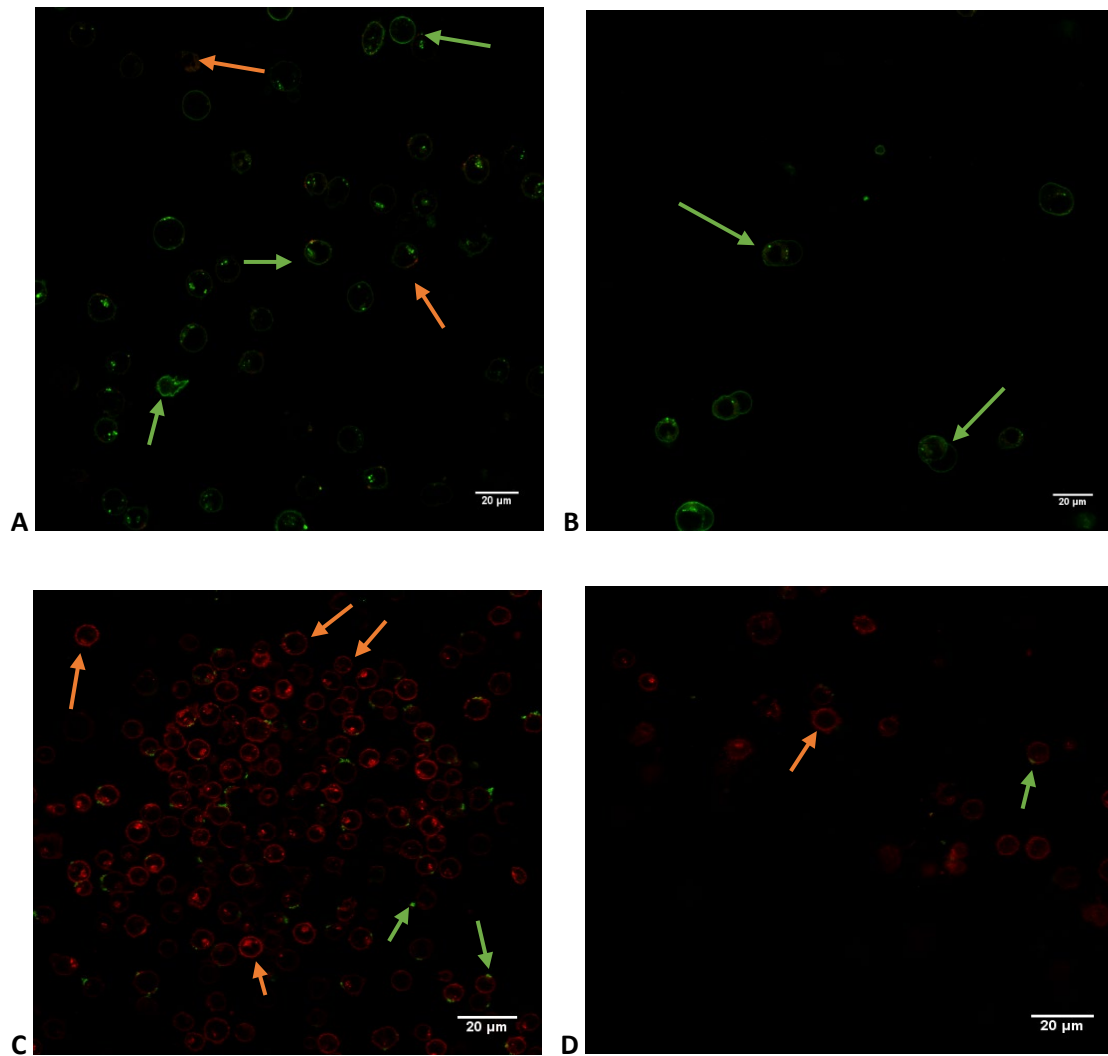
Figure 5.11 Confocal images showing heparin inhibiting the fusion of sEVs to the bystander cells via their membranes (A-B) and the subsequent release of sEVs' RNA into cells (C-D). In A and B, green arrow represents the cells whilst orange arrow represents the sEVs. In C and D, micrograhs illustrate the labelled RNA of sEVs (green arrow) on the outside or periphery of the cells (orange arrow). Original magnification, 20X. Scale bar, 20 μm

172

5.3.4 The effect of GW4869 on chemotherapy-induced bystander effects

Since the results have supported that sEVs secreted and released by HS-5 cells exposed to chemotherapy are taken up by the bystander TK6 cells; next the ability of GW4869 to inhibit the secretion and release of sEVs by HS-5 cells was explored. GW4869 is a neutral sphingomyelinase inhibitor that blocks the secretion of sEVs by inhibiting the ceramide-mediated inward budding of MVBs and the subsequent release of mature sEVs from MVBs (Essandoh *et al.,* 2015).

5.3.4.1 GW4689 is cytotoxic to HS-5 cells

As described in section 2.17, HS-5 cells were first treated with increasing doses of GW4869 (5 µm, 10 µm, 20 µm) for 24 hours to determine if the inhibitor has a possible cytotoxic effect on the cells. Cell viability was measured by trypan blue exclusion dye assay and acridine orange/propidium iodide assay. Untreated cells and cells treated with DMSO (solution used to dissolve GW4869) were used as negative and vehicle controls respectively.

As illustrated in figure 5.12, the results showed that cell viability was similar in cells treated with DMSO, non-treated group and cells treated with 5 µm. However, cell viability decreased as the dose of GW4869 was increased to 10 µM (untreated cells vs 10 µM p = 0.0064; cells + DMSO vs 10 µM p= 0.0243) and 20 µM (untreated cells vs 20 µM p < 0.0001; cells + DMSO vs 10 µM p < 0.0001). This suggests that GW4869 has a cytotoxic effect on HS-5 cells in a dose-dependent manner. Since GW4869 had little or no effect on the cells at 5 µm, this dose was chosen to drive the project forward as it is possible that GW4869-induced cytoxicity in HS-5 cells may alter the cargo of the sEVs.
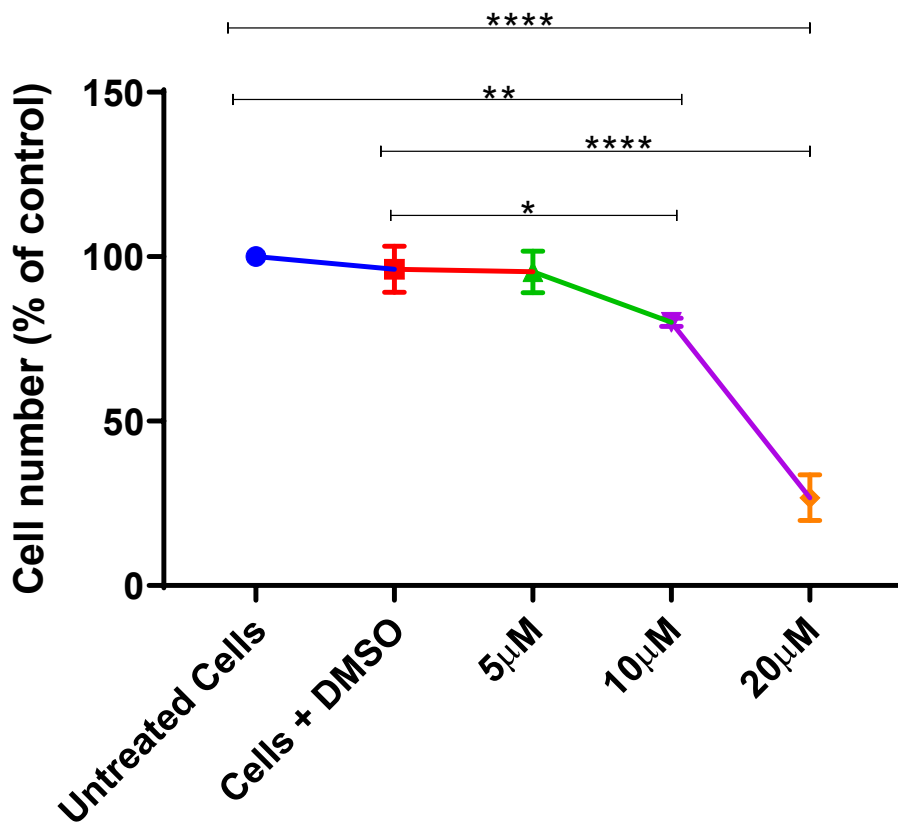
Figure 5.12 GW4869 has a cytotoxic effect on HS-5 cells at high concentrations. Cells were treated with three different doses of GW4869 (5 μM, 10 μM and 20 μM) for 24 hours. GW869 has a cytotoxic effect on the cells in a dose dependent manner. Statistical significance was done using the ANOVA for one-way factorial design (* $p<0.05$; ** $p<0.01$; ****$p<0.0001$).

5.3.4.2 GW4869 has no effect on chemotherapy-induced bystander effects

Next, the effect of GW4869 on CIBE was investigated as described in section 2.18 to ascertain if blocking the secretion and subsequent release of sEVs by HS-5 cells will ameliorate the BE in bystander TK6 cells. HS-5 cells were pre-treated with GW4869 (5 μM) for 24 hours prior to 24-hour chemotherapy treatment [CHL (40 μM), CAR (10 μg/ml), ETO (10 μM) and MTX (500 ng/ml)]. Afterwards, cells were co-cultured with bystander TK6 cells divided by a culture insert for 24

hours. TK6 cells were then harvested and analysed for cell death and genotoxicity via trypan blue exclusion assay and MN assay respectively.

The bystander TK6 cells maintained a good viability percentage of more than 90% in all drugs used in the absence of GW4689 except mitoxantrone (Figure 5.13). Mitoxantrone induced a reduction in cell number of the bystander cells relative to the control to 67.4% and this was statistically significant (p = 0.0311). This is supported by the findings in figure 4.3, which revealed an increase in cell number of bystander TK6 cells upon exposure to HS-5 cells treated with chlorambucil, carmustine and etoposide whilst mitoxantrone induced a reduction in cell number. Similarly, when the cells were exposed to HS-5 cells treated with drugs in the presence of GW4689, mitoxantrone induced a reduction in cell number to 62.4% (p = 0.0147) whilst number of cells exposed to carmustine, chlorambucil and etoposide-treated HS-5 cells did not subceed 89%.

Furthermore, mitoxantrone also induced the highest number of micronuclei formed in bystander TK6 cells (Figure 5.13). In cells exposed to drugs in the absence of GW4869, mitoxantrone induced the formation of 103 micronuclei. When compared to the control (cells only) and control + GW4869, the difference was statistically significant (p = 0.0012 vs p = 0.0009). However, when the cells were exposed to mitoxantrone in the presence of GW4869, the number of micronuclei formed in the bystander cells reduced to 86. The difference was also statistically significant when compared to the control (p = 0.0211) and control + GW4869 (p = 0.0152).

Collectively, these suggest that there is no difference in cytotoxic and genotoxic outcomes in bystander TK6 cells exposed to HS-5 cells treated with only drugs and HS-5 cells treated with drugs and GW4869. Nevertheless, it is important to note that whilst it is not significant, there is definitely in a decrease in MN with GW4869 especially in the mitoxantrone cohort. Therefore, it can be inferred from the data that whilst GW4869 does not remove CIBE, sEVs may play a contributory role to CIBE.
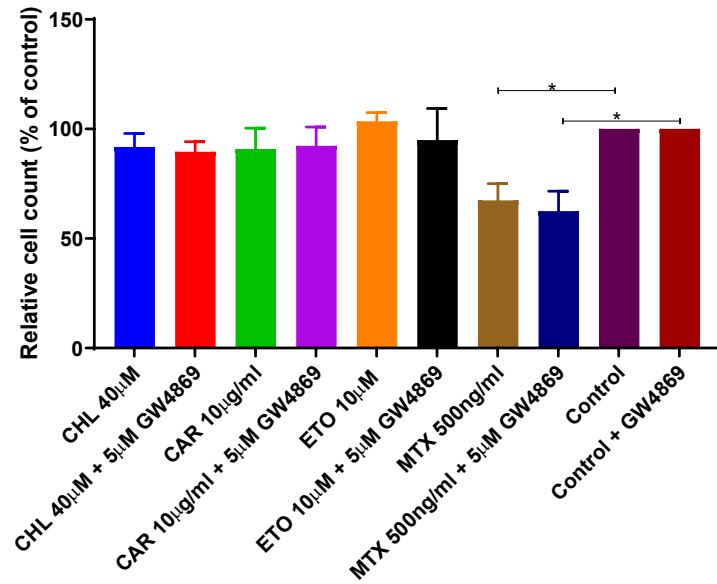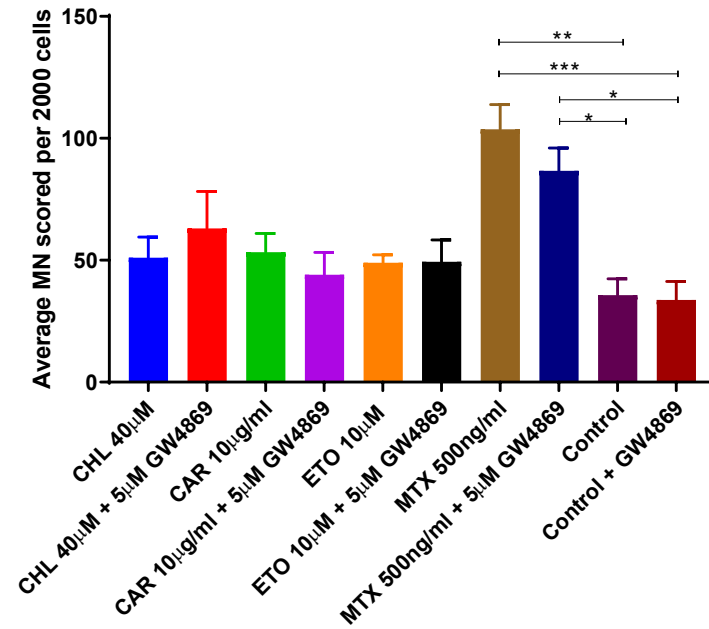
Figure 5.13 GW4869 does not have an effect on chemotherapy-induced bystander effect. A. Cell viability of bystander TK6 cells exposed to HS-5 cells that were pre-treated with drugs in the presence or absence of 5 μM GW4869. **B.** Micronuclei formed in the bystander TK6 cells exposed to HS-5 that were pre-treated with drugs in the presence or absence of 5 μM GW4869. Statistical significance was done using the ANOVA for one-way factorial design (* $p<0.05$; ** $p<0.01$; *** $p<0.001$).

5.3.5 sEVs induce a cytotoxic effect on TK6 cells that is ameliorated by heparin

In order to determine if sEVs from cellular communication are responsible for CIBE, TK6 cells were directly exposed to sEVs secreted from mitoxantrone-treated HS-5 cells for 24 hours as described in section 2.20. Prior to that, TK6 cells were pre-treated with or without heparin as it has been shown, in figure 5.11, to inhibit the uptake of sEVs by recipient TK6 cells. Afterwards, the total cell count relative to the control was determined to ascertain any cytotoxic effect on the cells.

As illustrated in figure 5.14, sEVs-derived from mitoxantrone-treated HS-5 cells induced a cytotoxic effect in the cells, reducing the relative cell count to 89.8% however when heparin was added to the cells, the relative cell count increased to 108.5%. In addition, heparin also increased the relative cell count of TK6 cells exposed to sEVs isolated from untreated HS-5 cells from 100.73% to 114.63%. However, when these were compared, there was statistical significant difference in the relative cell count of TK6 cells exposed to untreated HS-5-derived sEVs and treated HS-5-derived sEVs (p = 0.0154). Therefore, these infer that heparin may enhance the growth of TK6 cells by inhibiting the fusion and uptake of these sEVs by TK6 cells. However, this further suggests that heparin may abrogate the ability of mitoxantrone-treated sEVs to mediate cytotoxic effects in the TK6 cells.

Furthermore, sEVs-derived from mitoxantrone-treated HS-5 cells caused an increase in the number of MN formed in the cells (74) but this number was drastically reduced to 17.75 upon addition of heparin. In addition, heparin also decreased the number of MN observed in TK6 cells exposed to sEVs isolated from untreated HS-5 cells from 62.75 to 16.75. When the different set of cells were compared, there was statistical significant difference in the number of MN formed in TK6 cells exposed to the sEVs with and without heparin (p < 0.0001). These further infer that heparin may reduce DNA damage in these cells by enhancing their growth.
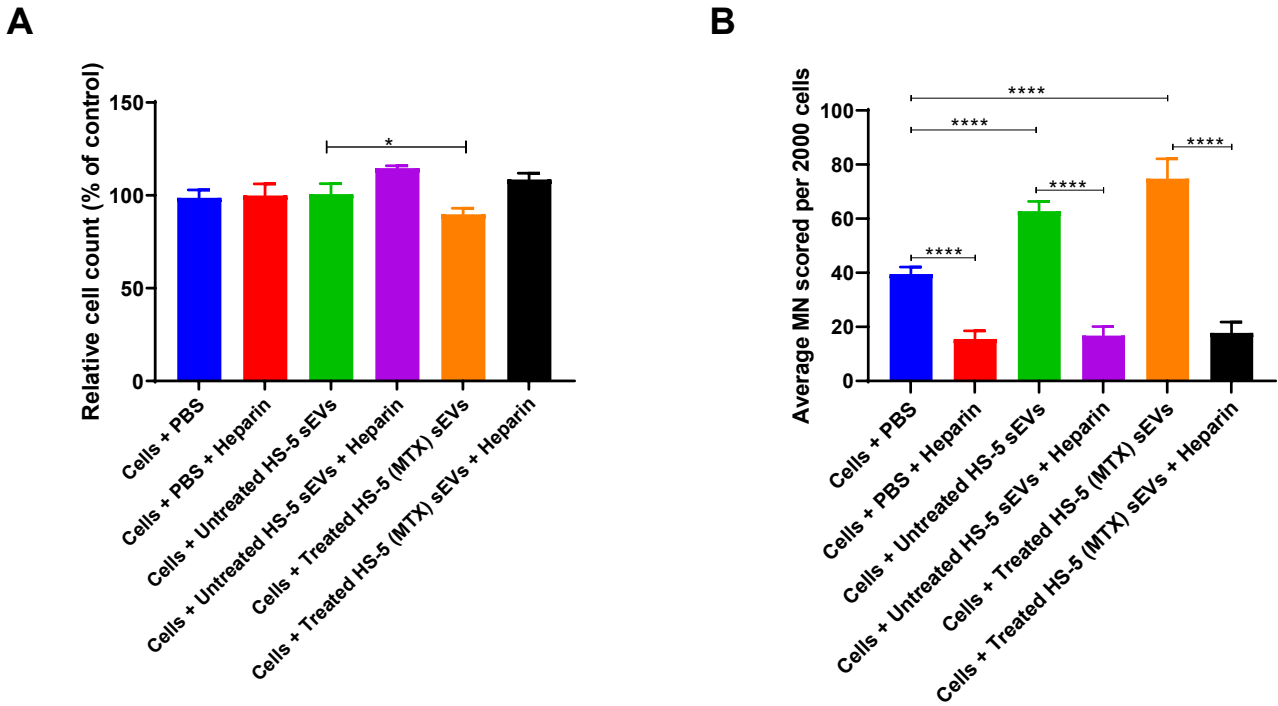
Figure 5.14 Small extracellular vesicles derived from mitoxantrone-treated HS-5 cells cause cytotoxic effects in TK6 cells. TK6 cells were treated with PBS (control), sEVs from mitoxantrone-treated cells or sEVs from untreated HS-5 cells with or without pre-treatment with heparin to inhibit sEVs uptake; 24 hours later, cells were harvested and relative cell count assessed (A) whilst DNA damage was assessed by counting the number of MN formed in these cells (B). Statistical significance was done using the ANOVA for one-way factorial design (* $p < 0.05$; **** $p < 0.0001$).

5.3.6 Exposure of cells to sEVs protects them from the effects of chemotherapy

Next, TK6 cells, directly treated with sEVs, were exposed to chemotherapy to investigate if these vesicles could modulate their response to chemotherapy. As described in section 2.21, TK6 cells that had been exposed to sEVs derived from mitoxantrone-treated and untreated HS-5 cells with or without pre-treatment with heparin, were treated with mitoxantrone for 24 hours. The relative cell count was determined afterwards.

As illustrated in figure 5.15, TK6 cells that were pre-treated with sEVs-derived from mitoxantrone-treated HS-5 cells were more resistant to mitoxantrone compared to the cells pre-

treated with PBS or untreated sEVs. This protective effect was decreased when the cells were pre-treated with heparin to inhibit the uptake of the sEVs. However, this difference was not statistically significant. Furthermore, there was an increase in the number of MN formed in these cells exposed to these sEVs upon addition of heparin. When compared to the control, there was no statistically significant difference between the MN formed in the control and cells exposed to sEVs. This infers that simple pre-treatment with sEVs is enough to be protective to mitoxantrone whilst heparin promotes the genotoxicity of mitoxantrone.
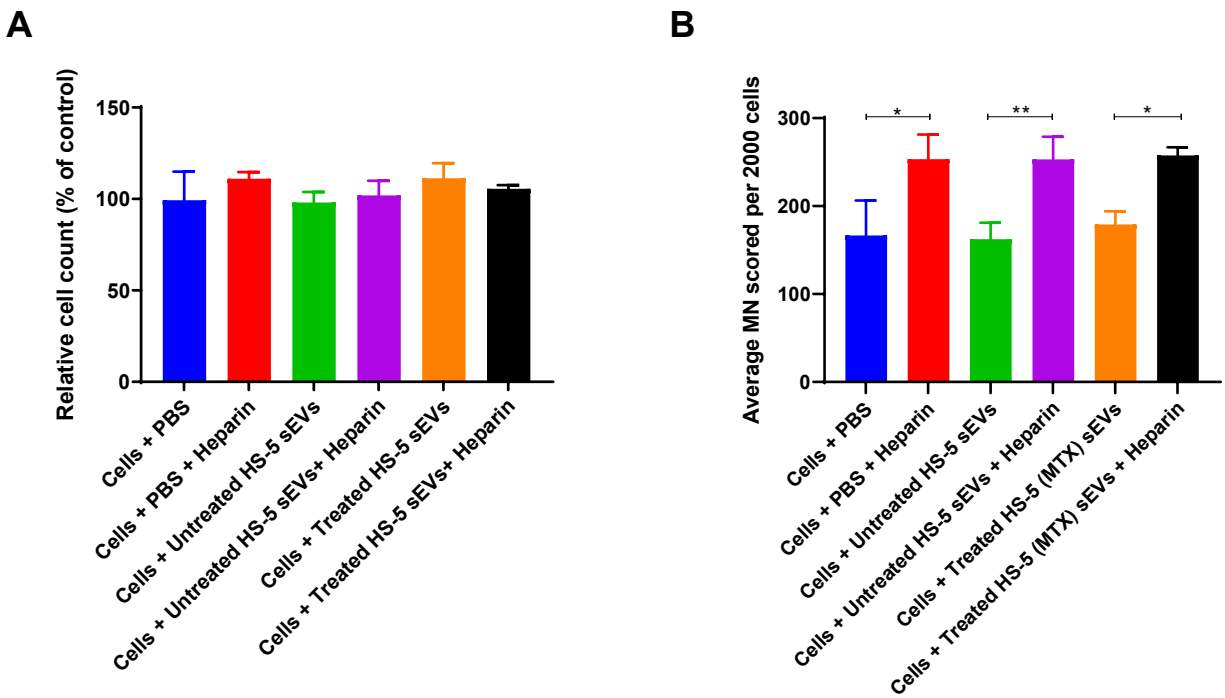
Figure 5.15 Small extracellular vesicles derived from mitoxantrone-treated HS-5 cells enhance survival of TK6 cells from the effects of chemotherapy. TK6 cells were treated with PBS (control), sEVs from mitoxantrone-treated cells or sEVs from untreated HS-5 cells with or without pre-treatment with heparin to inhibit sEVs uptake; 24 hours later, cells were further treated with mitoxantrone (500 ng/ml) for another 24 hours. Cells were then harvested and viability assessed (A). DNA damage was also assessed by counting the number of MN formed in these cells (B). Statistical significance was done using the ANOVA for one-way factorial design (* $p<0.05$; ** $p<0.01$).

Taken together, the results suggest that the treatment of cells with sEVs derived from mitoxantrone-treated HS-5 cells enhances their survival following mitoxantrone treatment. This

triggers an adaptive response in the cells that help them to resist and withstand the effects of mitoxantrone. However, the cells retain genotoxic effects of mitoxantrone (DNA damage), which may be detrimental to their long-term survival and may lead to the development of malignancy in these cells.

5.3.7 sEVs do not have an effect on TK6 cell cycle

As shown in section 4.3.3.3, the findings from the bioinformatics analysis revealed that cell cycle is one the biological processes regulated by the chosen miRNAs. Therefore, cell cycle analysis in TK6 cells was performed to further study whether the cell cycle of TK6 cells was affected by sEVs. TK6 cells were treated with sEVs derived from untreated and mitoxantrone-treated HS-5 cells for 24 hours. Prior to that, TK6 cells were pre-treated with or without heparin for 30 minutes. Cells were prepared as previously described in section 2.29 and cell cycle analysis by flow cytometry was performed. The cell cycle distribution was determined by flow cytometry with PI staining method. The flow cytometry analysis was done in duplicates and repeated at least three times.

As shown in figure 5.16, the results demonstrated that there was an evidence of cell death (13% in sub G1 phase) in cells that were treated with mitoxantrone alone, which served as the positive control. Aneuploidy was also found in the cells thus inferring that chemotherapy can cause chromosomal instability in these cells (data not shown, see appendix). This is in contrast to the untreated cells and cells treated with PBS (negative controls), which had less than 1% of the cells in sub G1 phase. Instead, the majority of the cells were in G0/G1 phase (69% vs 66%). In addition, the cells were also diploid thus suggesting that the cells had undergone one cell cycle. Similarly, cells treated with sEVs derived from untreated and mitoxantrone-treated HS-5 cells were mainly in G0/G1 phase (69% vs 67%). There was no statistical significant difference between any of them. However, the cells treated with sEVs from mitoxantrone-treated HS-5 cells were aneuploid thus inferring that these vesicles induce stress of some sort in these cells.

When the cells were pre-treated with heparin, the percentage of the cells in G0/G1 phase reduced to 53.7 % vs 53.2% in cells treated with sEVs derived from untreated and mitoxantrone-treated HS-5 cells respectively. In addition, the cells were found to be diploid. Similar cell percentages and diploidy were also observed in the negative controls (54% vs 53.2%). There was

no statistical significant difference between any of them. The return of the number of chromosomes in these cells from aneuploidy to diploidy as well as the reduction in percentage of the cells in different phases of cell cycle upon heparin treatment further suggest that heparin may have the capacity to alter the cell cycle of TK6 cells.

Taken together, these results suggest that sEVs do not affect cell cycle, as the percentage cells treated with sEVs in each phase of cell cycle was similar to the control. However, the amelioration of uncontrolled chromosome content in these cells following exposure to heparin thus further suggests that DNA damage may be sustained in these cells due to uncontrolled cycling. The regulation of the G0/G1 and G2/M phase checkpoints are necessary to prevent uncontrolled cycling and proliferation that may lead to tumorigenesis.

without heparin

with heparin

Cells only
Cells + MTX
Cells + PBS
Cells + Untreated HS-5 sEVs
Cells + MTX treated HS-5 sEVs

(A)

(B)
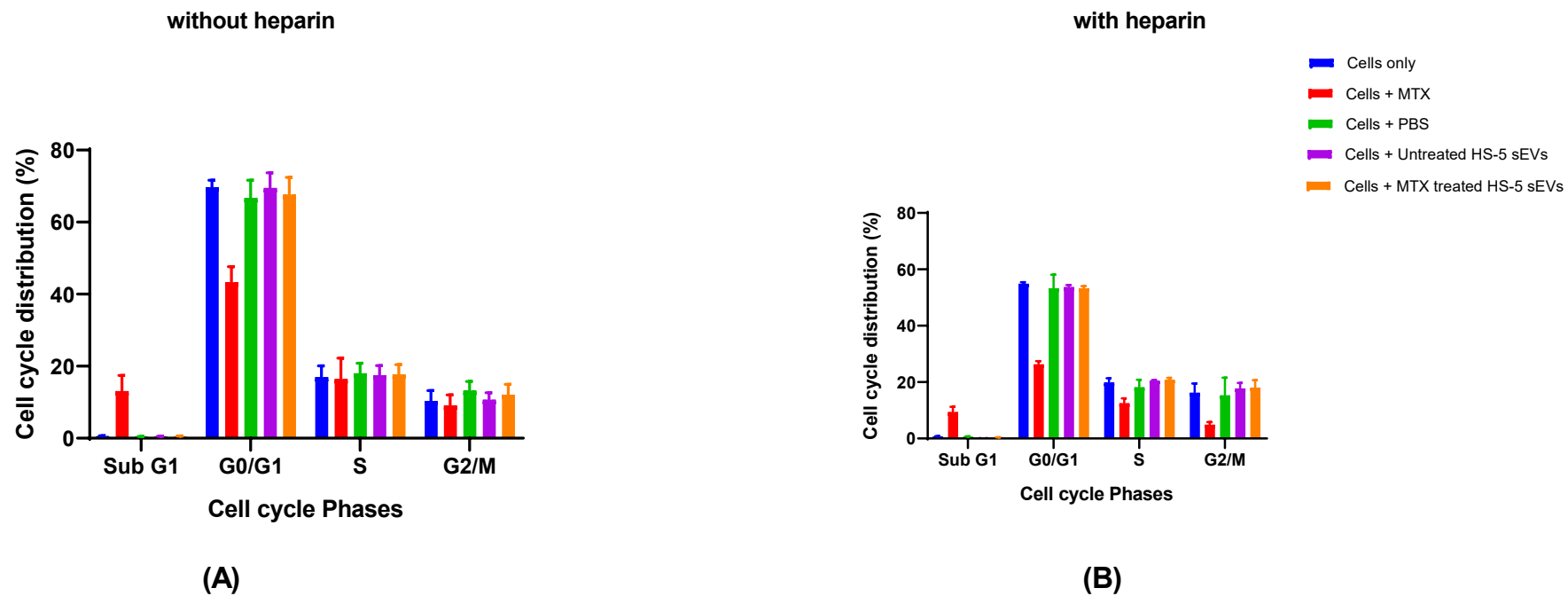
Figure 5.16 Effect of sEVs on cell cycle distribution in the presence and absence of heparin. TK6 cells were treated with sEVs derived from untreated and mitoxantrone-treated HS-5 cells for 24 hours without (A) and with (B) pre-treatment with heparin (10 μg/ml) for 30 minutes. Statistical significance was done using the ANOVA for two-way factorial design.

Next, cell cycle analysis was investigated in TK6 cells following treatment with chemotherapy. TK6 cells, directly treated with sEVs, were exposed to chemotherapy and analysed by flow cytometry to investigate if these vesicles are capable of altering the cell cycle of these cells. As described in section 2.21, bystander TK6 cells that had been exposed to sEVs derived from mitoxantrone-treated and untreated HS-5 cells were then treated with mitoxantrone for 24 hours. Flow cytometry analysis was performed by PI staining.

As illustrated in figure 5.17, the negative controls (untreated cells and cells treated with PBS) maintained a similar cell percentage as observed in figure 5.16. The majority of the cells were in G0/G1 phase (64% vs 64%) compared to the cells that were treated with mitoxantrone only and cells treated with sEVs. The percentage of cells in G0/G1 phase in these cells were 44%. These results also show that a percentage of these cells were in sub G1 phase as well. In addition, aneuploidy was found in these cells (cells treated with only mitoxantrone, cells treated with sEVs derived from untreated HS-5 cells and cells treated with sEVs derived from mitoxantrone-treated HS-5 cells) thus inferring chromosomal instability.

Taken together, the results suggest that sEVs appear to potentiate the cytotoxic effects of mitoxantrone and are equally the same as the positive control in G0/G1 phase. This is in contrast to the findings in section 5.6.4, which revealed that exposure to sEVs enhanced an adaptive response, in the cells, to mitoxantrone. Nevertheless, these data infer that although pre-exposure of cells to sEVs before treatment with mitoxantrone did not lead to a block in cell cycle at any of the cell cycle checkpoints or confer proliferative advantage to the cells, the cells may recover from the brink of cell death and undergo autonomous proliferation in a compensatory growth mechanism. In addition, mitoxantrone is considered cell cycle nonspecific however, the data herein infer that mitoxantrone may cause cell cycle arrest in G0/G1 phase in TK6 cells.
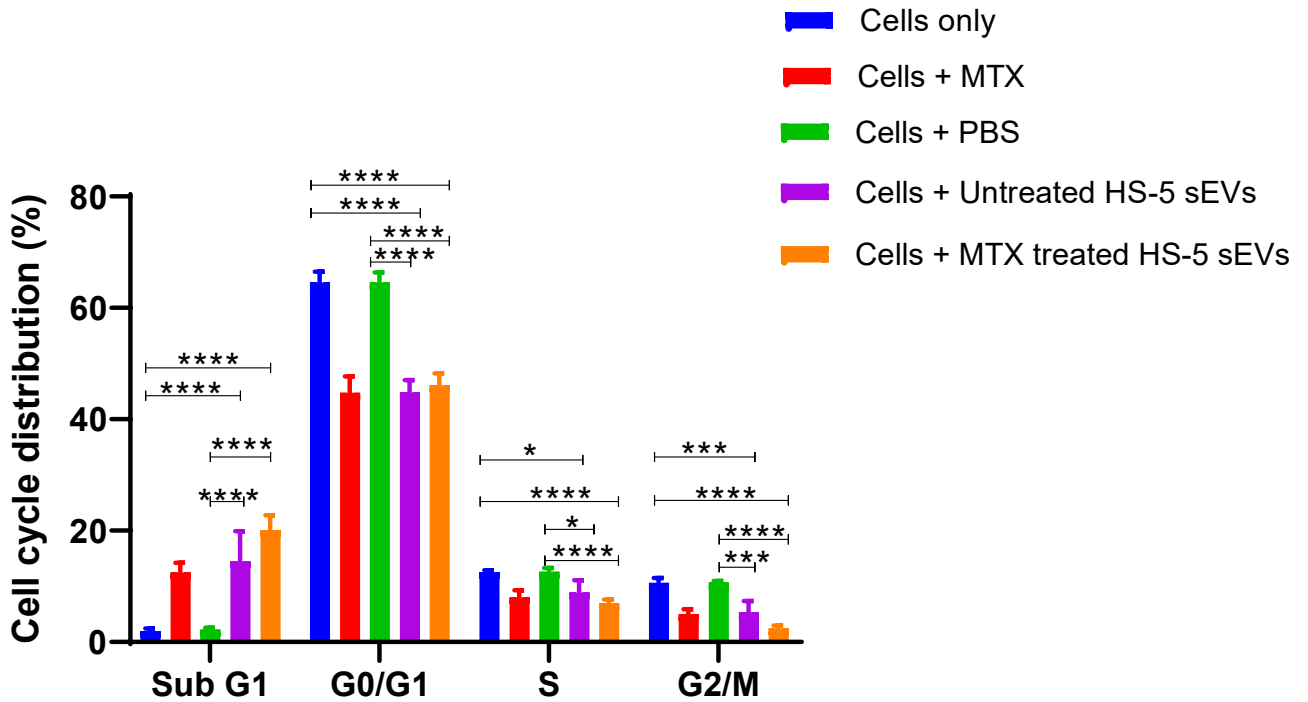
Figure 5.17 The combined effect of sEVs and mitoxantrone on cell cycle distribution. Bystander TK6 cells were treated with sEVs derived from untreated and mitoxantrone-treated HS-5 cells for 24 hours and then exposed to mitoxantrone (500 ng/ml) for 24 hours. Statistical significance was done using the ANOVA for two-way factorial design (* $p<0.05$; *** $p<0.001$; **** $p<0.0001$).

5.3.8 sEVs have an effect on the miRNA expression levels in TK6 cells

Next, the miRNA levels in TK6 cells following co-culture with sEVs was investigated. TK6 cells were co-cultured with HS-5-derived sEVs with or without pre-treatment with heparin as reported in section 2.21. RNA was isolated from the cells 24 hours later, and converted to cDNA. The cDNA was then relatively analysed with qRT-PCR to identify any changes in individual miRNA expression levels in these samples. The levels of candidate miRNAs (hsa-miR-146a-5p, hsa-miR-16-5p, hsa-miR-20a-5p, hsa-miR-30d-5p, hsa-miR-17-5p, and hsa-miR-200c-3p), chosen in section 4.3.3, were quantitatively measured by qRT-PCR as described in section 2.28. It is important to highlight

that the levels of these candidate miRNAs were upregulated in the bystander TK6 cells except hsa-miR-200c-3p, which was downregulated.

As depicted in figure 5.18, TK6 cells showed the presence of all miRNAs analysed in varying amounts. The levels of hsa-miR-146a-5p, hsa-miR-16-5p and hsa-miR-17-5p and hsa-miR-20a-5p were similar in TK6 cells treated with sEVs derived from untreated HS-5 cells and control (TK6 cells + PBS). However, when compared to cells treated with sEVs derived from mitoxantrone-treated HS-5 cells, the expression levels of these miRNAs - hsa-miR-146a-5p (33.80), hsa-miR-16-5p (31.28), hsa-miR-17-5p (30.60) and hsa-miR-20a-5p (31.26) were reduced.

The most abundant miRNA was hsa-miR-30d-5p, which had the lowest Ct value in all three samples – TK6 cells treated with sEVs derived from untreated HS-5 cells (27.26), TK6 cells treated with sEVs derived from mitoxantrone-treated HS-5 cells (27.76) and control (26.59). The second most abundant miRNA was hsa-miR-17-5p, which had Ct values of 28.00 and 30.60 in TK6 cells treated with sEVs derived from untreated and mitoxantrone-treated HS-5 cells respectively. However, its expression was higher in control with a Ct value of 27.49.

In addition, when the expression levels of these candidate miRNAs were compared between the cells treated with sEVs and the control, results show that the expression levels of these miRNAs were downregulated in cells treated with sEVs-derived from untreated HS-5 cells and sEVs-derived from mitoxantrone-treated HS-5 cells (figure 5.18B). When the expression levels of these miRNAs in these cells treated with sEVs were compared, data show that these miRNAs were further downregulated in the cells co-cultured with sEVs derived from mitoxantrone-treated HS-5 cells. This difference between the expression levels of these miRNAs in these two sets of cells was statistically significant ($p < 0.0001$). These data infer that sEVs can modulate the expression levels of these miRNAs in TK6 cells upon uptake.

Furthermore, when cells were pre-treated with heparin (figure 5.19), the expression level of hsa-miR-30d-5p in TK6 cells treated with sEVs-derived from mitoxantrone-treated HS-5 cells was reduced with a Ct value of 30.38 compared to control (27.99) and TK6 cells treated with sEVs derived from untreated HS-5 cells (27.99). When the expression level of hsa-miR-30d-5p was compared between the cells treated with sEVs and the control, results (figure 5.19B) show that

this miRNA was upregulated (1.61 folds) in cells treated with sEVs-derived from untreated HS-5 cells but downregulated (0.35 fold) in cells treated with sEVs-derived from mitoxantrone-treated HS-5 cells. This difference between the expression levels of these miRNAs in these two sets of cells was statistically significant ($p < 0.0001$). These data suggest that heparin has an effect on the expression levels of miRNAs. It can be inferred from the data tha the inhibition of sEVs' uptake by heparin causes an increase in the expression levels of miRNAs. However, it is important to mention that only one candidate miRNA was assessed due to financial constraints. SNORD61 and RNU6B/RNU6-2 were used as normalisers in both sets of experiments whilst hsa-miR-150-5p, which has been previously shown to have low expression level in TK6 cells (section 4.3.3), was used as negative control.

Collectively, these results suggest that sEVs can alter the expression levels of miRNAs in TK6 cells upon uptake. However, heparin-induced blockade of sEVs uptake led to an increase in the expression levels of these miRNAs in TK6 cells.
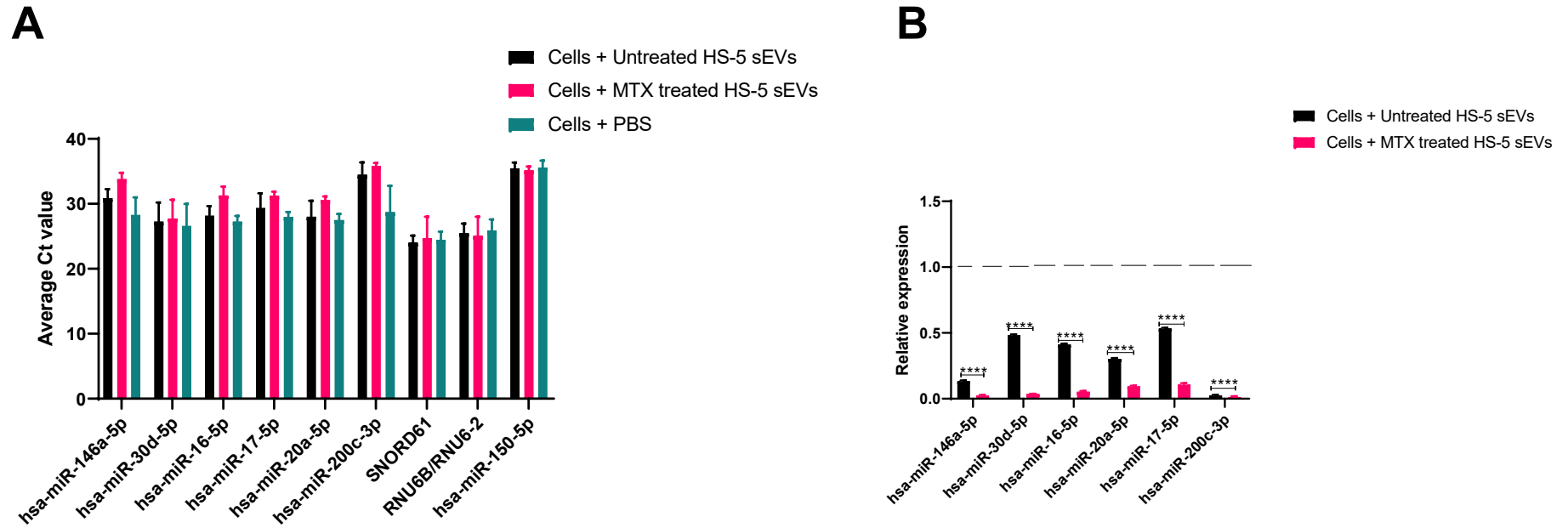
Figure 5.18 sEVs modulate miRNA expression in TK6 cells. TK6 cells were co-cultured with sEVs derived from untreated and mitoxantrone-treated HS-5 cells. RNA was isolated from the cells 24 hours later and analysed by qRT-PCR. Individual miRNA expression levels (A) and fold change (B) of six candidate miRNAs are shown. RNU6B/RNU6-2 and SNORD61 were used as normalisers whilst miR-150-5p was used as a negative control. Statistical significance was done using the ANOVA for two-way factorial design (**** $p < 0.0001$).
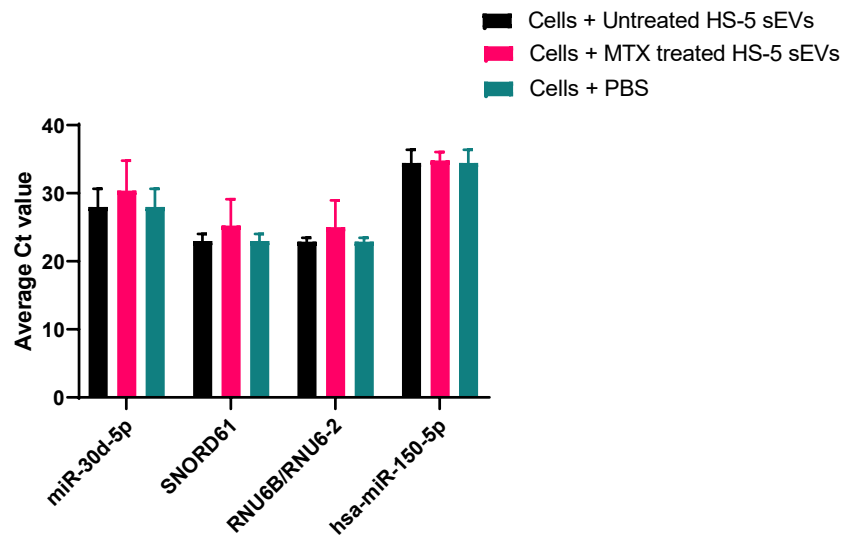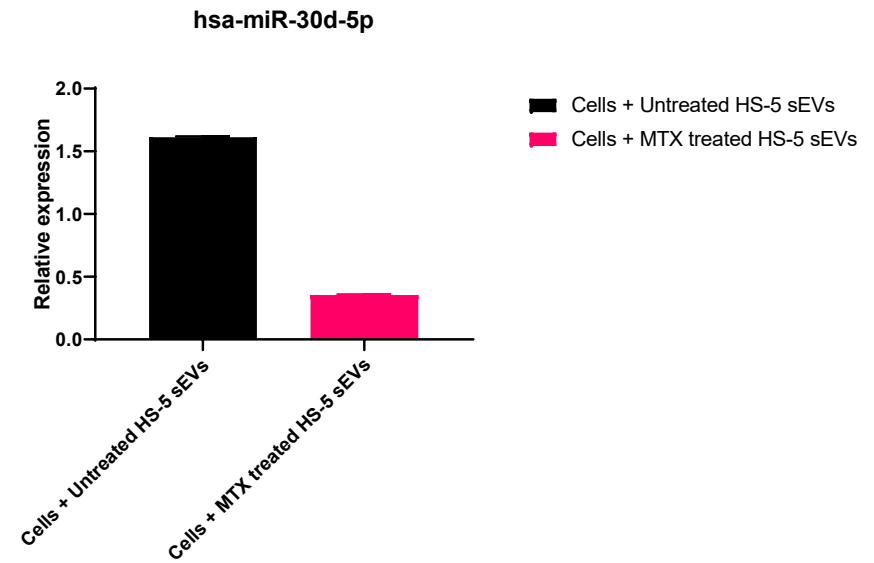
Figure 5.19 Heparin causes an increase in the expression levels of miRNA in TK6 cells. TK6 cells, pre-treated with heparin, were co-cultured with sEVs derived from untreated and mitoxantrone-treated HS-5 cells. RNA was isolated 24 hours later from the cells and analysed by qRT-PCR. The expression level of one miRNA (hsa-miR-30d-5p) is shown. RNU6B/RNU6-2 and SNORD61 were used as normalisers whilst miR-150-5p was used as a negative control. Statistical significance was performed by unpaired Student t-test (**** p<0.0001).

5.3.9 MiRNA trafficking to bystander TK6 cells

Previous results have shown that miRNA expression differ between HS-5 cells and bystander TK6 cells (section 4.3.3.4) and that sEVs, derived from HS-5 cells, release their cargo (RNA) into bystander cells (section 5.5). To test the transfer of these miRNAs via sEVs, the levels of miRNAs in sEVs and CM was explored. CM and sEVs samples were prepared as described in sections 2.22.2 and 2.22.3 respectively. RNA, extracted from these samples, was converted to cDNA as previously stated in section 2.25 and quantitatively analysed as directed in section 2.28.

5.3.9.1 RNA quality and yield

To assess the RNA yield of sEVs and CM, total RNA was analysed spectrophotometrically with the NanoDrop to obtain the concentration, yield and purity. It is important to note that extraction of RNA from the sEVs-depleted FBS, which was used to culture the cells, was also done. As illustrated in table 5.1, CM of untreated cells and CM of treated cells produced similar RNA amount and yield however, the amount of RNA produced by sEVs-depleted FBS was drastically reduced (7.98 ± 0.49 ng/µL). RNA concentration from CM of untreated cells was 28.99 ± 6.29 ng/µL whilst the concentration of RNA from CM of treated cells was 25.13 ± 8.34 ng/µL (figure 5.20). However, there was no statistical significant difference in the concentration of RNA isolated from CM of untreated and treated cells. The purity of the samples (OD at 260/280) were all within the range of 2.1 and 2.3.

Taken together, the results infer that RNA can be successfully isolated from cell-conditioned media and FBS in an *in vitro* setting. Successful RNA isolation is a prerequisite for expression analyses of secreted miRNAs. However, the reduced RNA constituent ratio in these samples suggests that although RNA are abundantly present in cells, some of these RNA may be present in extracellular samples or biological fluid such as cell-conditioned media and FBS but in minute amounts. Nevertheless, it is noteworthy to mention that cell-conditioned media containing all factors secreted by untreated and treated HS-5 cells, including EVs, were harvested and used in this study.

For sEVs, the RNA concentration and yield between the samples are illustrated in table 5.2. The sEVs extracted from both untreated and mitoxantrone-treated HS-5 cells produced a very small amount of RNA. However, there appears to be a slight difference between them. The concentration of RNA isolated from the treated sample was more (25.1 ± 6.54 ng/μL) than untreated samples (10.6 ± 0.56 ng/μL) but this difference was not statistically significant (figure 5.21; p = 0.146). RNA yield in sEVs-derived from treated HS-5 cells was also similar to the RNA yield in CM from untreated and treated cells illustrated in figure 5.21. Furthermore, the purity of the samples (OD at 260/280) were all within the range of 1.74 and 2.89, which is deviant from the accepted value of 2.0. These results further suggest that RNA isolated from extracellular samples are often depleted when compared to RNA isolated intercellularly. These data also support the data in figure 5.10 thus inferring that RNA is packaged into sEVs released by HS-5 cells.

Table 5.1 Summary of RNA isolated from conditioned medium and sEVs-depleted FBS

Samples	RNA concentration (ng/μl)	RNA yield	OD (260/280)	OD (260/230)
Untreated CM	16.897	1013.82	2.220	0.075
	43.311	2598.66	2.337	0.286
	26.746	1604.76	2.144	0.109
Treated CM	44.067	2644.02	2.381	0.083
	22.292	1337.52	2.121	0.206
	9.047	542.82	2.245	0.104
sEVs-depleted FBS	7.930	475.80	2.248	0.139
	9.047	542.82	2.245	0.104
	6.974	418.44	2.146	0.079

Conditioned medium of untreated and treated HS-5 cells were used. RNA concentration and RNA yield and RNA purity were evaluated spectrophotometrically at the absorbance 230, 260 and 280 nm. *OD, Optical density.
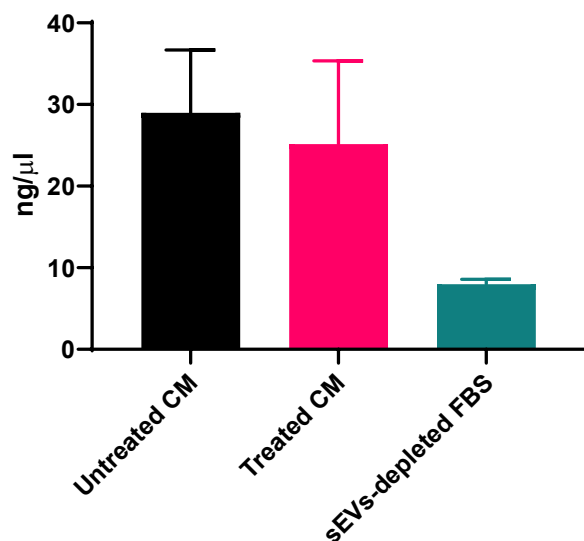
Figure 5.20 Concentration of RNA extracted from conditioned medium of untreated and mitoxantrone-treated HS-5 cells, and sEVs-depleted FBS used in cell culture. Data show mean values with standard deviation of the mean. Statistical significance was performed using the ANOVA for one-way factorial design.

Table 5.2 Summary of RNA isolated from sEVs extracted from HS-5 cells

Samples	RNA concentration (ng/µl)	RNA yield	OD (260/280)	OD (260/230)
Untreated sEVs	11.9	714	2.43	0.03
	9.6	576	2.16	0.02
	10.3	618	2.24	0.09
Mitoxantrone-treated sEVs	24.3	1458	2.93	0.04
	39.3	1768.5	2.89	0.04
	11.6	696	1.74	0.13

RNA concentration and RNA yield and RNA purity were evaluated spectrophotometrically at the absorbance 230, 260 and 280 nm. *OD, Optical density.
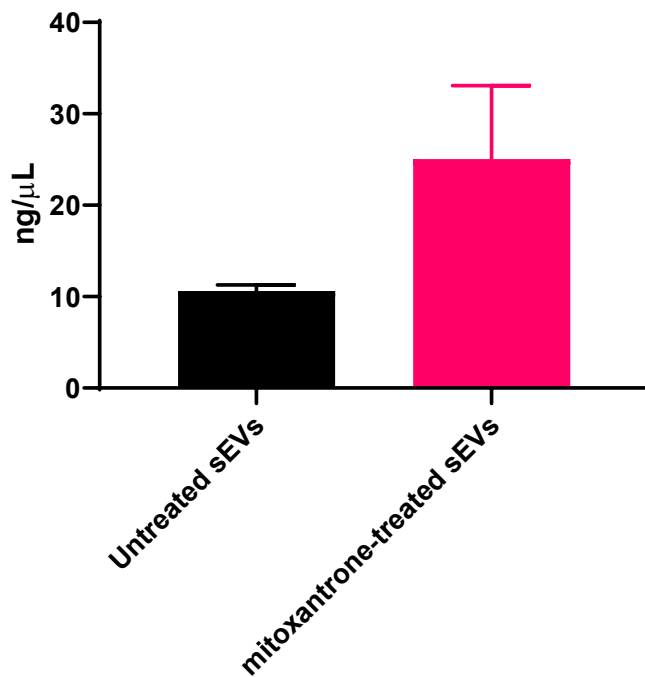
Figure 5.21 Concentration of RNA extracted from sEVs isolated from untreated and mitoxantrone-treated HS-5 cells. Data show mean values with standard error of the mean. Statistics was performed by unpaired student's t-test.

5.3.9.2 miRNAs are detected in cell-conditioned medium, sEVs and sEVs-depleted FBS

To determine the presence of miRNAs in CM, sEVs and sEVs-depleted FBS, RNA isolated from these samples were converted to cDNA (section 2.25). The levels of candidate miRNAs (hsa-miR-146a-5p, hsa-miR-16-5p, hsa-miR-20a-5p, hsa-miR-30d-5p, hsa-miR-17-5p, and hsa-miR-200c-3p), chosen in section 4.3.3, were quantitatively measured by qRT-PCR as described in section 2.28. It is important to highlight that the levels of these candidate miRNAs were upregulated in the bystander TK6 cells except hsa-miR-200c-3p, which was downregulated. These miRNA expression levels in CM, sEVs and sEV-depleted FBS were simultaneously analysed. The rationale behind this is to determine if treated HS-5 cells release miRNAs into the CM or package these miRNAs in sEVs to influence biological processes in the bystander TK6 cells. In addition, presence

of miRNAs in the sEVs-depleted FBS used in culturing the cells may represent confounding factors that may interfere with the downstream RNA analysis.

As illustrated in figure 5.22, these individual miRNAs were mostly not present in the samples except hsa-miR-30d-5p and hsa-miR-16-5p. In conditioned medium from both untreated and mitoxantrone-treated HS-5 cells, the only miRNA detected was hsa-miR-30d-5p however this was in a very minute amount as depicted by the low Ct values of 35.92 and 35.72 respectively (Figure 5.22A). Furthermore, hsa-miR-30d-5p was also low in sEVs-depleted FBS with a Ct value of 35.59 (Figure 5.22B). The other miRNA that was found in the sEVs-depleted FBS was hsa-miR-16-5p with Ct value of 35.85. These data do not support the transfer of free miRNAs through the CM from the drug exposed HS-5 cells to bystander TK6 cells. The results infer that it is likely that the measured hsa-miR-30d-5p in CM possibly originated from the sEVs-depleted FBS and not from the cells given the similar levels of this miRNA between CM and sEVs-depleted FBS. It is noteworthy to mention that the high Ct values in these samples meant that they were too low to be considered for delta delta Ct analysis.

Next, individual miRNA expression levels were detected in sEVs. Interestingly, two miRNAs were detected in sEVs isolated from both untreated and mitoxantrone-treated HS-5 cells, which were hsa-miR-30d-5p and hsa-miR-16-5p. However, there were no apparent differences in amounts of miRNAs, suggesting expression and/or trafficking is unaffected by mitoxantrone exposure. Furthermore, hsa-miR-17-5p was exclusively detected in the sEVs derived from the mitoxantrone-treated HS-5 cells inferring that hsa-miR-17-5p may play an important role in cellular communication following drug exposure. However, the presence of these individual miRNAs was low in both samples as indicated by the high Ct values shown in figure 5.22C. This is in contrast to the results in section 5.6.7, which revealed that TK6 cells treated with sEVs expressed these miRNAs 10 cycles earlier.

Collectively, these results suggest that a majority of the hsa-miR-30d-5p in the CM samples come from the serum used in cell culture rather than through cell secretion. This may explain why hsa-miR-30d-5p and hsa-miR-17-5p were the most abundant miRNAs in TK6 cells treated with sEVs (figure 5.18; section 5.6.7). Although the expression levels of all candidate miRNAs were

significantly reduced in TK6 cells co-cultured with sEVs-derived from mitoxantrone-treated HS-5 cells (figure 5.18; section 5.6.7), data from this vesicular study infer only hsa-miR-17-5p may be important, as it was the sole miRNA to be differentiated between untreated and treated sEVs. This further suggest that there may be selectivity in packaging of miRNA cargo into the sEVs and their subsequent uptake by the recipient cells. Here, hsa-miR-30d-5p, along with hsa-miR-16-5p and hsa-miR-17-5p, are enclosed in lipid bilayered vesicles.
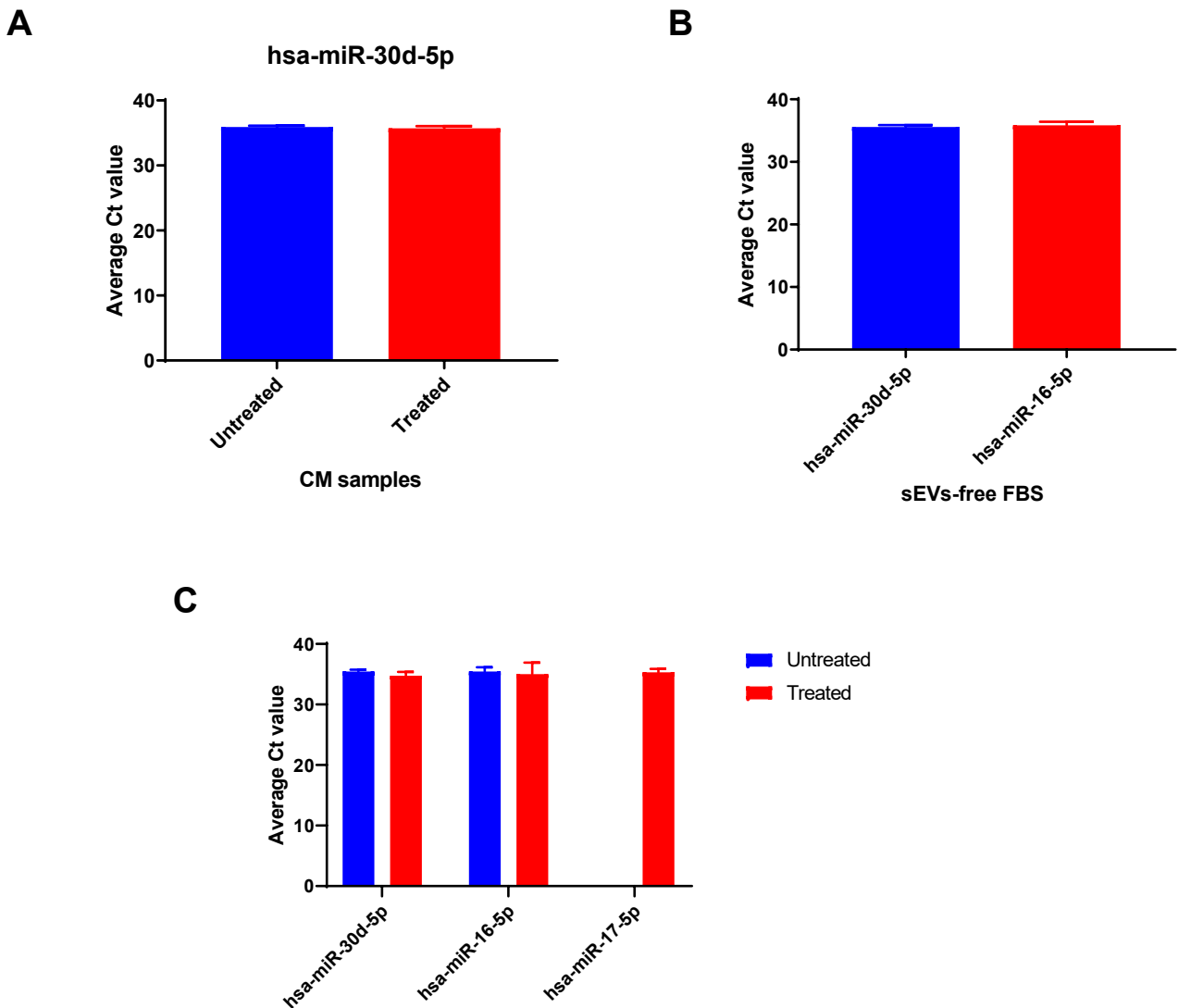
Figure 5.22 miRNA profiles in extracellular compartments. A. shows the average Ct value or threshold value of hsa-miR-30d-5p in conditioned media from untreated and mitoxantrone-treated HS-5 cells. B. shows the quantitative results of individual miRNAs (hsa-miR-30d-5p and hsa-miR-16-5p) in sEVs-depleted FBS. C. shows the relative levels of hsa-miR-30d-5p, hsa-miR-16-5p and hsa-miR-17-5p in sEV samples.

5.4 Discussion

Bystander effects depend on intercellular communication via direct cell contact, gap junctions and/or the transfer of signalling molecules from the secreting cells to the neighbouring cells. These signalling molecules, including miRNAs, can be exported in high concentrations, to the extracellular environment such as urine, breast milk, serum, saliva and plasma for wide-ranging effects. Cultured mammalian cells can also export miRNAs to the extracellular environment such as the culture medium. However, these secreted miRNAs, released through a ceramide-dependent secretory machinery, are often packaged into EVs such as exosomes, apoptotic bodies and microvesicles to maintain their integrity (Kosaka *et al.,* 2010; Wang *et al.,* 2010).

The classification of this diverse group of membranous vesicles depends on their sizes, functions, methods of biogenesis and RNA profiles. Regardless of the subtype, miRNAs are purposely and selectively sorted into EVs to be shuttled between cells thus allowing dissemination of genetically encoded messages (Nolte't Hoen *et al.,* 2012). Particularly, miRNAs and mRNA sorted and transferred via exosomes have been shown to induce and modify various functions of target cells (Xiao *et al.,* 2014: Muresan *et al.,* 2015; Sun *et al.,* 2018). There is still a debate about the extracellular RNA and miRNA content compared to the intercellular RNA and miRNA content. Some believe that EV RNA and miRNA content reflects that of the secreting cell whereas others believe there is a marked difference between the miRNA and RNA contents in the EVs and the secreting cells that drive the regulatory changes in recipient cells (O'Neill *et al.,* 2019; Groot and Lee, 2020). The latter infers that the secreting cell has the capacity to select what is trafficked irrespective of the quantity of a particular miRNA in the cell itself. Nevertheless, the miRNA and RNA content of EVs are tightly correlated with different pathological conditions, including cancer (Kosaka *et al.,* 2016; Groot and Lee, 2020). This suggests that quantification of circulating miRNAs packaged in EVs may be an extremely promising biomarker to assess and monitor the body's pathophysiological status.

Following illustration in chapter 4 (section 4.3.3.4), which revealed that there are significant differences in the miRNA content of treated HS-5 cells and bystander TK6 cells following co-

culture, it was pertinent to understand if these miRNAs are released into the medium or packaged into sEVs. This may explain the molecular changes in the treated cells as well as the phenotypic changes in the bystander cells. First, the ability of treated HS-5 cells to release EVs was determined by TEM. Secondly, the EVs were isolated from medium conditioned by treated HS-5 cells and characterised by TEM and NTA. Thirdly, the ability of these bystander cells to uptake EVs was ascertained. Afterwards, the secretion of EVs by HS-5 cells was blocked with an inhibitor of the ceramide synthesis pathway, GW4869, and its effects on CIBE were determined. The miRNA expression profiles in the extracellular components: conditioned medium, sEVs-depleted FBS and sEVs were then determined to understand if these cells release miRNAs into conditioned medium or packaged into sEVs. The miRNA content of serum used in culture was explored to understand if there are miRNAs present in the serum that can affect the results of this study. Lastly, the effects of these sEVs in bystander cells were explored.

5.4.1 HS-5 cells release sEVs following chemotherapy

The release of EVs by cells could be constitutively induced or stimulus-triggered. In particular, several researchers have reported that cells release EVs when faced with different kinds of stress, such as cytotoxic drugs, heat, hypoxia, radiation and oxidative stress (Xu *et al.,* 2015; Lin *et al.,* 2017; Aubertin *et al.,* 2018; Panigrahi *et al.,* 2018; Harmati *et al.,* 2019). MSC, derived from human umblical cord, also release EVs in response to hypoxia and proliferate faster in hypoxic conditions than in normoxic conditions *in vitro* and *in vivo* (Zhang *et al.,* 2012). There is a consensus that MSC release significant amounts of EVs, which contribute to their paracrine capacity and subsequent efficacy in regenerative therapies (Di Trapani *et al.,* 2016; Pachler *et al.,* 2017; Phinney and Pittenger, 2017). As shown here, in the first quantitative study of its type, HS-5 cells constitutively shed abundant vesicles however, this increases upon induction by cell activation or exposure to cytotoxic insult. This contrasts the previous findings of Javidi-Sharifi *et al.,* (2019), which revealed that untreated HS-5 cells shed abundant EVs in comparison to HS-27a, another MSC cell line. These two cell lines differ from each other by presence or absence of CD146; HS-27a contains CD146 whilst HS-5 cells lack CD146 (Iwata *et al.,* 2014). In addition, there was also heterogeneity in the sizes of EVs released by HS-5 cells following chemotherapy whereas

the opposite was found in untreated HS-5 cells. The reason for this is unclear but one overarching idea theorizes that different subtypes of EVs are released following cellular exposure to cytotoxic insult. The sac-like body or cocoon-shaped EV release is very informative and suggests that EVs are released in different ways depending on the subtype and sizes.

Extensive literature review suggested that this study provides the first *in vitro* evidence that mitoxantrone, chlorambucil, carmustine and etoposide may lead to increased EV release by HS-5 cells. Previous studies have shown that etoposide (5 µM, 10 µM, 25 µM) can induce abundant EV release by prostate cancer cells following two-hour exposure (Lin *et al.,* 2017). Although the cells used in their study differ from the one used in this study, the dose used in their study correlates to the clinically relevant dose (10 µM) used in this study. In another study, mitoxantrone was accumulated in EVs released by MCF-7/MR breast cancer cells following 12-hour incubation with 20 µmol/L mitoxantrone (Ifergan *et al.,* 2005; Carroll *et al.,* 2016). It is also noteworthy that the concentration of mitoxantrone (500 ng/ml) used in this study is less than the concentration used in their study. Furthermore, elevated EV production was also found in MCF-7 breast cancer cells undergoing doxorubicin-induced DNA damage response whilst a quantitative relationship between concentrations of doxorubicin and EV release after 24-hour and 1-hour treatments respectively was also illustrated in prostate cancer cells (Aubertin *et al.,* 2016). Etoposide, mitoxantrone and doxorubicin are well-established DNA topoisomerase inhibitors. However, these cancer cells behave differently from the normal cells used in this study but what is evident is that chemotherapy can induce the release of EVs by cells. Nevertheless, other studies failed to show that drug treatment itself can trigger EV release despite showing that EVs could transfer drugs such as doxorubicin and cisplatin to the extracellular medium (Shedden *et al.,* 2003; Chen *et al.,* 2006; Samuel *et al.,* 2017).

Although it has been reported that drugs can be loaded into purified preparations of EVs released by MSC to induce therapeutic effects (Pascucci *et al.,* 2014), these results suggest that drugs applied to MSC during pre-transplant conditioning may be incorporated and sorted into EVs and subsequently released by these cells to be taken up by the neighbouring cells with unfavourable outcome. Together, these data support the hypothesis that abundant cellular EV release induced

by pre-transplant conditioning regimens may in fact induce complications in cancer patients as these EVs may act as signalling molecules to incoming donor cells during HSCT thus promoting an oncogenic phenotype.

5.4.2 Characterisation of isolated sEVs

Since it has been shown that HS-5 cells release abundant EVs following chemotherapy, it was necessary to isolate these EVs from HS-5 cells and characterise them. Mitoxantrone was chosen as the appropriate drug to drive the study forward, as it was the drug that produced the highest CIBE. In order to ensure uniformity throughout the study, EVs were isolated from cells of the passage and seeded at the same density in DMEM-HG medium supplemented with sEVs-depleted FBS. These parameters can affect the production and characteristics of EVs by MSC (Szatanek *et al.,* 2015; Gudbergsson *et al.,* 2016; Patel *et al.,* 2017; Lee *et al.,* 2019). Two methods were employed during isolation of EVs following exposure of HS-5 cells to mitoxantrone: SEC and ExoQuick preparation. SEC entails the use of a column of porous beads, with radii smaller than the EVs of interest, to filter and separate biomolecules based on their hydrodynamic radius or a difference in size (Yamamoto *et al.,* 1970; Boing *et al.,* 2014). In contrast, ExoQuick uses polyethylene glycol or superhydrophilic polymers in order to decrease the solubility of EVs, forming a pellet precipitate consisting of EVs and some protein contaminants (Yamamoto *et al.,* 1970).

ExoQuick is usually used for isolation of EVs from cell culture medium because it has a relatively simple and easy-to-follow protocol, and requires no additional equipment, however it is expensive and high concentrations of impurities are usually co-isolated with these EVs (Yamamoto *et al.,* 1970; Sunkara *et al.,* 2016). Although differential centrifugation and density-gradient ultracentrifugation are the most widely used protocols for EV isolation, SEC was chosen as the alternative protocol as it has several major advantages over these other protocols. The processing time for SEC is relatively much faster and there is no risk of vesicle aggregation and protein complex formation due to purity of preparation and preservation of vesicle integrity (Gamez-Valero *et al.,* 2016; Carnino *et al.,* 2019). Due to this improved sensitivity and ability to maintain the biological properties of EVs, the accuracy of downstream assays is improved.

However, the process is a bit more complex than the ExoQuick as it requires specialised equipment and columns. Furthermore, the sample volume is limited by the size of the column and there may be 'contamination' of the sample by other molecules of similar size that elute at the same rate making it difficult to entirely isolate samples of EVs by their subtypes (Carnino *et al.,* 2019). The molecular weight of the column often range between 3 to 100 kDa hence ensuring only particles with molecular weights within this range are eluted (Gurreiro *et al.,* 2018). However, the molecular weight of the column used in concentrating the samples in this study was 100 kDa. In this study, SEC produced sEVs that had little or no protein contaminants hence it was chosen for downstream analysis of the contents of sEVs.

TEM analysis revealed that the morphology and structure (round or cup-shaped appearance) of the EV particles released by HS-5 cells were consistent with the particulate structure proposed by ISEV. TEM is a crucial tool in the characterisation of the morphology, size and phenotype of EVs. Due to its ability to provide a high-resolution image, TEM distinguishes EVs from possible contaminants of similar size that may be present after isolation of the EVs thereby ensuring the purity of sample (Linares *et al.,* 2017; Rikkert *et al.,* 2019). As a result, it provides visual verification that the sample used for the experiment is indeed EVs to refute any possibility that contaminants may skew experimental results during downstream assays and ensure accurate data analysis (Carnino *et al.,* 2019). Furthermore, EVs derived from HS-5 cells, using the two isolation methods in this study, were smaller than 200 nm and covered in a bilayer structure. Based on size, it is clear that the majority of the vesicles are probably small and as a result, the vesicles were regarded as sEVs to simplify the terminologies and prevent any confusion that may arise from the categorisation of the EVs. This is supported by the findings of Ramos *et al.,* (2016), which demonstrated that HS-5 cells release vesicles with a bilayer membrane. These vesicles also displayed the same immunophenotypic profile (CD73, CD63, CD81) as EVs from primary BM-MSC. In this study, the double-layer membrane of sEVs may protect the biomolecular cargo of these sEVs and may hugely contribute to their ability to convey cellular signals over long distances. Cellular signalling via EVs has been described as 'rececrine' and this involves the secretion of active cell receptors, including oncoproteins and growth factor receptors, as well as anchored and loaded signalling molecules (Dickey *et al.,* 2016).

Consequently, concentration and size distribution of the sEVs was characterized by NTA based on the Brownian motion of the sEVs particles (Enderle *et al.,* 2015). Similar to TEM, NTA offers a higher resolution and measures particle-by-particle ranging from 1 to 1000 nm thereby producing a number-based distribution and thus percentage of EVs (Vestad *et al.,* 2017). However, it is difficult to characterise heterogeneous EV particles especially apoptotic bodies that are larger than 1000 nm (Filipe *et al.,* 2010). There is also difficulty in distinguishing sEVs particles from non-sEVs particles that also display similar Brownian movement (Sunkara *et al.,* 2016).

As expected, all sEVs recovered by both isolation protocols were less than 1000 nm, most of them being in the 120-250 nm range. This is in support of the previous findings by Ramos *et al.,* (2016), which showed that the EVs released by HS-5 cells had an average size of 125.6 nm. However, in this study, particles isolated by SEC showed a broader size distribution and the principal population was larger with a mean diameter of 205 nm compared to sEVs isolated by the ExoQuick method with a mean diameter of 129 nm. Although these results suggest that the vesicles produced by ExoQuick and SEC are predominantly sEVs based on these measurements, this result was unexpected, as one would have expected that the vesicles isolated by ExoQuick method would have a broader particle size distribution profile detected by NTA. The sEVs isolated by this method were co-isolated with proteins. These proteins as well as lipoproteins, viruses or other aggregates are contaminants that may hinder precise analysis of the results, as the isolation of highly pure EVs is paramount to ensure the results are not misleading. These results further contrast the findings of Stranska *et al.,* (2018), which revealed that the majority of EVs isolated by precipitation method are larger than the particles isolated by SEC qEV columns. However, the precipitation method used in their study was the exoEasy kit manufactured by Qiagen.

Furthermore, the amount of sEVs recovered by the ExoQuick method was more than those from SEC thus suggesting that EV isolation method contributes to the amount of sEVs isolated from cells *in vitro*. These findings are further supported by the findings of Tang *et al.,* (2017) and Serrano-Pertierra *et al.,* (2019), which demonstrated that vesicle recovery is better with the ExoQuick method. The possible reason for this may be due to co-isolation of sEVs with contaminants or non-sEVs particles and other aggregates of similar size by the ExoQuick method. Similarly, the results in this study also corresponds to the findings of Gamez-Valero *et al.,* (2016)

who demonstrated that SEC isolates less sEVs than precipitation methods. This further reiterates the notion that the ExoQuick method gives more sEVs because the sample may not be as 'pure' as sEVs isolated by SEC. Furthermore, measurement of particle purity via assessment of the ratio of particle number to protein in these sEVs samples revealed that SEC-isolated sEVs had a higher ratio than those isolated by the ExoQuick method. A high ratio indicates the lowest level of protein contaminants and highest vesicular purity (Webber and Clayton, 2013; Tang *et al.,* 2017). This further implies that the sEVs isolated by SEC may be pure and maintain their integrity. These results are further corroborated by the reports that higher concentrations of total protein were found in EVs isolated with a precipitation kit compared to the EVs isolated from SEC qEV columns (Stranska *et al.,* 2018).

Additionally, the amount of sEVs particles recovered from untreated HS-5 cells by SEC was more than those recovered from treated HS-5 cells whereas treated HS-5 cells shed more sEVs than untreated HS-5 cells when EV isolation was performed by the ExoQuick method. The reason for this discrepancy in results may be due to differences in the isolation methods but since SEC provides the highest vesicular purity, it negates the notion that cells shed more sEVs during cytotoxic stress. However, since there is heterogeneity in sizes of EVs, the EVs released by HS-5 cells following chemotherapy may have different sizes but only the small vesicles are isolated. Isolation of large EV particles may be problematic thus making it difficult to differentiate the subtypes of EVs and consequently, one cannot identify which subtype of EVs contains any packaged nucleic acids during analysis (Taylor & Shah, 2015; Konoshenko *et al.,* 2018). However, it is important to mention that this is an important factor if the research requires this knowledge but this study was focused on discovering if miRNAs are trafficked between cells and if so, was it via EVs of any sort, so the process lends itself to the research question.

Nevertheless, the amount of sEVs shed by untreated HS-5 cells following SEC isolation (1.89 x 10^9 particles/ml) and ExoQuick method (6.01 x 10^9 particles/ml) in this study were much higher than the amount shed by untreated HS-5 cells demonstrated in another study (Javidi-Sharifi *et al.,* 2019). This difference in EV yield may be due to differences in cell culture conditions and EV isolation method. Whilst HS-5 cells were grown in DMEM-HG supplemented with 10% sEVs-depleted FBS in a 175cm^2 flask until 80-90% confluency before EV isolation in this study, their HS-

5 cells were grown to 80-90% confluency in RPMI 1640 supplemented with 10% FBS (not sEVs-depleted) in a 15cm dish. Their cells were sub-cultured in an EV-depleted medium overnight prior to EV isolation by density-gradient ultracentrifugation.

Further analysis of the fractions eluted from SEC qEV columns revealed that these fractions were rich in sEVs both in the control and treated samples. As suggested by the manufacturer's instructions, a pool of fractions 7-9 were used in this study, with fraction 8 showing the highest particle concentration (3.47×10^9 particles/ml). Similarly, SEC columns were used to isolate abundant EVs from cancer cells however, fractions 10-12 were analysed in their study (Guerreiro et al., 2018). The difference in the fractions utilised in this study and theirs may be due to differences in columns used. They used 30 mL sepharose CL-2B columns from GE Healthcare Biosciences, onto which a diluted sample of vesicles (4mL) was loaded to ensure proper yield of EVs. It is important to mention that since these columns differ, the molecular weight cutoffs of the membranes in these columns would also differ. In addition, Welton et al., (2015) and Baranyai et al., (2015) demonstrated that fraction 9 (6.0×10^{11} particles/ml) and fraction 2 (8.5×10^{12} particles/ml) respectively had the highest particle yield from plasma samples. This differs from the particle concentration in the fractions used in this study and this difference could be because their EVs were derived from plasma, which contains high lipid and protein content as well as platelets (Boing et al., 2013; Menezes-Neto et al., 2015). In contrast, low levels of protein were detected in these vesicle-rich fractions especially in the treated samples in this study.

Collectively, these results suggest that the HS-5 cells may release abundant EVs following exposure to chemotherapy however only the sEVs are isolated, from the cells. This further reiterates that secreting cell, cell culture conditions and EV isolation method contribute to the amount of EVs retrieved from cells in vitro. It also implies that no stand-alone EV isolation method results in a complete removal of contaminants. Although ExoQuick method represents a quick and easy method that could be implemented in clinical settings, these results suggest that SEC would be more suitable for clinical and therapeutic applications of sEVs derived from MSC due to its high yield of high-purity sEVs. However, these two isolation methods failed to separate the EVs based on their subtypes and produced EVs within 120-250 nm range hence the term sEVs. Since the different subtypes may contain different compositions (nucleic acids and/or proteins),

characterising these EVs as sEVs is important and would contribute to the analysis and interpretation of results from these vesicles. Furthermore, the integrity and amount of sEVs released by HS-5 cells under cytotoxic stress may provide additional information to determine if these sEVs are released to communicate damage signals to the bystander cells. The data, along with information about the miRNA contents of these sEVs may provide further insight into the role sEVs play in CIBE.

5.4.3 Uptake of sEVs by bystander cells

It is still unknown whether sEVs are selectively or non-selectively incorporated by bystander cells following release by parent cells. Following the evidence that HS-5 cells release sEVs following chemotherapy, the possibility of these sEVs being taken up by bystander TK6 cells was explored. By assessing cellular uptake of sEVs, the specificity of sEVs to bystander TK6 cells and their function upon uptake could be well understood.

However, the labelling of sEVs is a very difficult process due to their nano-size. Previously, researchers have used different lipophilic dyes such as DiO, DiL and PKH to label EVs however; these lipophilic dyes are not sEVs-specific and can label other cellular components (Tian *et al.,* 2013; Takov *et al,* 2017; Horibe *et al.,* 2018; Zhang *et al.,* 2019). The unbound dyes can also be retained in cells thereby producing false positive background signals that may skew experimental results. Another concern with the use of these lipophilic dyes is that they can cause an increase in vesicular size as well as changes in the homing characteristics of these vesicles and subsequently undermine cellular uptake and biodistribution studies (Dehghani *et al.,* 2019). Alternatively, protein dyes such as CFSE and antibodies to surface and intravesicular proteins such as CD63, CD9, CD81, calnexin and TSG10, which do not cause a shift in sizes of the labelled vesicles, have been suggested to be better options in labelling vesicles (Dehghani *et al.,* 2019; Mondal *et al.,* 2019).

In order to eliminate this problem of specificity of EV labelling and ensure EV uptake and visualisation, the membrane of sEVs was labelled with a red fluorescent dye that is commercially available (Exo-Glow-membrane) whilst the bystander TK6 cells were labelled with DiO in this study. The Exo-Glow-membrane dye has high specificity and high selectivity for sEVs membrane

with very low level of background noise. The time-lapse experiment revealed that sEVs membrane fused with the membrane of the bystander TK6 cells within an hour, and were internalised into the cells after 3 hours. However, it took 6-12 hours for the internalization process to be complete. These results imply that stromal cells could release sEVs into the BM microenvironment, which may be subsequently engulfed and internalised by incoming donor cells within a short time. The results also suggest that there may surface receptors on the membrane of the sEVs and cells that facilitate their uptake by the cells. In a similar study, sEVs released by HS-5 cells were internalised by leukemic cells and this protected the cells from the chemotherapeutic effects of tyrosine-kinase inhibitors *in vitro* (Javidi-Sharifi *et al.,* 2019). However, they stained the sEVs and leukemic cells with two lipophilic dyes, DiL and DiO, respectively.

Furthermore, another study also demonstrated that EVs do not remain attached to the outer cell membrane but are incorporated into the cytoplasm of the recipient cells (Durak-Kozica *et al.,* 2018). In the current research, the results suggest that the uptake process may be time-dependent and may depend on direct fusion between sEVs' membrane and the cell membrane based on molecules found on the surface of the vesicles and the bystander TK6 cells. This is similar to previous findings by Verdera *et al.,* (2017) that demonstrated that cellular internalization of EVs occurred within 4 hours in a time-dependent manner. However, their data suggest that lipid components such as cholesterol and phosphatidylserine (PS) found on the surface of the vesicles and cells play important role in EV uptake. These lipid components are very crucial to the maintenance and restoration of the cellular plasma membrane where they participate in macromolecular transport processes such as endocytosis and exocytosis (Zhang *et al.,* 2017). These lipid components have also been implicated in endocytic pathways that have been mentioned in EV internalization, which include clathrin-independent endocytosis, caveolae-dependent endocytosis, macropinocytosis and phagocytosis (Mulcahy *et al.,* 2014). Although this is beyond the scope of this study, the data in this study suggest that the sEVs are endocytosed or engulfed into the cells. These also suggest that the only live cells can engulf or internalise sEVs as disruption or loss of the plasma membrane integrity by damaging environmental forces will lead to cell death.

Furthermore, sEVs internalization was blocked by heparin, a soluble analogue of heparan sulfate proteoglycans (HSPG) in this study, as previously described by Atai *et al.,* (2013) and Christianson *et al.,* (2013). Heparin is a biological molecule that is primarily produced by mast cells and basophils, and thus influences a variety of biological processes such as cell adhesion, coagulation and growth factor signalling (Yang *et al.,* 2011; Balaj *et al.,* 2015). It acts primarily in preventing blood clotting through a complex with antithrombin, which prevents the formation of fibrin from fibrinogen but can also bind and sustain or control the release of cytokines including growth factors thereby enhancing the biological effects of proteins. Structurally, it is related to HSPG, which acts as receptors on the surface of many cells including MSC, where they play a key regulatory function in the interaction between the MSC and HSC within the BM niche (Papy-Garcia and Albanese, 2017).

Thus, heparin blocks off the ligand binding to HSPG but this effect may be dependent on the concentration used. A previous study demonstrated that time-dependent internalization of EVs by cells was abrogated in the presence of 10 µg/ml of heparin (Verdera *et al.,* 2017). It remains unclear how heparin disrupts EVs uptake but the results within the current study support the observations of Verdera *et al.,* (2017), suggesting a block of fusion of sEVs with TK6 cell membrane, possibly through a HSPG-mediated process. The sEVs seemed unable to fuse to the membrane of the cells (Figure 5.11) to facilitate the membrane-bound interaction between the cells and sEVs thus supporting the adhesive HSPG-mediated process. Therefore, the data from this study suggest that sEVs may be internalised into TK6 cells by receptor-mediated endocytosis as illustrated in figures 5.9 and 5.10. In support of this, heparin may bind to both sEVs and/or cells, and prevent adhesion of sEVs and subsequently cellular internalization (Sustar *et al.,* 2009; Atai *et al.,* 2013). However, since different inhibitors such as amilioride and dynasore can abrogate cellular internalization of sEVs into cells in different ways, it appears that sEVs can be internalised in a very complex mechanism via more than one route.

Although the detailed mechanism of sEVs uptake remains unknown, it has been suggested that the mechanism through which sEVs are taken up determine their ability to deliver their cargo and elicit a bio-molecular response. As a result, the RNA of the sEVs released by HS-5 cells was specifically labelled with a commercial dye (Exo-Glow-RNA) to understand if these sEVs deliver

their cargo once internalized by bystander TK6 cells. The Exo-Glow-RNA specifically binds to EV RNA with very low levels of background noise. The results suggested that these sEVs deliver their RNA cargo into the cytoplasm of bystander TK6 cells once taken up. In a similar fashion, it has been shown that the selected protocol is suitable for labelling and visualising isolated sEVs both in *in vitro* and *in vivo* systems (Li *et al.,* 2014; Reif *et al.,* 2015; Zhang *et al.,* 2019). These studies further support that sEVs are capable of adhering and fusing to the plasma membrane of the bystander TK6 cells, with the contents gradually released into the cytoplasm upon internalization – a classic mechanism used for cellular uptake of materials. Further pre-treatment of HS-5 cells-derived sEVs with heparin before labelling the RNA led to disruption of the sEVs uptake by the bystander cells. This further shows that the fusion of sEVs to the cells may be a very important step in the uptake of sEVs by bystander TK6 cells and may subsequently result in the ability of the sEVs to release their contents into sub-cellular compartments of these bystander cells to elicit bio-molecular effects.

Collectively, these results imply that stromal cells release sEVs that can be engulfed by the bystander cells within the BM microenvironment via direct fusion between the sEVs and bystander cells, which may be dependent on the surface molecules on their membranes. Once internalized, the RNA of sEVs could be seen within the cytoplasm of the recipient cells thus suggesting the release of sEVs' contents into the bystander cells. This is critical to further understanding how these sEVs may function as a delivery system in the human body as well as how they may be involved in the development or modulation of a second malignancy following HSCT. Any evidence of involvement in these processes may help clinicians to develop more effective methods to detect and monitor leukaemia patients following HSCT.

5.4.4 Effect of GW4869 on CIBE

The possibility that these sEVs may play important roles in the BM microenvironment highlights the importance to understand how their secretion can be inhibited. Thus, it was appropriate to inhibit sEVs secretion by stromal cells in a model of the BM microenvironment. Several researchers have explored the use of pharmacological agents, as potential therapeutic approaches, to inhibit the secretion and release of sEVs (Samuel *et al.,* 2017; Biemmi *et al.,* 2018).

However, the complexity and heterogeneity of the EV subtypes and their biogenesis pathways means using a single drug to block cellular production of EVs remains a challenge. Nevertheless, blocking the predominant EV subpopulation released by stromal cells, which are sEVs as seen in this study, may provide some answers.

The most widely used chemical in the inhibition of sEVs biogenesis and release is GW4869. In 2010, Kosaka *et al.,* became the first people to successfully inhibit the release of EVs in HEK293 cells using GW4869. GW4869 is a potent neutral sphingomyelinase inhibitor that acts by preventing the inward budding of MVBs and the subsequent release of exoosmes upon fusion of the MVBs with the plasma membrane (Essandoh *et al.,* 2015). Thus, neutral sphingomyelinase is ubiquitous and found in a range of compartments in all cells, including the membrane of cells where it acts as an enzyme that catalyses the hydrolysis of the membrane lipid sphingomyelin thereby leading to the generation of the bioactive lipid ceramide (Shamseddine *et al.,* 2015). The lipid bilayer of sEVs contains more ceramide, cholesterol and sphingolipids than cellular membrane as illustrated in a quantitative study (Catalano and O'Driscoll, 2019).

In the current study, GW4869 was used to inhibit the secretion and release of sEVs by stromal cells. However, GW4869 exerted a cytotoxic effect on the stromal cells in a dose dependent manner. The concentrations used in this study (5 µM, 10 µM, 20 µM) have been previously considered not to have any cytotoxic effect on RAW264.7 macrophages (Essandoh *et al.,* 2015). Thus, the reason for this discrepancy may be explained by the abundance of lipid bioactive molecules such as ceramide and sphingomyelin on the membrane of HS-5 stromal cells (Haraszati *et al.,* 2016). Although the structure of the cell membrane is similar in different cells, they are not exactly the same. The report by Haraszati *et al.,* (2016), which revealed that the MSC membrane is enriched in ceramide and sphingomyelin in comparison with glioblastoma and hepatocellular carcinoma cells, support these findings. It is well known that sphingomyelin, ceramide and phosphatidylserine are involved in a variety of biological functions such as proliferation, differentiation and apoptosis through the maintenance of the plamsa membrane integrity (Bartke and Hannun, 2009). Therefore, blocking the sphingomyelin pathway and thus formation of ceramide with GW4869 in these HS-5 stromal cells may explain this cytotoxic effect of GW4869 on the cells. GW869 was also cytotoxic to myeloma cells with highly expressed

phosphatidylserine on their cell membrane in a dose dependent manner (Vuckovic *et al.,* 2017). These suggest that at high dose, GW4869 may cause disruption or loss of plasma membrane integrity of the cells through interaction with anionic phospholipids. The loss of cell membrane integrity renders the cell vulnerable and may lead to cell death (M[c]Neil and Steinhardt, 1999). It is also likely that GW4869 causes deformation of the structure of the cell membrane, which may in turn cause irregularities in the fluidity of the cell membrane thereby disrupting critical signalling or transport pathways required for cell survival.

Since GW4869 is cytotoxic to these stromal cells, the non-toxic concentration (5 µM) of GW4869 was used to inhibit the secretion and release of sEVs. The hypothesis is that blocking the secretion of sEVs may reduce the CIBE in bystander TK6 cells. The anti-proliferative effects of the drugs were modestly promoted especially mitoxantrone but the difference in proliferation of the cells treated with or without GW4869 was not significant. Since the concentration of GW4869 used was not cytotoxic, hence it is assumed that the anti-proliferative effects recorded were solely dependent on the chemotherapeutic agents used. However, mitoxantrone induced more DNA damage in the bystander TK6 cells in the absence of GW4869 supporting a role for sEVs in the mutagenesis of the bystander cells. While this study does not necessarily confirm that GW4869 inhibits the secretion and release of sEVs by the stromal cells, the results suggest that the reduction in DNA damage in bystander TK6 cells could be attributed to blocking sEVs release. Extensive literature review supports that this is the first study to illustrate that GW4869 can reduce chemotherapy-induced DNA damage in a model of the BM using MSC. It is important to mention that this was a subtle change and not significant, and requires further assessment of definitive blocking of sEVs' secretion and release to be certain that this is a key process. The fact that the change was subtle, and that the lower doses of GW4869 were used, it is possible that some sEVs are still released at these lower doses and a reduction in MN could be more pronounced with complete blockade but this would need further validation.

However, the effect of GW4869 on vesicles' secretion and release, and subsequently CIBE has been extensively studied using fibroblasts. The ability of cancer-associated fibroblasts (CAF) to prime cancer stem cells in colorectal cancer and protect them from the chemotherapeutic effects of oxaliplatin or 5-fluorouracil was markedly reduced when the CAF were pre-treated with 10 µM

GW4869 (Hu *et al.,* 2015). In addition, exposure of CAF to gemcitabine induced an increase in the release of vesicles that conferred chemo-resistance on pancreatic epithelial cancer cells when co-cultured however, these survival benefits were significantly reduced when CAF were pre-treated with 20 μM GW4869 (Richards *et al.,* 2017). The concentrations of GW4869 used in both studies correspond to the concentrations used in this study however, they did not explore if GW4869 had any cytotoxic or anti-proliferative effects on the cells at these concentrations. Nevertheless, Richards *et al.,* (2017) showed that high concentration of GW4869 (20 μM) decreased CAF vesicles' secretion by 70% in both untreated and treated CAFs. In another study using lung cancer cells (PC9), Li *et al.,* (2016) showed that although GW4869 (5 μM, 10 μM, 20 μM) did not affect the proliferative ability of these cells, there was a significant decrease in vesicles secreted by lung cancer cells (PC9) treated with gefitinib. GW4869 (10 μM) also did not enhance the impact of gefitinib- or cisplatin-induced growth inhibition on these cells.

Collectively, these suggest that GW4869 is capable of inducing cytotoxic effects on stromal cells at high concentrations and this may be due to the enrichment of lipid bioactive molecules on their cell membrane. GW4869 may also block the secretion and release of sEVs by these cells in the BM microenvironment. Although this blockade may not be total, it may lead to a block in the transfer of residual effects of pre-transplant chemotherapy via sEVs to the neighbouring cells during HSCT.

5.4.5 Effect of sEVs on bystander cells

The evidence provided in this study supports a subtle role of sEVs in inducing CIBE. This concept is based on the observations that sEVs derived from stromal cells exposed to chemotherapeutic effects can induce CIBE in naïve TK6 cells and the inhibition of the secretion of these sEVs with GW4869 reduced the CIBE outcomes. Thus, it became necessary to directly treat the naïve TK6 cells with these sEVs derived from drug-treated stromal cells. Interestingly, the sEVs derived from mitoxantrone-treated HS-5 cells caused a reduction in bystander TK6 cell number, which was recovered upon treatment with heparin. This reduction in cell number coincided with increased MN frequency in the bystander cells. Furthermore, pre-treatment of bystander TK6 cells with sEVs from mitoxantrone-treated HS-5 cells conferred resistance to mitoxantrone despite

increased genotoxic events in the cells. However, the cells became sensitive to mitoxantrone upon heparin treatment. These suggest that sEVs may elicit bysander cellular response to different stimuli in diverse ways, and may be capable of sending both damaging and protective signals to the bystander cells despite the cells retaining genotoxic effects from mitoxantrone. However, these signals are negated when heparin blocks their uptake thereby making the bystander cells to be more prone to toxicity from the genototxic environment. The data from this study correspond to the previous findings by Samuel *et al.,* (2017), which demonstrated that sEVs derived from cisplatin-treated ovarian cancer cells, caused a reduction in cell numbers of naïve ovarian cancer cells when co-cultured and protected them from the chemotherapeutic effects of cisplatin. However, these effects were ameliorated upon treatment of the cells with inhibitors of sEVs uptake such as heparin, dynasore and amiloride.

Taken together, these data suggest that chemotherapy may alter the contents of released sEVs such that sEVs can cause damage in the bystander cells upon uptake but enhance the protective role of MSC towards the HSC within a genotoxic environment. It could be notionally assumed that the MSC are 'telling' the HSC to behave in such a way that would protect them from the toxic environment, such as controlling cell cycle, proliferation and exocytosis, pathways influenced by hsa-miR-16-5p, hsa-miR-17-5p, hsa-miR-200c-3p, hsa-miR-30d-5p and hsa-miR-20a-5p (section 4.3.3.4). In preventing the uptake of sEVs using heparin, the bystander cells do not get the protetctive messages and instead succumb in the presence of the chemotherapeutic agent. This protective effect may be due to the induction of signalling pathways that may be critical to their survival. Cell signalling to stress-response often takes a dual role thus activating both survival and death pathways to buffer and repair the damage but when the damage is beyond repair, cell death is triggered (Flusberg and Sorger, 2015). Stress-response and death signalling pathways seem to be tightly linked and involve cellular proteins that regulate cell death as well as normal cellular processes such as proliferation, differentiation and metabolism simultaneously (Yuan *et al.,* 2006; Munoz-Pinedo *et al.,* 2012).

Furthermore, these sEVs could contain molecules on their surfaces that may be able to promote resistance to chemotherapeutic drugs in these bystander cells upon uptake. Chemotherapy-induced sEVs released by myeloma cells have been shown to contain high levels of heparanase

on their surface (Bandari *et al.,* 2019). Heparanase is an enzyme that remodels the extracellular matrix thereby regulating multiple cellular processes and can be transferred to elicit biological activities in the neighbouring cells (Bandari *et al.,* 2019). Heparanase is also found on the cell membrane and its overexpression corresponds to tumour progression and poor prognosis (Mohan *et al.,* 2019). However, heparin is endowed with anti-heparanase activity (Cassinelli *et al.,* 2020). This may explain why heparin disrupted the uptake of sEVs and subsequent chemo-protective effects of sEVs in this study. It can be inferred that heparin digested the heparanase on the surface of the cells and sEVs thereby blocking the uptake of these sEVs by the bystander cells. However, this was beyond the scope of this study and needs further investigation to explore if heparanase can be found on the bystander TK6 cell membrane and the membrane of sEVs released by HS-5 stromal cells.

Other researchers have also demonstrated that chemotherapy-induced sEVs contain high levels of survivin and annexin A6 respectively, which were able to induce survival signals in neighbouring breast cancer cells (Kreger *et al.,* 2016; Keklikoglou *et al.,* 2019). Survivin is a pro-apoptotic protein that belongs to the group of inhibitor of apoptosis proteins whilst annexin A6 is a calcium-dependent protein that belongs to the annexin family. Expression of these proteins is elevated in several cancers (Cheung *et al.,* 2013; Qi *et al.,* 2015). Although there is no evidence in literature that shows that sEVs released by stromal cells express these proteins, annexin A6 found on vesicles derived from CAF enhanced the aggressiveness of pancreatic ductal adenocarcinoma *in vitro* (Leca *et al.,* 2016). Therefore, this needs further investigation in HS-5 cells-derived sEVs.

The survival of sEVs-treated bystander TK6 cells exposed to mitoxantrone may also depend on factors that control their cell cycle. Cells have a response system to combat deleterious genotoxic attacks on the DNA by inducing cell cycle arrest to allow sufficient time for the incurred damage to be repaired, and if this damage is irreparable, apoptosis is induced. Therefore, cell cycle and its checkpoints are tightly regulated and maintained in order to drive normal cellular processes including proliferation and differentiation; hence deregulation of the cell cycle may play an important role in the development of cancer (Satyanarayana and Kaldis, 2009). The G1- and G2-

phase checkpoints are crucial in preventing cancer cells from uncontrolled cycling and proliferation.

Previously, some researchers have shown that mitoxantrone can induce cell cycle arrest and growth inhibition by forcing G1- and G2 phase arrest in yeast cells (Khan *et al.,* 2010). No evidence of apoptotic peaks (sub-G1 phase) was also recorded with the different concentrations (0, 2.5, 5 µg/ml) used. Thus, mitoxantrone was used as a positive control in this study however when the bystander TK6 cells were treated with mitoxantrone, there was no evidence of cell cycle arrest instead there were apoptotic peaks even though the concentration of mitoxantrone (500 ng/ml) used in this study is smaller than the concentration used in their study. Therefore, the difference in results may be due to the differences in cell types and sampling times. The cycling time of TK6 cells in DMEM-HG media supplemented with sEVs-depleted FBS is about 18.3 hours (section 3.3.1.2) however; the cells were pre-treated with sEVs for 24 hours before exposing them to mitoxantrone for 24 hours. Therefore, the cells could well have moved through cell cycle block after accumulating genotoxic effects and either resumed cycling or died. A series of timepoints could have been useful in this study.

Furthermore, diploidy (a balanced complement of chromosomes) was found in the negative controls whilst uncontrolled chromosome content (aneuploidy) was found in the cells that were exposed to mitoxantrone. Aneuploidy is the gain or loss of chromosome in a cell, and is associated with significant cellular stress as well as cancer initiaition and progression (Molina *et al.,* 2020). However, aneuploidy is context-dependent and may depend on the cell type, genomic context, cellular microenvironment and immune system of the patient involved (Ben-David and Amon, 2019). Interestingly, aneuploidy was also found in the cells that were treated with sEVs from treated HS-5 cells but this chromosomal imbalance was corrected upon pre-exposure to heparin. This infers that the vesicles convey stress to the bystander cells perhaps chemotherapy-induced, which may be of great significance to their long-term survival.

Although the miRNAs such as hsa-miR-17-5p, hsa-miR-16-5p and hsa-miR-30d-5p that control cell cycle and cell death were found in sEVs released by treated HS-5 cells (Section 4.3.3.4), there was no evidence of cell cycle arrest in cells treated with sEVs from treated HS-5 cells. Most of the cells

were in G1 phase similar to the negative controls (untreated cells and cells treated with PBS). Similarly, there was no evidence of cell cycle arrest when the cells were pre-treated with heparin. These data further support the idea that bystander cell exposure to sEVs may trigger cell survival-signalling pathways such as cell cycle control, which also involves the apoptotic machinery to ensure cell cycle progression. However, exposure of the sEVs-treated bystander TK6 cells to mitoxantrone caused apoptotic peaks in the sub-G1 phase, which were more than the peaks found in cells treated with only mitoxantrone. This may explain the genotoxic events, which was interestingly accompanied by an increase in cell number, seen in sEVs-treated bystander TK6 cells upon exposure to mitoxantrone (section 5.6.4). Nevertheless, the data suggest that although that the cells progress through cell cycle, the DNA of these cells may become damaged upon exposure to mitoxantrone however, the data does not provide information on the mechanism of cell death (programmed or stress-induced). Therefore, the fate of these cells with damaged DNA remains unknown. Nevertheless, the sustained genotoxic effects in the bystander cells is of great concern and may cause genomic instability and cancer development.

Following extensive literature review, this is the first study of its kind to explore the effects of sEVs from drug-treated MSC on the cell cycle of the recipient cell. However, it has been previously shown that untreated MSC release sEVs that subsequently trigger breast cancer cells into dormancy or quiescence (G_0 phase) and protect them from the effects of chemotherapy (Lim *et al.,* 2011; Bliss *et al.,* 2016). This effect was mediated by miRNAs in the sEVs cargo, which are transported from the BM stroma to the breast cancer cells. These further suggest that the miRNA content of the sEVs released by HS-5 cells may have an important role in the adaptive response of TK6 cells to mitoxantrone through the regulation of cell cycle. Summarily, stromal cell-derived sEVs, which are released into the BM microenvironment following pre-transplant chemotherapy, may induce adaptive and invasive effects in the neighbouring cells, and protect them from the effects of chemotherapy. However, this protection from chemotherapy may be accompanied by sustained DNA damage in some of the cells. It is worth exploring the value of this sustained DNA damage in diagnosis.

5.4.6 miRNA expression profiles in extracellular components

It has been established that extracellular RNAs circulate in body fluids of healthy and diseased individuals, such as milk, urine, serum and plasma with sufficient integrity. Despite the presence of ribonuclease enzyme in these samples, circulating RNAs are stable and their stability is due to enclosure of these circulating RNAs within lipoprotein vesicles (Kosaka *et al.,* 2010). Nevertheless, there is selectivity in the packaging of the vesicular cargo and as a result, RNA and protein that make up a majority of the cargo may or may not reflect the nature of the parental cell (Li *et al.,* 2014; Groot and Lee, 2020). Recent studies have demonstrated that vesicles are targeted to recipient cells to exchange proteins and deliver nucleic acid cargo to facilitate intercellular communication within the BM microenvironment (Wang *et al.,* 2016).

Within the current study, analysis of RNA extracted from extracellular components such as sEVs, CM and sEVs-depleted FBS, was performed. FBS, usually used as a medium supplement, contains substantial particle population as well as bovine RNA in vesicular and non-vesicular particles that may skew the experimental results (Szatanek *et al.,* 2015*;* Wei *et al.,* 2016). In order to prevent the mixture of the serum EVs and cell-derived EVs during cell culture, which is a potential source of interference, the cells were grown in medium supplemented with commercially available sEVs-depleted FBS in this study. This eliminates the any bias from RNA species in the serum influencing or confusing the outcomes of the experiments.

Previously, it has been shown that the sEVs-depleted FBS has no negative effect on cell proliferation (Guerreiro *et al.,* 2018). Similarly in this study, HS-5 cells and TK6 cells grew in DMEM-HG medium supplemented with sEVs-depleted FBS at a similar rate as those grown in DMEM-HG medium supplemented with non-sEVs-depleted FBS (section 3.3). Whilst this confirms proliferation was unaffected, to ensure that no other experimental outcomes were affected, sEVs-depleted FBS was used throughout the experimentation to confirm that only the nucleic acid cargo of the sEVs released by HS-5 cells due to chemotherapeutic stress were present. Although there are very few published reports on the isolation of RNA from CM of cells, RNA was successfully extracted in this study from these extracellular components, of CM from HS-5 cells. The ability to achieve reliable and reproducible RNA yield from these extracellular components

is vital for the successful amplification of miRNAs by qRT-PCR. Successful miRNA analysis also relies heavily on the purity and integrity of extracted RNA. Thus, the concentration, yield and purity of these RNA were determined. The concentration of RNA from CM of untreated cells was 28.99 ± 6.29 ng/µl whilst the concentration of RNA from CM of treated cells was 25.13 ± 8.34 ng/µl. RNA from both sets of samples had purity ratios within the range of 2.1 and 2.3. This indicates that the samples were free of contaminants such as peptides, phenols, aromatic compounds, carbohydrates and proteins. These results correspond to the previous findings that demonstrated that the amount of RNA extracted from CM of primary stromal cells was 42.85 ng/µl (Glynn *et al.,* 2013). However, their data showed that the amount of RNA extracted from CM depends on the extraction method and cell type.

The amount of RNA isolated from sEVs derived from untreated and treated stromal cells in this study was 10.6 ± 1.18 ng/µl and 25.07 ± 13.87 ng/µl respectively. It should be noted that HS-5 cells contain about 19-fold more RNA and the fractions of vesicles isolated by SEC were not pooled together rather RNA was isolated from each 500 µl fraction containing vesicles. These suggest that the sEVs isolation method, starting material, RNA extraction method and cell type may have contributed to the reduction in sEVs-RNA recovery seen in this study. The sEVs' membrane may contain molecules that could cause incomplete lysis of the sEVs membrane during RNA isolation. However, this is above the scope of this study and needs to be further evaluated.

Furthermore, the sEVs-depleted FBS used in this study was tested for RNA to establish a baseline level of RNA as a control to minimise the confounding effect of FBS. RNA yield was also small in sEVs-depleted FBS used in cell culture (8.51 ± 0.56 ng/µl). This data is consistent with the previous assessments of the sEVs-depleted FBS used in culturing HEK293 kidney cells and A20 lymphoblast cells (Driedonks *et al.,* 2019). RNA yield in the serum samples ranged between 2-3 ng/µl. However, the RNA yield from 'crude' FBS was much larger and ranged between 5-40 ng/ml whilst sEVs-depleted FBS contained 34 ng/ml on average (Wei *et al.,* 2016). These indicate that FBS used as supplement for cell culture medium contains vesicle particles as well as RNA. Therefore, as a rule of thumb, medium and medium supplements including FBS that is free of vesicle particles as well as RNA should be prioritised.

Regardless of the extracellular component, it is worth mentioning that a fixed concentration of RNA of good quality was used for cDNA synthesis whilst the concentration of total cDNA used was the same in all samples analysed. These follow the suggestions proposed in the Minimum Information for Publication of Quantitative Real-Time PCR Experiments (MIQE) guidelines (Bustin *et al.,* 2009; Guenin *et al.,* 2009). This was to ensure that qRT-PCR analysis yields reliable results and enable the comparison of miRNA expression profiles in two different samples (treated and untreated). However, these small RNA species of non-miRNA origin, SNORD61 and RNU6B/RNU6-2, were either totally absent or present in trace amounts with significantly low Ct values (Ct > 34). This was expected as these small RNA species are produced intercellularly and may not be found in these extracellular components (Bustin *et al.,* 2009; Guenin *et al.,* 2009). As a result, normalisation of data with the endogenous controls and subsequent relative quantification could not be performed.

The only miRNA detected in the CM of untreated and treated stromal cells was hsa-miR-30d-5p, which has been previously reported to be a novel biomarker in the clinical therapy of human cancers (Gaziel-Sovran *et al.,* 2011; Zhang *et al.,* 2017). However, hsa-miR-30d-5p in the CM samples from HS-5 cells was in trace amount with Ct values above 35. A Ct value of 35 and above normally represents single template detection and is usually considered to be below detection level of the assays of intercellular miRNAs. However, these high Ct values in extracellular miRNAs suggest that miRNAs are highly expressed in the cell monolayers than in the CM, and only is released when intercellular communication is required. This is supported by the previous findings that demonstrated that the amount of miRNAs detected in CM (Ct values ranging from 32.6 to 33.8) was 180 times less than in cell monolayers (Turchinovich *et al.,* 2011). However, their data indicated that hsa-miR-16, hsa-miR-21 and hsa-miR-24 are common miRNAs that are readily detected in FBS used in cell culture. Instead, only hsa-miR-16-5p (Ct value 35.59) and hsa-miR-30d-5p (Ct value 35.85) were found in the sEVs-depleted FBS used in this study. It is important to note that the FBS used in their study was non-sEVs-depleted FBS. This may have contributed to the differences in the type and amount of miRNAs detected in this study. Nevertheless, other studies have also shown that miRNAs are present in sEVs-depleted FBS (Wei *et al.,* 2016; Mannerström *et al.,* (2019). These miRNAs include hsa-miR-122, hsa-miR-203a, hsa-miR-451a

and hsa-miR-1246, which do not correspond to the miRNAs detected in this study. These FBS-associated RNA species were also found to be protected from the effects of proteinase K and RNAse A treatment (Shelke *et al.,* 2014).

Therefore, it can be inferred that the hsa-miR-30d-5p detected in the CM of treated and untreated HS-5 cells in this study may stem from the sEVs-depleted FBS used in this study. This suggests that the prolonged bystander effects found in TK6 cells exposed to CM from mitoxantrone-treated HS-5 cells (section 4.3.2.3) may not be due to the miRNA content in CM but may be because of complex signals released into the medium by HS-5 cells upon drug treatment. Since this study has shown that CM from HS-5 cells contain EVs and miRNAs, CIBE may result from an interplay between different signalling molecules. It has been reported that a complex of growth factors, cytokines, chemokines, EVs and other extracellular matrix molecules can be found in CM from MSC (Benavides-Castellanos *et al.,* 2020). In addition, these components of CM from MSC may differ depending on their accumulation in the cell growth medium (Lee *et al.,* 2017; Sagaradze *et al.,* 2019). Taken together, these results suggest that the depletion of sEVs does not completely remove RNA from FBS thus highlighting the need and importance to carefully select the appropriate medium/supplements for the investigation of RNA biomarkers. The presence of RNA in FBS also suggests that RNA may have an effect on cell behaviour *in vitro* and may have interfered with the analysis of CM and sEVs-associated RNA in CIBE. However, the functional effect of this 'contaminant' RNA on recipient cells needs to be determined to understand their biological roles.

Lastly, the RNA cargo of the stromal cell-derived sEVs was analysed. Data revealed that two miRNAs, hsa-miR-30d-5p and hsa-miR-16-5p, were expressed in sEVs derived from both untreated and treated HS-5 cells. These were the miRNAs found in sEVs-depleted FBS thus suggesting these may have been trafficked via culture medium and incorporated into the sEVs. However, hsa-miR-17-5p was detected in treated sEVs but not in untreated HS-5 cells. This suggests that hsa-miR-17-5p may be an 'alarm signal' from the treated HS-5 cells and when trafficked to TK6 cells, may contribute to the CIBE seen in TK6 cells. Hsa-miR-17-5p is involved in the regulation of fundamental cellular processes such as proliferation, autophagy and apoptosis (Bobbili *et al.,* 2017). This supports the findings in this study that hsa-miR-17-5p control genes

involved in cell cycle and proliferation (Section 4.3.3.4) and may explain the reduction in cell numbers of TK6 cells following exposure to sEVs from treated HS-5 cells (section 5.5.3). It can also be inferred that the recovery of TK6 cell numbers following pre-treatment to heparin (section 5.5.3) may be due to inhibition of uptake of these treated sEVs containing hsa-miR-17-5p. Hsa-miR-17-5p also belongs to the miR-17-92 family, known as onco-miRs that are elevated in many human cancers wherein they promote unrestrained cell growth thereby enhancing cancer aggressiveness and responsiveness to chemotherapeutics (Li *et al.,* 2017; Kong *et al.,* 2018). The cluster could also act as tumour suppressors in some circumstances with pro-tumour properties (Li *et al.,* 2017). Despite the low detection in sEVs, these suggest that hsa-miR-17-5p may act as a biomarker of CIBE, which can trafficked to the recipient TK6 cells thus controlling their response to genotoxic effects of chemotherapy (section 5.5) as well as CIBE (section 4.3.2.2) seen in this study.

In support of this data, the expression of these miRNAs, including hsa-miR-17-5p, in bystander TK6 cells was downregulated following co-culture with sEVs from untreated and treated HS-5 cells (section 5.6.7). Interestingly, there was a significant difference in the miRNA levels detected in cells exposed to untreated sEVs and cells exposed to treated sEVs. These data support the findings in section 4.3.3.4, which revealed these miRNAs were detected at lower levels in TK6 cells exposed to drug treated HS-5 cells. Underexpression of these miRNAs have been implicated in tumourigenesis (Yan *et al.,* 2017; Zhang *et al.,* 2017; Chen *et al.,* 2018; Dong *et al.,* 2019). Therefore, it can be inferred that sEVs can sequester drugs from parent cells and transport them to neighbouring cells. Although only hsa-miR-17-5p was the differential miRNA between the untreated and treated sEVs, all miRNAs explored may have significant roles in CIBE seen in this study. These suggest that CIBE may be because of an interplay between complex molecular cues in TK6 cells. These further suggest that there may be selectivity in the packaging of miRNAs and not all the functional miRNAs are packaged into the sEVs. In addition, the expression of hsa-miR-30d-5p was elevated in these cells upon inhibition of sEVs uptake with heparin (section 5.6.7). These suggest that the cargo from the sEVs inhibits the expression of these miRNAs in bystander cells. These are further supported by the findings that heparin can differentially modulate gene expression of stromal cells (Laner-Plamberger *et al.,* 2019). Therefore, the CIBE in the bystander

TK6 cells may be through modulation of molecular cues that may regulate different cellular pathways such as proliferation, apoptosis and autophagy.

Collectively, these results suggest that CM, FBS and sEVs harbour miRNA but in low concentrations. One possible explanation for this low number is that cells harbour RNA intercellularly and only release a minute amount of RNA into the extracellular components, which may contain different cargos and functions. However, these extracellular components may reflect the functionality of the host cell and possess molecular and treatment signatures that are capable of inducing substantial biological effects in the bystander cells. In addition, these data infer that the majority of the hsa-miR-30d-5p and hsa-miR-16-5p in the CM and sEVs samples are free floating in the serum as the depleted medium had the same basic levels of these miRs despite the sEVs being removed. The presence of hsa-miR-17-5p in the treated sEVs samples also suggests a possible role of this miRNA as a diagnostic biomarker of CIBE during HSCT. Since these miRNAs are micro-managers of gene regulation, the biological effects found in the recipient cells could be because of the combined effects of hsa-miR-17-5p and other miRNAs on cellular pathways such as proliferation, apoptosis and autophagy.

5.5 Summary

This chapter has focused on the role of extracellular components and their associated miRNAs in CIBE. Stromal cells, HS-5 cells, release EVs into an *in vitro* model of the BM following exposure to drugs used in pre-transplant conditioning. These EVs were heterogeneous in size however when the EVs were isolated from these cells by two distinct methods and characterised, the cells were between 125 – 250 nm hence the term sEVs. These sEVs were then taken up by the bystander TK6 cells by fusing with the membrane of the cells. Once internalised, the sEVs released their RNA cargo into the cytoplasm of the bystander cells however this internalization was inhibited when the sEVs were pre-incubated with heparin. Further inhibitory studies using GW4869 to block the secretion and release of these sEVs led to a slight reduction in CIBE in the bystander TK6 cells.

In addition, co-culture of the bystander TK6 cells with sEVs led to a reduction in cell numbers and accumulation of genotoxic damage however, these were negated upon treatment with heparin. Exposure to sEVs also induced an adaptive response to mitoxantrone in these cells and resulted in a percentage of cells in the sub-G1 phase thus indicating cell death possibly due to the accumulation of the genotoxic effects in these cells. Small RNA molecules, miRNA, were successfully isolated from extracellular components such as CM, sEVs and FBS, and quantified. There could be several explanations for this difference between cellular and extracellular miRNA population, including cell lysis and packaging. This further supports the hypothesis that packaging and exporting of extracellular miRNAs is not specific. Two miRNAs, hsa-miR-30d-5p and hsa-miR-16-5p, were found in the FBS thus suggesting that these miRNA are free floating in the FBS and may interfere with the downstream analysis of miRNAs in CM and sEVs. As expected, hsa-miR-30d-5p was also found in the CM and sEVs samples however hsa-miR-17-5p was only found in the treated sEVs samples thus implying that this miRNA may act as a biomarker or 'alarm signal' to the bystander TK6 cells thereby inducing CIBE. However, when the miRNA expression in cells co-cultured with these sEVs was explored, the expression of all miRNAs explored were significantly downregulated thus indicating that the sEVs contribute to the reduction in detection levels of these miRNAs in TK6 cells.

Therefore, it is reasonable to speculate that pre-transplant conditioning may induce stromal cells to release sEVs that harbour RNA cargo, which may act as microenvironmental cues to neighbouring cells in the BM microenvironment thus inducing several molecular and physiological changes in the cells. Nevertheless, it could be inferred that the miRNAs not packaged into the sEVs or analysed in this study might also play a role, as might other cellular components and/or sequestered drugs. Furthermore, the CIBE seen in the bystander cells could be a combination of different biological stimuli such as cytokines, proteins and lipids in the CM and sEVs hence the need to strengthen and verify the current findings in order to propel this field forward. Additionally, there is need to develop a standardized method for isolating EVs from the cell culture supernatants to ensure that 'pure' vesicles devoid of contaminants are used for downstream analysis. There is also need to carefully identify an appropriate method to isolate RNA from these extracellular samples.

6.0 General Discussion

Pre-transplant conditioning is a double-edged sword that has improved the efficacy of HSCT and thence patient survival rates however, it has been associated with the development of secondary and *de novo* primary malignancies such as TRM and DCL after HSCT (Wiseman, 2011; McNerney *et al.,* 2017). Due to the intercellular communication between different cell populations within the BM microenvironment that can propagate a mutated clone and/or encourage the development of tumour, it is pertinent to understand how pre-transplant conditioning could remodel the BM microenvironment during HSCT. Pre-transplant conditioning is directed at clearing the BM for the incoming donor cells to ensure normal haematopoietic engraftment after HSCT (Carrancio *et al.,* 2011). Therefore, the conditioning regimen is toxic to both blood cells and leukaemic cells within the BM microenvironment such that all the cell populations within the BM microenvironment are all bathed in pre-transplant chemotherapy and under the influence of toxic effects (Spyridonidis *et al.,* 2005). This theory was hypothesized as a mechanism in DCL thus suggesting that stromal cells in the tumour microenvironment retain the effects of pre-transplant conditioning and then transfer toxic signals in response to the chemotherapy to the incoming cells from a donor (Wiseman, 2011; Hongbing and Liu, 2016). Using DCL as the pathological pivot of this study, this thesis is aimed at understanding how chemotherapeutic drugs used in pre-transplant conditioning can induce bystander effects (genotoxic and cytotoxic) in the neighbouring cells and the possible roles EVs and miRNAs play in propagating these effects.

Mammalian cell lines are a very useful source widely used as an experimental model to study and understand cellular mechanisms. Advances in cell culture have enhanced our understanding of cellular behaviour and responses *in vivo* (Duval *et al.,* 2017). *In vitro* research has also provided valuable information that has led to a better understanding of the genotypes and phenotypes of various diseases including leukaemia (Saunders and Amore, 1992; Bogdanowicz and Lu, 2013; Bian *et al.,* 2017). It has been widely reported that the human BM microenviroment can be modelled *in vitro* by MSC-HSC co-culture. However, most studies focus on how intimate interactions between MSC and HSC lead to the protection of the haematopoietic compartment from the toxic effects of drugs and in doing so, confer resistance to haematological malignancies

that may be present (Ede *et al.,* 2018; Usmani *et al.,* 2019; Kouzi *et al.,* 2020). Little research has been done on what the malignancy does to the BM or any transfer of drug-induced toxicity as in bystander.

Therefore, it is important to monitor the state of the BM stroma after pre-transplant conditioning, as the stroma is a source of pro-leukaemic signals. Although the BM stroma consists of different cell populations, mesenchymal stromal cells were chosen as they majorly produce cellular signals that protect leukaemia from the effects of anti-cancer treatment thus leading to the development of resistance to therapy. These stromal cells represent the stem cells that generate the stromal layer and within our laboratory, it has been shown that the HS-5 stromal cell line used in this study have the capacity to differentiate into a stromal layer (Saeed Kabra, personal communication). In addition, the interaction between these stromal cells and haematopoietic cells in the BM microenvironment is crucial to the regulation of haematopoiesis (Anthony and Link, 2014; Scadden, 2016). Since these stromal cells play a vital role in the self-renewal and differentiation of HSC, any compromise or damage to the functionality of the MSC stromal layer caused by conditioning regimens is likely to have far-reaching compromise to the haematopoietic compartment.

A literature search showed very limited data about the fate of these stromal cells after chemotherapy. The main fate *in vivo* is that these stromal cells survive and within the patient remain of patient origin thereby supporting the notion that they have the capacity to remain and transfer toxic signals to the incoming donor cells (Spyridonidis *et al.,* 2005; Bartsch *et al.,* 2009). However, these *in vivo* primary cells come from different patients, which would be difficult to obtain and would have inter-individual differences. These patients would have had combination therapy, which would make it difficult to determine if certain drugs were more important than others. In addition, treated primary cells have limited lifespan so would be limited for testing. Using HS-5 cells negated these problems and allowed for better reproducibility as well as ability to expose to single drugs at a time.

Using increasing doses of different chemotherapeutic agents, this study demonstrated that these drugs can induce cytotoxicity in the stromal cells however the stromal cells remained viable.

These findings are consistent with published reports that MSC are susceptible to chemotherapy-induced damage *in vitro* (Oliveira *et al.,* 2014; Nicolay *et al.,* 2016). Depending on the drug involved, anti-proliferative effects of the drugs on the stromal cells were either intermittent or sustained after 3 days. Although drug-resistant cells are able to survive and proliferate more than other cells, it is believed that cells capable of dividing over a long period of time are more likely to accumulate mutations leading to further neoplasia (Perumal *et al.,* 2017). The choice of chemotherapeutic agents used in this study is based on previous reports that alkylating agents and topoisomerase inhibitors are involved in the pathogenesis of TRM (Bhatia, 2013; McNerney *et al.,* 2017). Since these drugs have DNA-damaging capabilities, it can be inferred that these drugs might also be involved in DCL. In support of this theory, this research demonstrated that the clinically relevant doses of these drugs could induce variable bystander effects such as increased proliferation, cytotoxicity and genotoxicity. This suggests that the treated stromal cells are capable of releasing toxic signals within the BM microenvironment that may be taken up by incoming donor cells to exert bystander effects in these donor cells. However, it is noteworthy that the dosing used in this study is not reflective of the current status of chemotherapy treatment. Chemotherapy is usually fractionated and since the data in this study show that chemotherapeutic effects on stromal cells vary depending on the drug and dose given, this needs to be taken into consideration.

Nevertheless, the bystander cells exhibited an overall maintenance of good cell viability in contrast to the genotoxic events in the bystander cells. It has been previously suggested that presence of genotoxic effects along with a reduction in cell death may lead to the development of *de novo* primary malignancies (Swift and Golsteyn, 2014). This is supported by findings in literature that show that although genotoxic exposure causes genomic instability in cells, cells still proliferate and resist cell death thus suggesting mitosis entry as a major cellular response to damaged DNA (Kubara *et al.,* 2012; Blank *et al.,* 2015). Increased rate of cellular proliferation and resistance to cell death are hallmarks of cancer (Perumal *et al.,* 2017). This corresponds to recent reports in radiation studies, which revealed that low intensity conditioning regimen correlates with an increase in the incidence of DCL (Gonzalez *et al.,* 2018). Therefore, the evidence shown here that stromal cells can attempt to detoxify a drug-induced attack, and in doing so send toxic

signals to the neighbouring cells suggest that this may lead to the accumulation of genomic damage in the bystander cells over time, thus leading to the development of *de novo* primary malignancies.

Since the drug-treated HS-5 cells were separated from the bystander TK6 cells by a culture insert in co-culture, the over-arching theory suggests that soluble factors may play a role in mediating CIBE in bystander cells. In support of this theory, this research also demonstrated that exposure of the bystander TK6 cells to the CM of drug-treated HS-5 cells was also enough for these recipient cells to develop bystander effects. Therefore, it can inferred that CIBE may be as a result of drug elution into the CM by HS-5 cells, soluble factors released by HS-5 cells following chemotherapy into the extracellular environment or a combination of both. This is further supported by the findings that MSC express ATP-binding cassette (ABC) transmembrane pumps, multidrug resistance-associated protein (MRP) and breast cancer resistance protein (BCRP) but not P-glycoprotein (P-gp), which have been previously suggested as a general mechanism to expel anti-cancer drugs (Chen *et al.,* 2014; Bosco *et al.,* 2015; Perez *et al.,* 2019). Several chemotherapeutic agents used in pre-transplant conditioning are susceptible to ABC transporter-mediated efflux such as topoisomerase inhibitors, including etoposide and mitoxantrone, and DNA-damaging anthracyclines (Moitra, 2015; Cho and Kim, 2020). This may explain why mitoxantrone propagated more genotoxic bystander signals in this study.

Previously, bystander studies were based on radiation therapy thus RIBE have been well described with two categorized mechanisms: induction of soluble factors and gap-junction mediated cellular communication (Mothersill and Seymour, 2015; Klammer *et al.,* 2015). Therefore, the possible role of soluble factors in CIBE was determined. The soluble factors released into the extracellular milieu by treated HS-5 cells could be EVs, nucleic acids including miRNAs, metabolites, lipids, cytokines, chemokines, proteins including growth factors and hormones. This suggests that there may be a mulfactorial mechanism for the bystander effects seen in TK6 cells. The soluble factors and/or eluted drugs may act as extrinsic factors, which upon uptake by the bystander cells may lead to alteration in the regulation of bystander cell cycle in response to DNA damage. The results in this study revealed that exposure of bystander TK6 cells

to EVs isolated from treated HS-5 cells did not cause cell cycle arrest in TK6 cells despite the formation of aneuploidy in these cells. Aneuploidy is associated with significant cellular stress hence this infers that these EVs contain molecules that have the capacity to induce significant stress that may have detrimental effects in the bystander TK6 cells long term. This is supported by the findings in this study, which illustrated a reduction in cell numbers along with an accumulation of genotoxic events in TK6 cells following exposure to the EVs-derived from drug-treated HS-5 cells. However, these EVs-derived from drug-treated HS-5 cells also protected TK6 cells from mitoxantrone-induced genotoxic and cytotoxic effects. Nevertheless, aneuploidy may depend on the cell type, cellular microenviroment and immune system of the patient (Ben-David and Amon, 2019). This further supports the idea that EVs contain molecules, which may act as extrinsic factors that interplay with varied intrinsic factors in the bystander cells to exert these CIBE. Thus, this infers that things intrinsic to one person such as DNA repair mechanisms might predispose them to getting CIBE. These findings correspond to the fact that not every recipient of HSCT develops DCL hence DCL is a unique condition that can develop regardless of the pre-transplant conditioning. It has also been suggested that pathogenesis of DCL could be a multifactorial process involving extrinsic and intrinsic factors (Flynn and Kaufman, 2006).

Furthermore, the data here also showed that these EVs are taken up by the bystander cells by fusion of the membranes of the cell and vesicle and upon uptake, release their contents into the bystander cells to elicit biomolecular changes. This further support the notion that soluble factors play a vital role in mediating CIBE in bystander. The data suggest that these EVs may be a means of intercellular communication within the BM microenvironment whereby the vesicles act as messengers that convey toxic signals onto the incoming donor cells. These toxic signals could be nucleic acids, proteins or metabolites, which are enclosed within the EVs. The scientific and clinical field of EVs have been rapidly expanding over the past 15 years and there is evidence in literature that chemotherapeutic agents, nucleic acids and proteins can be loaded or incorporated into EVs to elicit therapeutic effects in the bystander cells (Pessina *et al.,* 2013; Pascucci *et al.,* 2014; Wu *et al.,* 2020). It has also been shown that EVs especially those derived from MSC have therapeutic effects in treating a variety of common and refractory diseases such as autoimmune disease, spinal cord injury, diabetes and cardiac repair (Zhang *et al.,* 2012; Wu *et*

al., 2020). Therefore, these EVs may have broad clinical application prospects as diagnostic and prognostic markers for CIBE due to their unique physiological and biochemical characteristics. In addition, specific and sensitive labelling of EVs with membrane and RNA fluorescent dyes as seen in this study may help in real-time tracking and imaging diagnosis of CIBE. Furthermore, inhibitors of EV secretion and uptake such as GW4869 and heparin respectively may also be of therapeutic value, as both chemicals seem to attenuate the propagation of CIBE signals to the bystander cells in this study. Therefore, inorder to develop and optimise EV-based diagnosis and therapy, it is critical to timely and dynamically monitor and understand the fate of these EVs and their CIBE capabilities *in vivo*.

Since molecules can be incorporated into EVs, the miRNA cargo of these EVs was determined. miRNAs are capable of inducing epigenetic changes in the cells via the regulation of genes post-transcription. Results in this study illustrated that miRNAs can extend their biological functions to outside of the cell and mediate CIBE thus inferring that these nucleic acids are protected from degradation by EVs in the extracellular milieu whilst traveling to the bystander cells. These also suggest that the miRNA cargo in the chemotherapy-induced EVs may act as extrinsic factors that interplay with varied intrinsic factors in the bystander cells to exert these CIBE. Nevertheless, it is important to mention that the miRNAs found in the EVs and CM were in low amounts. In addition, the results showed that miRNAs are differentially expressed in the treated HS-5 cells and the bystander TK6 cells following co-culture. This is similar to a previous report that illustrated that miRNAs are also differentially expressed in irradiated and non-irradiated cells (Chaudhury and Omaruddin, 2012). These suggest that the involvement of miRNA modulation in CIBE could be responsible for large-scale gene expression in the bystander cells leading to induction of non-targeted cellular effects. In support of this data, the predicted genes of these miRNAs were found to control different signalling pathways as well as pathways related to cell division and survival thus highlighting the importance of the decision between cell survival and cell death. Normal functional cell signalling pathway entails a series of biomolecular changes involving a group of molecules, which are induced when an extracellular messenger binds to the cell surface receptor in order to control a cell function. Normal functional cell signalling is vital to the role of MSC in protecting the HSC. Nevertheless, these miRNAs have all been associated with

the development and progression of cancer where they could act as tumour suppressors and/or oncogenic miRNAs (Fang *et al.,* 2017; Yang *et al.,* 2017; Ruan and Qian, 2019; Iacona and Lutz, 2019). Therefore, it could be inferred that these miRNAs could act as non-invasive biomarkers for early detection of CIBE that may lead to the development of *de novo* primary malignancies inorder to monitor response to treatment and guide prognosis post-HSCT.

The main aim of HSCT is to reconstitute haematopoiesis in the patient's BM after removing the leukaemic cells with pre-transplant conditioning. As a result, patients are usually given a 'safe period' of 2-3 days to recover from the effects of pre-transplant conditioning before infusing the donor cells. However, the outcome of this study further suggests that CIBE signals from the stromal cells may persist within the BM microenvironment *in vivo* and these treatment-induced effects can be seen in the recipient cells after 5 days. Thus, this suggests that the 'safe period' may not be safe after all and the phenotype and functionality of the donor cells may alter upon transplantation due to signals from the microenvironment. This further reiterates that the soluble factors released into the extracellular milieu may play a vital role in the propagation of CIBE signals to the incoming donor cells. However, it is important to note that inter-individual differences in donor might play a role in cellular response to CIBE.

Cellular response to DNA damage is often via a series of communication signalling pathways that promote both cell survival and cell death. The decision between cell survival and cell death is associated with development and progression of cancer. This would infer that the response of the bystander cells to the transferred treatment signals from the HS-5 cells could be to either repair (as seen in chlorambucil, carmustine and etoposide) or die (as seen in mitoxantrone). However, cell viability remained high regardless of the chemotherapeutic agent thus suggesting that the development of mutated clones in these cells or their progenies could likely be through uncontrolled proliferation. This further suggests that clonal expansion of these cells may lead to genomic instability that will be biologically relevant, as the time points used in this study may not tell the whole story *in vivo.* Nevertheless, this outcome illustrates the possible importance of pre-transplant conditioning in the development of *de novo* primary malignancies in contrast to a

previous report that refuted its importance as donor cells are not exposed to pre-transplant conditioning (Danylesko and Shimoni, 2018).

Summarily, the data presented in this thesis favours the theory that chemotherapeutic agents used in pre-transplant conditioning can propagate CIBE to the neighbouring cells. These CIBE could be mutagenic or anti-/pro-proliferative effects, which may explain the fate of donor cells within a HSCT setting. Although stromal cells may or may not recover from the effects of chemotherapy, it appears that chemotherapy causes a long-term disruption in the functionality of the BM microenvironment. Therefore, this may cause an alteration in the cargo of these chemotherapy-induced EVs released by stromal cells thus inferring that miRNAs enclosed in these EVs may play a role in CIBE. However, it is unlikely to be the sole mechanism involved as the contents of EVs are heterogeneous and may interact with other signalling molecules like cytokines to control multiple cellular pathways in the bystander cells. Additionally, it is possible that the mechanisms of CIBE vary depending on the drug involved. This study has also shed some light on the ability of stromal cells to extend genotoxic events beyond direct exposure however, the signalling pathways involved in non-directed cellular genotoxicity is not well understood hence why more complex multicellular or 3D models are likely to be more informative in the future.

6.1 <u>Limitations</u>

First, this study was limited by the use of an *in vitro* co-culture system that may not account for all the events that occur *in vivo* in response to chemotherapy. The two cell compartments used in this study were not in contact with each other but separated with culture inserts in the *in vitro* co-culture system. Therefore, bystander effects seen in this study may be pronounced if the cells were in contact with each other since it has been shown that gap junctions are vital in the propagation of RIBE signals. In addition, the use of one BM stromal cell line and lymphoblast cell line may not be enough to fully explain or understand CIBE. Instead, a future study may include the use of different stromal cell lines as well as primary MSC samples to compare the effects of these chemotherapeutic agents on these cells. Primary MSC samples would also help to explore

inter-individual differences that may influence CIBE. These may help explain why some individuals develop DCL after HSCT whilst others do not.

Second, current approaches to genotoxicity testing focuses on the measurement of the direct exposure of acute doses of toxic agents *in vitro* however; the development of genotoxic events in the bystander cells questions the validity of this approach (OECD, 2012). MN assay used in assessing genotoxicity in this study is a subjective assay as it entails visual and manual counting of MN thus this may lead to false positive or false negative results. Thus, there is need to develop a high thoroughput assay to eliminate these confounding effects. Currently, there is an equipment known as Metafer that is available for this however, it could not be purchased due to financial constriants.

Third, chemotherapy-induced EVs can also enhance our understanding of CIBE. The future in medical research in terms of prognosis or diagnosis of *de novo* primary malignancies like DCL could rely on EVs. The surface membrane proteins found on sEVs such as CD9, CD63, CD81, ALIX and TSG101 could not be identified by western blotting in this study. In addition, the nanosize of EVs makes it difficult to label these vesicles. One of the most common available strategies include use of lipophilic dyes such as the ones used in this study to label the bystander TK6 cells thus suggesting that these dyes are capable of labelling other cellular components, serum and proteins thereby generating false positive signals (Takov *et al.,* 2017; Mondal *et al.,* 2019). These lipophilic dyes also cause an increase in EV size (Deghani *et al.,* 2019). Therefore, the labelling experiments should have been carefully controlled with relevant controls such as staining PBS without EVs in order to make the data more robust. Thus, there are still many questions that need to be answered in EVs studies ranging from isolation, characterisation to downstream analysis of these EVs. Although this study focused on sEVs, EVs are heterogeneous and can overlap in terms of cargo thus different EV subtypes may have influenced the results found in this study. Overall, this study has laid the foundation for more work to be done in understanding the mechanism of CIBE and needs modification. Direct targeting of EVs that act as biomarkers may enhance precision medicine and thence overall patient survival.

6.2 Future Work

CIBE may be a complicated process that is probably influenced by multiple signalling molecules such as EVs, nucleic acid, proteins, metabolites and cytokines. The secretome of stromal cells following chemotherapy should also be investigated for cytokines and other signalling molecules. Currently, proteomic analysis of the CM from treated stromal cells by mass spectrometry is ongoing within our laboratory to identify the complete complement of proteins that may be involved in CIBE (Sultan Al-Malki, personal communication). However, there is also need to perform metabolomics to understand the complete set of metabolites that may be released into the CM by stromal cells following exposure to drugs as proteomics and microarray analysis may not be sufficient to fully understand the role of soluble factors in CIBE. In addition, next generation sequencing of the CM from the treated stromal cells should also be performed in order to identify nucleic acids that may have been neglected or omitted in this study.

Furthermore, the contents of the EVs also need to be explored as only miRNA was assessed in this study. According to Wu *et al.,* (2020), EVs contain mRNA, DNA, proteins, long noncoding RNA (lncRNA) and other short noncoding RNA molecules. Thus, EVs released by stromal cells may contain these components and need to be explored. Therefore, next generation sequencing, proteomics and metabolomics using EV samples may provide more information to understand the contents of the EVs and their possible roles in CIBE. In addition, the miRNAs identified could also be knocked down using antagomirs to ascertain if these will ameliorate or enhance CIBE in bystander cells.

Mitoxantrone produced more bystander cytotoxic and genotoxic effects in this study however this study could not ascertain if alkylating agents or topoisomerase inhibitors play major roles in CIBE as the drugs had different bystander outcomes hence this area of study should be further explored. Although the doses of these drugs used in this study are clinically relevant, it is noteworthy that different mechanisms are involved in the efficacy of a drug *in vivo,* which may not be possible to reconstruct *in vitro.* For example, drug safety and efficacy vary amongst patients, and are dependent on clinical and molecular factors hence prescribing the optimal dose

for a drug for each patient is often a problem for physicians. Therefore, this raises an important issue that these bystander effects may be under-measured and under-represented in standard *in vitro* tests where a single cell source is considered. This also raises the question that there may be inter-individual differences in the patients that could make them susceptible to the risk of CIBE. Therefore, there is need to modify the monocultures used in genotoxicity testing thus reconsidering the drug dosage and treatment duration. Hence why more complex multicellular or 3D models are likely to provide a better understanding of the risks posed by these toxic agents *in vivo* in the future.

Furthermore, the *in vitro* bystander model used in this study needs to be modified with cells grown in a hypoxic environment to mimic the hypoxic nature of BM microenvironment (Cheng *et al.,* 2018). In addition, collecting and isolating stromal cell samples from leukaemia patients should be considered in order to understand the full scope of CIBE signalling pathways *in vivo.* Using patient samples will also help us understand the duration of CIBE and thence ways we can modulate pre-transplant conditioning as it has been shown in this study that the safe period of 5 days after pre-transplant conditioning is not safe after all. Alternatively, hTERT immortalised cell lines, which have been shown to possess karyotypic, morphologic and phenotypic similarities with primary MSC can also be used as they have the advantage of an extended lifespan (Lee *et al.,* 2004). Since the bystander endpoints in this study varied from increased proliferation, genotoxicity and cell death, primary MSC from healthy and leukaemia patients, hTERT immortalised cell lines and 3D multicellular models could be combined to compare bystander endpoints in these cells. This will help ascertain a standard endpoint for CIBE to aid uniformity of data and subsequent comparative studies.

Lastly, there is need to produce standardized techniques that will enable the isolation and quantification of pure EVs. In addition, the mechanism by which chemotherapy alters the contents of the heterogeneous EV population is not understoodand and should be explored. Nevertheless, the overall effects of chemotherapy-induced EVs should be further investigated as they may play important roles in tipping the pro- and anti-tumorigenic balance in the BM microenvironment.

7.0 References

Abo-Aziza, F.A.-A.M. and Zaki, A.E.-K.A. (2016) The impact of confluence on BMMSC proliferation and osteogenic differentiation. *International Journal of Hematology-Oncology and Stem Cell Research*. **11** (2), pp. 121–132.

Ach, R.A., Wang, H. and Curry, B. (2008) Measuring microRNAs: Comparisons of microarray and quantitative PCR measurements, and of different total RNA prep methods. *BMC Biotechnology* [online]. **8**. Available from: http://www.biomedcentral.com/1472-6750/8/69doi:10.1186/1472-6750-8-69 [Accessed 5 September 2020].

Al-Mayah, A., Bright, S., Chapman, K., Irons, S., Luo, P., Carter, D., Goodwin, E. and Kadhim, M. (2015) The non-targeted effects of radiation are perpetuated by exosomes. *Mutation Research - Fundamental and Molecular Mechanisms of Mutagenesis*. **772** pp. 38–45. doi:10.1016/j.mrfmmm.2014.12.007.

Alexandre, J., Hu, Y., Lu, W., Pelicano, H. and Huang, P. (2007) Novel Action of Paclitaxel against Cancer Cells: Bystander Effect Mediated by Reactive Oxygen Species. *Cancer Res* [online]. **67** (8), pp. 3512–3529. Available from: www.aacrjournals.orgdoi:10.1158/0008-5472.CAN-06-3914 [Accessed 11 December 2019].

Alonso, S., Su, M., Jones, J.W., Ganguly, S., Kane, M.A., Jones, R.J. and Ghiaur, G. (no date) Human bone marrow niche chemoprotection mediated by cytochrome p450 enzymes *Oncotarget* [online]. **6** (17). Available from: www.impactjournals.com/oncotarget/ [Accessed 28 August 2020].

Ann, J., Byl, W., Cline, S.D., Utsugi, T., Kobunai, T., Yamada, Y. and Osheroff, N. (2001) *DNA Topoisomerase II as the Target for the Anticancer Drug TOP-53: Mechanistic Basis for Drug Action*. Available from: https://pubs.acs.org/sharingguidelinesdoi:10.1021/bi0021838 [Accessed 22 November 2019].

Anon (no date) *FAB M7: Acute Megakaryoblastic Leukemia-Beyond Morphology* [online]. Available from: https://annals.org/

Anon (1996) Bcl-2 and clonogenic survival in human tumour cells.

Anon (no date) *FAB M7: Acute Megakaryoblastic Leukemia-Beyond Morphology* [online]. Available from: https://annals.org/.

Appelbaum, F.R., Gundacker, H., Head, D.R., Slovak, M.L., Willman, C.L., Godwin, J.E., Anderson, J.E. and Petersdorf, S.H. (2006) Age and acute myeloid leukemia. *Blood*. **107** (9), pp. 3481–3485. doi:10.1182/blood-2005-09-3724.

Arber, D.A., Orazi, A., Hasserjian, R., Thiele, J., Borowitz, M.J., Le Beau, M.M., Bloomfield, C.D., Cazzola, M. and Vardiman, J.W. (2016) The 2016 revision to the World Health Organization classification of myeloid neoplasms and acute leukemia *Blood* [online]. **127** (20), pp. 2391–2405. Available from: https://ashpublications.org/blood/article-pdf/127/20/2391/1017805/2391.pdfdoi:10.1182/blood-2016-03-643544

Ariyoshi, K., Miura, T., Kasai, K., Fujishima, Y., Nakata, A. and Yoshida, M. (2019) Radiation-Induced Bystander Effect is Mediated by Mitochondrial DNA in Exosome-Like Vesicles. *Scientific Reports* [online]. **9** (1). Available from: https://doi.org/10.1038/s41598-019-45669-zdoi:10.1038/s41598-019-45669-z [Accessed 16 July 2020].

Arora, M. (2013) Cell Culture Media: A Review. *Materials and Methods*. **3**. doi:10.13070/mm.en.3.175.

Arora, S., Heyza, J.R., Chalfin, E.C., Ruch, R.J. and Patrick, S.M. (2018) Gap junction intercellular communication positively regulates cisplatin toxicity by inducing dna damage through bystander signaling. *Cancers* [online]. **10** (10). Available from: www.mdpi.com/journal/cancersdoi:10.3390/cancers10100368 [Accessed 11 December 2019].

Asada, N. (2018) Regulation of malignant hematopoiesis by bone marrow microenvironment *Frontiers in Oncology* 8 (APR). doi:10.3389/fonc.2018.00119.

Asur, R.S., Thomas, R.A. and Tucker, J.D. (2009) Chemical induction of the bystander effect in normal human lymphoblastoid cells. *Mutation Research - Genetic Toxicology and Environmental Mutagenesis*. **676** (1), pp. 11–16. doi:10.1016/j.mrgentox.2009.02.012

Aswad, H., Jalabert, A. and Rome, S. (2016) Depleting extracellular vesicles from fetal bovine serum alters proliferation and differentiation of skeletal muscle cells in vitro. *BMC Biotechnology*. **16** (1). doi:10.1186/s12896-016-0262-0.

Atai, N.A., Balaj, L., Van Veen, H., Breakefield, X.O., Jarzyna, P.A., Van Noorden, C.J.F., Skog, J. and Maguire, C.A. (2013) Heparin blocks transfer of extracellular vesicles between donor and recipient cells. *Journal of Neuro-Oncology*. **115** (3), pp. 343–351. doi:10.1007/s11060-013-1235-y.

Auber, M., Fröhlich, D., Drechsel, O., Karaulanov, E. and Krämer-Albers, E.M. (2019) Serum-free media supplements carry miRNAs that co-purify with extracellular vesicles. *Journal of Extracellular Vesicles*. **8** (1). doi:10.1080/20013078.2019.1656042.

Aubertin, K., Silva, A.K.A., Luciani, N., Espinosa, A., Djemat, A., Charue, D., Gallet, F., Blanc-Brude, O. and Wilhelm, C. (2016) Massive release of extracellular vesicles from cancer cells after photodynamic treatment or chemotherapy. *Nature Publishing Group* [online]. Available from: www.nature.com/scientificreportsdoi:10.1038/srep35376

Awan, F.M., Naz, A., Obaid, A., Ikram, A., Ali, A., Ahmad, J., Naveed, A.K. and Janjua, H.A. (2017) MicroRNA pharmacogenomics based integrated model of miR-17-92 cluster in sorafenib resistant HCC cells reveals a strategy to forestall drug resistance. *Scientific Reports* [online]. **7** (1), pp. 1–21. Available from: http://dx.doi.org/10.1038/s41598-017-11943-1doi:10.1038/s41598-017-11943-1

Azarova, A.M., Lisa Lyu, Y., Lin, C.-P., Tsai, Y.-C., Yiu-Nam Lau, J., Wang, J.C. and Liu, L.F. (2007) *Sciences of the USA 11014-11019 PNAS* [online] 104 (26). Available from: www.pnas.orgcgidoi10.1073pnas.0704002104 [Accessed 22 November 2019].

Baccarani, M., Saglio, G., Goldman, J., Hochhaus, A., Simonsson, B., Appelbaum, F., Apperley, J., Cervantes, F., Cortes, J., Deininger, M., Gratwohl, A., Guilhot, F., Horowitz, M., Hughes, T., et al. (2006) Evolving concepts in the management of chronic myeloid leukemia: Recommendations from an expert panel on behalf of the European Leukemia Network. *Blood* [online]. **108** (6) p.pp. 1809–1820. Available from: https://ashpublications.org/blood/article-pdf/108/6/1809/914134/zh801806001809.pdfdoi:10.1182/blood-2006-02-005686

Baccarani, M., Cortes, J., Pane, F., Niederwieser, D., Saglio, G., Apperley, J., Cervantes, F., Deininger, M., Gratwohl, A., Guilhot, F., Hochhaus, A., Horowitz, M., Hughes, T., Kantarjian, H., et al. (2009) Chronic myeloid leukemia: An update of concepts and management recommendations of European LeukemiaNet *Journal of Clinical Oncology* [online] **27** (35), pp. 6041–6051. Available from: www.jco.org.doi:10.1200/JCO.2009.25.0779

Bai, H., Weng, Y., Bai, S., Jiang, Y., Li, B., He, F., Zhang, R., Yan, S., Deng, F., Wang, J. and Shi, Q. (2014) CCL5 secreted from bone marrow stromal cells stimulates the migration and invasion of Huh7 hepatocellular carcinoma cells via the PI3K-Akt pathway. *International Journal of Oncology*. **45** (1), pp. 333–343. doi:10.3892/ijo.2014.2421.

Bain, B.J. (2017). *Leukaemia diagnosis*. John Wiley & Sons.

Baixauli, F., López-Otín, C. and Mittelbrunn, M. (2014) Exosomes and autophagy: Coordinated mechanisms for the maintenance of cellular fitness. *Frontiers in Immunology* [online]. **5** (AUG). Available from: www.frontiersin.orgdoi:10.3389/fimmu.2014.00403

Balakrishnan, I., Yang, X., Brown, J., Ramakrishnan, A., Torok-Storb, B., Kabos, P., Hesselberth, J.R. and Pillai, M.M. (2014) Genome-Wide Analysis of miRNA-mRNA Interactions in Marrow Stromal Cells. *Stem Cells* [online]. **32** (3), pp. 662–673. Available from: www.StemCells.comdoi:10.1002/stem.1531

Balaj, L., Atai, N.A., Chen, W., Mu, D., Tannous, B.A., Breakefield, X.O., Skog, J. and Maguire, C.A. (2015) Heparin affinity purification of extracellular vesicles. *Nature Publishing Group* [online]. Available from: www.nature.com/scientificreportsdoi:10.1038/srep10266 [Accessed 23 June 2020].

Ball, L.M., Bernardo, M.E., Roelofs, H., Lankester, A., Cometa, A., Maarten Egeler, R., Locatelli, F. and Fibbe, W.E. (2007) *Cotransplantation of ex vivo-expanded mesenchymal stem cells accelerates lymphocyte recovery and may reduce the risk of graft failure in haploidentical hematopoietic stem-cell transplantation*. doi:10.1182/blood-2007-04-087056.

Bandari, S.K., Purushothaman, A., Ramani, V.C., Brinkley, G.J., Chandrashekar, D.S., Varambally, S., Mobley, J.A., Zhang, Y., Brown, E.E., Vlodavsky, I. and Sanderson, R.D. (2018) Chemotherapy induces secretion of exosomes loaded with heparanase that degrades extracellular matrix and impacts tumor and host cell behavior HHS Public Access. *Matrix Biol*. 35294 pp. 104–118. doi:10.1016/j.matbio.2017.09.001.

Baranyai, T., Herczeg, K., Onódi, Z., Voszka, I., Módos, K., Marton, N., Nagy, G., Mäger, I., Wood, M.J., Andaloussi, S. El, Pálinkás, Z., Kumar, V., Nagy, P., Kittel, Á., et al. (2015) *Isolation of Exosomes from Blood Plasma: Qualitative and Quantitative Comparison of Ultracentrifugation and Size Exclusion Chromatography Methods*. doi:10.1371/journal.pone.0145686.

Barnouin, K., Leier, I., Jedlitschky, G., Pourtier-Manzanedo, A., König, J., Lehmann, W.D. and Keppler, D. (1998) Multidrug resistance protein-mediated transport of chlorambucil and melphalan conjugated to glutathione. *British Journal of Cancer*. **77** (2), pp. 201–209. doi:10.1038/bjc.1998.34.

Bartel, D.P. (2009) MicroRNAs: Target Recognition and Regulatory Functions *Cell*. **136** (2) p.pp. 215–233. doi:10.1016/j.cell.2009.01.002.

Bartenhagen, C., Fischer, U., Korn, K., Pfister, S.M., Gombert, M., Chen, C., Okpanyi, V., Hauer, J., Rinaldi, A., Bourquin, J.P., Eckert, C., Hu, J., Ensser, A., Dugas, M., et al. (2017) Infection as a cause

of childhood leukemia: Virus detection employing whole genome sequencing *Haematologica.* **102** (5) p.pp. e179–e183. doi:10.3324/haematol.2016.155382.

Bartke, N. and Hannun, Y.A. (2008) *Bioactive sphingolipids: metabolism and function*. Available from: http://www.jlr.orgdoi:10.1194/jlr.R800080-JLR200 [Accessed 24 June 2020].

Bartsch, K., Al-Ali, H., Reinhardt, A., Franke, C., Hudecek, M., Kamprad, M., Tschiedel, S., Cross, M., Niederweiser, D., Gentilini, C (2009) Mesenchymal stem cells remain host-derived independent of the source of the stem-cell graft and conditioning regimen used. *Transplantation.* **87 (**2); 217-221.

Beer, L., Zimmermann, M., Mitterbauer, A., Ellinger, A., Gruber, F., Narzt, M.S., Zellner, M., Gyöngyösi, M., Madlener, S., Simader, E., Gabriel, C., Mildner, M. and Ankersmit, H.J. (2015) Analysis of the secretome of apoptotic peripheral blood mononuclear cells: Impact of released proteins and exosomes for tissue regeneration. *Scientific Reports* [online]. **5.** Available from: www.nature.com/scientificreportsdoi:10.1038/srep16662

Bellagamba, B.C., Abreu, B.R.R. De, Grivicich, I., Markarian, C.F., Chem, E., Camassola, M., Nardil, N.B. and Dihl, R.R. (2016) Human mesenchymal stem cells are resistant to cytotoxic and genotoxic effects of cisplatin in vitro. *Genetics and Molecular Biology*. **39** (1), pp. 129–134. doi:10.1590/1678-4685-GMB-2015-0057.

Ben-David, U. and Amon, A. Context is everything: aneuploidy in cancer. *Nature Reviews Genetics.* **21,** 44–62 (2020). https://doi.org/10.1038/s41576-019-0171-x [Accessed 18 December 2020].

Benavides-Castellanos, M.P., Garzón-Orjuela, N. and Linero, I. (2020) Effectiveness of mesenchymal stem cell-conditioned medium in bone regeneration in animal and human models: a systematic review and meta-analysis. *Cell Regeneration*. 9 (1), pp. 1–22. doi:10.1186/s13619-020-00047-3.

Bennett, J.M., Catovsky, D., Daniel, M. -T, Flandrin, G., Galton, D.A.G., Gralnick, H.R. and Sultan, C. (1976) Proposals for the Classification of the Acute Leukaemias French-American-British (FAB) Co-operative Group. *British Journal of Haematology*. **33** (4), pp. 451–458. doi:10.1111/j.1365-2141.1976.tb03563.x.

Bhatia, S. (2013) Therapy-related myelodysplasia and acute myeloid leukemia. *Semin Oncol*. 40 (6). doi:10.1053/j.seminoncol.2013.09.013.

Bian, X., Yang, Z., Feng, H., Sun, H. and Liu, Y. (2017) A Combination of Species Identification and STR Profiling Identifies Cross-contaminated Cells from 482 Human Tumor Cell Lines. *Scientific Reports* [online]. **7** (1). Available from: www.nature.com/scientificreportsdoi:10.1038/s41598-017-09660-w [Accessed 17 July 2020].

Biemmi, V., Milano, G., Ciullo, A., Cervio, E., Burrello, J., Cas, M.D., Paroni, R., Tallone, T., Moccetti, T., Pedrazzini, G., Longnus, S., Vassalli, G. and Barile, L. (2020) Inflammatory extracellular vesicles prompt heart dysfunction via TRL4-dependent NF-κB activation. *Theranostics* [online]. **10** (6), pp. 2773–2790. Available from: http://www.thno.org//creativecommons.org/licenses/by/4.0/doi:10.7150/thno.39072 [Accessed 24 June 2020].

Binet, J.L., Leporrier, M., DIghiero, G., Charron, D., Vaugier, G., Merle Beral, H., Natali, J.C., Raphael, M., Nizet, B. and J.Y.F. (1977) Clinical staging system for chronic lymphocytic leukemia. *Cancer*. **40** pp. 855–864. doi:10.1002/1097-0142(197708)40:2<855::AID-CNCR2820400239>3.0.CO;2-1.

Bithell, J.F., Murphy, M.F.G., Stiller, C.A., Toumpakari, E., Vincent, T. and Wakeford, R. (2013) Leukaemia in young children in the vicinity of British nuclear power plants: A case-control study. *British Journal of Cancer* [online]. **109** (11), pp. 2880–2885. Available from: www.bjcancer.comdoi:10.1038/bjc.2013.560

Björk, J., Albin, M., Mauritzson, N., Strömberg, U., Johansson, B. and Hagmar, L. (2001) Smoking and acute myeloid leukemia: Associations with morphology and karyotypic patterns and

evaluation of dose-response relations. *Leukemia Research*. **25** (10), pp. 865–872. doi:10.1016/S0145-2126(01)00048-0.

Blank, H. M., Sheltzer, J. M., Meehl, C. M., & Amon, A. (2015). Mitotic entry in the presence of DNA damage is a widespread property of aneuploidy in yeast. *Molecular biology of the cell*. **26** (8), 1440–1451. https://doi.org/10.1091/mbc.E14-10-1442

Bliss, S.A., Sinha, G., Sandiford, O.A., Williams, L.M., Engelberth, D.J., Guiro, K., Isenalumhe, L.L., Greco, S.J., Ayer, S., Bryan, M., Kumar, R., Ponzio, N.M. and Rameshwar, P. (2016) *Therapeutics, Targets, and Chemical Biology Mesenchymal Stem Cell-Derived Exosomes Stimulate Cycling Quiescence and Early Breast Cancer Dormancy in Bone Marrow*. Available from: http://cancerres.aacrjournals.org/doi:10.1158/0008-5472.CAN-16-1092 [Accessed 25 June 2020].

Bobadilla-Morales, L., Pimentel-Gutiérrez, H.J., Gallegos-Castorena, S., Paniagua-Padilla, J.A., Ortega-De-la-torre, C., Sánchez-Zubieta, F., Silva-Cruz, R., Corona-Rivera, J.R., Zepeda-Moreno, A., González-Ramella, O. and Corona-Rivera, A. (2015) Pediatric donor cell leukemia after allogeneic hematopoietic stem cell transplantation in AML patient from related donor. *Molecular Cytogenetics*. **8** (1). doi:10.1186/s13039-014-0105-4.

Bogdanowicz, D.R. and Lu, H.H. (2013) Studying cell-cell communication in co-culture. *Biotechnology Journal*. **8** (4), pp. 395–396. doi:10.1002/biot.201300054.

Böing, A.N., van der Pol, E., Grootemaat, A.E., Coumans, F.A.W., Sturk, A. and Nieuwland, R. (2014) Single-step isolation of extracellular vesicles by size-exclusion chromatography. *Journal of Extracellular Vesicles* [online]. **3** (1). Available from: http://dx.doi.org/10.3402/jev.v3.23430doi:10.3402/jev.v3.23430 [Accessed 15 June 2020].

Boland, M.P. (2000) Topoisomerase II is required for mitoxantrone to signal NFkB activation in HL60 cells. *Journal of Biological Chemistry* [online]. Available from: http://www.jbc.org/doi:10.1074/jbc.m003794200 [Accessed 23 November 2019].

Bonomi, A., Sordi, V., Dugnani, E., Ceserani, V., Dossena, M., Coccè, V., Cavicchini, L., Ciusani, E., Bondiolotti, G., Piovani, G., Pascucci, L., Sisto, F., Alessandri, G., Piemonti, L., et al. (2015) Gemcitabine-releasing mesenchymal stromal cells inhibit in vitro proliferation of human pancreatic carcinoma cells. *Cytotherapy*. **17** (12), pp. 1687–1695. doi:10.1016/j.jcyt.2015.09.005.

Bosco, D.B., Kenworthy, R., Zorio, D.A.R. and Sang, Q.-X.A. (2015) *Human Mesenchymal Stem Cells Are Resistant to Paclitaxel by Adopting a Non-Proliferative Fibroblastic State*. doi:10.1371/journal.pone.0128511.

Brassesco, M.S., Montaldi, A.P. and Sakamoto-Hojo, E.T. (2009) *Preferential induction of MLL (Mixed Lineage Leukemia) rearrangements in human lymphocyte cultures treated with etoposide* [online]. Available from: www.sbg.org.br [Accessed 28 November 2019].

Bryce, S.M., Bernacki, D.T., Bemis, J.C., Spellman, R.A., Engel, M.E., Schuler, M., Lorge, E., Heikkinen, P.T., Hemmann, U., Thybaud, V., Wilde, S., Queisser, N., Sutter, A., Zeller, A., et al. (2017) Interlaboratory evaluation of a multiplexed high information content in vitro genotoxicity assay. *Environmental and Molecular Mutagenesis* [online]. 58 (3), pp. 146–161. Available from: http://doi.wiley.com/10.1002/em.22083doi:10.1002/em.22083 [Accessed 9 September 2020].

Bryce, S.M., Bernacki, D.T., Smith-Roe, S.L., Witt, K.L., Bemis, J.C. and Dertinger, S.D. (2018) Investigating the Generalizability of the MultiFlow V R DNA Damage Assay and Several Companion Machine Learning Models With a Set of 103 Diverse Test Chemicals. Available from: https://doi.org/doi:10.1093/toxsci/kfx235 [Accessed 9 September 2020].

Bustin, S.A., Benes, V., Garson, J.A., Hellemans, J., Huggett, J., Kubista, M., Mueller, R., Nolan, T., Pfaffl, M.W., Shipley, G.L., Vandesompele, J. and Wittwer, C.T. (2009) The MIQE guidelines: Minimum information for publication of quantitative real-time PCR experiments. *Clinical Chemistry*. **55** (4), pp. 611–622. doi:10.1373/clinchem.2008.112797.

Cai, S., Shi, G.S., Cheng, H.Y., Zeng, Y.N., Li, G., Zhang, M., Song, M., Zhou, P.K., Tian, Y., Cui, F.M. and Chen, Q. (2017) Exosomal miR-7 mediates bystander autophagy in lung after focal brain

irradiation in mice. *International Journal of Biological Sciences*. **13** (10), pp. 1287–1296. doi:10.7150/ijbs.18890.

Cammarata, G., Augugliaro, L., Salemi, D., Agueli, C., Rosa, M. La, Dagnino, L., Civiletto, G., Messana, F., Marfia, A., Bica, M.G., Cascio, L., Floridia, P.M., Mineo, A.M., Russo, M., et al. (2010) Differential expression of specific microRNA and their targets in acute myeloid leukemia. *American Journal of Hematology* [online]. pp. NA-NA. Available from: http://doi.wiley.com/10.1002/ajh.21667doi:10.1002/ajh.21667 [Accessed 13 December 2019].

Canal, P., Attal, M., Chatelut, E., Guichard, S., Huguet, oise, Muller, C., Schlaifer, D., Laurent, G., Houin, G. and Bugat, R. (1993) Plasma and Cellular Pharmacokinetics of Mitoxantrone in High-Dose Chemotherapeutic Regimen for Refractory Lymphomas *CANCER RESEARCH* [online] 53. Available from: https://bloodcancerdiscov.aacrjournals.org [Accessed 28 August 2020].

Cancer Research UK (2016) Leukaemia statistics. Available from: https://www.cancerresearchuk.org/health-professional/cancer-statistics/statistics-by-cancer-type/leukaemia#heading-Zero [Accessed 29 December 2020].

Caplan, A.I. (1991) Mesenchymal Stem Cells. *Orthopaedic Research*. **9** pp. 641–650. doi:10.1016/0009-2614(70)87009-9.

Cárceles-Álvarez, A., Ortega-García, J.A., López-Hernández, F.A., Orozco-Llamas, M., Espinosa-López, B., Tobarra-Sánchez, E., Alvarez, L., Antonio Ortega García, J., Environmental Health, P. and Res Author manuscript, E. (2017) Spatial clustering of childhood leukaemia with the integration of the Paediatric Environmental History Human subjects' ethics review: HHS Public Access Author manuscript. *Environ Res*. **156** pp. 605–612. doi:10.1016/j.envres.2017.04.019.

Carnino, J.M., Lee, H. and Jin, Y. (2019) Isolation and characterization of extracellular vesicles from Broncho-alveolar lavage fluid: a review and comparison of different methods. *Respiratory research* [online]. **20** (1), pp. 240. Available from: https://doi.org/10.1186/s12931-019-1210-zdoi:10.1186/s12931-019-1210-z [Accessed 15 June 2020].

Carrancio, S., Blanco, B., Romo, C., Muntion, S., Lopez-Holgado, N., Blanco, J.F., Briñon, J.G., San Miguel, J.F., Sanchez-Guijo, F.M. and del Cañizo, M.C. (2011) Bone marrow mesenchymal stem cells for improving hematopoietic function: an in vitro and in vivo model. Part 2: Effect on bone marrow microenvironment. *PLoS One*. **6** (10):e26241. doi: 10.1371/journal.pone.0026241.

Carroll, B.L., Pulkoski-Gross, M.J., Hannun, Y.A. and Obeid, L.M. (2016) CHK1 regulates NF-κB signaling upon DNA damage in p53-deficient cells and associated tumor-derived microvesicles *Oncotarget* [online]. **7** (14). Available from: www.impactjournals.com/oncotarget/ [Accessed 11 June 2020].

Casabonne, D., Benavente, Y., Seifert, J., Costas, L., Armesto, M., Arestin, M., Besson, C., Hosnijeh, F.S., Duell, E.J., Weiderpass, E., Masala, G., Kaaks, R., Canzian, F., Chirlaque, M.D., et al. (2020) Serum levels of hsa-miR-16-5p, hsa-miR-29a-3p, hsa-miR-150-5p, hsa-miR-155-5p and hsa-miR-223-3p and subsequent risk of chronic lymphocytic leukemia in the EPIC study. *International Journal of Cancer* [online]. 147 (5), pp. 1315–1324. Available from: https://onlinelibrary.wiley.com/doi/abs/10.1002/ijc.32894doi:10.1002/ijc.32894 [Accessed 5 September 2020].

Cassinelli, G., Torri, G. and Naggi, A. (2020) Non-anti-coagulant heparins as heparanase inhibitors. In: Vlodavsky, I., Sanderson, R., Ilan N. (eds) Heparanase. Advances in experimental medicine and Biology. Vol. 1221. Springer, Charm.

Catacchio, I., Berardi, S., Reale, A., De Luisi, A., Racanelli, V., Vacca, A. and Ria, R. (2013) Evidence for bone marrow adult stem cell plasticity: Properties, molecular mechanisms, negative aspects, and clinical applications of hematopoietic and mesenchymal stem cells transdifferentiation *Stem Cells International* [online]. 2013 p.pp. 11. Available from: http://dx.doi:10.1155/2013/589139 [Accessed 24 October 2019].

Catalano, M. and O'driscoll, L. (2019) Inhibiting extracellular vesicles formation and release: a review of EV inhibitors. Available from:

https://doi.org/10.1080/20013078.2019.1703244doi:10.1080/20013078.2019.1703244

[Accessed 24 June 2020].

Cavnar, S.P., Xiao, A., Gibbons, A.E., Rickelmann, A.D., Neely, T., Luker, K.E., Takayama, S. and Luker, G.D. (2016) Imaging Sensitivity of Quiescent Cancer Cells to Metabolic Perturbations in Bone Marrow Spheroids. *Tomography*. 2 (2), pp. 146–157. doi:10.18383/j.tom.2016.00157.

Cetin, Z., Tezcan, G., Karauzum, S.B., Kupesiz, A., Esra Manguoglu, A., Yesilipek, A., Luleci, G. and Hazar, V. (2006) Donor Cell-derived Acute Myeloblastic Leukemia After Allogeneic Peripheral Blood Hematopoietic Stem Cell Transplantation for Juvenile Myelomonocytic Leukemia *J Pediatr Hematol Oncol*. **28** (11).

Chakraborty, C., Sharma, A. R., Patra, B. C., Bhattacharya, M., Sharma, G., and Lee, S. S. (2016). MicroRNAs mediated regulation of MAPK signaling pathways in chronic myeloid leukemia. *Oncotarget*. **7** (27); 42683–42697. https://doi.org/10.18632/oncotarget.7977 [Accessed 01 March 2020].

Chapuy, B., Koch, R., Radunski, U., Corsham, S., Cheong, N., Inagaki, N., Ban, N., Wenzel, D., Reinhardt, D., Zapf, A., Schweyer, S., Kosari, F., Klapper, W., Truemper, L., et al. (2008) Intracellular ABC transporter A3 confers multidrug resistance in leukemia cells by lysosomal drug sequestration. *Leukemia* [online]. 22 pp. 1576–1586. Available from: www.nature.com/leudoi:10.1038/leu.2008.103 [Accessed 27 March 2021].

Chaudhry, M.A. and Omaruddin, R.A. (2012) Differential regulation of MicroRNA expression in irradiated and bystander cells. *Molecular Biology*. **46** (4), pp. 569–578. doi:10.1134/S0026893312030041.

Chelghoum, Y., Danaíla, C., Belhabri, A., Charrin, C., Le, Q.H., Michallet, M., Fiere, D. and Thomas, X. (2002) Influence of cigarette smoking on the presentation and course of acute myeloid leukemia. *Annals of Oncology* [online]. **13** (10), pp. 1621–1627. Available from: https://academic.oup.com/annonc/article-abstract/13/10/1621/167659doi:10.1093/annonc/mdf269

Chen, X., Ba, Y., Ma, L., Cai, X., Yin, Y., Wang, K., Guo, J., Zhang, Y., Chen, J., Guo, X., Li, Q., Li, X., Wang, W., Zhang, Y., et al. (2008) Characterization of microRNAs in serum: a novel class of biomarkers for diagnosis of cancer and other diseases. *Cell Research* [online]. **18** pp. 997–1006. Available from: www.nature.com/crdoi:10.1038/cr.2008.282 [Accessed 13 December 2019].

Chen, X., Liang, H., Zhang, J., Zen, K. and Zhang, C.Y. (2012) Horizontal transfer of microRNAs: Molecular mechanisms and clinical applications *Protein and Cell.* **3** (1) p.pp. 28–37. doi:10.1007/s13238-012-2003-z.

Chen, G., Huang, A.C., Zhang, W., Zhang, G., Wu, M., Xu, W., Yu, Z., Yang, J., Wang, B., Sun, H., Xia, H., Man, Q., Zhong, W., Antelo, L.F., et al. (2018) Exosomal PD-L1 contributes to immunosuppression and is associated with anti-PD-1 response. *Nature* [online]. **560** (7718), pp. 382–386. Available from: http://www.nature.com/authors/editorial_policies/license.html#termsdoi:10.1038/s41586-018-0392-8 [Accessed 16 July 2020].

Chen, V.Y., Posada, M.M., Blazer, L.L., Zhao, T. and Rosania, G.R. (2006) The role of the VPS4a-exosome pathway in the intrinsic egress route of a DNA-binding anticancer drug. *Pharmaceutical Research*. **23** (8), pp. 1687–1695. doi:10.1007/s11095-006-9043-0.

Chen, D., Lu, D., Lin, H. and Yeh, W. (2014) Mesenchymal stem cell-induced doxorubicin resistance in triple negative breast cancer. *BioMed Research International.* ID 532161. 10 pages. https://doi.org/10.115/2014/532161 [Accessed 27 December 2020].

Chen, P., Huang, H., Wu, J., Lu, R., Wu, Y., Jiang, X., Yuan, Q. and Chen, Y. (2015) Bone marrow stromal cells protect acute myeloid leukemia cells from anti-CD44 therapy partly through regulating PI3K/Akt-p27Kip1 axis. *Molecular Carcinogenesis*. **54** (12), pp. 1678–1685. doi:10.1002/mc.22239.

Chen, L., Lu, F. bin, Chen, D. zhi, Wu, J. lu, Hu, E. de, Xu, L. man, Zheng, M. Hua, Li, H., Huang, Y., Jin, X. ya, Gong, Y. wen, Lin, Z., Wang, X. dong and Chen, Y. ping (2018) BMSCs-derived miR-223-

containing exosomes contribute to liver protection in experimental autoimmune hepatitis. *Molecular Immunology*. **93** pp. 38–46. doi:10.1016/j.molimm.2017.11.008.

Chen, T., Zhang, G., Kong, L., Xu, S., Wang, Y. and Dong, M. (2019) Leukemia-derived exosomes induced IL-8 production in bone marrow stromal cells to protect the leukemia cells against chemotherapy. *Life Sciences*. **221** pp. 187–195. doi:10.1016/j.lfs.2019.02.003.

Chen, J., Tian, W., He, H., Chen, F., Huang, J., Wang, X. and Chen, Z. (2018) Downregulation of miR-200c-3p contributes to the resistance of breast cancer cells to paclitaxel by targeting SOX2. *Oncology Reports*. 40 (6), pp. 3821–3829. doi:10.3892/or.2018.6735.

Chen, W., Cai, Y., Lv, M., Chen, L., Zhong, S., Ma, T., Zhao, J. and Tang, J. (no date) *Exosomes from docetaxel-resistant breast cancer cells alter chemosensitivity by delivering microRNAs*. Available from: www.targetscan.org/doi:10.1007/s13277-014-2242-0 [Accessed 16 December 2019].

Cheng, H., Sun, G. and Cheng, T. (2018) Hematopoiesis and microenvironment in hematological malignancies *Cell Regeneration.* **7** (1) p.pp. 22–26. doi:10.1016/j.cr.2018.08.002.

Cheuk, D.K. (2013) Optimal stem cell source for allogeneic stem cell transplantation for hematological malignancies. *World Journal of Transplantation*. **3** (4), pp. 99. doi:10.5500/wjt.v3.i4.99.

Chiarini, F., Lonetti, A., Evangelisti, C., Buontempo, F., Orsini, E., Evangelisti, C., Cappellini, A., Neri, L.M., McCubrey, J.A. and Martelli, A.M. (2016) Advances in understanding the acute lymphoblastic leukemia bone marrow microenvironment: From biology to therapeutic targeting. *Biochimica et Biophysica Acta - Molecular Cell Research*. doi:10.1016/j.bbamcr.2015.08.015.

Chinnadurai, M., Chidambaram, S., Ganesan, V., Baraneedharan, U., Sundaram, L., Paul, S.F.D. and Venkatachalam, P. (2011) Bleomycin, neocarzinostatin and ionising radiation-induced bystander effects in normal diploid human lung fibroblasts, bone marrow mesenchymal stem cells, lung adenocarcinoma cells and peripheral blood lymphocytes. *International Journal of Radiation Biology* [online]. **87** (7), pp. 673–682. Available from:

https://www.tandfonline.com/action/journalInformation?journalCode=irab20doi:10.3109/09553002.2010.549536 [Accessed 11 December 2019].

Chinnadurai, M., Paul, S.F.D. and Venkatachalam, P. (2013) The effect of growth architecture on the induction and decay of bleomycin and X-ray-induced bystander response and genomic instability in lung adenocarcinoma cells and blood lymphocytes. *International Journal of Radiation Biology*. **89** (2), pp. 69–78. doi:10.3109/09553002.2012.726397.

Chinnasamy, N., Rafferty, J.A., Hickson, I., Ashby, J., Tinwell, H., Margison, G.P., Dexter, T.M. and Fairbairn, L.J. (1997) O6-benzylguanine potentiates the in vivo toxicity and clastogenicity of temozolomide and BCNU in mouse bone marrow. *Blood.* **89** (5); pp. 1566-1573.

Cho, Y. and Kim, Y.K. (2020) Cancer stem cells as a potential target to overcome multidrug resistance. *Frontiers in Oncology.* **10.** 764 pages. https://www.frontiersin.org/article/10.3389/fonc.2020.00764 [Accessed 27 December 2020].

Christianson, H.C., Svensson, K.J., Van Kuppevelt, T.H., Li, J.-P. and Belting, M. (2013) *Cancer cell exosomes depend on cell-surface heparan sulfate proteoglycans for their internalization and functional activity*. **110** (43). doi:10.1073/pnas.1304266110.

Chulpanova, D.S., Kitaeva, K. V, James, V., Rizvanov, A.A. and Solovyeva, V. V (2018) Therapeutic Prospects of Extracellular Vesicles in Cancer Treatment. *Front. Immunol* [online]. **9** pp. 1534. Available from: www.frontiersin.orgdoi:10.3389/fimmu.2018.01534

Chyall, L., Gauny, S. and Kronenberg, A. (2006) Characterization of a TK6-Bcl-xl gly-159-ala human lymphoblast clone.U.S. Department of Energy Journal of Undergraduate Research [online]. Pp. 35-39. Available from: https://www.osti.gov/servlets/purl/1051797 [Accessed 15 September 2020].

Clark, P.I., Slevin, M.L., Joel, S.P., Osborne, R.J., Talbot, D.I., Johnson, P.W.M., Reznek, R., Masud, T., Gregory, W. and Wrigley, P.F.M. (1994) A randomized trial of two etoposide schedules in small-cell lung cancer: The influence of pharmacokinetics on efficacy and toxicity.

Journal of Clinical Oncology. 12; 1427-1435.

Clauson, C., Schärer, O.D. and Niedernhofer, L. (2013) Advances in understanding the complex mechanisms of DNA inter strand cross-link repair. *Cold Spring Harbor Perspectives in Medicine* [online]. 3 (10). Available from: www.cshperspectives.orgdoi:10.1101/cshperspect.a012732 [Accessed 4 November 2019].

Colvin M. Alkylating Agents. In: Kufe DW, Pollock RE, Weichselbaum RR, *et al.,* (2003). Holland-Frei Cancer Medicine. 6th edition. Hamilton (ON): BC Decker;. Available from: https://www.ncbi.nlm.nih.gov/books/NBK12772/

Cominal, J.G., Da Costa Cacemiro, M., Pinto-Simões, B., Kolb, H.-J., Cristina, K., Malmegrim, R. and Attié De Castro, F. (2019) *Emerging Role of Mesenchymal Stromal Cell-Derived Extracellular Vesicles in Pathogenesis of Haematological Malignancies*. Available from: https://doi.org/10.1155/2019/6854080doi:10.1155/2019/6854080 [Accessed 5 March 2020].

Concepcion, C. P., Bonetti, C., and Ventura, A. (2012). The microRNA-17-92 family of microRNA clusters in development and disease. *Cancer journal (Sudbury, Mass.)*. **18** (3); 262–267. https://doi.org/10.1097/PPO.0b013e318258b60a [Accessed 01 March 2020].

Cory, S. (1990) bcr-abl, the hallmark of chronic myeloid leukaemia in man, induces multiple haemopoietic neoplasms in mice. *The EMBO Journal*. **9** (4), pp. 1069–1078. doi:10.1002/j.1460-2075.1990.tb08212.x.

Costa Verdera, H., Gitz-Francois, J.J., Schiffelers, R.M. and Vader, P. (2017) Cellular uptake of extracellular vesicles is mediated by clathrin-independent endocytosis and macropinocytosis. *Journal of Controlled Release*. **266** pp. 100–108. doi:10.1016/j.jconrel.2017.09.019.

Crespi, C.L. and Thiuy, W.G. (1984) Assay for gene mutation in a human lymphoblast line, AHH-1, competent for xenobiotic metabolism *Mutation Research* 128.

Crow, J., Youens, K., Michalowski, S., Perrine, G., Emhart, C., Johnson, F., Gerling, A., Kurtzberg, J., Goodman, B.K., Sebastian, S., Rehder, C.W. and Datto, M.B. (2010) Donor cell leukemia in umbilical cord blood transplant patients: A case study and literature review highlighting the Danylesko, I. and Shimoni, A. (2018) Second Malignancies after Hematopoietic Stem Cell Transplantation *Current Treatment Options in Oncology*. **19** (2); 9. doi:10.1007/s11864-018-0528-y.

Dal Bo, M., Bomben, R., Hernández, L. and Gattei, V. (2015) The MYC/miR-17-92 axis in lymphoproliferative disorders: A common pathway with therapeutic potential. *Oncotarget* [online]. 6 (23), pp. 19381–19392. Available from: www.impactjournals.com/oncotarget/doi:10.18632/oncotarget.4574 [Accessed 5 September 2020].

Davis, C., Dukes, A., Drewry, M., Helwa, I., Johnson, M.H., Isales, C.M., Hill, W.D., Liu, Y., Shi, X., Fulzele, S. and Hamrick, M.W. (2017) MicroRNA-183-5p Increases with Age in Bone-Derived Extracellular Vesicles, Suppresses Bone Marrow Stromal (Stem) Cell Proliferation, and Induces Stem Cell Senescence. *Tissue Engineering - Part A*. **23** (21–22), pp. 1231–1240. doi:10.1089/ten.tea.2016.0525.

Davies, I.D., Allanson, J.P. and Causon, R.C. (1999) Rapid determination of the anti-cancer drug chlorambucil (Leukeran) and its phenyl acetic acid mustard metabolite in human serum and plasma by automated solid-phase extraction and liquid chromatography-tandem mass spectrometry. *Journal of chromatography. B, Biomedical sciences and applications* [online]. **732** (1), pp. 173–184. Available from: http://www.ncbi.nlm.nih.gov/pubmed/10517234doi:10.1016/s0378-4347(99)00280-7 [Accessed 22 November 2019].

De Luca, L., Trino, S., Laurenzana, I., Simeon, V., Calice, G., Raimondo, S., Podestà, M., Santodirocco, M., Di Mauro, L., La Rocca, F., Caivano, A., Morano, A., Frassoni, F., Cilloni, D., et al. (2016) MiRNAs and piRNAs from bone marrow mesenchymal stem cell extracellular vesicles induce cell survival and inhibit cell differentiation of cord blood hematopoietic stem cells: A new

insight in transplantation. *Oncotarget* [online]. **7** (6), pp. 6676–6692. Available from: www.impactjournals.com/oncotarget/doi:10.18632/oncotarget.6791

de Jong, O.G., Verhaar, M.C., Chen, Y., Vader, P., Gremmels, H., Posthuma, G., Schiffelers, R.M., Gucek, M. and van Balkom, B.W.M. (2012) Cellular stress conditions are reflected in the protein and RNA content of endothelial cell-derived exosomes. *Journal of Extracellular Vesicles* [online]. **1** (1). Available from: http://dx.doi.org/10.3402/jev.v1i0.18396doi:10.3402/jev.v1i0.18396 [Accessed 16 December 2019].

de Jong, O.G., Kooijmans, S.A.A., Murphy, D.E., Jiang, L., Evers, M.J.W., Sluijter, J.P.G., Vader, P. and Schiffelers, R.M. (2019) Drug Delivery with Extracellular Vesicles: From Imagination to Innovation. *Accounts of Chemical Research*. **52** (7), pp. 1761–1770. doi:10.1021/acs.accounts.9b00109.

De Kouchkovsky, I. and Abdul-Hay, M. (2016) 'Acute myeloid leukemia: A comprehensive review and 2016 update' *Blood Cancer Journal* [online]. **6** (7) p.pp. 441. Available from: www.nature.com/bcjdoi:10.1038/bcj.2016.50

De Menezes-Neto, A., José, M., Sáez, F., Lozano-Ramos, I., Segui-Barber, J., Martin-Jaular, L., Ullate, J.M.E., Fernandez-Becerra, C., Borrás, F.E. and Del Portillo, H.A. (2015) *Journal of Extracellular Vesicles Size-exclusion chromatography as a stand-alone methodology identifies novel markers in mass spectrometry analyses of plasma-derived vesicles from healthy individuals.* Available from: https://www.tandfonline.com/action/journalInformation?journalCode=zjev20doi:10.3402/jev.v4.27378 [Accessed 19 June 2020].

Dehghani, M., Gulvin, S.M., Flax, J. and Thomas, R. (2019) Exosome labeling by lipophilic dye PKH26 results in significant increase in vesicle size. *BioRxiv* [online]. Available from: https://doi.org/10.1101/532028doi:10.1101/532028 [Accessed 22 June 2020].

Delk, N.A. and Farach-Carson, M.C. (2012) Interleukin-6: A bone marrow stromal cell paracrine signal that induces neuroendocrine differentiation and modulates autophagy in bone metastatic PCa cells. *Autophagy*. **8** (4), pp. 650–663. doi:10.4161/auto.19226.

Demidem, A., Morvan, D. and Madelmont, J.C. (2006) Bystander effects are induced by CENU treatment and associated with altered protein secretory activity of treated tumor cells A relay for chemotherapy? *International Journal of Cancer* [online]. **119** (5), pp. 992–1004. Available from: http://doi.wiley.com/10.1002/ijc.21761doi:10.1002/ijc.21761 [Accessed 10 December 2019].

Demiriz, I.S., Tekgunduz, E. and Altuntas, F. (2012) What Is the Most Appropriate Source for Hematopoietic Stem Cell Transplantation? Peripheral Stem Cell/Bone Marrow/Cord Blood. *Bone Marrow Research*. 2012. doi:10.1155/2012/834040.

Dertinger, S.D., Kraynak, A.R., Wheeldon, R.P., Bernacki, D.T., Bryce, S.M., Hall, N., Bemis, J.C., Galloway, S.M., Escobar, P.A. and Johnson, G.E. (2019) Predictions of genotoxic potential, mode of action, molecular targets, and potency via a tiered multiflow® assay data analysis strategy. *Environmental and Molecular Mutagenesis* [online]. 60 (6), pp. 513–533. Available from: http://doi.wiley.com/10.1002/em.22274doi:10.1002/em.22274 [Accessed 9 September 2020].

Desdín-Micó, G. and Mittelbrunn, M. (2017) Role of exosomes in the protection of cellular homeostasis *Cell Adhesion and Migration* [online]. **11** (2) p.pp. 127–134. Available from: https://www.tandfonline.com/action/journalInformation?journalCode=kcam20doi:10.1080/19336918.2016.1251000

Devereux T.R., Risinger J.I. and Barrett J.C. (1999) Mutations and altered expression of the human cancer genes: what they tell us about causes. *IARC Sci Publ*. **146:**19-42.

Dexheimer, V., Mueller, S., Braatz, F. and Richter, W. (2011) Reduced reactivation from dormancy but maintained lineage choice of human mesenchymal stem cells with donor age. *PLoS ONE*. **6** (8). doi:10.1371/journal.pone.0022980.

Deynoux, M., Sunter, N., Ducrocq, E., Dakik, H., Guibon, R., Burlaud-Gaillard, J., Brisson, L., Rouleux-Bonnin, F., le Nail, L.R., Hérault, O., Domenech, J., Roingeard, P., Fromont, G. and Mazurier, F. (2020) A comparative study of the capacity of mesenchymal stromal cell lines to form spheroids. *PLoS ONE* [online]. **15** (6). Available from: https://doi.org/10.1101/834390doi:10.1371/journal.pone.0225485

Di, X., Bright, A.T., Bellott, R., Gaskins, E., Robert, J., Holt, S., Gewirtz, D.A. and Elmore, L. (2008) A chemotherapy-associated senescence bystander effect in breast cancer cells. *Cancer Biology & Therapy* [online]. **7** (6), pp. 864–872. Available from: https://doi.org/10.4161/cbt.7.6.5861doi:10.4161/cbt.7.6.5861 [Accessed 11 December 2019].

Di Antonio, M., McLuckie, K.I.E. and Balasubramanian, S. (2014) Reprogramming the mechanism of action of chlorambucil by coupling to a G-quadruplex ligand. *Journal of the American Chemical Society*. **136** (16), pp. 5860–5863. doi:10.1021/ja5014344.

Di Trapani, M., Bassi, G., Midolo, M., Gatti, A., Kamga, P.T., Cassaro, A., Carusone, R., Adamo, A. and Krampera, M. (2016) Differential and transferable modulatory effects of mesenchymal stromal cell-derived extracellular vesicles on T, B and NK cell functions. *Scientific Reports* [online]. **6.** Available from: www.nature.com/scientificreportsdoi:10.1038/srep24120

Dickey, J.S., Baird, B.J., Redon, C.E., Sokolov, M. V, Sedelnikova, O.A. and Bonner, W.M. (2009) Intercellular communication of cellular stress monitored by g-H2AX induction. *Carcinogenesis*. **30** (10), pp. 1686–1695. doi:10.1093/carcin/bgp192.

Dickey, J.S., Zemp, F.J., Martin, O.A. and Kovalchuk, O. (2011) The role of miRNA in the direct and indirect effects of ionizing radiation *Radiation and Environmental Biophysics.* **50** (4) p.pp. 491–499. doi:10.1007/s00411-011-0386-5.

Driedonks, T.A.P., Nijen Twilhaar, M.K. and Nolte't Hoen, E.N.M. (2019) Technical approaches to reduce interference of Fetal calf serum derived RNA in the analysis of extracellular vesicle RNA from cultured cells. *Journal of Extracellular Vesicles*. **8** (1). doi:10.1080/20013078.2018.1552059.

Drela, K., Stanaszek, L., Nowakowski, A., Kuczynska, Z. and Lukomska, B. (2019) Experimental strategies of mesenchymal stem cell propagation: Adverse events and potential risk of functional changes *Stem Cells International* [online] 2019. Available from: https://doi.org/10.1155/2019/7012692doi:10.1155/2019/7012692 [Accessed 6 January 2020].

Dominici, M., Le Blanc, K., Mueller, I., Slaper-Cortenbach, I., Marini, F., Krause, D., Deans, R., Keating, A., Prockop, Dj and Horowitz, E. (2006) Minimal criteria for defining multipotent mesenchymal stromal cells. The International Society for Cellular Therapy position statement. *Cytotherapy.* **8** (4); 315-317.

Dong, Z., Yu, C., Rezhiya, K., Gulijiahan, A. and Wang, X. (2019) Downregulation of miR-146a promotes tumorigenesis of cervical cancer stem cells via VEGF/CDC42/PAK1 signaling pathway. *Artificial Cells, Nanomedicine and Biotechnology* [online]. 47 (1), pp. 3711–3719. Available from: https://doi.org/10.1080/21691401.2019.1664560doi:10.1080/21691401.2019.1664560.

Dunn, C.J. and Goa, K.L. (1996) Mitoxantrone. A review of its pharmacological properties and use in acute nonlymphoblastic leukaemia *Drugs and Aging.* **9** (2) p.pp. 122–147. doi:10.2165/00002512-199609020-00007.

Durak-Kozica, M., Baster, Z., Kubat, K. and Stępień, E. (2018) 3D visualization of extracellular vesicle uptake by endothelial cells. *Cellular and Molecular Biology Letters*. **23** (1). doi:10.1186/s11658-018-0123-z.

Duval, K., Grover, H., Han, L.-H., Mou, Y., Pegoraro, A.F., Fredberg, J., Chen, Z., Duval, * K, Grover, H. and Han, L.-H. (2017) *Modeling Physiological Events in 2D vs. 3D Cell Culture*. Available from: www.physiologyonline.orgdoi:10.1152/physiol.00036.2016 [Accessed 6 January 2020].

Ede, B.C., Asmaro, R.R., Moppett, J.P., Diamanti, P. and Blair, A. (2018) Investigating chemoresistance to improve sensitivity of childhood T-cell acute lymphoblastic leukemia to parthenolide. *Haematologica* [online]. **103** (9), pp. 1493–1501. Available from: www.haematologica.org/content/103/9/1493doi:10.3324/haematol.2017.186700 [Accessed 17 July 2020].

Ehninger, G., Schuler, U., Proksch, B. *et al.,* (1990) Pharmacokinetics and metabolism of mitoxantrone: A review. Clinical Pharmacokinetics. **18** (5); 365-380. Available from: https://doi.org/10.2165/00003088-199018050-0000

Eitan, E., Zhang, S., Witwer, K.W. and Mattson, M.P. (2015) Extracellular vesicle-depleted fetal bovine and human sera have reduced capacity to support cell growth. *Journal of Extracellular Vesicles*. **4** (2015), pp. 1–10. doi:10.3402/jev.v4.26373.

Eldh, M., Lötvall, J., Malmhäll, C. and Ekström, K. (2012) Importance of RNA isolation methods for analysis of exosomal RNA: Evaluation of different methods. *Molecular Immunology*. **50** (4), pp. 278–286. doi:10.1016/j.molimm.2012.02.001.

Elefanty, A.G., Hariharan, I.K. and Gaziel-Sovran, A., Segura, M.F., Di Micco, R., Collins, M.K., Hanniford, D., Vega-Saenz de Fagerberg, L., Strömberg, S., El-Obeid, A., Gry, M., Nilsson, K., Uhlen, M., Ponten, F. and Asplund, A. (2011) Large-scale protein profiling in human cell lines using antibody-based proteomics. *Journal of Proteome Research*. **10** (9), pp. 4066–4075. doi:10.1021/pr200259v.

Elefanty, A.G., Hariharan, I.K. and Cory, S. (1990) bcr-abl, the hallmark of chronic myeloid leukaemia in man, induces multiple haemopoietic neoplasms in mice. *The EMBO Journal*. 9 (4), pp. 1069–1078. doi:10.1002/j.1460-2075.1990.tb08212.x.

Escrevente, C., Keller, S., Altevogt, P. and Costa, J. (2011) Interaction and uptake of exosomes by ovarian cancer cells [online]. Available from: http://rsb.info.nih.gov/ij/.doi:10.1186/1471-2407-11-108 [Accessed 13 December 2019].

Esmaeli, S., Allameh, A., Aleagha, M.S.E., Kazemnejad, S. and Soleimani, M. (2012) Expression of cytochrome P450 and glutathione S-transferase in human bone marrow mesenchymal stem cells. *Iranian Journal of Biotechnology*. 10 (4), pp. 270–274.

Estey, E.H. (2018) Acute myeloid leukemia: 2019 update on risk-stratification and management. *American Journal of Hematology*. **93** (10), pp. 1267–1291. doi:10.1002/ajh.25214.

Fang, L.L., Wang, X.H., Sun, B.F., Zhang, X.D., Zhu, X.H., Yu, Z.J. and Luo, H. (2017) Expression, regulation and mechanism of action of the miR-17-92 cluster in tumor cells (Review) *International Journal of Molecular Medicine.* **40** (6) p.pp. 1624–1630. doi:10.3892/ijmm.2017.3164.

Faulds, D., Balfour, J.A., Chrisp, P. et al., (1991) Mitoxantrone: A review of its pharmacodynamics and pharmacokinetic properties, and therapeutic potential in the chemotherapy of cancer. **41** (3); 400 -409. Available from: https://doi.org/10.2165/00003495-199141030-00007

Federici, C., Petrucci, F., Caimi, S., Cesolini, A., Logozzi, M., Borghi, M., D'ilio, S., Lugini, L., Violante, N., Azzarito, T., Majorani, C., Brambilla, D. and Fais, S. (2014) *Exosome Release and Low pH Belong to a Framework of Resistance of Human Melanoma Cells to Cisplatin*. Available from: www.plosone.orgdoi:10.1371/journal.pone.0088193 [Accessed 27 March 2021].

Fenech, M., Kirsch-Volders, M., Natarajan, A.T., Surralles, J., Crott, J.W., Parry, J., Norppa, H., Eastmond, D.A., Tucker, J.D. and Thomas, P. (2011) Molecular mechanisms of micronucleus, nucleoplasmic bridge and nuclear bud formation in mammalian and human cells *Mutagenesis.* **26** (1) p.pp. 125–132. doi:10.1093/mutage/geq052.

Filip, A.A., Grenda, A., Popek, S., Koczkodaj, D., Michalak-Wojnowska, M., Budzyński, M., Wąsik-Szczepanek, E., Zmorzyński, S., Karczmarczyk, A. and Giannopoulos, K. (2017) Expression of circulating miRNAs associated with lymphocyte differentiation and activation in CLL—another piece in the puzzle. *Annals of Hematology*. 96 (1), pp. 33–50. doi:10.1007/s00277-016-2840-6.

Fircanis, S., Merriam, P., Khan, N. and Castillo, J.J. (2014) The relation between cigarette smoking and risk of acute myeloid leukemia: An updated meta-analysis of epidemiological studies. *American Journal of Hematology*. **89** (8), pp. 125–132. doi:10.1002/ajh.23744.

Fischer, J., Rossetti, S., Datta, A., Eng, K., Beghini, A., & Sacchi, N. (2015). miR-17 deregulates a core RUNX1-miRNA mechanism of CBF acute myeloid leukemia. *Molecular cancer.* **14**; 7. https://doi.org/10.1186/s12943-014-0283-z [Accessed 01 March 2020].

Fischer, K., Bahlo, J., Maria Fink, A., Goede, V., Diana Herling, C., Cramer, P., Langerbeins, P., von Tresckow, J., Engelke, A., Maurer, C., Kovacs, G., Herling, M., Tausch, E., Kreuzer, K.-A., et al. (2016) Long-term remissions after FCR chemoimmunotherapy in previously untreated patients with CLL: updated results of the CLL8 trial and 9 Cluster of Excellence Cellular Stress Responses in Aging Associated. *Blood* [online]. **127** (2), pp. 208–215. Available from: www.bloodjournal.orgdoi:10.1182/blood-2015-06

Flusberg, D.A. and Sorger, P.K. (2015) Surviving apoptosis: Life-death signaling in single cells *Trends in Cell Biology.* **25** (8) p.pp. 446–458. doi:10.1016/j.tcb.2015.03.003.

Flynn, C.M. and Kaufman, D.S. (2007) *Donor cell leukemia: insight into cancer stem cells and the stem cell niche*. **109** pp. 2688–2692. Available from: https://ashpublications.org/blood/article-pdf/109/7/2688/1289358/zh800707002688.pdfdoi:10.1182/blood-2006-07-021980 [Accessed 7 December 2019].

Fonseca, S.B., Pereira, M.P., Mourtada, R., Gronda, M., Horton, K.L., Hurren, R., Minden, M.D., Schimmer, A.D. and Kelley, S.O. (2011) Rerouting chlorambucil to mitochondria combats drug deactivation and resistance in cancer cells. *Chemistry and Biology*. doi:10.1016/j.chembiol.2011.02.010.

Fracchiolla, N.S., Fattizzo, B. and Cortelezzi, A. (2017) Mesenchymal Stem Cells in Myeloid Malignancies: A Focus on Immune Escaping and Therapeutic Implications *Stem Cells International* 2017. doi:10.1155/2017/6720594.

Fraser, C.J., Hirsch, B.A., Dayton, V., Creer, M.H., Neglia, J.P., Wagner, J.E. and Baker, K.S. (2005) First report of donor cell-derived acute leukemia as a complication of umbilical cord blood transplantation. *Blood*. **106** (13), pp. 4377–4380. doi:10.1182/blood-2005-06-2551.

Freedman, H.J., Gurtoo, H.L., Minowada, J., Paigen, B. and Vaught4, J.B. (1979) *Aryl Hydrocarbon Hydroxylase in a Stable Human B-Lymphocyte Cell Line, RPMI-1788, Cultured in the Absence of Mitogens1*.

Freedman, H.J., Parker, N.B., Mannello, A.J., Gurtoo, M.L. and Minowada, J. (1979) *Induction, Inhibition, and Biological Properties of Aryl Hydrocarbon Hydroxylase in a Stable Human B-Lymphocyte Cell Line, RPMI-17881*.

Frei, H., Clements, J., Howe, D. and Würgler, F.E. (1992) The genotoxicity of the anti-cancer drug mitoxantrone in somatic and germ cells of Drosophila melanogaster. *Mutation Research/Genetic Toxicology* [online]. **279** (1), pp. 21–33. Available from: https://www.sciencedirect.com/science/article/abs/pii/016512189290262X?via%3Dihubdoi:10.1016/0165-1218(92)90262-X [Accessed 24 November 2019].

Friedenstein, A.J., Chailakhjan, R.K. and Lalykina, K.S. (1970) The development of fibroblast colonies in monolayer cultures of guinea-pig bone marrow and spleen cells. *Cell Tissue Kinetics.* **3**: 393 – 403.

Foukakis, T., Lö Vrot, J., Matikas, A., Zerdes, I., Lorent, J., Tobin, N., Suzuki, C., Egyhá Zi Brage, S., Carlsson, L., Einbeigi, Z., Linderholm, B., Loman, N., Malmberg, M., Fernö, M., et al. (2018) *Immune gene expression and response to chemotherapy in advanced breast cancer*. Available from: www.bjcancer.comdoi:10.1038/bjc.2017.446 [Accessed 29 May 2020].

Fu, F., Jiang, W., Zhou, L. and Chen, Z. (2018) Circulating Exosomal miR-17-5p and miR-92a-3p Predict Pathologic Stage and Grade of Colorectal Cancer. *Translational Oncology* [online]. **11** (2), pp. 221–232. Available from: https://doi.org/10.1016/j.tranon.2017.12.012doi:10.1016/j.tranon.2017.12.012 [Accessed 2 July 2020].

Furukawa, M., Ohkawara, H., Ogawa, K., Ikeda, K., Ueda, K., Shichishima-Nakamura, A., Ito, E., Imai, J.I., Yanagisawa, Y., Honma, R., Watanabe, S., Waguri, S., Ikezoe, T. and Takeishi, Y. (2017) Autocrine and paracrine interactions between multiple myeloma cells and bone marrow stromal cells by growth arrest-specific gene 6 cross-talk with interleukin-6. *Journal of Biological Chemistry*. **292** (10), pp. 4280–4292. doi:10.1074/jbc.M116.733030.

Gámez-Valero, A., Monguió-Tortajada, M., Carreras-Planella, L., Franquesa, M., Beyer, K. and Borràs, F.E. (2016) Size-Exclusion Chromatography-based isolation minimally alters Extracellular Vesicles' characteristics compared to precipitating agents OPEN. *Nature Publishing Group* [online]. Available from: www.nature.com/scientificreports/doi:10.1038/srep33641 [Accessed 15 June 2020].

Garavelli, S., De Rosa, V., & de Candia, P. (2018). The Multifaceted Interface Between Cytokines and microRNAs: An Ancient Mechanism to Regulate the Good and the Bad of Inflammation. *Frontiers in immunology*, *9*, 3012. https://doi.org/10.3389/fimmu.2018.03012 [Accessed 15 June 2020].

Garrido, S.M., Appelbaum, F.R., Willman, C.L. and Banker, D.E. (2001) Acute myeloid leukemia cells are protected from spontaneous and drug-induced apoptosis by direct contact with a human bone marrow stromal cell line (HS-5). *Experimental Hematology*. **29** (4), pp. 448–457. doi:10.1016/S0301-472X(01)00612-9.

Gatto, B. and Leo, E. (2003) Drugs acting on the beta isoform of human topoisomerase II (p180) *Current Medicinal Chemistry - Anti-Cancer Agents.* **3** (3) p.pp. 173–185. doi:10.2174/1568011033482486.

Ge, Q., Zhou, Y., Lu, J., Bai, Y., Xie, X. and Lu, Z. (2014) molecules miRNA in Plasma Exosome is Stable under Different Storage Conditions. *Molecules* [online]. **19** pp. 1568–1575. Available from: www.mdpi.com/journal/moleculesArticledoi:10.3390/molecules19021568 [Accessed 13 December 2019].

Gelfond, J. Al, McManus, L.M. and Shireman, P.K. (2009) Reproducibility of quantitative RT-PCR array in miRNA expression profiling and comparison with microarray analysis. *BMC Genomics* [online]. 10 pp. 407. Available from: http://www.biomedcentral.com/1471-2164/10/407doi:10.1186/1471-2164-10-407 [Accessed 5 September 2020].

Georgiou, K.R., Foster, B.K. and Xian, C.J. (2010) Damage and Recovery of the Bone Marrow Microenvironment Induced by Cancer Chemotherapy – Potential Regulatory Role of Chemokine

CXCL12/Receptor CXCR4 Signalling. *Current Molecular Medicine*. 10 (5), pp. 440–453. doi:10.2174/156652410791608243.

Georgiou, K.R., Scherer, M.A., King, T.J., Foster, B.K. and Xian, C.J. (2012) Deregulation of the CXCL12/CXCR4 axis in methotrexate chemotherapy-induced damage and recovery of the bone marrow microenvironment. *International Journal of Experimental Pathology*. **93** (2), pp. 104–114. doi:10.1111/j.1365-2613.2011.00800.x.

Geyh, S., Cadeddu, R.-P., Frö Bel, J., Brü Ckner, B., Kü Ndgen, A., Fenk, R., Bruns, I., Zilkens, C., Hermsen, D., Gattermann, N., Kobbe, G., Germing, U., Lyko, F., Haas, R., et al. (2013) Insufficient stromal support in MDS results from molecular and functional deficits of mesenchymal stromal cells. *Leukemia* [online]. **27** pp. 1841–1851. Available from: www.nature.com/leudoi:10.1038/leu.2013.193 [Accessed 15 May 2020].

Ghia, P., Ferreri, A.M. and Galigaris-Cappio, F. (2007) Chronic lymphocytic leukemia *Critical Reviews in Oncology/Hematology* [online]. **64** (3) p.pp. 234–246. Available from: https://linkinghub.elsevier.com/retrieve/pii/S1040842807000844doi:10.1016/j.critrevonc.2007.04.008 [Accessed 14 October 2019].

Ghidoni, R., Benussi, L. and Binetti, G. (2008) Exosomes: The Trojan horses of neurodegeneration *Medical Hypotheses.* **70** (6) p.pp. 1226–1227. doi:10.1016/j.mehy.2007.12.003.

Ginzburg, Y. and Rivella, S. (2011) β-thalassemia: A model for elucidating the dynamic regulation of ineffective erythropoiesis and iron metabolism *Blood.* **118** (16) p.pp. 4321–4330. doi:10.1182/blood-2011-03-283614.

Glynn, C.L., Khan, S., Kerin, M.J. and Dwyer, R.M. (2013) Isolation of Secreted microRNAs (miRNAs) from Cell-conditioned Media. *MicroRNA*. **2** (1), pp. 14–19. doi:10.2174/2211536611302010003.

Jiang Goh, W., Lee, K., Zou, S., Woon, C., Czarny, B. and Pastorin, G. (2017) Doxorubicin-loaded cell-derived nanovesicles: an alternative targeted approach for anti-tumor therapy. *International*

Journal of Nanomedicine [online]. pp. 12–2759. Available from: http://dx.doi.org/10.2147/IJN.S131786doi:10.2147/IJN.S131786 [Accessed 27 March 2021].

Goldin, L.R., Pfeiffer, R.M., Li, X. and Hemminki, K. (2004) Familial risk of lymphoproliferative tumors in families of patients with chronic lymphocytic leukemia: Results from the Swedish Family-Cancer Database. *Blood* [online]. **104** (6), pp. 1850–1854. Available from: www.bloodjournal.orgdoi:10.1182/blood-2004-01-0341

Goler-Baron, V. and Assaraf, Y.G. (2011) Structure and Function of ABCG2-Rich Extracellular Vesicles Mediating Multidrug Resistance. *PLoS ONE* [online]. **6** (1), pp. 16007. Available from: www.plosone.orgdoi:10.1371/journal.pone.0016007 [Accessed 27 March 2021].

Gomari, H., Moghadam, M.F. and Soleimani, M. (2018) Targeted cancer therapy using engineered exosome as a natural drug delivery vehicle. *OncoTargets and Therapy*. **11** pp. 5753–5762. doi:10.2147/OTT.S173110.

Gorman, S., Tosetto, M., Lyng, F., Howe, O., Sheahan, K., O'Donoghue, D., Hyland, J., Mulcahy, H. and O'Sullivan, J. (2009) Radiation and chemotherapy bystander effects induce early genomic instability events: Telomere shortening and bridge formation coupled with mitochondrial dysfunction. *Mutation Research - Fundamental and Molecular Mechanisms of Mutagenesis*. **669** (1–2), pp. 131–138. doi:10.1016/j.mrfmmm.2009.06.003.

Groot, M. and Lee, H. (2020) Sorting Mechanisms for MicroRNAs into Extracellular Vesicles and Their Associated Diseases *Cells* [online]. **9** (4). Available from: www.mdpi.com/journal/cellsdoi:10.3390/cells9041044 [Accessed 8 June 2020].

Guadamillas, M.C., Cerezo, A. and del Pozo, M.A. (2011) Overcoming anoikis - pathways to anchorageindependent growth in cancer *Journal of Cell Science.* **124** (19) p.pp. 3189–3197. doi:10.1242/jcs.072165

Guan, D., Qing, W., Ma, C., Zhang, Z., Wei, H. and Wu, G. (2018) Bone marrow stromal-cell line hs-5 affects apoptosis of acute myeloid leukemia cells hl-60 through gli1 activation. *Biomedical*

Research (India) [online]. **29** (5), pp. 865–868. Available from: www.biomedres.infodoi:10.4066/biomedicalresearch.29-17-2410.

Gudbergsson, J.M., Johnsen, K.B., Skov, M.N. and Duroux, M. (2016) Systematic review of factors influencing extracellular vesicle yield from cell cultures *Cytotechnology*. **68** (4) p.pp. 579–592. doi:10.1007/s10616-015-9913-6.

Guénin, S., Mauriat, M., Pelloux, J., Van Wuytswinkel, O., Bellini, C. and Gutierrez, L. (2009) Normalization of qRT-PCR data: The necessity of adopting a systematic, experimental conditions-specific, validation of references. *Journal of Experimental Botany* [online]. **60** (2), pp. 487–493. Available from: https://academic.oup.com/jxb/article-abstract/60/2/487/631727doi:10.1093/jxb/ern305 [Accessed 30 June 2020].

Guerreiro, E.M., Vestad, B., Steffensen, L.A., Christian, H., Aass, D., Saeed, M., Øvstebø, R., Elena Costea, D., Kanli, H., 1☺, G., Søland, T.M. and Ahmad, A. (2018) *Efficient extracellular vesicle isolation by combining cell media modifications, ultrafiltration, and size-exclusion chromatography*. Available from: https://doi.org/10.1371/journal.pone.0204276doi:10.1371/journal.pone.0204276 [Accessed 19 June 2020].

Guo, S., S-w, L., Kalimuthu, S., Gangadaran, P., Lakshmi Rajendran, R., Zhu, L., Min Oh, J., Won Lee, H., Gopal, A., Hwan Baek, S., Young Jeong, S., Lee, S.-W., Lee, J. and Ahn, B.-C. (2018) *A New Approach for Loading Anticancer Drugs Into Mesenchymal Stem Cell-Derived Exosome Mimetics for Cancer Therapy*. Available from: www.frontiersin.orgdoi:10.3389/fphar.2018.01116

Gustafson, D., Veitch, S. and Fish, J.E. (2017) Extracellular Vesicles as Protagonists of Diabetic Cardiovascular Pathology. *Frontiers in Cardiovascular Medicine*. 4. doi:10.3389/fcvm.2017.00071.

Gyurkocza, B., & Sandmaier, B. M. (2014). Conditioning regimens for hematopoietic cell transplantation: one size does not fit all. *Blood*, *124*(3), 344–353. https://doi.org/10.1182/blood-2014-02-514778 [Accessed 31 December 2020].

Haglund, U., Stellan, B., Juliusson, G. and Gahrton, G. (1997) Increased frequency of chromosome abnormalities in fibroblasts from hairy cell leukemia patients *Leukemia* 11.

Haltrich, I., Müller, J., Szabó, J., Kovács, G., Kóos, R., Poros, A., Dobos, M. and Fekete, G. (2003) Donor-cell myelodysplastic syndrome developing 13 years after marrow grafting for aplastic anemia. *Cancer Genetics and Cytogenetics*. **142** (2), pp. 124–128. doi:10.1016/S0165-4608(02)00804-X.

Hampel, P.J., Chaffee, K.G., King, R.L., Simonetto, D., Larson, M.C., Achenbach, S., Call, T.G., Ding, W., Kenderian, S.S., Leis, J.F., Chanan-Khan, A.A., Bowen, D.A., Conte, M.J., Schwager, S.M., et al. (2017) Liver dysfunction in chronic lymphocytic leukemia: Prevalence, outcomes, and pathological findings. *American Journal of Hematology*. **92** (12), pp. 1362–1369. doi:10.1002/ajh.24915.

Han, N., Song, Y.K., Burckart, G.J., Ji, E., Kim, I.W. and Oh, J.M. (2017) Regulation of pharmacogene expression by microRNA in the cancer genome atlas (TCGA) research network. *Biomolecules and Therapeutics*. 25 (5), pp. 482–489. doi:10.4062/biomolther.2017.122.

Hande, K.R. (2008) Topoisomerase II inhibitors *Update on Cancer Therapeutics*. **3** (1) p.pp. 13–26. doi:10.1016/j.uct.2008.02.001.

Hashimoto, H., Chatterjee, S. and Berger, N.A. (1995) Inhibition of Etoposide (VP-16)-induced DNA Recombination and Mutant Frequency by Bcl-2 Protein Overexpression. *Cancer Research*. **55** (18), pp. 4029–4035.

Hasle, H., Haunstrup Clemmensen, I. and Mikkelsen, M. (2000) Risks of leukaemia and solid tumours in individuals with Down's syndrome. *Lancet*. **355** (9199), pp. 165–169. doi:10.1016/S0140-6736(99)05264-2.

Haug, B.H., Hald, Ø.H., Utnes, P., Roth, S.A., Løkke, C., Flægstad, T. and Einvik, C. (2015) Exosome-like extracellular vesicles from MYCN-amplified neuroblastoma cells contain oncogenic miRNAs. *Anticancer Research*. **35** (5), pp. 2521–2530.

Haraszti, R.A., Didiot, M.C., Sapp, E., Leszyk, J., Shaffer, S.A., Rockwell, H.E., Gao, F., Narain, N.R., DiFiglia, M., Kiebish, M.A., Aronin, N. and Khvorova, A. (2016) High-resolution proteomic and lipidomic analysis of exosomes and microvesicles from different cell sources. *Journal of Extracellular Vesicles*. **5** (1). doi:10.3402/jev.v5.32570.

Harmati, M., Gyukity-Sebestyen, E., Dobra, G., Janovak, L., Dekany, I., Saydam, O., Hunyadi-Gulyas, E., Nagy, I., Farkas, A., Pankotai, T., Ujfaludi, Z., Horvath, P., Piccinini, F., Kovacs, M., et al. (2019) Small extracellular vesicles convey the stress-induced adaptive responses of melanoma cells. *Scientific Reports* [online]. **9** (1). Available from: https://doi.org/10.1038/s41598-019-51778-6doi:10.1038/s41598-019-51778-6 [Accessed 10 June 2020].

Hasford, J., Pfirrmann, M., Hehlmann, R., Allan, N.C., Baccarani, M., Kluin-Nelemans, J.C., Alimena, G., Steegmann, J.L. and Ansari, H. (1998) A New Prognostic Score for Survival of Patients With Chronic Myeloid Leukemia Treated With Interferon Alfa Writing Committee for the Collaborative CML Prognostic Factors Project Group. *JNCI: Journal of the National Cancer Institute* [online]. **90** (11), pp. 850–859. Available from: https://academic.oup.com/jnci/article-abstract/90/11/850/916627doi:10.1093/jnci/90.11.850

Hasford, J., Baccarani, M., Hoffmann, V., Guilhot, J., Saussele, S., Rosti, G., Guilhot, F., Porkka, K., Ossenkoppele, G., Lindoerfer, D., Simonsson, B., Pfirrmann, M. and Hehlmann, R. (2011) Predicting complete cytogenetic response and subsequent progression-free survival in 2060 patients with CML on imatinib treatment: The EUTOS score. *Blood* [online]. **118** (3), pp. 686–692. Available from: https://ashpublications.org/blood/article-pdf/118/3/686/976964/zh802911000686.pdfdoi:10.1182/blood-2010-12-319038

Hasle, H., Haunstrup Clemmensen, I. and Mikkelsen, M. (2000) Risks of leukaemia and solid tumours in individuals with Down's syndrome. *Lancet*. **355** (9199), pp. 165–169. doi:10.1016/S0140-6736(99)05264-2.

Hattangadi, S.M., Wong, P., Zhang, L., Flygare, J. and Lodish, H.F. (2011) From stem cell to red cell: Regulation of erythropoiesis at multiple levels by multiple proteins, RNAs, and chromatin modifications *Blood* **118** (24) p.pp. 6258–6268. doi:10.1182/blood-2011-07-356006.

Hecker, J., Miller, I., Götze, K.S. and Verbeek, M. (2018) Bridging strategies to allogeneic transplant for older AML patients *Cancers* [online] 10 (7). Available from: www.mdpi.com/journal/cancersdoi:10.3390/cancers10070232 [Accessed 3 September 2020].

Hei Antonio Cheung, C., Huang, C.-C., Tsai, F.-Y., Ying-Chieh Lee, J., Muk Cheng, S., Chang, Y.-C., Huang, Y.-C., Chen, S.-H. and Chang, J.-Y. (2013) OTT-33374-survivin---biology-and-potential-as-a-therapeutic-target-in-. *National Health Research institutes* [online]. Available from: http://dx.doi.org/10.2147/OTT.S33374doi:10.2147/OTT.S33374 [Accessed 25 June 2020].

Hematology Fc, G.N.A.N.A. (1993); and Edith Nourse Rogers Memorial Veterans Hospital *Cellular Immunology*. 53.

Henner, W.D., Peters, W.P., Eder, J.P., Antman, K., Schnipper, L. and Frei, E. (1997) Pharmacokinetics and immediate effects of high-dose carmustine in man. *Clinical Chemistry*. **43** (4); 615-618. Drug monitoring and toxicology.

Hertenstein, B., Hambach, L., Bacigalupo, A., Schmitz, N., McCann, S., Slavin, S., Gratwohl, A., Ferrant, A., Elmaagacli, A., Schwertfeger, R., Locasciulli, A., Zander, A., Bornhäuser, M., Niederwieser, D., et al. (2005) Development of leukemia in donor cells after allogeneic stem cell transplantation - A survey of the European Group for Blood and Marrow Transplantation (EBMT). *Haematologica*. **90** (7), pp. 969–975.

Hijiya, N., Ness, K. K., Ribeiro, R. C., and Hudson, M. M. (2009). Acute leukemia as a secondary malignancy in children and adolescents: current findings and issues. *Cancer.* **115** (1); 23–35. https://doi.org/10.1002/cncr.23988 [Accessed 03 February 2020].

Hijiya, N., Schultz, K. R., Metzler, M., Millot, F., & Suttorp, M. (2016). Pediatric chronic myeloid leukemia is a unique disease that requires a different approach. *Blood.* **127** (4); 392–399. https://doi.org/10.1182/blood-2015-06-648667 [Accessed 03 February 2020].

Holthuis, J.J.M., Postmus, P.E., Van Oort, W.J., Hulshoff, B., Verleun, H., Sleijfer, D.T. and Mulder, N.H. (1986) Pharmacokinetics of high dose etoposide (VP 16-213). *European Journal of Cancer and Clinical Oncology.* 22 (10), pp. 1149–1155. doi:10.1016/0277-5379(86)90315-9.

Hong, W.K., Bast, R.C., Hait, W.N., Kufe, D.W., Pollock, R.E., Weichselbaum, R.R., Holland, J.F. and Frei, E. (2010) Holland-Frei Cancer Medicine 8th. Ed. *American association for cancer Research.* Peoples medical publishing house-USA, Shelton, Connecticut.

Horibe, S., Tanahashi, T., Kawauchi, S., Murakami, Y. and Rikitake, Y. (no date) *Mechanism of recipient cell-dependent differences in exosome uptake*. doi:10.1186/s12885-017-3958-1.

Hu, G., Drescher, K.M. and Chen, X.M. (2012) Exosomal miRNAs: Biological properties and therapeutic potential. *Frontiers in Genetics.* 3 (APR), . doi:10.3389/fgene.2012.00056.

Hu, Y., Yan, C., Mu, L., Huang, K., Li, X., Tao, D., Wu, Y. and Qin, J. (2015) *Fibroblast-Derived Exosomes Contribute to Chemoresistance through Priming Cancer Stem Cells in Colorectal Cancer*. doi:10.1371/journal.pone.0125625.

Hu, W., Xu, S., Yao, B., Hong, M., Wu, X., Pei, H., Chang, L., Ding, N., Gao, X., Ye, C., Wang, J., Hei, T.K. and Zhou, G. (2014) MiR-663 inhibits radiation-induced bystander effects by targeting TGFB1 in a feedback mode. *RNA Biology.* **11** (9), pp. 1189–1198. doi:10.4161/rna.34345.

Huang, J., Woods, P., Normolle, D., Goff, J.P., Benos, P. V, Stehle, C.J., Steinman, R.A. and Steinman, R. (2017) Downregulation of estrogen receptor and modulation of growth of breast

cancer cell lines mediated by paracrine stromal cell signals HHS Public Access. *Breast Cancer Res Treat*. **161** (2), pp. 229–243. doi:10.1007/s10549-016-4052-0.

Huang, Y. and Li, L. (2013) DNA crosslinking damage and cancer - a tale of friend and foe *Translational Cancer Research.* **2** (3) p.pp. 144–154. doi:10.3978/j.issn.2218-676X.2013.03.01.

Huh, D., Hamilton, G.A. and Ingber, D.E. (2011) From 3D cell culture to organs-on-chips. *Trends in Cell Biology.* **21** (12) p.pp. 745–754. doi:10.1016/j.tcb.2011.09.005.

IARC Working Group on the Evaluation of Carcinogenic Risk to Humans. Pharmaceuticals. Lyon (FR): International Agency for Research on Cancer; 2012. (IARC Monographs on the Evaluation of Carcinogenic Risks to Humans, No. 100A.) Chlorambucil. Available from: https://www.ncbi.nlm.nih.gov/books/NBK304324/ [Accessed 15 July 2020].

Iacona, J.R. and Lutz, C.S. (2019) miR-146a-5p: Expression, regulation, and functions in cancer *Wiley Interdisciplinary Reviews: RNA* [online]. **10** (4) p.pp. e1533. Available from: https://onlinelibrary.wiley.com/doi/abs/10.1002/wrna.1533doi:10.1002/wrna.1533 [Accessed 16 July 2020].

Ifergan, I., Scheffer, G.L. and Assaraf, Y.G. (2005) Novel Extracellular Vesicles Mediate an ABCG2-Dependent Anticancer Drug Sequestration and Resistance. *Cancer Res* [online]. **65** (23), pp. 10952–10960. Available from: www.aacrjournals.orgdoi:10.1158/0008-5472.CAN-05-2021 [Accessed 11 June 2020].

Improgo, M.R., Tesar, B., Klitgaard, J.L., Magori-Cohen, R., Yu, L., Kasar, S., Chaudhary, D., Miao, W., Fernandes, S.M., Hoang, K., Westlin, W.F., Kim, H.T. and Brown, J.R. (2019) MYD88 L265P mutations identify a prognostic gene expression signature and a pathway for targeted inhibition in CLL. *British Journal of Haematology* [online]. 184 (6), pp. 925–936. Available from: https://onlinelibrary.wiley.com/doi/abs/10.1111/bjh.15714doi:10.1111/bjh.15714 [Accessed 5 September 2020].

Jabbour, E., O'Brien, S., Ravandi, F. and Kantarjian, H., (2015) Monoclonal antibodies in acute lymphoblastic leukemia. *Blood.* **125** (26); 4010-4016.

Jacob, D.A., Mercer, S.L., Osheroff, N. and Deweese, J.E. (2011) Etoposide Quinone Is a Redox-Dependent Topoisomerase II Poison † NIH Public Access. *Biochemistry.* **50** (25), pp. 5660–5667. doi:10.1021/bi200438m.

Jaganathan, B.G., Tisato, V., Vulliamy, T., Dokal, I., Marsh, J., Dazzi, F. and Bonnet, D. (2010) *Effects of MSC co-injection on the reconstitution of aplastic anemia patient following hematopoietic stem cell transplantation*. doi:10.1038/leu.2010.164.

Jain, C. K., Majumder, H. K., and Roychoudhury, S. (2017). Natural Compounds as Anticancer Agents Targeting DNA Topoisomerases. *Current genomics.* **18** (1), 75–92. Available from: https://doi.org/10.2174/1389202917666160808125213 [Accessed on 01 January 2021].

Jedrzejczak-Silicka, M. (2017) History of Cell Culture. In: *New Insights into Cell Culture Technology*. (no place) InTech. doi:10.5772/66905.

Jensen, R., Glazer, P.M. and Cleaver, J.E. (2004) Cell-interdependent cisplatin killing by KuDNA-dependent protein kinase signaling transduced through gap junctions [online]. Available from: www.pnas.orgcgidoi10.1073pnas.0400051101 [Accessed 10 December 2019].

Jethava, Y.S., Sica, S., Savani, B., Socola, F., Jagasia, M., Mohty, M., Nagler, A., and Bacigalupo, A. (2017) Conditioning regimens for allogeneic hematopoietic stem cell transplants in acute myeloid leukemia. *Bone Marrow Transplant*. **52** (11):1504-1511. doi: 10.1038/bmt.2017.83. Epub 2017 May 15. PMID: 28504666.

Jiang, Y., Chen, X., Tian, W., Yin, X., Wang, J. and Yang, H. (2014) The role of TGF-β1-miR-21-ROS pathway in bystander responses induced by irradiated non-small-cell lung cancer cells. *British Journal of Cancer*. **111** (4), pp. 772–780. doi:10.1038/bjc.2014.368.

Jin, C., Wu, S., Lu, X., Liu, Q., Qi, M., Lu, S., Xi, Q. and Cai, Y. (2011) Induction of the bystander effect in Chinese hamster V79 cells by actinomycin D. *Toxicology Letters*. **202** (3), pp. 178–185. doi:10.1016/j.toxlet.2011.02.002.

Joannides, M. and Grimwade, D. (2010) Molecular biology of therapy-related leukaemias *Clinical and Translational Oncology.* **12** (1) p.pp. 8–14. doi:10.1007/s12094-010-0460-5.

Johnstone, R.M., Adam, M., Hammond, J.R., Orr, L. and Turbide, C. (1987) Vesicle formation during reticulocyte maturation. Association of plasma membrane activities with released vesicles (exosomes). *Journal of Biological Chemistry*. **262** (19), pp. 9412–9420.

Kaatsch, P., Spix, C., Jung, I. and Blettner, M. (2008) Childhood leukemia in the vicinity of nuclear power plants in Germany. *Deutsches Arzteblatt*. **105** (42), pp. 725–732. doi:10.3238/arztebl.2008.0725.

Kamesaki, S., Kamesaki, H., Jorgensen, T.J., Tanizawa, A., Pommier, Y. and Cossman, J. (1993) bcl-2 Protein Inhibits Etoposide-induced Apoptosis through Its Effects on Events Subsequent to Topoisomerase II-induced DNA Strand Breaks and Their Repair. *Cancer Research*. **53** (18), pp. 4251–4256.

Kanemoto, S., Nitani, R., Murakami, T., Kaneko, M., Asada, R., Matsuhisa, K., Saito, A. and Imaizumi, K. (2016) Multivesicular body formation enhancement and exosome release during endoplasmic reticulum stress. *Biochemical and Biophysical Research Communications*. **480** (2), pp. 166–172. doi:10.1016/j.bbrc.2016.10.019.

Kathiravan, M.K., Khilare, M.M., Nikoomanesh, K., Chothe, A.S. and Jain, K.S. (2012) *Journal of Enzyme Inhibition and Medicinal Chemistry Topoisomerase as target for antibacterial and anticancer drug discovery*. Available from: https://www.tandfonline.com/action/journalInformation?journalCode=ienz20doi:10.3109/14756366.2012.658785 [Accessed 22 November 2019].

Katsuda, T., Ikeda, S., Yoshioka, Y., Kosaka, N., Kawamata, M. and Ochiya, T. (2014) Physiological and pathological relevance of secretory microRNAs and a perspective on their clinical application *Biological Chemistry.* **395** (4) p.pp. 365–373. doi:10.1515/hsz-2013-0222.

Keklikoglou, I., Cianciaruso, C., Güç, E., Squadrito, M.L., Spring, L.M., Tazzyman, S., Lambein, L., Poissonnier, A., Ferraro, G.B., Baer, C., Cassará, A., Guichard, A., Luisa Iruela-Arispe, M., Lewis, C.E., et al. (2019) Chemotherapy elicits pro-metastatic extracellular vesicles in breast cancer models Europe PMC Funders Group. *Nat Cell Biol* [online]. **21** (2), pp. 190–202. Available from: http://www.nature.com/authors/editorial_policies/license.html#terms%23Correspondence:michele.depalma@epfl.chdoi:10.6019/PXD010362 [Accessed 25 June 2020].

Kemp, K., Morse, R., Sanders, K., Hows, J. and Donaldson, C. (2011) Alkylating chemotherapeutic agents cyclophosphamide and melphalan cause functional injury to human bone marrow-derived mesenchymal stem cells. *Annals of Hematology*. **90** (7), pp. 777–789. doi:10.1007/s00277-010-1141-8.

Khalade, A., Jaakkola, M.S., Pukkala, E. and Jaakkola, J.J. (2010) Exposure to benzene at work and the risk of leukemia: A systematic review and meta-analysis. *Environmental Health: A Global Access Science Source* [online]. **9** (1). Available from: http://www.ehjournal.net/content/9/1/31doi:10.1186/1476-069X-9-31

Kilian, P.H., Skrzypek, S., Becker, N. and Havemann, K. (2001) Exposure to armament wastes and leukemia: A case-control study within a cluster of AML and CML in Germany. *Leukemia Research*. **25** (10), pp. 839–845. doi:10.1016/S0145-2126(01)00035-2.

Kim, M.Y. (2017) Intracellular and extracellular factors influencing the genotoxicity of nitric oxide and reactive oxygen species. *Oncology Letters*. **13** (3), pp. 1417–1424. doi:10.3892/ol.2017.5584.

Kim, M.S., Haney, M.J., Zhao, Y., Mahajan, V., Deygen, I., Klyachko, N.L., Inskoe, E., Piroyan, A., Sokolsky, M., Okolie, O., Hingtgen, S.D., Kabanov, A. V and Batrakova, E. V (2016) Development of Exosome-encapsulated Paclitaxel to Overcome MDR in Cancer cells HHS Public Access. *Nanomedicine*. 12 (3), pp. 655–664. doi:10.1016/j.nano.2015.10.012.

King, H.W., Michael, M.Z. and Gleadle, J.M. (2012) Hypoxic enhancement of exosome release by breast cancer cells. *BMC Cancer*. 12 . doi:10.1186/1471-2407-12-421.

Klammer, H., Mladenov, E., Li, F. and Iliakis, G. (2015) Bystander effects as manifestation of intercellular communication of DNA damage and of the cellular oxidative status *Cancer Letters.* **356** (1) p.pp. 58–71. doi:10.1016/j.canlet.2013.12.017.

Koch, R., Aung, T., Vogel, D., Chapuy, B., Wenzel, D., Becker, S., Sinzig, U., Venkataramani, V., Von Mach, T., Jacob, R., Truemper, L. and Wulf, G.G. (2016) *Cancer Therapy: Preclinical Nuclear Trapping through Inhibition of Exosomal Export by Indomethacin Increases Cytostatic Efficacy of Doxorubicin and Pixantrone*. Available from: www.graphpad.comdoi:10.1158/1078-0432.CCR-15-0577 [Accessed 27 March 2021].

Kogure, T., Lin, W.-L., Yan, I.K., Braconi, C. and Patel, T. (2011) Intercellular nanovesicle-mediated microRNA transfer: A mechanism of environmental modulation of hepatocellular cancer cell growth. *Hepatology* [online]. **54** (4), pp. 1237–1248. Available from: http://doi.wiley.com/10.1002/hep.24504doi:10.1002/hep.24504 [Accessed 16 December 2019].

Kolb, G., Becker, N., Scheller, S., Zugmaier, G., Pralle, H., Wahrendorf, J. and Havemann, K. (1993) Increased risk of acute myelogeneous leukemia (AML) and chronic myelogenous leukemia (CML) in a county of Hesse, Germany. *Sozial- und Präventivmedizin SPM*. **38** (4), pp. 190–195. doi:10.1007/BF01624535.

Kondo, N., Takahashi, A., Ono, K. and Ohnishi, T. (2010) DNA damage induced by alkylating agents and repair pathways *Journal of Nucleic Acids* 2010. doi:10.4061/2010/543531.

Konoshenko, M.Y., Lekchnov, E.A., Vlassov, A. V and Laktionov, P.P. (2018) *Isolation of Extracellular Vesicles: General Methodologies and Latest Trends*. Available from: https://doi.org/10.1155/2018/8545347doi:10.1155/2018/8545347 [Accessed 15 June 2020].

Kornek, M., Melo, S.A., Bidarimath, M., Vader pvader, P., Willms, E., Cabañas, C., Mäger, I., A Wood, M.J. and Vader, P. (2018) *extracellular vesicle Heterogeneity: Subpopulations, isolation Techniques, and Diverse Functions in Cancer Progression*. **9** pp. 1. Available from: www.frontiersin.orgdoi:10.3389/fimmu.2018.00738.

Kortubash, I., Boyko, A., Rodriguez-Juarez, R., McDonald, R.J., Tryndyak, V.P., Kovalchuk, I., Pogribny, I.P. and Kovalchuk, O. (2007) Role of epigenetic effectors in maintenance of the long-term persistent bystander effect in spleen in vivo. *Carcinogenesis*. **28** (8); 1831-1838.

Kortubash, I., Zemp, F.J., Kutanzi, K., Luzhna, L., Loree, J., Kolb, B. and Kovalchuk, O. (2008) *Cell Cycle Sex-specific microRNAome deregulation in the shielded bystander spleen of cranially exposed mice*. Available from: https://www.tandfonline.com/action/journalInformation?journalCode=kccy20doi:10.4161/cc.7.11.5981 [Accessed 29 May 2020].

Kosaka, N., Iguchi, H., Yoshioka, Y., Takeshita, F., Matsuki, Y. and Ochiya, T. (2010) *Secretory Mechanisms and Intercellular Transfer of MicroRNAs in Living Cells * □ S*. Available from: http://www.jbc.orgdoi:10.1074/jbc.M110.107821 [Accessed 24 June 2020].

Kosaka, N., Yoshioka, Y., Fujita, Y. and Ochiya, T. (2016) Versatile roles of extracellular vesicles in cancer *Journal of Clinical Investigation.* **126** (4) p.pp. 1163–1172. doi:10.1172/JCI81130.

Koumangoye, R.B., Sakwe, A.M., Goodwin, J.S., Patel, T. and Ochieng, J. (2011) Detachment of Breast Tumor Cells Induces Rapid Secretion of Exosomes Which Subsequently Mediate Cellular Adhesion and Spreading. *PLoS ONE* [online]. **6** (9), pp. 24234. Available from: www.plosone.orgdoi:10.1371/journal.pone.0024234 [Accessed 16 December 2019].Koussounadis, A., Langdon, S.P., Harrison, D.J. and Smith, V.A. (2014) *Chemotherapy-induced dynamic gene expression changes in vivo are prognostic in ovarian cancer*. Available from: www.bjcancer.comdoi:10.1038/bjc.2014.258 [Accessed 29 May 2020].

Kovalchuk, O., Zemp, F.J., Filkowski, J.N., Altamirano, A.M., Dickey, J.S., Jenkins-Baker, G., Marino, S.A., Brenner, D.J., Bonner, W.M. and Sedelnikova, O.A. (2010) microRNAome changes in

bystander three-dimensional human tissue models suggest priming of apoptotic pathways. *Carcinogenesis*. **31** (10), pp. 1882–1888. doi:10.1093/carcin/bgq119.

Kouzi, F., Zibara, K., Bourgeais, J., Picou, F., Gallay, N., Brossaud, J., Dakik, H., Roux, B., Hamard, S., Le Nail, L.R., Hleihel, R., Foucault, A., Ravalet, N., Rouleux-Bonnin, F., et al. (2020) Disruption of gap junctions attenuates acute myeloid leukemia chemoresistance induced by bone marrow mesenchymal stromal cells. *Oncogene* [online]. **39** (6), pp. 1198–1212. Available from: https://doi.org/10.1038/s41388-019-1069-ydoi:10.1038/s41388-019-1069-y [Accessed 17 July 2020].

Kovalchuk, O. and Baulch, J.E. (2008) Epigenetic changes and nontargeted radiation effects - Is there a link? *Environmental and Molecular Mutagenesis.* **49** (1) p.pp. 16–25. doi:10.1002/em.20361.

Kovalchuk, O., Zemp, F.J., Filkowski, J.N., Altamirano, A.M., Dickey, J.S., Jenkins-Baker, G., Marino, S.A., Brenner, D.J., Bonner, W.M. and Sedelnikova, O.A. (2010) microRNAome changes in bystander three-dimensional human tissue models suggest priming of apoptotic pathways. *Carcinogenesis*. **31** (10), pp. 1882–1888. doi:10.1093/carcin/bgq119.

Kreger, B.T., Johansen, E.R., Cerione, R.A. and Antonyak, M.A. (no date) *The Enrichment of Survivin in Exosomes from Breast Cancer Cells Treated with Paclitaxel Promotes Cell Survival and Chemoresistance*. Available from: www.mdpi.com/journal/cancersdoi:10.3390/cancers8120111 [Accessed 25 June 2020].

Kubara, P. M., Kernéis-Golsteyn, S., Studény, A., Lanser, B. B., Meijer, L., & Golsteyn, R. M. (2012). Human cells enter mitosis with damaged DNA after treatment with pharmacological concentrations of genotoxic agents. *The Biochemical journal*. **446** (3), 373–381. https://doi.org/10.1042/BJ20120385 [Accessed 28 February 2019].

Kumar, A., Bhattacharyya, J. and Jaganathan, B.G. (2017) Adhesion to stromal cells mediates imatinib resistance in chronic myeloid leukemia through ERK and BMP signaling pathways. *Scientific Reports* [online]. **7** (1). Available from:

www.nature.com/scientificreports/doi:10.1038/s41598-017-10373-3 [Accessed 25 February 2020].

Kumar, A., Anand, T., Bhattacharyya, J., Sharma, A. and Grace Jaganathan, B. (2018) *K562 chronic myeloid leukemia cells modify osteogenic differentiation and gene expression of bone marrow stromal cells*. Available from: https://doi.org/10.1007/s12079-017-0412-8doi:10.1007/s12079-017-0412-8 [Accessed 25 February 2020].

Kumar, B., Garcia, M., Weng, L., Jung, X., Murakami, J.L., Hu, X., Mcdonald, T., Lin, A., Kumar, A.R., Digiusto, D.L., Stein, A.S., Pullarkat, V.A., Hui, S.K., Carlesso, N., et al. (2017) Acute myeloid leukemia transforms the bone marrow niche into a leukemia-permissive microenvironment through exosome secretion. *Nature Publishing Group* [online]. **32**. Available from: www.nature.com/leudoi:10.1038/leu.2017.259 [Accessed 28 October 2019].

Kumar, R., Godavarthy, P.S. and Krause, D.S. (2018) The bone marrow microenvironment in health and disease at a glance. *Journal of Cell Science*. **131** (4). doi:10.1242/jcs.201707.

Kumar, S., Gupta, V., Bharti, A., Meena, L., Gupta, V. and Shukla, J. (2019) A study to determine the clinical, hematological, cytogenetic, and molecular profile in CML patient in and around Eastern UP, India. *Journal of Family Medicine and Primary Care*. **8** (7), pp. 2450. doi:10.4103/jfmpc.jfmpc_307_19.

Kumari, R., Sharma, A., Kumar Ajay, A. and Kumar Bhat, M. (2009) *Mitomycin C induces bystander killing in homogeneous and heterogeneous hepatoma cellular models*. Available from: http://www.molecular-cancer.com/content/8/1/87doi:10.1186/1476-4598-8-87 [Accessed 10 December 2019].

Kyle, R.A., Jacobus, S., Friedenberg, W.R., Slabber, C.F., Rajkumar, S.V. and Greipp, P.R. (2009) The treatment of multiple myeloma using vincristine, carmustine, melphalan, cyclophosphamide, and prednisone (VBMCP) alternating with high-dose cyclophosphamide and α2β interferon versus VBMCP: Results of a Phase III Eastern Cooperative Oncology Group Stu. *Cancer*. **115** (10), pp. 2155–2164. doi:10.1002/cncr.24221.

Laner-Plamberger, S., Oeller, M., Poupardin, R., Kirsch, L., Kalathur, R., Hochmann, S., Pachler, K., Kreutzer, C., Erdmann, G., Rohde, E., Strunk, D. and Schallmoser, K. (2019) Heparin Differentially Impacts Gene Expression of Stromal Cells from Various Tissues. *Scientific Reports.* **9,** 7258 (2019).

Lapi, S., Nocchi, F., Lamanna, R., Passeri, S., Iorio, M., Paolicchi, A., Urciuoli, P., Coli, A., Abramo, F., Miragliotta, V., Giannessi, E., Stornelli, M.R., Vanacore, R., Stampacchia, G., et al. (2008) Different media and supplements modulate the clonogenic and expansion properties of rabbit bone marrow mesenchymal stem cells. *BMC Research Notes* [online]. 1 . Available from: http://www.biomedcentral.com/1756-0500/1/53doi:10.1186/1756-0500-1-53 [Accessed 9 September 2020].

Larsen, M.C., Almeldin, A., Tong, T., Rondelli, C.M., Maguire, M., Jaskula-Sztul, R. and Jefcoate, C.R. (2020) Cytochrome P4501B1 in bone marrow is co-expressed with key markers of mesenchymal stem cells. BMS2 cell line models PAH disruption of bone marrow niche development functions. Available from: https://doi.org/10.1016/j.taap.2020.115111doi:10.1016/j.taap.2020.115111 [Accessed 28 August 2020].

Le Hégarat, L., Huet, S. and Fessard, V. (2012) A co-culture system of human intestinal Caco-2 cells and lymphoblastoid TK6 cells for investigating the genotoxicity of oral compounds. *Mutagenesis*. **27** (6), pp. 631–636. doi:10.1093/mutage/ges028.

Leca, J., Martinez, S., Lac, S., Nigri, J., Secq, V., Rubis, M., Bressy, C., Sergé, A., Lavaut, M.N., Dusetti, N., Loncle, C., Roques, J., Pietrasz, D., Bousquet, C., et al. (2016) Cancer-associated fibroblast-derived annexin A6+ extracellular vesicles support pancreatic cancer aggressiveness. *Journal of Clinical Investigation*. **126** (11), pp. 4140–4156. doi:10.1172/JCI87734.

Lee, S.S., Won, J.H., Lim, G.J., Han, J., Lee, J.Y., Cho, K.O. and Bae, Y.K. (2019) A novel population of extracellular vesicles smaller than exosomes promotes cell proliferation. *Cell Communication and Signaling*. **17** (1). doi:10.1186/s12964-019-0401-z.

Lee, K. M., Choi, K. H., & Ouellette, M. M. (2004). Use of exogenous hTERT to immortalize primary human cells. *Cytotechnology*, **45** (1-2); pp. 33–38. https://doi.org/10.1007/10.1007/s10616-004-5123-3 [Accessed 28 December 2020].

Lee, H., Groot, M., Pinilla-Vera, M., Fredenburgh, L.E. and Jin, Y. (2019) Identification of miRNA-rich vesicles in bronchoalveolar lavage fluids: Insights into the function and heterogeneity of extracellular vesicles HHS Public Access. *J Control Release*. **294** pp. 43–52. doi:10.1016/j.jconrel.2018.12.008.

Lee, J.K., Park, S.R., Jung, B.K., Jeon, Y.K., Lee, Y.S., Kim, M.K., Kim, Y.G., Jang, J.Y. and Kim, C.W. (2013) Exosomes derived from mesenchymal stem cells suppress angiogenesis by down-regulating VEGF expression in breast cancer cells. *PLoS ONE*. **8** (12). doi:10.1371/journal.pone.0084256.

Lee, R.C., Feinbaum, R.L. and Ambros, V. (1993) The C. elegans heterochronic gene lin-4 encodes small RNAs with antisense complementarity to lin-14. *Cell*. **75** (5), pp. 843–854. doi:10.1016/0092-8674(93)90529-Y.

Lee, E.J., Pollak, A., Leavitt, R.D., Testa, J.R. and Schiffer, C.A. (1987) Minimally differentiated acute nonlymphocytic leukemia: A distinct entity. *Blood* [online]. **70** (5), pp. 1400–1406. Available from: https://ashpublications.org/blood/article/70/5/1400/109346/Minimally-differentiated-acute-nonlymphocyticdoi:10.1182/blood.v70.5.1400.bloodjournal7051400

Lee, H.Y. and Hong, I.S. (2017) Double-edged sword of mesenchymal stem cells: Cancer-promoting versus therapeutic potential *Cancer Science.* **108** (10) p.pp. 1939–1946. doi:10.1111/cas.13334.

Lee, M.S., Youn, C., Kim, J.H., Park, B.J., Ahn, J., Hong, S., Kim, Y.D., Shin, Y.K. and Park, S.G. (2017) Enhanced cell growth of adipocyte-derived mesenchymal stem cells using chemically-defined serum-free media. *International Journal of Molecular Sciences*. 18 (8). doi:10.3390/ijms18081779.

Lehnert, B.E. and Goodwin, E.H. (1997) A New Mechanism for DNA Alterations Induced by Alpha Particles Such as Those Emitted by Radon and Radon Progeny *Environ Health Perspect* **1** (5).

Li, J., Lai, Y., Ma, J., Liu, Y., Bi, J., Zhang, L., Chen, L., Yao, C., Lv, W., Chang, G., Wang, S., Ouyang, Kong, W., Cheng, Y., Liang, H., Chen, Q., Xiao, C., Li, K., Huang, Z. and Zhang, J. (2018) Prognostic value of miR-17-5p in cancers: A meta-analysis. *OncoTargets and Therapy* [online]. **11** pp. 3541–3549. Available from: http://dx.doi.org/10.2147/OTT.S150340doi:10.2147/OTT.S150340 [Accessed 2 July 2020].

Li, J., Law, H.K.W., Lau, Y.L. and Chan, G.C.F. (2004) Differential damage and recovery of human mesenchymal stem cells after exposure to chemotherapeutic agents. *British Journal of Haematology* [online]. **127** (3), pp. 326–334. Available from: http://doi.wiley.com/10.1111/j.1365-2141.2004.05200.xdoi:10.1111/j.1365-2141.2004.05200.x [Accessed 15 January 2020].

Li, J., Lee, Y., Johansson, H.J., Mäger, I., Vader, P., Nordin, J.Z., Wiklander, O.P.B., Lehtiö, J., Wood, M.J.A. and El Andaloussi, S. (2015) Serum-free culture alters the quantity and protein composition of neuroblastoma-derived extracellular vesicles. *Journal of Extracellular Vesicles*. **4** (2015), pp. 1–12. doi:10.3402/jev.v4.26883.

Li, J., Lai, Y., Ma, J., Liu, Y., Bi, J., Zhang, L., Chen, L., Yao, C., Lv, W., Chang, G., Wang, S., Ouyang, M. and Wang, W. (2017) miR-17-5p suppresses cell proliferation and invasion by targeting ETV1 in triple-negative breast cancer. *BMC Cancer*. **17** (1). doi:10.1186/s12885-017-3674-x.

Li, M., Zeringer, E., Barta, T., Schageman, J., Cheng, A. and Vlassov, A. V (2014) Analysis of the RNA content of the exosomes derived from blood serum and urine and its potential as biomarkers. *Philosophical Transactions of the Royal Society B: Biological Sciences* [online]. **369** (1652). Available from: http://dx.doi.org/10.1098/rstb.2013.0502doi:10.1098/rstb.2013.0502 [Accessed 23 June 2020].

Li, X.Q., Liu, J.T., Fan, L.L., Liu, Y., Cheng, L., Wang, F., Yu, H.Q., Gao, J., Wei, W., Wang, H. and Sun, G.P. (2016) Exosomes derived from gefitinib-treated EGFR-mutant lung cancer cells alter cisplatin

sensitivity via up-regulating autophagy. *Oncotarget*. **7** (17), pp. 24585–24595. doi:10.18632/oncotarget.8358.

Liang, W., Xia, H., Li, J. and Zhao, R.C. (2011) Human adipose tissue derived mesenchymal stem cells are resistant to several chemotherapeutic agents. *Cytotechnology*. **63** (5), pp. 523–530. doi:10.1007/s10616-011-9374-5.

Liao, W. and Sharma, S. (2016) Modulation of B-cell receptor and microenvironment signaling by a guanine exchange factor in B-cell malignancies. *Cancer Biology and Medicine*. **13** (2), pp. 277–285. doi:10.20892/j.issn.2095-3941.2016.0026.

Liao, H., He, H., Chen, Y., Zeng, F., Huang, J., Wu, L. and Chen, Y. (2014) Effects of long-term serial cell passaging on cell spreading, migration, and cell-surface ultrastructures of cultured vascular endothelial cells. *Cytotechnology*. **66** (2), pp. 229–238. doi:10.1007/s10616-013-9560-8.

Lim, P.K., Bliss, S.A., Patel, S.A., Taborga, M., Dave, M.A., Gregory, L.A., Greco, S.J., Bryan, M., Patel, P.S. and Rameshwar, P. (2011) *Gap Junction-Mediated Import of MicroRNA from Bone Marrow Stromal Cells Can Elicit Cell Cycle Quiescence in Breast Cancer Cells*. Available from: http://cancerres.aacrjournals.org/doi:10.1158/0008-5472.CAN-10-2372 [Accessed 25 June 2020].

Lin, X., Wei, F., Major, P., Al-Nedawi, K., Al Saleh, H.A. and Tang, D. (2017) Microvesicles contribute to the bystander effect of DNA damage. *International Journal of Molecular Sciences* [online]. **18** (4). Available from: www.mdpi.com/journal/ijmsdoi:10.3390/ijms18040788 [Accessed 11 June 2020].

Lin, Y.-M., Zhang, G.-Z., Leng, Z.-X., Zhen-Xia, L.U., Bu, L.-S., Shen, G. and Shao-Juan, Y. (2006) Study on the bone marrow mesenchymal stem cells induced drug resistance in the U937 cells and its mechanism *Chinese Medical Journal*. **119** (11).

Liu, Y., Zhao, J., Jiang, J., Chen, F. and Fang, X. (2020) Doxorubicin Delivered Using Nanoparticles Camouflaged with Mesenchymal Stem Cell Membranes to Treat Colon Cancer. *International Journal of Nanomedicine*. Volume **15** pp. 2873–2884. doi:10.2147/ijn.s242787.

Liu, C. and Su, C. (2019) Design strategies and application progress of therapeutic exosomes. *Theranostics* [online]. **9** (4), pp. 1015–1028. Available from: http://www.thno.orgdoi:10.7150/thno.30853

Loeber, R., Michaelson, E., Fang, Q., Campbell, C., Pegg, A., Tretyakova, N., Res, C. and Author, T. (2008) Cross-linking of the DNA repair protein O 6-alkylguanine DNA alkyltransferase to DNA in the presence of antitumor nitrogen mustards NIH Public Access Author Manuscript. *Chem Res Toxicol* [online]. **21** (4), pp. 787–795. Available from: http://pubs.acs.org.doi:10.1021/tx7004508 [Accessed 12 November 2019].

Lopatina, T., Gai, C., Deregibus, M.C., Kholia, S. and Camussi, G. (2016) Cross Talk between Cancer and Mesenchymal Stem Cells through Extracellular Vesicles Carrying Nucleic Acids. *Frontiers in Oncology*. **6**. doi:10.3389/fonc.2016.00125LiverTox: Clinical and Research Information on Drug-Induced Liver Injury (2012) Bethesda (MD): National Institute of Diabetes and Digestive and Kidney Diseases; Carmustine. Available from: https://www.ncbi.nlm.nih.gov/books/NBK548307/ [Updated 2017 Jan 17].

Lopez Perez, R., Münz, F., Vidoni, D., Rühle, A., Trinh, T., Sisombath, S., Zou, B., Wuchter, P., Debus, J., Grosu, A.L., Saffrich, R., Huber, P.E. and Nicolay, N.H. (2019) Mesenchymal stem cells preserve their stem cell traits after exposure to antimetabolite chemotherapy. *Stem Cell Res.* **40.** 101536. ISSN 1873-5061. https://doi.org/10.1016/j.scr.2019.101536 [Accessed 27 December 2020].

Lorge, E., Moore, M.M., Clements, J., O'Donovan, M., Fellows, M.D., Honma, M., Kohara, A., Galloway, S., Armstrong, M.J., Thybaud, V., Gollapudi, B., Aardema, M.J. and Tanir, J.Y. (2016) Standardized cell sources and recommendations for good cell culture practices in genotoxicity

testing. *Mutation Research - Genetic Toxicology and Environmental Mutagenesis*. **809** pp. 1–15. doi:10.1016/j.mrgentox.2016.08.001.

Lou, G., Chen, Z., Zheng, M. and Liu, Y. (2017) Mesenchymal stem cell-derived exosomes as a new therapeutic strategy for liver diseases. *Nature Publishing Group* [online]. pp. 346.

Lovat, F., Fassan, M., Gasparini, P., Rizzotto, L., Cascione, L., Pizzi, M., Vicentini, C., Balatti, V., Palmieri, D., Costinean, S., & Croce, C. M. (2015). miR-15b/16-2 deletion promotes B-cell malignancies. *Proceedings of the National Academy of Sciences of the United States of America.* **112 (**37); 11636–11641. https://doi.org/10.1073/pnas.1514954112 [Accessed 01 March 2020].

Ludwig, N., Whiteside, T.L. and Reichert, T.E. (2019) Challenges in exosome isolation and analysis in health and disease *International Journal of Molecular Sciences.* **20** (19). doi:10.3390/ijms20194684.

Lv, L.-H., Wan, Y.-L., Lin, Y., Zhang, W., Yang, M., Li, G.-L., Lin, H.-M., Shang, C.-Z., Chen, Y.-J. and Min, J. (2012) *Anticancer Drugs Cause Release of Exosomes with Heat Shock Proteins from Human Hepatocellular Carcinoma Cells That Elicit Effective Natural Killer Cell Antitumor Responses in Vitro *. doi:10.1074/jbc.M112.340588.

M. Lyng, F., B. Semour, C. and Mothersill, C. (2002) Early Events in the Apoptotic Cascade Initiated in Cells Treated with Medium from the Progeny of Irradiated Cells. *Radiation Protection Dosimetry* [online]. **99** (1), pp. 169–172. Available from: https://academic.oup.com/rpd/article-abstract/99/1-4/169/1687763doi:10.1093/oxfordjournals.rpd.a006753 [Accessed 27 May 2020].

Ma, H. and Liu, T. (2016) Development of donor cell leukemia following peripheral blood stem cell transplantation for severe aplastic anemia: A case report. *Oncology Letters*. **11** (6), pp. 3858–3862. doi:10.3892/ol.2016.4452.

Maghazachi, A., Olive, D., Brenner, A.K., Nepstad, I. and Bruserud, Ø. (2017) Mesenchymal stem cells support survival and Proliferation of Primary human acute Myeloid leukemia cells through

heterogeneous Molecular Mechanisms. *Article* [online]. **8** pp. 1. Available from: www.frontiersin.orgdoi:10.3389/fimmu.2017.00106 [Accessed 16 May 2020].

Mahalingaiah, P.K., Palenski, T. and Van Vleet, T.R., (2018). An In Vitro Model of Hematotoxicity: Differentiation of Bone Marrow–Derived Stem/Progenitor Cells into Hematopoietic Lineages and Evaluation of Lineage-Specific Hematotoxicity. *Current protocols in toxicology*, **76** (1), e45.

Mallam, E., Kemp, K., Wilkins, A., Rice, C. and Scolding, N. (2010) Characterization of in vitro expanded bone marrow-derived mesenchymal stem cells from patients with multiple sclerosis. *Multiple Sclerosis*. 16 (8), pp. 909–918. doi:10.1177/1352458510371959.

Mannerström, B., Paananen, R.O., Abu-Shahba, A.G., Moilanen, J., Seppänen-Kaijansinkko, R. and Kaur, S. (2019) Extracellular small non-coding RNA contaminants in fetal bovine serum and serum-free media. *Scientific Reports* [online]. **9** (1). Available from: https://doi.org/10.1038/s41598-019-41772-3doi:10.1038/s41598-019-41772-3 [Accessed 30 June 2020].

Mansour, I., Zayed, R.A., Said, F. and Latif, L.A. (2016) Indoleamine 2,3-dioxygenase and regulatory T cells in acute myeloid leukemia. *Hematology* [online]. **21** (8), pp. 447–453. Available from: https://doi.org/10.1080/10245332.2015.1106814doi:10.1080/10245332.2015.1106814 [Accessed 28 October 2019].

Marchetti, F., Bishop, J.B., Lowe, X., Generoso, W.M., Hozier, J. and Wyrobek, A.J. (2001) Etoposide induces heritable chromosomal aberrations and aneuploidy during male meiosis in the mouse. *Proceedings of the National Academy of Sciences of the United States of America* [online]. **98** (7), pp. 3952–3957. Available from: www.pnas.orgcgidoi10.1073pnas.061404598doi:10.1073/pnas.061404598 [Accessed 28 November 2019].

Marchetti, F., Pearson, F.S., Bishop, J.B. and Wyrobek, A.J. (2006) Etoposide induces chromosomal abnormalities in mouse spermatocytes and stem cell spermatogonia. *Human Reproduction* [online]. **21** (4), pp. 888–895. Available from:

https://academic.oup.com/humrep/article-abstract/21/4/888/585521doi:10.1093/humrep/dei416 [Accessed 28 November 2019].

Mareschi, K., Rustichelli, D., Calabrese, R., Gunetti, M., Sanavio, F., Castiglia, S., Risso, A., Ferrero, I., Tarella, C. and Fagioli, F. (2012) Multipotent mesenchymal stromal stem cell expansion by plating whole bone marrow at a low cellular density: A more advantageous method for clinical use. *Stem Cells International*. doi:10.1155/2012/920581.

Marín, A., Martín, M., Liñán, O., Alvarenga, F., López, M., Fernández, L., Büchser, D. and Cerezo, L. (2015) Bystander effects and radiotherapy *Reports of Practical Oncology and Radiotherapy* [online] **20** (1);12–21. Available from: www.sciencedirect.comdoi:10.1016/j.rpor.2014.08.004 [Accessed 17 July 2020].

Marzi, M.J., Montani, F., Rose, †, Carletti, M., Dezi, F., Dama, E., Bonizzi, G., Sandri, M.T., Rampinelli, C., Bellomi, M., Maisonneuve, P., Spaggiari, L., Veronesi, G., Bianchi, F., et al. (2016) *Optimization and Standardization of Circulating MicroRNA Detection for Clinical Application: The miR-Test Case*. Available from: http://www.clinchem.org/content/vol62/issue5.doi:10.1373/clinchem.2015.251942

Mathews, E., Laurie, T., O'Riordan, K. and Nabhan, C. (2008) Liver Involvement with Acute Myeloid Leukemia. *Case Reports in Gastroenterology* [online]. **2** (1), pp. 121–124. Available from: www.karger.com/crgdoi:10.1159/000120756

Mattei, F., Cabrera-Fuentes, H.A., Bei, R., Wu, en, Ding, J., Yang, J., Guo, X. and Zheng, Y. (2018) MicroRNA Roles in the Nuclear Factor Kappa B Signaling Pathway in Cancer. *Front. Immunol* [online]. **9** pp. 546. Available from: www.frontiersin.orgdoi:10.3389/fimmu.2018.00546 [Accessed 29 May 2020].

Mathews, E., Laurie, T., O'Riordan, K. and Nabhan, C. (2008) Liver Involvement with Acute Myeloid Leukemia. *Case Reports in Gastroenterology* [online]. 2 (1), pp. 121–124. Available from: www.karger.com/crgdoi:10.1159/000120756

May, J.E., Donaldson, C., Gynn, L. and Ruth Morse, H. (2018) Chemotherapy-induced genotoxic damage to bone marrow cells: Long-term implications. *Mutagenesis*. **33** (3), pp. 241–251. doi:10.1093/mutage/gey014.

McLean, A., Woods, R.L., Farmer, P. *et al.,* (1979) Pharmacokinetics and metabolism of chlorambucil in patients with malignant disease. Cancer Treatment Reviews. **6**; IN3-42.

McMahon, M., Javidi-Sharifi, N., Martinez, J., English, I., Joshi, S.K., Scopim-Ribeiro, R., Viola, S.K., Edwards V, D.K., Agarwal, A., Lopez, C., Jorgens, D., Tyner, J.W., Druker, B.J. and Traer, E. (2019) *FGF2-FGFR1 signaling regulates release of Leukemia-Protective exosomes from bone marrow stromal cells*. Available from: https://doi.org/10.7554/eLife.40033.001doi:10.7554/eLife.40033.001

McNally, R.J.Q., Stiller, C., Vincent, T.J. and Murphy, M.F.G. (2014) Cross-space-time clustering of childhood cancer in Great Britain: Evidence for a common aetiology. *International Journal of Cancer*. **134** (1), pp. 136–143. doi:10.1002/ijc.28332.

McNeil, P.L. and Steinhardt, R.A. (1997) Mini-Review Loss, Restoration, and Maintenance of Plasma Membrane Integrity *The Journal of Cell Biology.* **137** (1).

McNerney, M.E., Godley, L.A. and Le Beau, M.M. (2017) Therapy-related myeloid neoplasms: When genetics and environment collide *Nature Reviews Cancer* [online]. **17** (9) p.pp. 513–527. Available from: www.nature.com/nrcdoi:10.1038/nrc.2017.60 [Accessed 17 July 2020].

Meier, C., Steinhauer, T.N., Koczian, F., Plitzko, B., Jarolim, K., Girreser, U., Braig, S., Marko, D., Vollmar, A.M. and Clement, B. (2017) A dual topoisomerase inhibitor of intense pro-apoptotic and antileukemic nature for cancer treatment. *ChemMedChem*. **12** (5), pp. 347–352. doi:10.1002/cmdc.201700026.

Meikrantz, W., Bergom, M.A., Memisoglu, A. and Samson, L. (1998) O6-alkylguanine DNA lesions trigger apoptosis. *Carcinogenesis.* **19** (2); pp. 369-72. doi: 10.1093/carcin/19.2.369.

Mergenthaler, H.G., Bruhl, P., Ehninger, G. and Heidemann, E. (1987) Comparative in vitro toxicity of mitoxanatrone and adriamycin in human granulocyte-macrophage progenitor cells. *Cancer Chemotherapy and Pharmacology*. **20** (1), pp. 8–12. doi:10.1007/BF00252951.

Merle, P., Morvan, D., Caillaud, D. and Demidem, A. (2008) Chemotherapy-induced bystander effect in response to several chloroethylnitrosoureas: An origin independent of DNA damage? *Anticancer Research*. **28** (1 A), pp. 21–28.

Merten, O.W. (2015) Advances in cell culture: Anchorage dependence *Philosophical Transactions of the Royal Society B: Biological Sciences.* **370** (1661). doi:10.1098/rstb.2014.0040.

Mian, Y.A. and Zeleznik-Le, N.J. (2016) The miR-17~92 cluster contributes to MLL leukemia through the repression of MEIS1 competitor PKNOX1. *Leukemia Research*. 46 pp. 51–60. doi:10.1016/j.leukres.2016.04.006.

Miera, E., Rakus, J.F., Dankert, J.F., Shang, S., Kerbel, R.S., Bhardwaj, N., Shao, Y., Darvishian, F., Zavadil, J., et al. (2011) MiR-30b/30d Regulation of GalNAc Transferases Enhances Invasion and Immunosuppression during Metastasis. *Cancer Cell*. **20** (1), pp. 104–118. doi:10.1016/j.ccr.2011.05.027.

Millard, M., Gallagher, J.D., Olenyuk, B.Z. and Neamati, N. (2013) *A Selective Mitochondrial-Targeted Chlorambucil with Remarkable Cytotoxicity in Breast and Pancreatic Cancers*. Available from: https://pubs.acs.org/sharingguidelinesdoi:10.1021/jm4012438 [Accessed 27 November 2019].

Millward, M.J., Newell, D.R., Yuen, K., Matthews, J.P., Balmanno, K., Charlton, C.J., Gumbrell, L., Lind, M.J., Chapman, F., Proctor, M. (1995) Pharmacokinetics and pharmacodynamics of prolonged oral etoposide in women with metastatic breast cancer. *Cancer Chemotherapy and Pharmacology.* 37; 161–167.

Miranda-Filho, A., Piñeros, M., Ferlay, J., Soerjomataram, I., Monnereau, A. and Bray, F. (2018) Epidemiological patterns of leukaemia in 184 countries: a population-based study. *The Lancet Haematology*. **5** (1), pp. e14–e24. doi:10.1016/S2352-3026(17)30232-6.

Mitchell, C., Hall, G. and Clarke, R.T. (2009) Acute leukaemia in children: Diagnosis and management *BMJ (Online)*. **338** (7709) p.pp. 1491–1495. doi:10.1136/bmj.b2285.

Molina O., Abad M.A., Solé F. and Menéndez P. (2020) Aneuploidy in Cancer: Lessons from Acute Lymphoblastic Leukemia. Trends Cancer. Sep 17:S2405-8033(20)30240-5. doi: 10.1016/j.trecan.2020.08.008. Epub ahead of print. PMID: 32952102.

Monaghan KN, Acierno MJ. Extracorporeal removal of drugs and toxins. Vet Clin North Am Small Anim Pract. 2011 Jan;41(1):227-38. doi: 10.1016/j.cvsm.2010.09.005. Epub 2010 Dec 4. PMID: 21251519.

Mondal, A., Ashiq, K.A., Phulpagar, P., Singh, D.K. and Shiras, A. (2019) Effective Visualization and Easy Tracking of Extracellular Vesicles in Glioma Cells. *Biological Procedures Online*. **21** (1). doi:10.1186/s12575-019-0092-2.

Moorman, A. V, Roman, E., Cartwright, R.A. and Morgan, G.J. (2002) Smoking and the risk of acute myeloid leukaemia in cytogenetic subgroups. *British Journal of Cancer*. **86** (1), pp. 60–62. doi:10.1038/sj.bjc.6600010.

Morales-Kastresana, A., Telford, B., Musich, T.A., McKinnon, K., Clayborne, C., Braig, Z., Rosner, A., Demberg, T., Watson, D.C., Karpova, T.S., Freeman, G.J., Dekruyff, R.H., Pavlakis, G.N., Terabe, M., et al. (2017) Labeling extracellular vesicles for nanoscale flow cytometry. *Scientific Reports* [online]. **7** (1). Available from: www.nature.com/scientificreports/doi:10.1038/s41598-017-01731-2 [Accessed 15 June 2020].

Mori, H., Colman, S.M., Xiao, Z., Ford, A.M., Healy, L.E., Donaldson, C., Hows, J.M., Navarrete, C. and Greaves, M. (2002) Chromosome translocations and covert leukemic clones are generated during normal fetal development. *Proceedings of the National Academy of Sciences of the United*

States of America [online]. **99** (12), pp. 8242–8247. Available from: www.pnas.orgcgidoi10.1073pnas.112218799doi:10.1073/pnas.112218799

Mothersill, C. and Seymour, C. (2015) Radiation-induced non-targeted effects: Some open questions. *Radiation Protection Dosimetry* [online]. **166** (1–4), pp. 125–130. Available from: https://academic.oup.com/rpd/article-abstract/166/1-4/125/1610969doi:10.1093/rpd/ncv155 [Accessed 16 July 2020].

Moitra K. (2015). Overcoming Multidrug Resistance in Cancer Stem Cells. *BioMed research international*, *2015*, 635745. https://doi.org/10.1155/2015/635745 [Accessed 27 December 2020].

Mouriaux, F., Zaniolo, K., Bergeron, M.A., Weidmann, C., De La Fouchardière, A., Fournier, F., Droit, A., Morcos, M.W., Landreville, S. and Guérin, S.L. (2016) Effects of long-term serial passaging on the characteristics and properties of cell lines derived from uveal melanoma primary tumors. *Investigative Ophthalmology and Visual Science*. **57** (13), pp. 5288–5301. doi:10.1167/iovs.16-19317.

Mueller, L.P., Luetzkendorf, J., Mueller, T., Reichelt, K., Simon, H. and Schmoll, H.-J. (2006) Presence of Mesenchymal Stem Cells in Human Bone Marrow After Exposure to Chemotherapy: Evidence of Resistance to Apoptosis Induction. *Stem Cells* [online]. **24** (12), pp. 2753–2765. Available from: http://doi.wiley.com/10.1634/stemcells.2006-0108doi:10.1634/stemcells.2006-0108 [Accessed 15 January 2020].

Mulcahy, L.A., Pink, R.C. and Carter, D.R.F. (2014) Routes and mechanisms of extracellular vesicle uptake *Journal of Extracellular Vesicles.* **3** (1). doi:10.3402/jev.v3.24641.

Mughal, T.I., Radich, J.P., Deininger, M.W., Apperley, J.F., Hughes, T.P., Harrison, C.J., Gambacorti-Passerini, C., Saglio, G., Cortes, J. and Daley, G.Q. (2016) Chronic myeloid leukemia: Reminiscences and dreams *Haematologica* [online]. **101** (5) p.pp. 541–558. Available from: www.haematologica.org/content/101/5/541doi:10.3324/haematol.2015.139337

Muirhead, C.R. (2013) Childhood leukaemia near nuclear power plants *British Journal of Cancer* [online]. **109** (11) p.pp. 2763–2764. Available from: http://www.comare.org.uk/.doi:10.1038/bjc.2013.674

Munoz, J.L., Bliss, S.A., Greco, S.J., Ramkissoon, S.H., Ligon, K.L. and Rameshwar, P. (2013) Delivery of functional anti-miR-9 by mesenchymal stem cell-derived exosomes to glioblastoma multiforme cells conferred chemosensitivity. *Molecular Therapy - Nucleic Acids*. 2 (OCT). doi:10.1038/mtna.2013.60.

Muñoz-Pinedo, C. (2012) Signaling pathways that regulate life and cell death: Evolution of apoptosis in the context of self-defense. *Advances in Experimental Medicine and Biology*. **738** pp. 124–143. doi:10.1007/978-1-4614-1680-7_8.

Muralidharan-Chari, V., Gilzad Kohan, H., Asimakopoulos, A.G., Sudha, T., Sell, S., Kannan, K., Boroujerdi, M., Davis, P.J. and Mousa, S.A. (2016) *Microvesicle removal of anticancer drugs contributes to drug resistance in human pancreatic cancer cells* [online] 7 (31). Available from: www.impactjournals.com/oncotarget [Accessed 27 March 2021].

Musselman, J.R.B., Blair, C.K., Cerhan, J.R., Nguyen, P., Hirsch, B. and Ross, J.A. (2013) Risk of adult acute and chronic myeloid leukemia with cigarette smoking and cessation. *Cancer Epidemiology*. **37** (4), pp. 410–416. doi:10.1016/j.canep.2013.03.012

Nagamura-Inoue, T., Kodo, H., Takahashi, T., Mugishima, H., Tojo, A. and Asano, S. (2007) Four cases of donor cell-derived AML following unrelated cord blood transplantation for adult patients: Experiences of the Tokyo Cord Blood Bank *Cytotherapy*. doi:10.1080/14653240701466339.

Nagasawa, H. and Little, J.B. (1992) Induction of Sister Chromatid Exchanges by Extremely Low Doses of a-Particles. *Cancer Research*. **52** (22), pp. 6394–6396.

Najafi, M., Fardid, R., Hadadi, G. and Fardid, M. (2014) The mechanisms of radiation-induced bystander effect. *Journal of biomedical physics & engineering* [online]. **4** (4), pp. 163–172. Available from: www.jbpe.org [Accessed 9 December 2019].

Nakada, S., Inazawa, J., Mizutani, S., Katsuki, Y., Imoto, I., Yokoyama, T. and Nagasawa, M. (2006) Early G2/M checkpoint failure as a molecular mechanism underlying etoposide-induced chromosomal aberrations. *The Journal of Clinical Investigation*. **116** (1). doi:10.1172/JCI25716.

Nakamura-Ishizu, A., Takizawa, H. and Suda, T. (2014) The analysis, roles and regulation of quiescence in hematopoietic stem cells *Development (Cambridge)* [online]. **141** (24) p.pp. 4656–4666. Available from: http://www.ncbi.nlm.nih.gov/pubmed/25468935doi:10.1242/dev.106575 [Accessed 28 October 2019].

Neuhuber, B., Swanger, S.A., Howard, L., Mackay, A. and Fischer, I. (2008) Effects of plating density and culture time on bone marrow stromal cell characteristics. *Experimental Hematology*. 36 (9), pp. 1176–1185. doi:10.1016/j.exphem.2008.03.019.

Newell, D.R., Shepherd, C.R. and Harrap, K.R. (1981) The pharmacokinetics of prednimustine and chlorambucil in the rat. *Cancer chemotherapy and pharmacology* [online]. **6** (1), pp. 85–91. Available from: http://www.ncbi.nlm.nih.gov/pubmed/7273268doi:10.1007/bf00253015 [Accessed 11 November 2019].

Ng, A., Taylor, G.M. and Eden, O.B. (2000) Treatment-related leukaemia - A clinical and scientific challenge *Cancer Treatment Reviews.* **26** (5) p.pp. 377–391. doi:10.1053/ctrv.2000.0186.

Ngo, L.P., Chan, T.K., Ge, J., Samson, L.D. and Engelward, B.P. (2019) Microcolony Size Distribution Assay Enables High-Throughput Cell Survival Quantitation. *Cell Reports* [online]. **26** (6), pp. 1668-1678.e4. Available from: https://doi.org/10.1016/j.celrep.2019.01.053doi:10.1016/j.celrep.2019.01.053 [Accessed 15 September 2020].

Nicolay, N.H., Lopez Perez, R., Rühle, A., Trinh, T., Sisombath, S., Weber, K.-J., Ho, A.D., Debus, J., Saffrich, R. and Huber, P.E. (2015) *Mesenchymal stem cells maintain their defining stem cell characteristics after treatment with cisplatin*. Available from: www.nature.com/scientificreportsdoi:10.1038/srep20035 [Accessed 16 May 2020].

Nicolay, N.H., Rühle, A., Lopez Perez, R., Trinh, T., Sisombath, S., Weber, K.-J., Ho, A.D., Debus, J., Saffrich, R. and Huber, P.E. (2016) *Mesenchymal stem cells are sensitive to bleomycin treatment*. Available from: www.nature.com/scientificreportsdoi:10.1038/srep26645 [Accessed 16 May 2020].

Nifontova, I., Svinareva, D., Petrova, T. and Drize, N. (2008) Sensitivity of mesenchymal stem cells and their progeny to medicines used for the treatment of hematoproliferative diseases. *Acta Haematologica*. **119** (2), pp. 98–103. doi:10.1159/000120440.

Nikolova, T., Roos, W.P., Krämer, O.H., Strik, H.M. and Kaina, B. (2017) Chloroethylating nitrosoureas in cancer therapy: DNA damage, repair and cell death signaling *Biochimica et Biophysica Acta - Reviews on Cancer*. doi:10.1016/j.bbcan.2017.01.004.

Nolte't Hoen, E.N.M., Buermans, H.P.J., Waasdorp, M., Stoorvogel, W., Wauben, M.H.M. and 'T Hoen, P.A.C. (2012) Deep sequencing of RNA from immune cell-derived vesicles uncovers the selective incorporation of small non-coding RNA biotypes with potential regulatory functions. *Nucleic Acids Research*. **40** (18), pp. 9272–9285. doi:10.1093/nar/gks658.

Nombela-Arrieta, C., Ritz, J. and Silberstein, L.E. (2011) The elusive nature and function of mesenchymal stem cells *Nature Reviews Molecular Cell Biology*. **12** (2) p.pp. 126–131. doi:10.1038/nrm3049.

Norbury, C. and Zhivotovsky, B. (2004) DNA damage-induced apoptosis. *Oncogene*. **23,** 2797–2808. https://doi.org/10.1038/sj.onc.1207532 [Accessed 01 January 2021].

Nunhart, P., Konkoľová, E., Janovec, L., Jendželovský, R., Vargová, J., Ševc, J., Matejová, M., Miltáková, B., Fedoročko, P. and Kozurkova, M. (2019) Fluorinated 3,6,9-trisubstituted acridine

derivatives as DNA interacting agents and topoisomerase inhibitors with A549 antiproliferative activity. *Bioorganic Chemistry*. doi:10.1016/j.bioorg.2019.103393.

O'Brien, K., Breyne, K., Ughetto, S., Laurent, L.C. and Breakefield, X.O. (2020) RNA delivery by extracellular vesicles in mammalian cells and its applications *Nature Reviews Molecular Cell Biology* [online]. Available from: www.nature.com/nrmdoi:10.1038/s41580-020-0251-y [Accessed 26 June 2020].

O'Neill, C.P., Gilligan, K.E. and Dwyer, R.M. (2019) Role of extracellular vesicles (EVs) in cell stress response and resistance to cancer therapy. *Cancers*. **11** (2). doi:10.3390/cancers11020136.

O'Reilly, A., Murphy, J., Rawe, S. and Garvey, M. (2018) Chronic Lymphocytic Leukemia: A Review of Front-line Treatment Options, With a Focus on Elderly CLL Patients *Clinical Lymphoma, Myeloma and Leukemia*. **18** (4) p.pp. 249–256. doi:10.1016/j.clml.2018.02.003.

Ohshima, A., Miura, L., Chubachi, A., Hashimoto, K., Nimura, T., Utsumi, S., Takahashi, N., Hayashi, Y., Seto, M., Ueda, R. and Miura, A.B. (no date) 1 q23 Aberration Is an Additional Chromosomal Change in De Novo Acute Leukemia After Treatment With Etoposide and Mitoxantrone *American Journal of Hematology* 53.

Okay, M., Büyükaşik, Y., Demiroğlu, H., Malkan, Ü.Y., Çiftçiler, R., Aladağ, E., Aksu, S., Haznedaroğlu, İ.C., Sayinalp, N., Özcebe, O.İ. and Göker, H. (2019) Mitoxantrone-melphalan conditioning regimen for autologous stem cell transplantation in relapsed/refractory lymphoma. *Turkish Journal of Medical Sciences* [online]. 49 (4), pp. 985–992. Available from: http://journals.tubitak.gov.tr/medical/doi:10.3906/sag-1809-36 [Accessed 3 September 2020].

Oliveira, M.S., Carvalho, J.L., Campos, A.C.D.A., Gomes, D.A., de Goes, A.M. and Melo, M.M. (2014) Doxorubicin has in vivo toxicological effects on ex vivo cultured mesenchymal stem cells. *Toxicology Letters*. **224** (3), pp. 380–386. doi:10.1016/j.toxlet.2013.11.023.

Ortega, F.G., Roefs, M.T., de Miguel Perez, D., Kooijmans, S.A., de Jong, O.G., Sluijter, J.P., Schiffelers, R.M. and Vader, P. (2019) Interfering with endolysosomal trafficking enhances release

of bioactive exosomes. *Nanomedicine: Nanotechnology, Biology, and Medicine*. **20.** doi:10.1016/j.nano.2019.102014.

Osaki, L.H. and Gama, P. (2013) MAPKs and Signal Transduction in the Control of Gastrointestinal Epithelial Cell Proliferation and Differentiation. *Int. J. Mol. Sci* [online]. **14** pp. 10143–10161. Available from: www.mdpi.com/journal/ijmsdoi:10.3390/ijms140510143 [Accessed 29 May 2020].

Pachler, K., Lener, T., Streif, D., Dunai, Z.A., Desgeorges, A., Feichtner, M., Öller, M., Schallmoser, K., Rohde, E. and Gimona, M. (2017) A Good Manufacturing Practice–grade standard protocol for exclusively human mesenchymal stromal cell–derived extracellular vesicles. *Cytotherapy*. **19** (4), pp. 458–472. doi:10.1016/j.jcyt.2017.01.001.

Paggetti, J., Haderk, F., Seiffert, M., Janji, B., Distler, U., Ammerlaan, W., Kim, Y.J., Adam, J., Lichter, P., Solary, E., Berchem, G. and Moussay, E. (2015) Exosomes released by chronic lymphocytic leukemia cells induce the transition of stromal cells into cancer-associated fibroblasts. *Blood* [online]. **126** (9), pp. 1106–1117. Available from: http://www.ncbi.nlm.nih.gov/pubmed/26100252doi:10.1182/blood-2014-12-618025 [Accessed 28 October 2019].

Palviainen, M., Saari, H., Kärkkäinen, O., Pekkinen, J., Auriola, S., Yliperttula, M., Puhka, M., Hanhineva, K. and R-M Siljander, P. (2019) Metabolic signature of extracellular vesicles depends on the cell culture conditions. *Journal of Extracellular Vesicles* [online]. **8** (1), pp. 1596669. Available from: https://www.tandfonline.com/action/journalInformation?journalCode=zjev20doi:10.1080/20013078.2019.1596669 [Accessed 15 June 2020].

Panigrahi, G.K., Praharaj, P.P., Peak, T.C., Long, J., Singh, R., Rhim, J.S., Elmageed, Z.Y.A. and Deep, G. (2018) Hypoxia-induced exosome secretion promotes survival of African-American and Caucasian prostate cancer cells. *Scientific Reports* [online]. **8** (1). Available from: www.nature.com/scientificreports/doi:10.1038/s41598-018-22068-4 [Accessed 11 June 2020].

Panousis, C., Kettle, A.J. & Phillips, D.R. (1995) Myeloperoxidase oxidizes mitoxantrone to metabolites, which bind covalently to DNA and RNA. *Anticancer Drug Research.* **10;** 593-605.

Papy-Garcia, D. and Albanese, P. (2017) Heparan sulfate proteoglycans as key regulators of the mesenchymal niche of hematopoietic stem cells. *Glycoconjugate Journal.* **34** (3):377-391. doi: 10.1007/s10719-017-9773-8. Epub 2017

Pardini, B., Viberti, C., Naccarati, A., Allione, A., Oderda, M., Critelli, R., Preto, M., Zijno, A., Cucchiarale, G., Gontero, P., Vineis, P., Sacerdote, C. and Matullo, G. (2017) Increased micronucleus frequency in peripheral blood lymphocytes predicts the risk of bladder cancer. *British Journal of Cancer*. **116** (2), pp. 202–210. doi:10.1038/bjc.2016.411.

Parikh, S.A. (2018) Chronic lymphocytic leukemia treatment. *Blood Cancer Journal* **8** (10) p.pp. 93. doi:10.1038/s41408-018-0131-2.

Pascucci, L., Coccè, V., Bonomi, A., Ami, D., Ceccarelli, P., Ciusani, E., Viganò, L., Locatelli, A., Sisto, F., Doglia, S.M., Parati, E., Bernardo, M.E., Muraca, M., Alessandri, G., et al. (2014) Paclitaxel is incorporated by mesenchymal stromal cells and released in exosomes that inhibit in vitro tumor growth: A new approach for drug delivery. *Journal of Controlled Release*. **192** pp. 262–270. doi:10.1016/j.jconrel.2014.07.042.

Pasmant, E., Vidaud, D. and Ballerini, P. (no date) *Oncoscience 930 www.impactjournals.com/oncoscience RAS MAPK inhibitors deregulation in leukemia* [online]. Available from: www.impactjournals.com/oncoscience/ [Accessed 5 September 2020].

Patel, D.B., Gray, K.M., Santharam, Y., Lamichhane, T.N., Stroka, K.M. and Jay, S.M. (2017) Impact of cell culture parameters on production and vascularization bioactivity of mesenchymal stem cell-derived extracellular vesicles. *Bioengineering & Translational Medicine*. **2** (2), pp. 170–179. doi:10.1002/btm2.10065.

Paulson, R.F., Shi, L. and Wu, D.C. (2011) Stress erythropoiesis: New signals and new stress progenitor cells. *Current Opinion in Hematology*. **18** (3), pp. 139–145. doi:10.1097/MOH.0b013e32834521c8.

Pedersen-Bjergaard, J., Andersen, M.K., Andersen, M.T. and Christiansen, D.H. (2008) Genetics of therapy-related myelodysplasia and acute myeloid leukemia *Leukemia* [online] **22** (2) p.pp. 240–248. Available from: www.nature.com/leudoi:10.1038/sj.leu.2405078 [Accessed 19 February 2020].

Pessina, A., Coccè, V., Pascucci, L., Bonomi, A., Cavicchini, L., Sisto, F., Ferrari, M., Ciusani, E., Crovace, A., Falchetti, M.L., Zicari, S., Caruso, A., Navone, S., Marfia, G., et al. (2013) Mesenchymal stromal cells primed with Paclitaxel attract and kill leukaemia cells, inhibit angiogenesis and improve survival of leukaemia-bearing mice. *British Journal of Haematology*. **160** (6), pp. 766–778. doi:10.1111/bjh.12196.

Pessina, A., Bonomi, A., Coccè, V., Invernici, G., Navone, S., Cavicchini, L., Sisto, F., Ferrari, M., Viganò, L., Locatelli, A., Ciusani, E., Cappelletti, G., Cartelli, D., Arnaldo, C., et al. (no date) *Mesenchymal Stromal Cells Primed with Paclitaxel Provide a New Approach for Cancer Therapy*. Available from: www.plosone.orgdoi:10.1371/journal.pone.0028321

Pettersen Hessvik, N. and Llorente, A. (2018) Current knowledge on exosome biogenesis and release. *Cell. Mol. Life Sci* [online]. **75** pp. 193–208. Available from: https://doi.org/10.1007/s00018-017-2595-9doi:10.1007/s00018-017-2595-9

Peterson-Roth, E., Brdlik, C.M. and Glazer, P.M. (2009) Src-Induced Cisplatin resistance mediated by cell-to-cell communication. *Cancer Research*. **69** (8), pp. 3619–3624. doi:10.1158/0008-5472.CAN-08-0985.

Perumal, V., Chinnadurai, M., Raavi, V., Kanagaraj, K., Shangamithra, V. and Paul, S.F.D. (2017) *Perspectives on the Role of Bystander Effect and Genomic Instability on Therapy-induced Secondary Malignancy*. Available from: www.journalrcr.orgdoi:10.4103/jrcr.jrcr_22_16 Pink, R.C., Samuel, P., Massa, D., Caley, D.P., Brooks, S.A. and Carter, D.R.F. (2015) The passenger

strand, miR-21-3p, plays a role in mediating cisplatin resistance in ovarian cancer cells. *Gynecologic Oncology*. **137** (1), pp. 143–151. doi:10.1016/j.ygyno.2014.12.042.

Phinney, D.G. and Pittenger, M.F. (2017) Concise Review: MSC-Derived Exosomes for Cell-Free Therapy. *Stem Cells*. **35** (4), pp. 851–858. doi:10.1002/stem.2575.

Pinto, N., Ludeman, S.M. and Dolan, M.E. (2009) Pharmacogenetic studies related to cyclophosphamide-based therapy. *Pharmacogenomics*. 10 (12), pp. 1897–1903. doi:10.2217/pgs.09.134.

Podrimaj-Bytyqi, A., Borovečki, A., Selimi, Q., Manxhuka-Kerliu, S., Gashi, G. and Elezaj, I.R. (2018) The frequencies of micronuclei, nucleoplasmic bridges and nuclear buds as biomarkers of genomic instability in patients with urothelial cell carcinoma. *Scientific Reports*. **8** (1). doi:10.1038/s41598-018-35903-5.

Podszywalow-Bartnicka, P., Kominek, A., Wolczyk, M., Kolba, M.D., Swatler, J. and Piwocka, K. (2018) Characteristics of live parameters of the HS-5 human bone marrow stromal cell line cocultured with the leukemia cells in hypoxia, for the studies of leukemia–stroma cross-talk. *Cytometry Part A*. 93 (9), pp. 929–940. doi:10.1002/cyto.a.23580.

Preston DL, Kusumi S, Tomonaga M, Izumi S, Ron E, Kuramoto A et al. (1994). Cancer incidence in atomic bomb survivors. Part III. Leukemia, lymphoma and multiple myeloma, 1950–1987. Radiat Res 137 (Suppl. 2): S68–S97.

Preston, R.J. (2005) Bystander effects, genomic instability, adaptive response, and cancer risk assessment for radiation and chemical exposures. In: *Toxicology and Applied Pharmacology*. 1 September 2005 (no place) Academic Press Inc. pp. 550–556. doi:10.1016/j.taap.2004.12.024.

Prieto-Bermejo, R., Romo-González, M., Pérez-Fernández, A., Ijurko, C. and Hernández-Hernández, Á. (2018) Reactive oxygen species in haematopoiesis: Leukaemic cells take a walk on the wild side *Journal of Experimental and Clinical Cancer Research* [online]. **37** (1). Available from:

https://doi.org/10.1186/s13046-018-0797-0doi:10.1186/s13046-018-0797-0 [Accessed 28 October 2019].

Prise, K.M. and O'Sullivan, J.M. (2009) Radiation-induced bystander signalling in cancer therapy *Nature Reviews Cancer* [online]. **9** (5) p.pp. 351–360. Available from: http://www.qub.ac.uk/research-centres/CentreforCancerResearchCellBiology/doi:10.1038/nrc2603 [Accessed 9 December 2019].

Przepiorka, D., Luo, L., Subramaniam, S., Qiu, J., Gudi, R., Cunningham, L.C., Nie, L., Leong, R., Ma, L., Sheth, C., Deisseroth, A., Goldberg, K.B., Blumenthal, G.M. and Pazdur, R. (2020) FDA Approval Summary: Ruxolitinib for Treatment of Steroid-Refractory Acute Graft-Versus-Host Disease. *The Oncologist*. **25** (2), pp. theoncologist.2019-0627. doi:10.1634/theoncologist.2019-0627.

Pulte, D., Redanie, M.T., Jansen, L., Brenner, H. and Jeffreys, M. (2013) Recent trends in survival of adult patients with acute leukemia: Overall improvements, but persistent and partly increasing disparity in survival of patients from minority groups. *Haematologica*. **98** (2), pp. 222–229. doi:10.3324/haematol.2012.063602.

Qi, H., Liu, S., Guo, C., Wang, J., Greenaway, F.T. and Sun, M.Z. (2015) Role of annexin A6 in cancer (Review). *Oncology Letters*. **10** (4), pp. 1947–1952. doi:10.3892/ol.2015.3498.

Qiu, G., Zheng, G., Ge, M., Wang, J., Huang, R., Shu, Q. and Xu, J. (2018) Mesenchymal stem cell-derived extracellular vesicles affect disease outcomes via transfer of microRNAs *Stem Cell Research and Therapy* [online]. **9** (1). Available from: https://doi.org/10.1186/s13287-018-1069-9doi:10.1186/s13287-018-1069-9 [Accessed 3 March 2020].

Rai, K.R., Sawitsky, A., Cronkite, E.P., Chanana, A.D., Levy, R.N. and Pasternack, B.S. (no date) Clinical Staging of Chronic Lymphocytic Leukemia *Blood* [online]. **46** (2). Available from: https://ashpublications.org/blood/article-pdf/46/2/219/203436/219.pdf

Ralhan, R. and Kaur, J. (2007) Alkylating agents and cancer therapy *Expert Opinion on Therapeutic Patents.* **17** (9) p.pp. 1061–1075. doi:10.1517/13543776.17.9.1061.

Ramirez, C.B., Barrientos, J. and Jhaveri, K.D. (2018) Renal involvement in chronic lymphocytic leukemia *Clinical Kidney Journal* [online]. **11** (5) p.pp. 670–680. Available from: https://academic.oup.com/ckj/article- abstract/11/5/670/4967844 doi:10.1093/ckj/sfy026

Ramirez, M.I., Amorim, M.G., Gadelha, C., Milic, I., Welsh, J.A., Freitas, V.M., Nawaz, M., Akbar, N., Couch, Y., Makin, L., Cooke, F., Vettore, A.L., Batista, P.X., Freezor, R., et al. (2018) Technical challenges of working with extracellular vesicles. *Nanoscale REVIEW Cite this: Nanoscale* [online]. **10** pp. 881. Available from: http://www.isev.orgdoi:10.1039/c7nr08360b

Ramos, T.L., Sánchez-Abarca, L.I., Muntión, S., Preciado, S., Puig, N., López-Ruano, G., Hernández-Hernández, Á., Redondo, A., Ortega, R., Rodríguez, C., Sánchez-Guijo, F. and Del Cañizo, C. (2016) MSC surface markers (CD44, CD73, and CD90) can identify human MSC-derived extracellular vesicles by conventional flow cytometry. *Cell Communication and Signaling* [online]. 14 (1), pp. 1–14. Available from: http://dx.doi.org/10.1186/s12964-015-0124-8doi:10.1186/s12964-015-0124-8

Rao, X., Huang, X., Zhou, Z. and Lin, X. (2013) An improvement of the 2ˆ(-delta delta CT) method for quantitative real-time polymerase chain reaction data analysis. Biostatistics, bioinformatics and biomathematics [online]. 3 (3), pp. 71-85. Available from: http://www.ncbi.nlm.nih.gov/pubmed/25558171%0Ahttp://www.pubmedcentral.nih.gov/articlerender.fcgi?artid=PMC4280562 [Accessed 24 August 2020].

Razak, N.S., Ab Mutalib, N.S., Mohtar, M.A. and Abu, N. (2019) Impact of Chemotherapy on Extracellular Vesicles: Understanding the Chemo-EVs. *Frontiers in Oncology*. **9.** doi:10.3389/fonc.2019.01113.

Reagan, M.R. and Rosen, C.J. (2016) Navigating the bone marrow niche: Translational insights and cancer-driven dysfunction *Nature Reviews Rheumatology*. **12** (3) p.pp. 154–168. doi:10.1038/nrrheum.2015.160.

Reif, S., Elbaum Shiff, Y. and Golan-Gerstl, R. (2019) Milk-derived exosomes (MDEs) have a different biological effect on normal fetal colon epithelial cells compared to colon tumor cells in a miRNA-dependent manner. *Journal of Translational Medicine*. 17 (1). doi:10.1186/s12967-019-2072-3.

Ren, K. (123AD) Exosomes in perspective: a potential surrogate for stem cell therapy. *Odontology* [online]. **1** pp. 271–284. Available from: https://doi.org/10.1007/s10266-018-0395-9doi:10.1007/s10266-018-0395-9

Richards, K.E., Zeleniak, A.E., Fishel, M.L., Wu, J., Littlepage, L.E. and Hill, R. (2017) Cancer-associated fibroblast exosomes regulate survival and proliferation of pancreatic cancer cells. *Oncogene* [online]. **36** (13), pp. 1770–1778. Available from: http://www.nature.com/authors/editorial_policies/license.html#termsdoi:10.1038/onc.2016.353 [Accessed 24 June 2020].

Richard, B., Launay-Iliadis, M.C., Iliadis, A., Just-Landi, S., Blaise, D., Stoppa, A.M., Viens, P., Gaspard, M.H., Maraninchi, D., Cano, J.P. and Carcassonne, Y. (1992) Pharmacokinetics of mitoxantrone in cancer patients treated by high-dose chemotherapy and autologous bone marrow transplantation. *British Journal of Cancer*. 65 (3), pp. 399–404. doi:10.1038/bjc.1992.81.

Rivella, S. (2012) The role of ineffective erythropoiesis in non-transfusion-dependent thalassemia. *Blood Reviews*. **26** (SUPPL.1). doi:10.1016/S0268-960X(12)70005-X.

Roecklein, B.A., Remis, J.A., Rowley, S. and Torok-Storb, B. (1998) Ex vivo expansion of immature 4-hydroperoxycyclophosphamide-resistant progenitor cells from G-CSF-mobilized peripheral blood. *Biology of Blood and Marrow Transplantation*. **4** (2), pp. 61–68. doi:10.1053/bbmt.1998.v4.pm9763108

Roodhart, J.M.L., Daenen, L.G.M., Stigter, E.C.A., Prins, H.-J., Gerrits, J., Houthuijzen, J.M., Gerritsen, M.G., Schipper, H.S., Backer, M.J.G., Van Amersfoort, M., Vermaat, J.S.P., Moerer, P., Ishihara, K., Kalkhoven, E., et al. (2011) *Article Mesenchymal Stem Cells Induce Resistance to*

Chemotherapy through the Release of Platinum-Induced Fatty Acids. doi:10.1016/j.ccr.2011.08.010.

Ruan, L. and Qian, X. (2019) MIR-16-5p inhibits breast cancer by reducing AKT3 to restrain NF-κB pathway. *Bioscience Reports* [online]. **39** (8), pp. 20191611. Available from: https://doi.org/10.1042/BSR20191611doi:10.1042/BSR20191611 [Accessed 16 July 2020].

Rugo, R.E., Almeida, K.H., Hendricks, C.A., Jonnalagadda, V.S. and Engelward, B.P. (2005) A single acute exposure to a chemotherapeutic agent induces hyper-recombination in distantly descendant cells and in their neighbors. *Oncogene* [online]. **24** (32), pp. 5016–5025. Available from: www.nature.com/oncdoi:10.1038/sj.onc.1208690 [Accessed 10 December 2019].

Rukov, J.L., Wilentzik, R., Jaffe, I., Vinther, J. and Shomron, N. (2014) Pharmaco-miR: Linking microRNAs and drug effects. *Briefings in Bioinformatics* [online]. **15** (4), pp. 648–659. Available from: www.Pharmaco-miR.org.doi:10.1093/bib/bbs082 [Accessed 29 May 2020].

Russell, L.B., Hunsicker, P.R., Cacheiro, N.L.A., Bangham, J.W., Russell, W.L. and Shelbyt, M.D. (1989) Chlorambucil effectively induces deletion mutations in mouse germ cells (chemical mutagenesis/speciflc-locus mutations/chromosome rearrangements/dominant lethals/germ-cell killing) *Genetics* 86.

Rylova, J. V, Andreeva, E.R., Gogvadze, V.G., Zhivotovsky, B.D. and Buravkova, L.B. (2012) Etoposide and hypoxia do not activate apoptosis of multipotent mesenchymal stromal cells in vitro. *Bulletin of Experimental Biology and Medicine*. **154** (1), pp. 141–144. doi:10.1007/s10517-012-1895-1.

Safaei, R., Larson, B.J., Cheng, T.C., Gibson, M.A., Otani, S., Naerdemann, W., Howell Rebecca, S.B. and Moore, J. (2005) Abnormal lysosomal trafficking and enhanced exosomal export of cisplatin in drug-resistant human ovarian carcinoma cells. *Molecular Cancer Therapeutics* [online]. 4 (10), pp. 1595–1604. Available from: http://www.microarray.orgdoi:10.1158/1535-7163.MCT-05-0102 [Accessed 27 March 2021].

Sacha, T. (2014) Imatinib in Chronic Myeloid Leukemia: an Overview. *Open Journal System MEDITERRANEAN JOURNAL OF HEMATOLOGY AND INFECTIOUS DISEASES Citation: Mediterr J Hematol Infect Dis* [online]. **6** (1), pp. 2014007. Available from: www.mjhid.orgdoi:10.4084/MJHID.2014.007 [Accessed 8 November 2019].

Sagaradze, G., Grigorieva, O., Nimiritsky, P., Basalova, N., Kalinina, N., Akopyan, Z. and Efimenko, A. (2019) Conditioned medium from human mesenchymal stromal cells: Towards the clinical translation. *International Journal of Molecular Sciences*. 20 (7), pp. 1–16. doi:10.3390/ijms20071656.

Saji Joseph, J., Tebogo Malindisa, S. and Ntwasa, M. (2019) Two-Dimensional (2D) and Three-Dimensional (3D) Cell Culturing in Drug Discovery. In: *Cell Culture*. (no place) IntechOpen. doi:10.5772/intechopen.81552.

Salimu, J., Webber, J., Gurney, M., Al-Taei, S., Clayton, A., Tabi, Z. and Vizio, D. Di (2017) Dominant immunosuppression of dendritic cell function by prostate-cancer-derived exosomes. *Journal of Extracellular Vesicles* [online]. 6 (1). Available from: https://www.tandfonline.com/action/journalInformation?journalCode=zjev20doi:10.1080/20013078.2017.1368823 [Accessed 27 March 2021].

Samuel, P., Mulcahy, L.A., Furlong, F., McCarthy, H.O., Brooks, S.A., Fabbri, M., Pink, R.C. and Francisco Carter, D.R. (2018) Cisplatin induces the release of extracellular vesicles from ovarian cancer cells that can induce invasiveness and drug resistance in bystander cells. *Philosophical Transactions of the Royal Society B: Biological Sciences*. **373** (1737). doi:10.1098/rstb.2017.0065.

Sancho-Albero, M., Navascués, N., Mendoza, G., Sebastián, V., Arruebo, M., Martín-Duque, P. and Santamaría, J. (2019) Exosome origin determines cell targeting and the transfer of therapeutic nanoparticles towards target cells. *Journal of Nanobiotechnology* [online]. 17 (1), pp. 1–13. Available from: https://doi.org/10.1186/s12951-018-0437-zdoi:10.1186/s12951-018-0437-z [Accessed 1 October 2020].

Sane, M.S., Misra, N., Mousa, O.M., Czop, S., Tang, H., Khoo, L.T., Jones, C.D. and Mustafi, S.B. (2018) Cytokines in umbilical cord blood-derived cellular product: A mechanistic insight into bone repair. *Regenerative Medicine*. **13** (8), pp. 881–898. doi:10.2217/rme-2018-0102.

Sankila, R., Martos Jiménez, M.C., Miljus, D., Pritchard-Jones, K., Steliarova-Foucher, E., Stiller, C., Petrovich, S. V., Budanov, O., Storm, H., Christensen, N., Aareleid, T., Hakulinen, T., Pukkala, E., Le Gall, E., et al. (2006) Geographical comparison of cancer survival in European children (1988-1997): Report from the Automated Childhood Cancer Information System project. *European Journal of Cancer*. **42** (13), pp. 1972–1980. doi:10.1016/j.ejca.2006.05.013.

Satyanarayana, A. and Kaldis, P. (2009) Mammalian cell-cycle regulation: several Cdks, numerous cyclins and diverse compensatory mechanisms. *Oncogene* [online]. **28** pp. 2925–2939. Available from: www.nature.com/oncdoi:10.1038/onc.2009.170 [Accessed 25 June 2020].

Saunders, K.B. and D'Amore, P.A. (1992) An in vitro model for cell-cell interactions. *In Vitro Cellular & Developmental Biology - Animal*. **28** (7–8), 521–528. doi:10.1007/BF02634136

Saury, C., Lardenois, A., Schleder, C., Leroux, I., Lieubeau, B., David, L., Charrier, M., Guével, L., Viau, S., Delorme, B. and Rouger, K. (2018) Human serum and platelet lysate are appropriate xeno-free alternatives for clinical-grade production of human MuStem cell batches. *Stem Cell Research and Therapy* [online]. **9** (1). Available from: https://doi.org/10.1186/s13287-018-0852-ydoi:10.1186/s13287-018-0852-y [Accessed 13 January 2020].

Savage, D.G., Szydlo, R.M. and Goldman, J.M. (1997) Clinical features at diagnosis in 430 patients with chronic myeloid leukaemia seen at a referral centre over a 16-year period. *British Journal of Haematology*. **96** (1), pp. 111–116. doi:10.1046/j.1365-2141.1997.d01-1982.x.

Schageman, J., Zeringer, E., Li, M., Barta, T., Lea, K., Gu, J., Magdaleno, S., Setterquist, R. and Vlassov, A. V (2013) The complete exosome workflow solution: From isolation to characterization of RNA cargo. *BioMed Research International* [online]. **2013** pp. 15. Available from: http://dx.doi:10.1155/2013/253957 [Accessed 2 July 2020].

Schmidmaier, R., Baumann, P. and Meinhardt, G. (2006) Cell-cell contact mediated signalling - No fear of contact. *Experimental Oncology*. **28** (1), pp. 12–15.

Schoefinius, J.S., Brunswig-Spickenheier, B., Speiseder, T., Krebs, S., Just, U. and Lange, C. (2017) Mesenchymal Stromal Cell-Derived Extracellular Vesicles Provide Long-Term Survival After Total Body Irradiation Without Additional Hematopoietic Stem Cell Support. *Stem Cells*. **35** (12), pp. 2379–2389. doi:10.1002/stem.2716.

Segel, G.B. and Lichtman, M.A. (2004) Familial (inherited) leukemia, lymphoma, and myeloma: An overview. *Blood Cells, Molecules, and Diseases*. **32** (1), pp. 246–261. doi:10.1016/j.bcmd.2003.10.005.

Seifriz, W. (1943) Protoplasmic streaming. *The Botanical Review* [online]. **9** (2), pp. 49–123. Available from: http://science.sciencemag.org/doi:10.1007/BF02872461

Seifrtova, M., Havelek, R., Soukup, T., Filipova, A., Mokry, J. and Rezacova, M. (2013) Mitoxantrone ability to induce premature senescence in human dental pulp stem cells and human dermal fibroblasts. *Journal of Physiology and Pharmacology*. 64 (2).

Serrano-Pertierra, E., Oliveira-Rodríguez, M., Rivas, M., Oliva, P., Villafani, J., Navarro, A., Carmen Blanco-López, M. and Cernuda-Morollón, E. (2019) *Characterization of Plasma-Derived Extracellular Vesicles Isolated by Different Methods: A Comparison Study*. Available from: www.mdpi.com/journal/bioengineeringdoi:10.3390/bioengineering6010008 [Accessed 15 June 2020].

Sever, R. and Brugge, J.S. (2015) Signal transduction in cancer. *Cold Spring Harbor Perspectives in Medicine* [online]. **5** (4). Available from: www.cshperspectivesinmedicine.orgdoi:10.1101/cshperspect.a006098 [Accessed 29 May 2020].

Sevilla, J., Querol, S., Molines, A., González-Vicent, M., Balas, A., Carrió, A., Estella, J., Angel Díaz, M. and Madero, L. (2006) Transient donor cell-derived myelodysplastic syndrome with

monosomy 7 after unrelated cord blood transplantation. *European Journal of Haematology*. **77** (3), pp. 259–263. doi:10.1111/j.1600-0609.2006.00716.x.

Shafer, A.W. and Jolla, L. (no date) *CATHOLIC MEDICAL CENTER CENTRAL MEDICAL LIBRA Y B8-25 153rd STREET Etiology of Leukemia A Review*.

Shahar Gabay, T., Chapal-Ilani, N., Moskovitz, Y., Biezuner, T., Oron, B., Brilon, Y., Fridman-Dror, A., Sabah, R., Balicer, R., Tanay, A., Mendelson-Cohen, N., Dann, E.J., Fineman, R., Kaushansky, N., et al. (2020) Donor cell leukemia: reappearance of gene mutations in donor cells - more than an incidental phenomenon? *Haematologica*. pp. haematol.2019.242347. doi:10.3324/haematol.2019.242347.

Shahnazi, M., Khatami, A., Shamsian, B., Haerizadeh, B. and Mehrafarin, M. (2012) Bony lesions in pediatric acute leukemia: Pictorial essay. *Iranian Journal of Radiology* [online]. **9** (1), pp. 261–267. Available from: www.iranjradiol.comdoi:10.5812/iranjradiol.6765

Shamseddine, A.A., Airola, M. V and Hannun, Y.A. (2015) Roles and regulation of neutral sphingomyelinase-2 in cellular and pathological processes *Advances in Biological Regulation* **57** p.pp. 24–41. doi:10.1016/j.jbior.2014.10.002.

Shedden, K., Xie, T., Chandaroy, P., Chang, Y.T. and Rosania, G.R. (2003) Expulsion of Small Molecules in Vesicles Shed by Cancer Cells: Association with Gene Expression and Chemosensitivity Profiles 1,2 *CANCER RESEARCH* [online] 63. Available from: http://www.genome.wi.mit.edu/MPR/NC160/NC160.html

Shelke, G.V., Lässer, C., Gho, Y.S. and Lötvall, J. (2014) Importance of exosome depletion protocols to eliminate functional and RNA-containing extracellular vesicles from fetal bovine serum. *Journal of Extracellular Vesicles* [online]. **3** (1). Available from: http://dx.doi.org/10.3402/jev.v3.24783doi:10.3402/jev.v3.24783 [Accessed 30 June 2020].

Shipounova, I.N., Petinati, N.A., Bigildeev, A.E., Drize, N.J., Sorokina, T. V., Kuzmina, L.A., Parovichnikova, E.N. and Savchenko, V.G. (2017) Alterations of the bone marrow stromal

microenvironment in adult patients with acute myeloid and lymphoblastic leukemias before and after allogeneic hematopoietic stem cell transplantation. *Leukemia and Lymphoma*. **58** (2), pp. 408–417. doi:10.1080/10428194.2016.1187277.

Shiozaki, H., Yoshinaga, K., Kondo, T., Imai, Y., Shiseki, M., Mori, N., Teramura, M. and Motoji, T. (2014) Donor cell-derived leukemia after cord blood transplantation and a review of the literature: Differences between cord blood and BM as the transplant source *Bone Marrow Transplantation* [online] 49 (1) p.pp. 102–109. Available from: www.nature.com/bmtdoi:10.1038/bmt.2013.127 [Accessed 5 September 2020].

Siddik, Z.H. (2020) Alkylating agents and platinum anti-tumour compounds. *OncohemaKey.* Available from: https://oncohemakey.com/alkylating-agents-and-platinum-antitumor-compounds/ [Accessed 01 January 2021].

Singh, S. V, Ajay, A.K., Mohammad, N., Malvi, P., Chaube, B., Meena, A.S. and Bhat, M.K. (1934) Proteasomal inhibition sensitizes cervical cancer cells to mitomycin C-induced bystander effect: the role of tumor microenvironment. *Cell Death and Disease* [online]. 6. Available from: www.nature.com/cddisdoi:10.1038/cddis.2015.292 [Accessed 10 December 2019].

Skalska, J., Oliveira, F.D., Figueira, T.N., Mello, É.O., Gomes, V.M., McNaughton-Smith, G., Castanho, M.A.R.B. and Gaspar, D. (2019) Plant defensin: Pv D1 modulates the membrane composition of breast tumour-derived exosomes. *Nanoscale*. **11** (48), pp. 23366–23381. doi:10.1039/c9nr07843f.

Skolekova, S., Matuskova, M., Bohac, M., Toro, L., Demkova, L., Gursky, J. and Kucerova, L. (2016) *Cisplatin-induced mesenchymal stromal cells-mediated mechanism contributing to decreased antitumor effect in breast cancer cells*. doi:10.1186/s12964-016-0127-0.

Skopelitis, D.S., Hill, K., Klesen, S., Marco, C.F., von Born, P., Chitwood, D.H. and Timmermans, M.C.P. (2018) Gating of miRNA movement at defined cell-cell interfaces governs their impact as positional signals. *Nature Communications* [online]. 9 (1), . Available from:

www.nature.com/naturecommunicationsdoi:10.1038/s41467-018-05571-0 [Accessed 5 September 2020].

Smart, D.J., Helbing, F.R., Verardo, M., Huber, A., McHugh, D. and Vanscheeuwijck, P. (2020) Development of an integrated assay in human TK6 cells to permit comprehensive genotoxicity analysis in vitro. *Mutation Research/Genetic Toxicology and Environmental Mutagenesis.* **849.** [Accessed 9 September 2020].

Smith, P.J., Soues, S., Gottlieb, T., Falk, S.J., Watson, J. V, Osborne, R.J. and Bleehen, N.M. (1994) Etoposide-induced cell cycle delay and arrest-dependent modulation of DNA topoisomerase H in small-cell lung cancer cells *Br. J. Cancer* 914.

Sohel, M.M.H., Hoelker, M., Noferesti, S.S., Salilew-Wondim, D., Tholen, E., Looft, C., Rings, F., Uddin, M.J., Spencer, T.E., Schellander, K. and Tesfaye, D. (2013) Exosomal and non-exosomal transport of extra-cellular microRNAs in follicular fluid: Implications for bovine oocyte developmental competence. *PLoS ONE*. **8** (11). doi:10.1371/journal.pone.0078505.

Sokolov, M. and Neumann, R. (2018) Changes in gene expression as one of the key mechanisms involved in radiation-induced bystander effect (Review) *Biomedical Reports.* **9** (2) p.pp. 99–111. doi:10.3892/br.2018.1110.

Sokal, J.E., Cox, E.B., Baccarani, M., Tura, S., Gomez, G.A., Robertson, J.E., Tso, C.Y., Braun, T.J., Clarkson, B.D., Cervantes, F., *et al.,* (1984) Prognostic discrimination in "good-risk" chronic granulocytic leukaemia. *Blood* **63** (4); 789-799.

Somaiah, C., Kumar, A., Sharma, R., Sharma, A., Anand, T., Bhattacharyya, J., Das, D., Deka Talukdar, S. and Jaganathan, B.G. (2018) Mesenchymal stem cells show functional defect and decreased anti-cancer effect after exposure to chemotherapeutic drugs. *Journal of Biomedical Science*. **25** (1). doi:10.1186/s12929-018-0407-7.

Song, M., Wang, Y., Shang, Z.-F., Liu, X.-D., Xie, D.-F., Wang, Q., Guan, H. and Zhou, P.-K. (2016) Bystander autophagy mediated by radiation-induced exosomal miR-7-5p in non-targeted human

bronchial epithelial cells. *Nature Publishing Group* [online]. Available from: www.nature.com/scientificreports/doi:10.1038/srep30165 [Accessed 9 December 2019].

Song, M., Wang, H. and Ye, Q. (no date) Increased circulating vascular endothelial growth factor in acute myeloid leukemia patients: a systematic review and meta-analysis. Available from: https://doi.org/10.1186/s13643-020-01368-9doi:10.1186/s13643-020-01368-9 [Accessed 5 September 2020].

Spagnuolo, M., Regazzo, G., De Dominici, M., Sacconi, A., Pelosi, A., Korita, E., Marchesi, F., Pisani, F., Magenta, A., Lulli, V., Cordone, I., Mengarelli, A., Strano, S., Blandino, G., et al. (2019) Transcriptional activation of the miR-17-92 cluster is involved in the growth-promoting effects of MYB in human Ph-positive leukemia cells. *Haematologica*. 104 (1), pp. 82–92. doi:10.3324/haematol.2018.191213.

Spix, C., Schmiedel, S., Kaatsch, P., Schulze-Rath, R. and Blettner, M. (no date) *Case-control study on childhood cancer in the vicinity of nuclear power plants in Germany 1980-2003*. Available from: http://www.kinderkrebsregister.dedoi:10.1016/j.ejca.2007.10.024

Spyridonidis A, Küttler T, Wäsch R, Samek E, Waterhouse M, Behringer D, Bertz H, Finke J. (2005) Reduced intensity conditioning compared to standard conditioning preserves the in vitro growth capacity of bone marrow stroma, which remains of host origin. *Stem Cells Dev.* **14** (2); pp. 213-22. doi: 10.1089/scd.2005.14.213.

St-Pierre, J., Gregoire, J.C. and Vaillancourt, C. (2017) A simple method to assess group difference in RT_qPCR reference gene selection using GeNorm: The case of the placental sex. Scientific Reports [online]. 7 (1), pp. 1-7. Available from: www.nature.com/scientificreportsdoi:10.1038/s41598-017-16916-y [Accessed 25 August 2020].

Stranska, R., Gysbrechts, L., Wouters, J., Vermeersch, P., Bloch, K., Dierickx, D., Andrei, G. and Snoeck, R. (2018) Comparison of membrane affinity-based method with size-exclusion chromatography for isolation of exosome-like vesicles from human plasma Open Access Journal

of Translational Medicine. *J Transl Med* [online]. **16** pp. 1. Available from: https://doi.org/10.1186/s12967-017-1374-6doi:10.1186/s12967-017-1374-6 [Accessed 19 June 2020].

Stopper, H., Boos, G., Clark, M. and Gieseler, F. (1999) Are topoisomerase II inhibitor-induced micronuclei in vitro a predictive marker for the compounds' ability to cause secondary leukemias after treatment? *Toxicology Letters* 104.

Suárez-González, J., Martínez-Laperche, C., Kwon, M., Balsalobre, P., Carbonell, D., Chicano, M., Rodríguez-Macías, G., Serrano, D., Gayoso, J., Díez-Martín, J.L. and Buño, I. (2018) Donor Cell–Derived Hematologic Neoplasms after Hematopoietic Stem Cell Transplantation: A Systematic Review. *Biology of Blood and Marrow Transplantation*. **24** (7), pp. 1505–1513. doi:10.1016/j.bbmt.2018.01.033.

Sukumari-Ramesh, S., Prasad, N., Alleyne, C.H., Vender, J.R. and Dhandapani, K.M. (2015) *Overexpression of Nrf2 attenuates Carmustine-induced cytotoxicity in U87MG human glioma cells*. doi:10.1186/s12885-015-1134-z.

Sun, Z., Shi, K., Yang, S., Liu, J., Zhou, Q., Wang, G., Song, J., Li, Z., Zhang, Z. and Yuan, W. (2018) Effect of exosomal miRNA on cancer biology and clinical applications *Molecular Cancer* [online]. **17** (1). Available from: https://doi.org/10.1186/s12943-018-0897-7doi:10.1186/s12943-018-0897-7 [Accessed 10 June 2020].

Sunkara, V., Woo, H.-K. and Cho, Y.-K. (2016) Emerging techniques in the isolation and characterization of extracellular vesicles and their roles in cancer diagnostics and prognostics. *Cite this: Analyst* [online]. **141** pp. 371. Available from: www.rsc.org/analystdoi:10.1039/c5an01775k [Accessed 15 June 2020].

Šuštar, V., Janša, R., Frank, M., Hagerstrand, H., Kržan, M., Iglič, A. and Kralj-Iglič, V. (2009) Suppression of membrane microvesiculation - A possible anticoagulant and anti-tumor progression effect of heparin. *Blood Cells, Molecules, and Diseases*. **42** (3), pp. 223–227. doi:10.1016/j.bcmd.2009.01.012.

Suzuki, H. and Nakane, S. (1994) Differential induction of chromosomal aberrations by topoisomerase inhibitors in cultured Chinese hamster cells. *Biological Pharmaceutical Bulletins.* **17** (2); 222-226.

Suzuki, Y., Katayama, K., Ishikawa, E., Mizoguchi, S., Oda, K., Hirabayashi, Y., Haruki, A., Ito, T., Fujimoto, M., Murata, T. and Ito, M. (2017) Granulomatous interstitial nephritis due to chronic lymphocytic leukemia: A case report. In: *BMC Nephrology.* 2017 doi:10.1186/s12882-017-0775-3.

Suzuki, H., Ikeda, T., Yamagishi, T., Nakaike, S., Nakane, S. and Ohsawa, M. (1995) Efficient induction of chromosome-type aberrations by topoisomerase II inhibitors closely associated with stabilization of the cleavable complex in cultured fibroblastic cells *Mutation Research.* 328.

Sverdlov, E.D. (2012) Amedeo Avogadro's cry: What is 1µg of exosomes? *BioEssays.* **34** (10), pp. 873–875. doi:10.1002/bies.201200045.

Swift, L. H., & Golsteyn, R. M. (2014). Genotoxic anti-cancer agents and their relationship to DNA damage, mitosis, and checkpoint adaptation in proliferating cancer cells. *International journal of molecular sciences.* **15** (3), 3403–3431. https://doi.org/10.3390/ijms15033403 [Accessed 27 December 2020].

Szatanek, R., Baran, J., Siedlar, M. and Baj-Krzyworzeka, M. (2015) Isolation of extracellular vesicles: Determining the correct approach (review) *International Journal of Molecular Medicine* **36** (1) p.pp. 11–17. doi:10.3892/ijmm.2015.2194.

Szatmári, T., Kis, D., Bogdándi, E.N., Benedek, A., Bright, S., Bowler, D., Persa, E., Kis, E., Balogh, A., Naszályi, L.N., Kadhim, M., Sáfrány, G. and Lumniczky, K. (2017) Extracellular vesicles mediate radiation-induced systemic bystander signals in the bone marrow and spleen. *Frontiers in Immunology.* **8** (MAR). doi:10.3389/fimmu.2017.00347.

Takasugi, M., Okada, R., Takahashi, A., Virya Chen, D., Watanabe, S. and Hara, E. (2017) Small extracellular vesicles secreted from senescent cells promote cancer cell proliferation through

EphA2. *Nature Communications* [online]. **8**. Available from: www.nature.com/naturecommunicationsdoi:10.1038/ncomms15728 [Accessed 16 July 2020].

Takov, K., Yellon, D.M. and Davidson, S.M. (2017) Confounding factors in vesicle uptake studies using fluorescent lipophilic membrane dyes. *Journal of Extracellular Vesicles*. **6** (1). doi:10.1080/20013078.2017.1388731.

Tang, Y.T., Huang, Y.Y., Zheng, L., Qin, S.H., Xu, X.P., An, T.X., Xu, Y., Wu, Y.S., Hu, X.M., Ping, B.H. and Wang, Q. (2017) Comparison of isolation methods of exosomes and exosomal RNA from cell culture medium and serum. *International Journal of Molecular Medicine*. **40** (3), pp. 834–844. doi:10.3892/ijmm.2017.3080.

Taylor, D.D. and Shah, S. (2015) Methods of isolating extracellular vesicles impact down-stream analyses of their cargoes *Methods.* **87** p.pp. 3–10. doi:10.1016/j.ymeth.2015.02.019.

Terwilliger, T. and Abdul-Hay, M. (2017) Acute lymphoblastic leukemia: a comprehensive review and 2017 update. *Blood cancer journal* [online]. **7** (6), pp. e577. Available from: www.nature.com/bcjdoi:10.1038/bcj.2017.53

Testa, U. (2004) Apoptotic mechanisms in the control of erythropoiesis *Leukemia* [online]. **18** (7) p.pp. 1176–1199. Available from: www.nature.com/leudoi:10.1038/sj.leu.2403383 [Accessed 24 October 2019].

Théry, C., Witwer, K.W., Aikawa, E., Jose Alcaraz, M., Anderson, J.D., Jay, S.M., Jayachandran, M., Jenster, G., Jiang, L., Johnson, S.M., Jones, J.C., Jong, A., Jovanovic-Talisman, T., Jung, S., et al. (2018) Minimal information for studies of extracellular vesicles 2018 (MISEV2018): a position statement of the International Society for Extracellular Vesicles and update of the MISEV2014 guidelines. *Anabela Cordeiro-da-Silva* [online]. **119**. Available from: https://doi.org/10.1080/20013078.2018.1535750doi:10.1080/20013078.2018.1535750 [Accessed 14 January 2020].

Thiede C. (2004) Diagnostic chimerism analysis after allogeneic stem cell transplantation: new methods and markers. *American Journal of Pharmacogenomics*. **4** (3); 177-187.

Tian, T., Zhu, Y.-L., Hu, F.-H., Wang, Y.-Y., Huang, N.-P. and Xiao, Z.-D. (2013) Dynamics of exosome internalization and trafficking. *Journal of Cellular Physiology* [online]. **228** (7), pp. 1487–1495. Available from: http://doi.wiley.com/10.1002/jcp.24304doi:10.1002/jcp.24304 [Accessed 20 June 2020].

Torra, O.S. and Loeb, K.R. (2011) Donor Cell-Derived Leukemia and Myelodysplastic Neoplasm Unique Forms of Leukemia. *Am J Clin Pathol* [online]. **135** pp. 501. Available from: https://academic.oup.com/ajcp/article-abstract/135/4/501/1760425doi:10.1309/AJCPXW8DKEG5QMTB [Accessed 7 December 2019].

Trams, E.G., Lauter, C.J., Norman Salem, J. and Heine, U. (1981) Exfoliation of membrane ecto-enzymes in the form of micro-vesicles. *Biochimica et Biophysica Acta (BBA) - Biomembranes* [online]. **645** (1), pp. 63–70. Available from: https://www.sciencedirect.com/science/article/pii/0005273681905125?via%3Dihubdoi:10.1016/0005-2736(81)90512-5 [Accessed 13 August 2019].

Turchinovich, A., Weiz, L., Langheinz, A. and Burwinkel, B. (2011) Characterization of extracellular circulating microRNA. *Nucleic Acids Research*. **39** (16), pp. 7223–7233. doi:10.1093/nar/gkr254.

Umezu, T., Ohyashiki, K., Kuroda, M. and Ohyashiki, J.H. (2013) Leukemia cell to endothelial cell communication via exosomal miRNAs. *Oncogene* [online]. **32** pp. 2747–2755. Available from: www.nature.com/oncdoi:10.1038/onc.2012.295 [Accessed 16 December 2019].

Usmani, S., Sivagnanalingam, U., Tkachenko, O., Nunez, L., Shand, J.C. and Mullen, C.A. (2019). Support of acute lymphoblastic leukemia cells by nonmalignant bone marrow stromal cells. *Oncology Letters*. **17** (6), pp. 5039–5049. doi:10.3892/ol.2019.10188.

Valadi, H., Ekström, K., Bossios, A., Sjöstrand, M., Lee, J.J. and Lötvall, J.O. (2007) Exosome-mediated transfer of mRNAs and microRNAs is a novel mechanism of genetic exchange between cells. *Nature Cell Biology*. **9** (6), pp. 654–659. doi:10.1038/ncb1596.

Vallabhaneni, K.C., Penfornis, P., Dhule, S., Guillonneau, F., Adams, K. V, Yuan Mo, Y., Xu, R., Liu, Y., Watabe, K., Vemuri, M.C. and Pochampally, R. (2014) Oncotarget 4953 www.impactjournals.com/oncotarget Extracellular vesicles from bone marrow mesenchymal stem/ stromal cells transport tumor regulatory microRNA, proteins, and metabolites *Oncotarget* [online]. **6** (7). Available from: www.impactjournals.com/oncotarget/ [Accessed 16 December 2019].

van Belle, S.J.P., de Planque, M.M., Smith, I.E., van Oosterom, A.T., Schoemaker, T.J., Deneve, W. and McVie, J.G. (1986) Pharmacokinetics of mitoxantrone in humans following single agent infusion or intra-arterial injection therapy or combined-agent infusion therapy. *Cancer Chemotherapy and Pharmacology*. 18; 27–32.

van Dommelen, S.M., van der Meel, R., van Solinge, W.W., Coimbra, M., Vader, P. and Schiffelers, R.M. (2016) Cetuximab treatment alters the content of extracellular vesicles released from tumor cells. *Nanomedicine (London, England)* [online]. **11** (8), pp. 881–890. Available from: http://www.ncbi.nlm.nih.gov/pubmed/27021928doi:10.2217/nnm-2015-0009 [Accessed 16 August 2019].

van Niel, G. and Raposo, G. (2018) *Shedding light on the cell biology of extracellular vesicles*. Available from: www.nature.com/nrmdoi:10.1038/nrm.2017.125

Vangapandu, H. V., Ayres, M.L., Bristow, C.A., Wierda, W.G., Keating, M.J., Balakrishnan, K., Stellrecht, C.M. and Gandhi, V. (2017) The Stromal Microenvironment Modulates Mitochondrial Oxidative Phosphorylation in Chronic Lymphocytic Leukemia Cells. *Neoplasia (United States)*. **19** (10), pp. 762–771. doi:10.1016/j.neo.2017.07.004.

Vardiman, J.W., Thiele, J., Arber, D.A., Brunning, R.D., Borowitz, M.J., Porwit, A., Harris, N.L., Le Beau, M.M., Hellström-Lindberg, E., Tefferi, A. and Bloomfield, C.D. (2009) The 2008 revision of

the World Health Organization (WHO) classification of myeloid neoplasms and acute leukemia: Rationale and important changes *Blood* [online]. **114** (5) p.pp. 937–951. Available from: https://ashpublications.org/blood/article-pdf/114/5/937/1090302/zh803109000937.pdfdoi:10.1182/blood-2009-03-209262

Veal, G.J., Cole, M., Chinnaswamy, G., Sludden, J., Jamieson, D., Errington, J., Malik, G., Hill, C.R., Chamberlain, T. and Boddy, A. V (2016) Cyclophosphamide pharmacokinetics and pharmacogenetics in children with B-cell non-Hodgkin's lymphoma. *European Journal of Cancer* [online]. 55 pp. 56–64. Available from: http://creativecommons.org/licenses/by/4.0/doi:10.1016/j.ejca.2015.12.007 [Accessed 28 August 2020].

Veisani, Y., Khazaei, S. and Delpisheh, A. (2018) Review Article 5-year survival rates based on the type of leukemia in Iran, a Meta-analysis. *Caspian J Intern Med*. **9** (4), pp. 316–324. doi:10.22088/cjim.9.4.316.

Vuckovic, S., Vandyke, K., Rickards, D.A., McCauley Winter, P., Brown, S.H.J., Mitchell, T.W., Liu, J., Lu, J., Askenase, P.W., Yuriev, E., Capuano, B., Ramsland, P.A., Hill, G.R., Zannettino, A.C.W., et al. (2017) The cationic small molecule GW4869 is cytotoxic to high phosphatidylserine-expressing myeloma cells. *British Journal of Haematology* [online]. **177** (3), pp. 423–440. Available from: http://doi.wiley.com/10.1111/bjh.14561doi:10.1111/bjh.14561 [Accessed 24 June 2020].

Wanchoo, R., Ramirez, C.B., Barrientos, J. and Jhaveri, K.D. (2018) Renal involvement in chronic lymphocytic leukemia *Clinical Kidney Journal* [online] 11 (5) p.pp. 670–680. Available from: https://academic.oup.com/ckj/article-abstract/11/5/670/4967844/doi:10.1093/ckj/sfy026

Wang, X., Gu, H., Qin, D., Yang, L., Huang, W., Essandoh, K., Wang, Y., Caldwell, C.C., Peng, T., Zingarelli, B. and Fan, G.-C. (2015) Exosomal miR-223 Contributes to Mesenchymal Stem Cell-Elicited Cardioprotection in Polymicrobial Sepsis OPEN. *Nature Publishing Group* [online]. Available from: www.nature.com/scientificreports/doi:10.1038/srep13721 [Accessed 3 March 2020].

Wang, E., Hutchinson, C.B., Huang, Q., Lu, C.M., Crow, J., Wang, F.F., Sebastian, S., Rehder, C., Lagoo, A., Horwitz, M., Rizzieri, D., Yu, J., Goodman, B., Datto, M., et al. (2011) Donor cell-derived leukemias/myelodysplastic neoplasms in allogeneic hematopoietic stem cell transplant recipients: A clinicopathologic study of 10 cases and a comprehensive review of the literature. *American Journal of Clinical Pathology*. **135** (4), pp. 525–540. doi:10.1309/AJCPPJUQ9DNR1GHP.

Wang, J., Zhao, J., Fei, X., Yin, Y., Cheng, H., Zhang, W., Gu, J., Yang, F., Yang, Y., Xue, S., Tian, Z., He, J., Zhang, S. and Wang, X. (2018) A new intensive conditioning regimen for allogeneic hematopoietic stem cell transplantation in patients with refractory or relapsed acute myeloid leukemia. *Medicine (United States)* [online]. 97 (17). Available from: http://dx.doi.org/10.1097/MD.0000000000010228doi:10.1097/MD.0000000000010228 [Accessed 3 September 2020].

Wang, J., Faict, S., Maes, K., De Bruyne, E., Van Valckenborgh, E., Schots, R., Vanderkerken, K. and Menu, E. (2016) Extracellular vesicle cross-talk in the bone marrow microenvironment: Implications in multiple myeloma. *Oncotarget*. 7 (25), pp. 38927–38945. doi:10.18632/oncotarget.7792.

Wasnik, S., Kantipudi, S., Kirkland, M.A. and Pande, G. (2016) Enhanced Ex Vivo Expansion of Human Hematopoietic Progenitors on Native and Spin Coated Acellular Matrices Prepared from Bone Marrow Stromal Cells. *Stem Cells International*. 2016 . doi:10.1155/2016/7231567.

Webber, J. and Clayton, A. (2013) *How pure are your vesicles?* Available from: http://dx.doi.org/10.3402/jev.v2i0.19861doi:10.3402/jev.v2i0.19861 [Accessed 12 June 2020].

Wei, Z., Batagov, A.O., Carter, D.R.F. and Krichevsky, A.M. (2016) Fetal Bovine Serum RNA Interferes with the Cell Culture derived Extracellular RNA. *Scientific Reports*. **6**. doi:10.1038/srep31175.

Wei, Y., Lai, X., Yu, S., Chen, S., Ma, Y., Zhang, Y., Li, H., Zhu, X., Yao, L. and Zhang, J. (2014) Exosomal miR-221/222 enhances tamoxifen resistance in recipient ER-positive breast cancer

cells. *Breast Cancer Research and Treatment*. **147** (2), pp. 423–431. doi:10.1007/s10549-014-3037-0.

Weisberg, E., Wright, R.D., McMillin, D.W., Mitsiades, C., Ray, A., Barrett, R., Adamia, S., Stone, R., Galinsky, I., Kung, A.L. and Griffin, J.D. (2008) Stromal-mediated protection of tyrosine kinase inhibitor-treated BCR-ABL-expressing leukemia cells. *Molecular Cancer Therapeutics*. **7** (5), pp. 1121–1129. doi:10.1158/1535-7163.MCT-07-2331.

Welton, J.L., Webber, J.P., Botos, L.A., Jones, M. and Clayton, A. (2015) Ready-made chromatography columns for extracellular vesicle isolation from plasma. *Journal of Extracellular Vesicles* [online]. **4** (2015), pp. 1–9. Available from: http://dx.doi.org/10.3402/jev.v4.27269doi:10.3402/jev.v4.27269 [Accessed 19 June 2020].

Wenk, C., Garz, A.K., Grath, S., Huberle, C., Witham, D., Weickert, M., Malinverni, R., Niggemeyer, J., Kyncl, M., Hecker, J., Pagel, C., Mulholland, C.B., Müller-Thomas, C., Leonhardt, H., et al. (2018) Direct modulation of the bone marrow mesenchymal stromal cell compartment by azacitidine enhances healthy hematopoiesis. *Blood Advances*. **2** (23), pp. 3447–3461. doi:10.1182/bloodadvances.2018022053.

Willms, E., Cabañas, C., Mäger, I., Wood, M.J.A. and Vader, P. (2018) Extracellular vesicle heterogeneity: Subpopulations, isolation techniques, and diverse functions in cancer progression *Frontiers in Immunology.* 9 (APR). doi:10.3389/fimmu.2018.00738.

Wiseman, D.H. (2011) Donor Cell Leukemia: A Review. *Biology of Blood and Marrow Transplantation.* **17** (6) p.pp. 771–789. doi:10.1016/j.bbmt.2010.10.010.

Wiseman, L.R. and Spencer, C.M. (1997) Mitoxantrone: A review of its pharmacology and clinical efficacy in the management of hormone-resistant advanced prostate cancer *Drugs and Aging.* **10** (6) p.pp. 473–485. doi:10.2165/00002512-199710060-00007.

World Cancer Research Fund (2018) Worldwide cancer data. Available from: https://www.wcrf.org/dietandcancer/cancer-trends/worldwide-cancer-data [Accessed 29 December 2020].

Wu, H., Zhou, J., Mei, S., Wu, D., Mu, Z., Chen, B., Xie, Y., Ye, Y. and Liu, J. (2017) Circulating exosomal microRNA-96 promotes cell proliferation, migration and drug resistance by targeting LMO7. *Journal of Cellular and Molecular Medicine*. **21** (6), pp. 1228–1236. doi:10.1111/jcmm.13056.

Wu, J., Ding, J., Yang, J., Guo, X. and Zheng, Y. (2018) MicroRNA roles in the nuclear factor kappa B signaling pathway in cancer *Frontiers in Immunology* [online] 9 (MAR) p.pp. 546. Available from: www.frontiersin.orgdoi:10.3389/fimmu.2018.00546 [Accessed 29 May 2020].

Wu, P., Zhang, B., Ocansey, D.K.W., Xu, W. and Qian, H. (2020) Extracellular vesicles: A bright star of nanomedicine. Biomaterials. **6**:120467. doi: 10.1016/j.biomaterials.2020.120467. Epub ahead of print. PMID: 33189359. https://doi.org/10.1016/j.biomaterials.2020.120467 [Accessed 27 December 2020].

Xavier, C.P.R., Caires, H.R., Barbosa, M.A.G., Bergantim, R., Guimarães, J.E. and Vasconcelos, M.H. (2020) The Role of Extracellular Vesicles in the Hallmarks of Cancer and Drug Resistance *Cells.* **9** (5). doi:10.3390/cells9051141.

Xiao, X., Yu, S., Li, S., Wu, J., Ma, R., Cao, H., Zhu, Y. and Feng, J. (2014) Exosomes: Decreased sensitivity of lung cancer A549 cells to cisplatin. *PLoS ONE*. **9** (2). doi:10.1371/journal.pone.0089534.

Xie, H., Sun, L., Zhang, L., Liu, T., Chen, L., Zhao, A., Lei, Q., Gao, F., Zou, P., Li, Q., Guo, A.-Y., Chen, Z. and Wang, H. (2016) *Mesenchymal Stem Cell-Derived Microvesicles Support Ex Vivo Expansion of Cord Blood-Derived CD34 + Cells*. Available from: http://dx.doi.org/10.1155/2016/6493241doi:10.1155/2016/6493241 [Accessed 5 March 2020].

Xin, H., Katakowski, M., Wang, F., Qian, J.Y., Liu, X.S., Ali, M.M., Buller, B., Zhang, Z.G. and Chopp, M. (2017) MicroRNA cluster miR-17-92 Cluster in Exosomes Enhance Neuroplasticity and Functional Recovery after Stroke in Rats. In: *Stroke*. 2017 pp. 747–753. doi:10.1161/STROKEAHA.116.015204.

Xu, S., Ding, N., Pei, H., Hu, W., Wei, W., Zhang, X., Zhou, G. and Wang, J. (2014) *MiR-21 is involved in radiation-induced bystander effects*. Available from: http://dx.doi.org/10.4161/rna.34380doi:10.4161/rna.34380 [Accessed 29 May 2020].

Xu, S., Wang, J., Ding, N., Hu, W., Zhang, X., Wang, B., Hua, J., Wei, W. and Zhu, Q. (2015) *Exosome-mediated microRNA transfer plays a role in radiation-induced bystander effect*. Available from: http://dx.doi.org/10.1080/15476286.2015.1100795doi:10.1080/15476286.2015.1100795 [Accessed 9 December 2019].

Yamamoto, K.R., Alberts, B.M., Benzinger, R., Lawhorne, L. and Treiber, G. (1970) Rapid Bacteriophage Sedimentation in the Presence of Polyethylene Glycol and Its Application to Large-Scale Virus Purification *VIROLOGY* 40.

Yan, L., Qiu, J. and Yao, J. (2017) Downregulation of microRNA-30d promotes cell proliferation and invasion by targeting LRH-1 in colorectal carcinoma. *International Journal of Molecular Medicine*. 39 (6), pp. 1371–1380. doi:10.3892/ijmm.2017.2958.

Yang, B., Solakyildirim, K., Chang, Y. and Linhardt, R.J. (2011) Hyphenated techniques for the analysis of heparin and heparan sulfate *Analytical and Bioanalytical Chemistry.* **399** (2) p.pp. 541–557. doi:10.1007/s00216-010-4117-6.

Yang, W.I. (2002) Neoplastic Diseases of the Hematopoietic and Lymphoid Tissues: New World Health Organization Classification. *Korean Journal of Pathology*. **36** (3), pp. 137–145.

Yang, S.-J. and Rafla, S. (1985) Temperature Effect on Mitoxantrone Cytotoxicity in Chinese Hamster Cells in Vitro *CANCER RESEARCH* 45.

Yang, S.J., Yang, S.Y., Wang, D.D., Chen, X., Shen, H.Y., Zhang, X.H., Zhong, S.L., Tang, J.H. and Zhao, J.H. (2017) The miR-30 family: Versatile players in breast cancer *Tumor Biology.* **39** (3). doi:10.1177/1010428317692204.

Yin, X., Tian, W., Wang, L., Wang, J., Zhang, S., Cao, J. and Yang, H. (2015) Radiation quality-dependence of bystander effect in unirradiated fibroblasts is associated with TGF-β1-Smad2 pathway and miR-21 in irradiated keratinocytes. *Scientific Reports*. **5**. doi:10.1038/srep11373.

Zeng, Z., Li, Y., Pan, Y., Lan, X., Song, F., Sun, J., Zhou, K., Liu, X., Ren, X., Wang, F., Hu, J., Zhu, X., Yang, W., Liao, W., et al. (2018) Cancer-derived exosomal miR-25-3p promotes pre-metastatic niche formation by inducing vascular permeability and angiogenesis. *Nature Communications* [online]. **9** (1). Available from: https://doi.org/10.1038/s41467-018-07810-wdoi:10.1038/s41467-018-07810-w [Accessed 2 July 2020].

Zhang, L., Zhou, L., Shi, M., Kuang, Y. and Fang, L. (2018) Downregulation of miRNA-15a and miRNA-16 promote tumor proliferation in multiple myeloma by increasing CABIN1 expression. *Oncology Letters*. 15 (1), pp. 1287–1296. doi:10.3892/ol.2017.7424.

Zhang, C., Soori, M., Miles, F.L., Sikes, R.A., Carson, D.D., Chung, L.W.K. and Farach-Carson, M.C. (2011) Paracrine factors produced by bone marrow stromal cells induce apoptosis and neuroendocrine differentiation in prostate cancer cells. *Prostate* [online]. **71** (2), pp. 157–167. Available from: www.interscience.wiley.comdoi:10.1002/pros.21231 [Accessed 27 May 2020].

Zhang, H.C., Liu, X. Bin, Huang, S., Bi, X.Y., Wang, H.X., Xie, L.X., Wang, Y.Q., Cao, X.F., Lv, J., Xiao, F.J., Yang, Y. and Guo, Z.K. (2012) Microvesicles derived from human umbilical cord mesenchymal stem cells stimulated by hypoxia promote angiogenesis both in vitro and in vivo. *Stem Cells and Development*. **21** (18), pp. 3289–3297. doi:10.1089/scd.2012.0095.

Zhang, R., Xu, J., Zhao, J. and Bai, J. (2017) Mir-30d suppresses cell proliferation of colon cancer cells by inhibiting cell autophagy and promoting cell apoptosis. *Tumor Biology*. **39** (6). doi:10.1177/1010428317703984.

Zhang, J., Liu, J., Xu, X. and Li, L. (2017) Curcumin suppresses cisplatin resistance development partly via modulating extracellular vesicle-mediated transfer of MEG3 and miR-214 in ovarian cancer. *Cancer Chemotherapy and Pharmacology* [online]. **79** pp. 479–487. Available from: http://bibiserv2.cebitec.uni-bielefeld.de/rnahybriddoi:10.1007/s00280-017-3238-4 [Accessed 16 December 2019].

Zhang, J., Li, S., Li, L., Li, M., Guo, C., Yao, J. and Mi, S. (2015) Exosome and exosomal microRNA: Trafficking, sorting, and function *Genomics, Proteomics and Bioinformatics.* **13** (1) p.pp. 17–24. doi:10.1016/j.gpb.2015.02.001.

Zhang, Y., Chen, X., Gueydan, C. and Huan, J. (2017) Plasma membrane changes during programmed cell deaths. *Cell Research.* **28,** 9–21 (2018). https://doi.org/10.1038/cr.2017.133 [Accessed 30 April 2020].

Zhang, D., Lee, H., Wang, X., Rai, A., Groot, M. and Jin, Y. (2018) Exosome-Mediated Small RNA Delivery: A Novel Therapeutic Approach for Inflammatory Lung Responses. *Molecular Therapy*. **26** (9), pp. 2119–2130. doi:10.1016/j.ymthe.2018.06.007.

Zhang, Y., Jin, X., Liang, J., Guo, Y., Sun, G., Zeng, X. and Yin, H. (2019) Extracellular vesicles derived from ODN-stimulated macrophages transfer and activate Cdc42 in recipient cells and thereby increase cellular permissiveness to EV uptake *Sci. Adv* [online] **5**. Available from: http://advances.sciencemag.org/ [Accessed 20 June 2020].

Zhang, Y., Zhang, Y., Yin, Y. and Li, S. (2019) Detection of circulating exosomal miR-17-5p serves as a novel non-invasive diagnostic marker for non-small cell lung cancer patients. *Pathology Research and Practice* [online]. 215 (8). Available from: https://doi.org/10.1016/j.prp.2019.152466doi:10.1016/j.prp.2019.152466 [Accessed 2 July 2020].

Zhang, Y., Liu, Y., Liu, H. and Tang, W.H. (2019) Exosomes: Biogenesis, biologic function and clinical potential. *Cell and Bioscience* [online]. **9** (1), pp. 1–18. Available from:

https://doi.org/10.1186/s13578-019-0282-2doi:10.1186/s13578-019-0282-2 [Accessed 1 October 2020].

Zhao, E., Xu, H., Wang, L., Kryczek, I., Wu, K., Hu, Y., Wang, G. and Zou, W. (2012) Bone marrow and the control of immunity *Cellular and Molecular Immunology* [online]. **9** (1) p.pp. 11–19. Available from: www.nature.com/cmidoi:10.1038/cmi.2011.47 [Accessed 24 October 2019].

Zhou, J., Ching, Y.Q. and Chng, W.J. (2015) Aberrant nuclear factor-kappa B activity in acute myeloid Leukemia: From molecular pathogenesis to therapeutic target. *Oncotarget* [online]. 6 (8), pp. 5490–5500. Available from: www.impactjournals.com/oncotargetdoi:10.18632/oncotarget.3545 [Accessed 5 September 2020].

Zhou, J. dong, Zhang, L. chao, Zhang, T. juan, Gu, Y., Wu, D. hong, Zhang, W., Ma, J. chun, Wen, X. mei, Guo, H., Lin, J. and Qian, J. (2018) Dysregulation of miR-200s clusters as potential prognostic biomarkers in acute myeloid leukemia. *Journal of Translational Medicine* [online]. 16 (1), pp. 135. Available from: https://doi.org/10.1186/s12967-018-1494-7doi:10.1186/s12967-018-1494-7 [Accessed 5 September 2020].

8.0 Appendix

Table 8.1 List of upregulated miRNAs that are in bystander TK6 cells with Ct values more than 34.

MiRNA(s)	Control (Average Ct value)	Treatment (Average Ct value)	Fold change	Fold Regulation	95% CI	P-value
hsa-miR-150-5p	35	35	2.03	2.03	0.00001. 10.07	0.396
hsa-miR-32-5p	35	35	2.03	2.03	0.00001. 10.07	0.396
hsa-miR-101-3p	34.7	34.88	1.79	1.79	0.00001. 8.67	0.397
hsa-miR-302b-3p	35	35	2.03	2.03	0.00001. 10.07	0.396
hsa-miR-376c-3p	35	35	2.03	2.03	0.00001. 10.07	0.396
hsa-miR-122-5p	35	35	2.03	2.03	0.00001. 10.07	0.396
hsa-miR-144-3p	35	35	2.03	2.03	0.00001. 10.07	0.396
hsa-miR-126-3p	35	35	2.03	2.03	0.00001. 10.07	0.396
hsa-miR-143-3p	35	35	2.03	2.03	0.00001. 10.07	0.396
hsa-miR-28-5p	35	35	2.03	2.03	0.00001. 10.07	0.396
hsa-miR-96-5p	35	34.95	2.10	2.10	0.00001. 10.45	0.396
hsa-miR-223-3p	34.81	35	1.18	1.18	0.00001. 8.81	0.397
hsa-miR-141-3p	35	35	2.03	2.03	0.00001. 10.07	0.396
hsa-miR-302a-3p	34.73	35	1.69	1.69	0.00001. 8.34	0.398
hsa-miR-196b-5p	35	35	2.03	2.03	0.00001. 10.07	0.396
hsa-miR-302c-3p	35	35	2.03	2.03	0.00001. 10.07	0.396
hsa-miR-96-5p	35	34.95	2.10	2.10	0.00001. 10.45	0.396

Relative expression levels of the miRNAs with Ct values of more than 34 are shown. Student *t*-test of the replicate normalized miRNA expression values was performed for each miRNA in the control and treatment groups. Red colour indicates the candidate miRNA that was chosen as the negative control in this study. Fold change values greater than one indicate an upregulation whilst fold regulation represents the negative inverse of the fold change hence the fold regulation is equal to the fold change.

Table 8.2 List of some of the genes controlled by the candidate miRNAs as identified by bioinformatics.

S/N	Genes	MicroRNA(s) involved

1	TP53	hsa-miR-30d-5p, hsa-miR-16-5p
2	SMAD1	hsa-miR-30d-5p
3	RUNX2	hsa-miR-30d-5p
4	SOCS1	hsa-miR-30d-5p
5	FADD	hsa-miR-146a-5p
6	BRCA1	hsa-miR-146a-5p
7	IL-8	hsa-miR-146a-5p, hsa-miR-146a-5p
8	CDKN1A	hsa-miR-146a-5p, hsa-miR-20a-5p, hsa-miR-17-5p
9	EGFR	hsa-miR-146a-5p, hsa-miR-16-5p
10	SMAD4	hsa-miR-146a-5p, hsa-miR-17-5p, hsa-miR-20a-5p
11	ICAM-1	hsa-miR-146a-5p, hsa-miR-17-5p, hsa-miR-20a-5p
12	SMAD2	hsa-miR-146a-5p
13	PTGS2	hsa-miR-146a-5p, hsa-miR-16-5p
14	RAC1	hsa-miR-146a-5p
15	CCNE1	hsa-miR-16-5p
16	PTEN	hsa-miR-20a-5p, hsa-miR-17-5p
17	TIMP3	hsa-miR-17-5p
18	MYB	hsa-miR-16-5p, hsa-miR-200C-3p
19	HIF1A	hsa-miR-20a-5p, hsa-miR-17-5p
20	TCEAL1	hsa-miR-20a-5p, hsa-miR-17-5p
21	CCND1	hsa-miR-20a-5p, hsa-miR-16-5p, hsa-miR-17-5p
22	E2F1	hsa-miR-20-5p, hsa-miR-17-5p
23	BMPR2	hsa-miR-20-5p, hsa-miR-17-5p
24	TGFBR2	hsa-miR-20-5p, hsa-miR-17-5p
25	MAP3K12	hsa-miR-20-5p, hsa-miR-17-5p
26	BCL2	hsa-miR-20-5p, hsa-miR-17-5p, hsa-miR-16-5p, hsa-miR-200c-3p
27	MEF2D	hsa-miR-20-5p, hsa-miR-17-5p
28	APP	hsa-miR-20-5p, hsa-miR-17-5p
29	RUNX1	hsa-miR-20-5p, hsa-miR-17-5p
30	VEGFA	hsa-miR-20-5p, hsa-miR-17-5p, hsa-miR-16-5p, hsa-miR-200c-3p
31	MYC	hsa-miR-20-5p, hsa-miR-17-5p
32	CCND2	hsa-miR-20-5p, hsa-miR-17-5p
33	E2F3	hsa-miR-20-5p, hsa-miR-17-5p
34	MAPK9	hsa-miR-20-5p, hsa-miR-17-5p
35	RB1	hsa-miR-20-5p, hsa-miR-17-5p
36	RBL1	hsa-miR-20-5p, hsa-miR-17-5p
37	RBL2	hsa-miR-20-5p, hsa-miR-17-5p
38	WEE1	hsa-miR-20-5p, hsa-miR-17-5p, hsa-miR-16-5p
39	PURA	hsa-miR-20-5p, hsa-miR-17-5p
40	SIRP-α	hsa-miR-20-5p, hsa-miR-17-5p
41	UBE2	hsa-miR-20-5p, hsa-miR-17-5p
42	STAT3	hsa-miR-20-5p, hsa-miR-17-5p
43	LIMK1	hsa-miR-20-5p, hsa-miR-17-5p
44	ITGB8	hsa-miR-20-5p, hsa-miR-17-5p
45	TP531NP1	hsa-miR-20-5p, hsa-miR-17-5p
46	ETV1	hsa-miR-20-5p, hsa-miR-17-5p

| 47	EPAS1	hsa-miR-20-5p, hsa-miR-17-5p
48	FBX031	hsa-miR-20-5p, hsa-miR-17-5p
49	DNMT1	hsa-miR-20-5p, hsa-miR-17-5p
50	SOX6	hsa-miR-16-5p
51	KRAS	hsa-miR-16-5p, hsa-miR-200c-3p
52	SELE	hsa-miR-17-5p
53	HBP1	hsa-miR-17-5p
54	CASP3	hsa-miR-30d-5p
55	BCL9	hsa-miR-30d-5p
56	NOTCH1	hsa-miR-30d-5p, hsa-miR-200c-3p
57	ATG9	hsa-miR-16-5p
58	ATG5	hsa-miR-30d-5p
59	BECN1	hsa-miR-30d-5p
60	ATG2B	hsa-miR-30d-5p
61	ATG12	hsa-miR-30d-5p
62	BNP3L	hsa-miR-30d-5p
63	GNAI2	hsa-miR-30d-5p
64	EZH2	hsa-miR-30d-5p
65	GPRR78	hsa-miR-30d-5p
66	CXCR4	hsa-miR-146a-5p
67	TLR2	hsa-miR-146a-5p
68	BRCA2	hsa-miR-146a-5p
69	NFKB1	hsa-miR-146a-5p
70	STAT1	hsa-miR-146a-5p
71	CDKN3	hsa-miR-146a-5p
72	CCNA2	hsa-miR-146a-5p
73	IRAK1	hsa-miR-146a-5p
74	FAS	hsa-miR-146a-5p
75	TLR4	hsa-miR-146a-5p
76	CD40LG	hsa-miR-146a-5p
77	NUMB	hsa-miR-146a-5p
78	MTOR	hsa-miR-200c-3p
79	AKT3	hsa-miR-200c-3p
80	NOTCH2	hsa-miR-200c-3p
81	RAF1	hsa-miR-200c-3p
82	IGF1R	hsa-miR-200c-3p
83	FGFR1	hsa-miR-200c-3p
84	DNMT3A	hsa-miR-200c-3p
85	DNMT3B	hsa-miR-200c-3p
86	CCNE2	hsa-miR-200c-3p
87	GATA4	hsa-miR-200c-3p
88	KIT	hsa-miR-17-5p
89	TSG101	hsa-miR-17-5p
90	MAP2K3	hsa-miR-17-5p
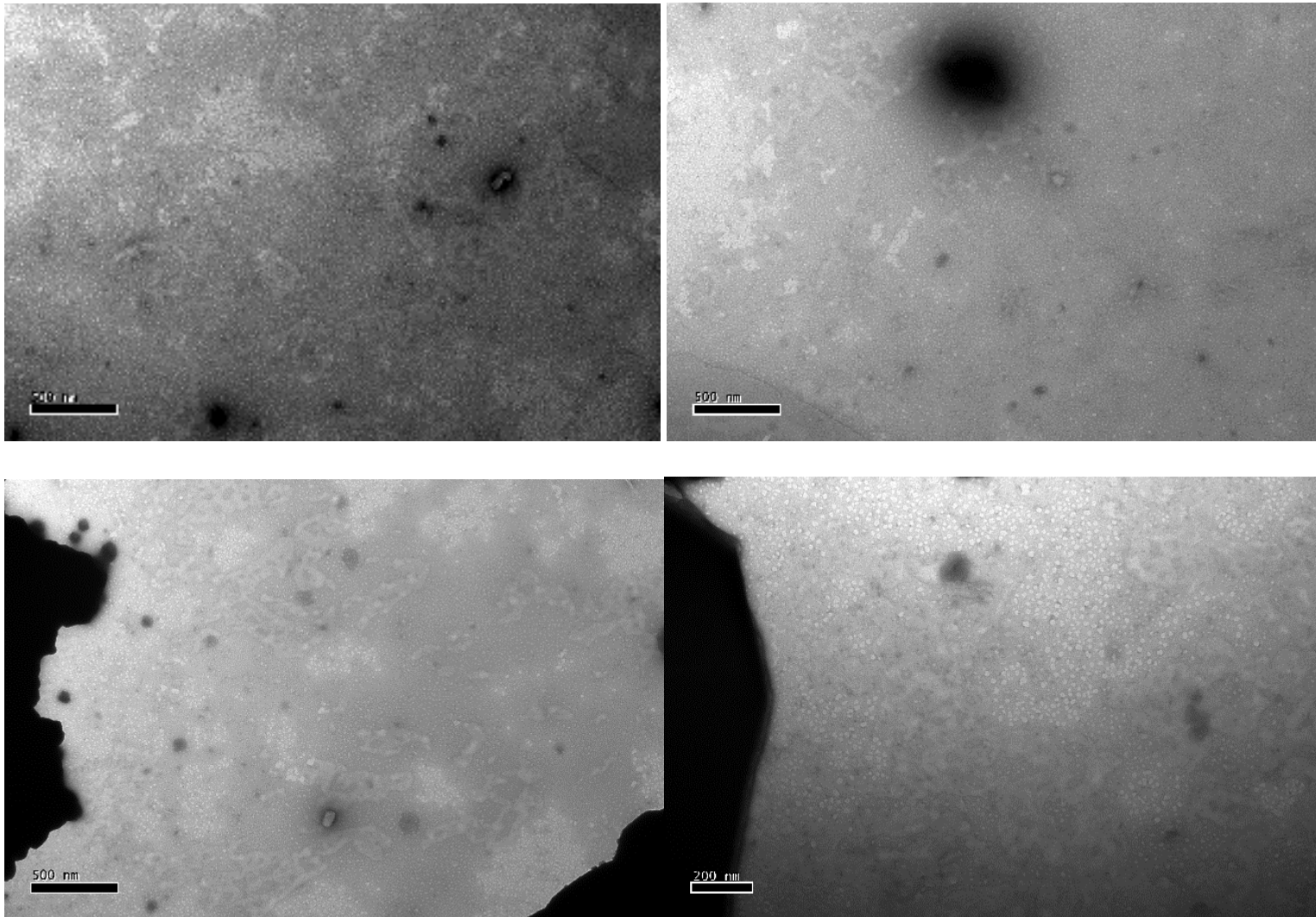
Figure 8.1 Transmission elecron micrographs of the control (PBS only). The electron micrographs show that there is no vesicle within PBS, which was used as the suspension buffer for the vesicles. Scale bar, 500 nm.
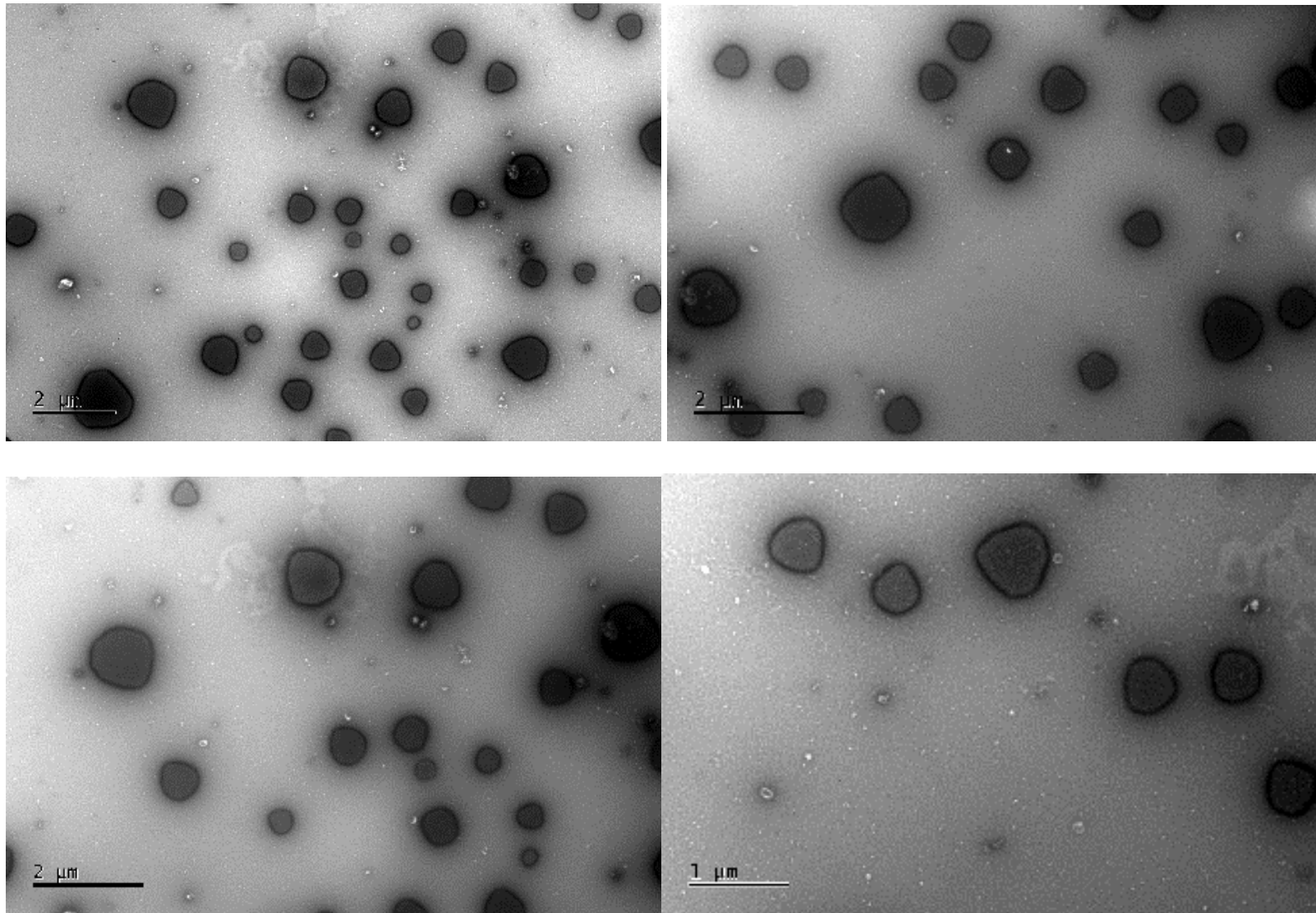
Figure 8.2 HS-5 cells release large extracellular vesicles following exposure to chemotherapy. Large vesicles were also observed following exposure of stromal cells to treatment with drugs. Scale bar, 2 µm.
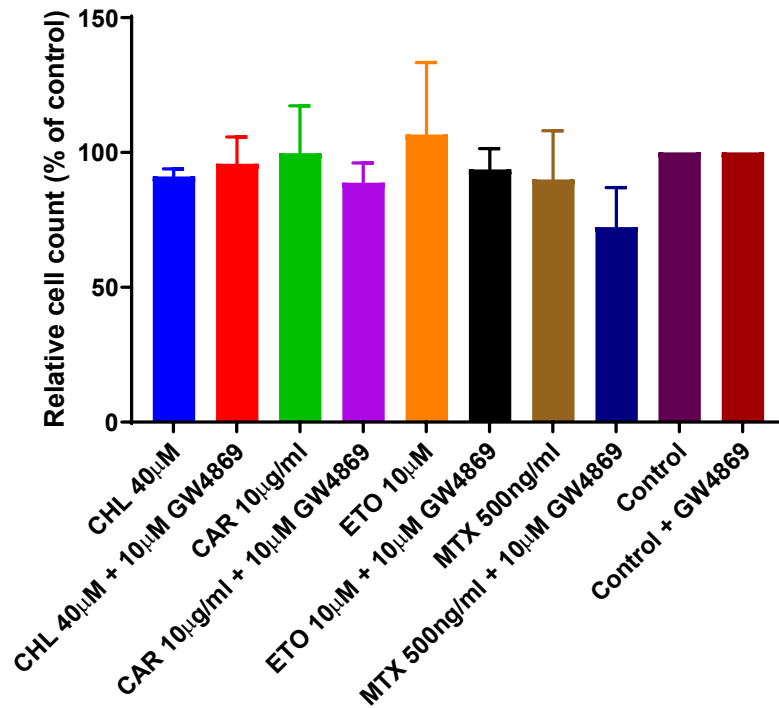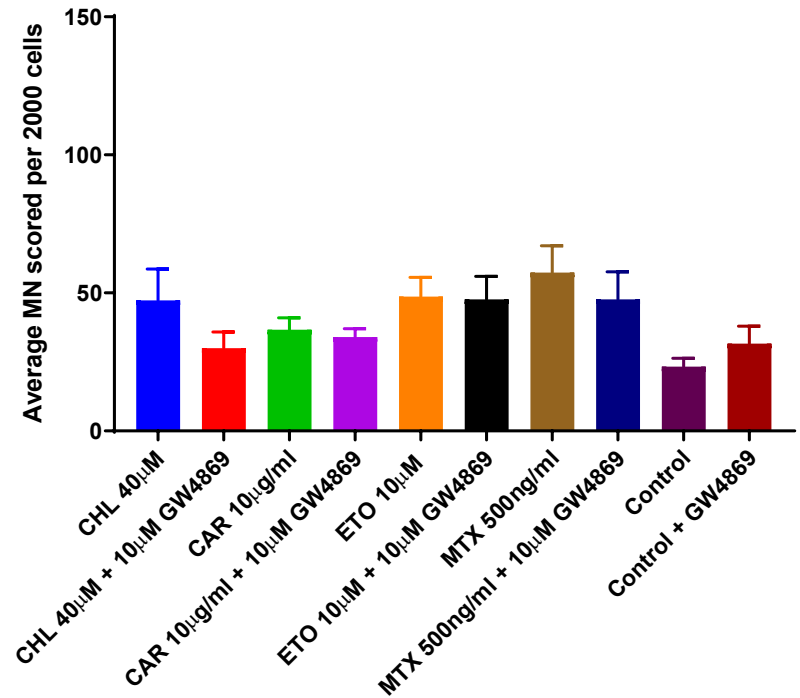
Figure 8.3 GW4869 does not have an effect on chemotherapy-induced bystander effect. A. Cell viability of bystander TK6 cells exposed to HS-5 cells that were pre-treated with drugs in the presence or absence of 10 μM GW4869. **B.** Micronuclei formed in the bystander TK6 cells exposed to HS-5 that were pre-treated with drugs in the presence or absence of 10 μM GW4869.
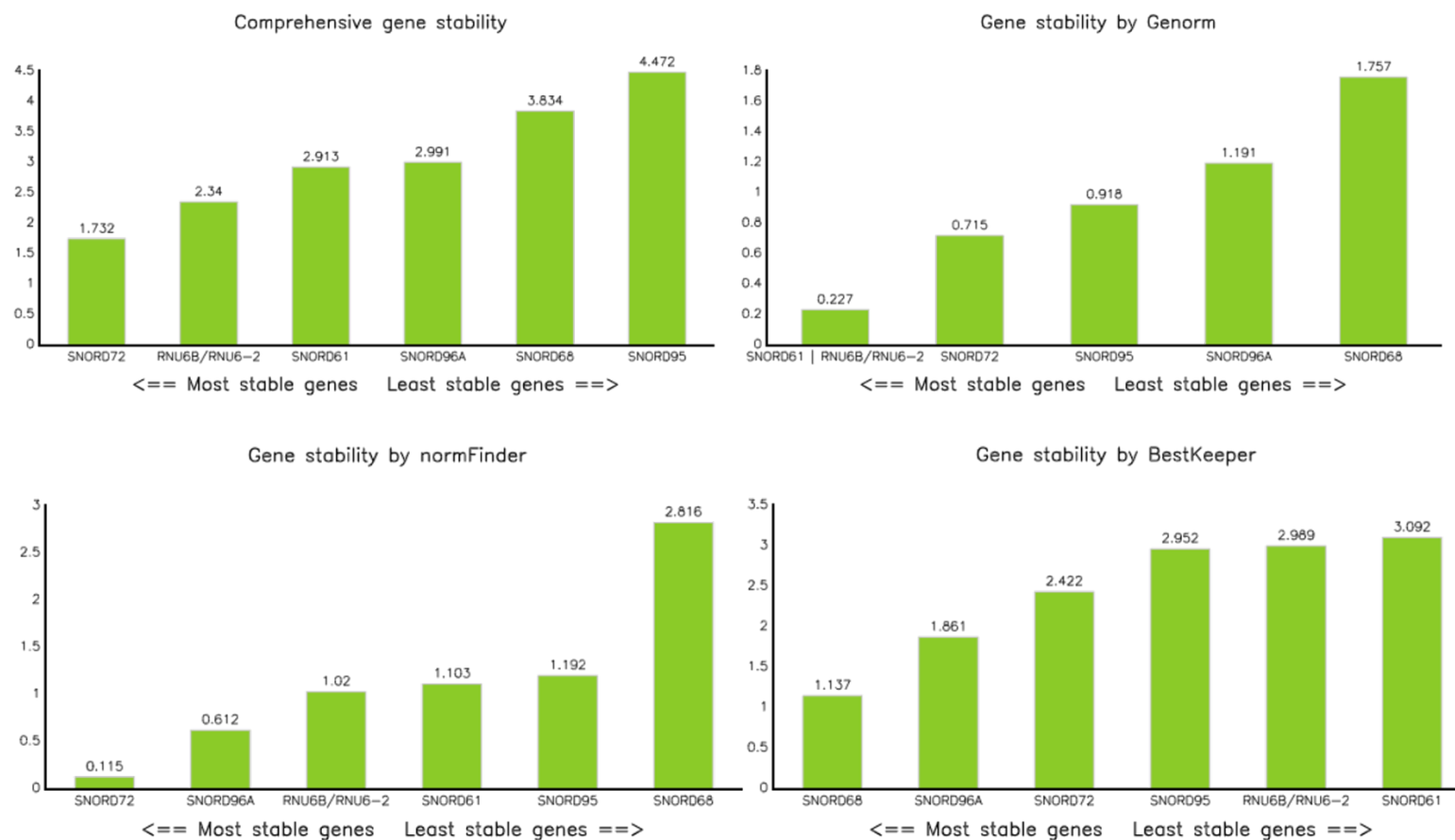
Figure 8.4 Normalisation of small nuclear RNAs. The Ct values of small nuclear RNAs used as normalisers in microarray of bystander TK6 cells' RNA were put through three normalization software tools (GeNorm, NormFinder and BestKeeper) to identify the candidate normalisers for the validation of miRNA expression in this study. A normalisation miRNA candidate has to fulfil two criteria: it has be stably expressed in the cells of interest and it has to have an expression level above background.
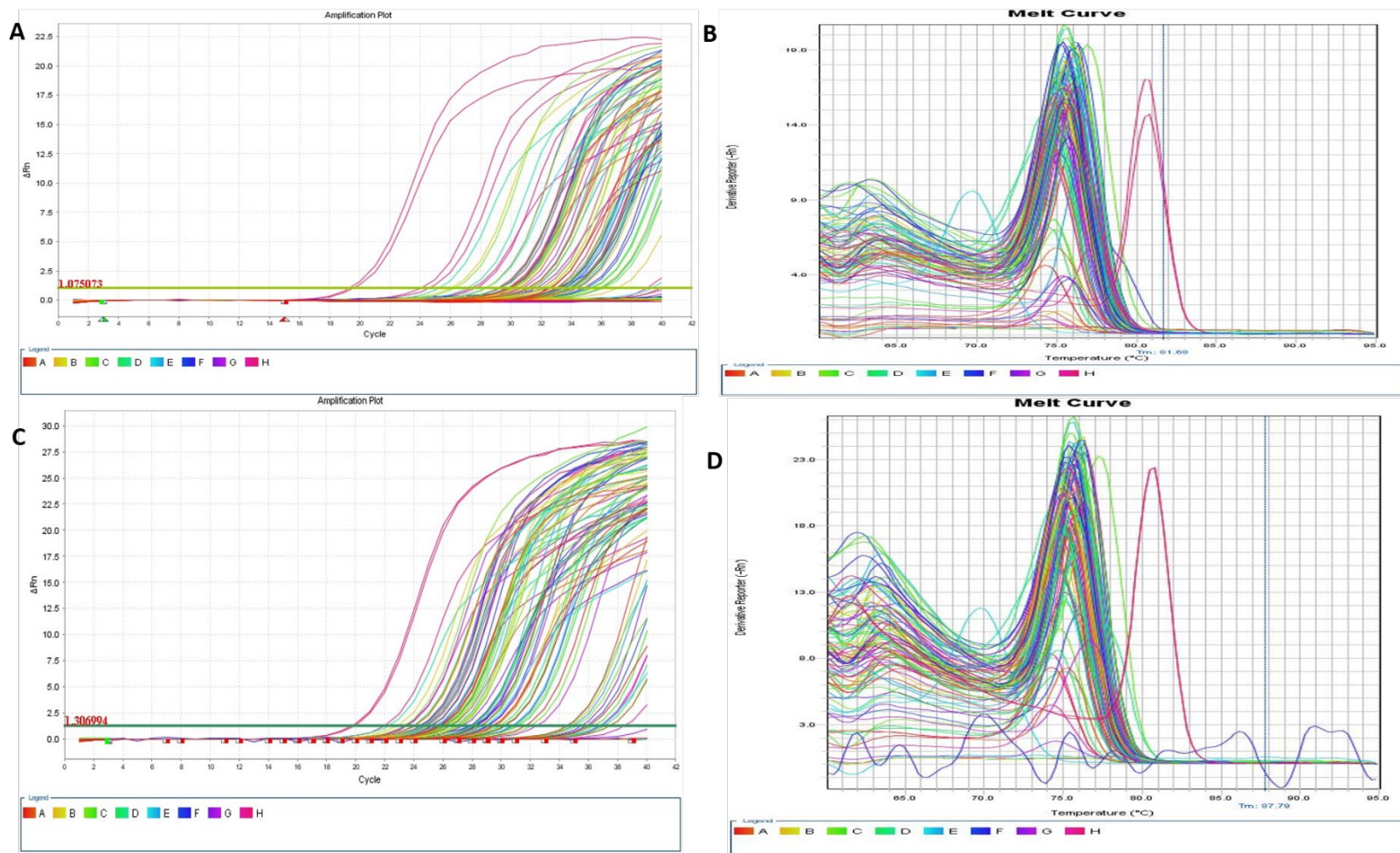
Figure 8.5 Linear amplification plots and melt curves from microarray of bystander TK6 cells' RNA. The amplicons from RNA isolated from bystander TK6 cells exposed to untreated HS-5 cells (A) and treated HS-5 cells (C) are shown. These linearly amplified RNA samples indicate that abundant amplicons were generated. These linear amplicons also reveal a single peak following melt curve analysis thus idnicating sinle amplicons were geneated in both untreated (B) and treated (D) samples.
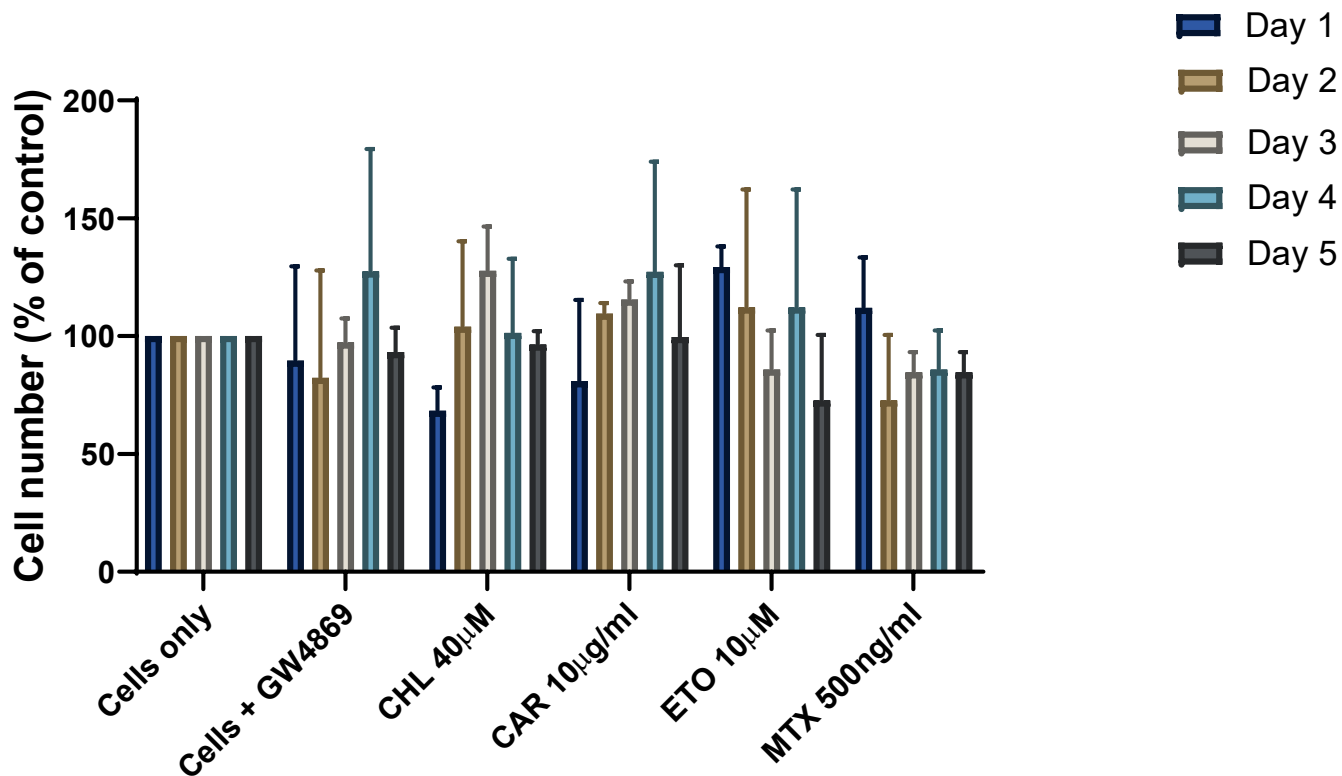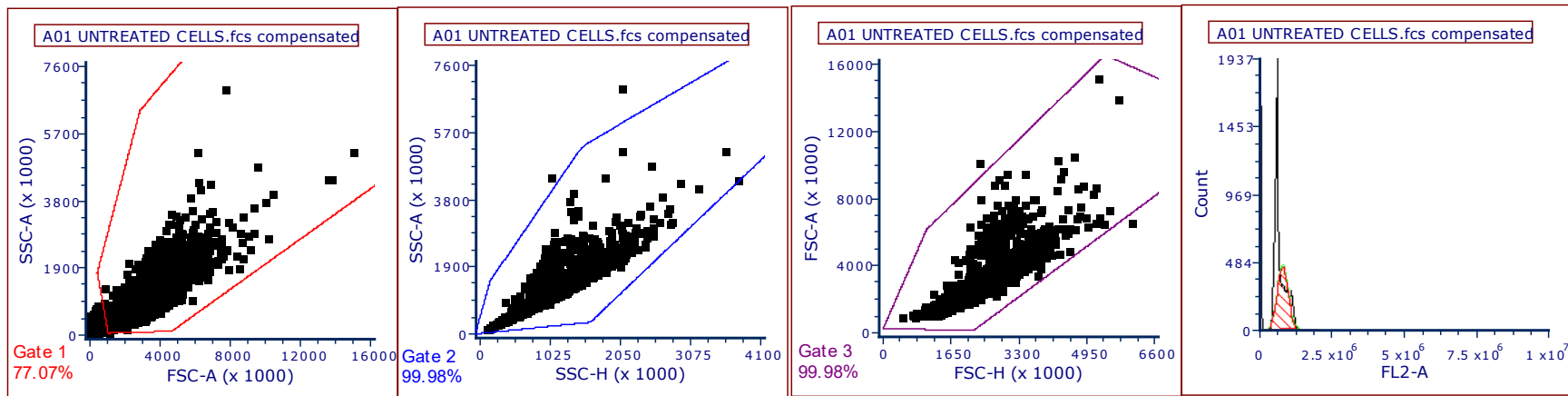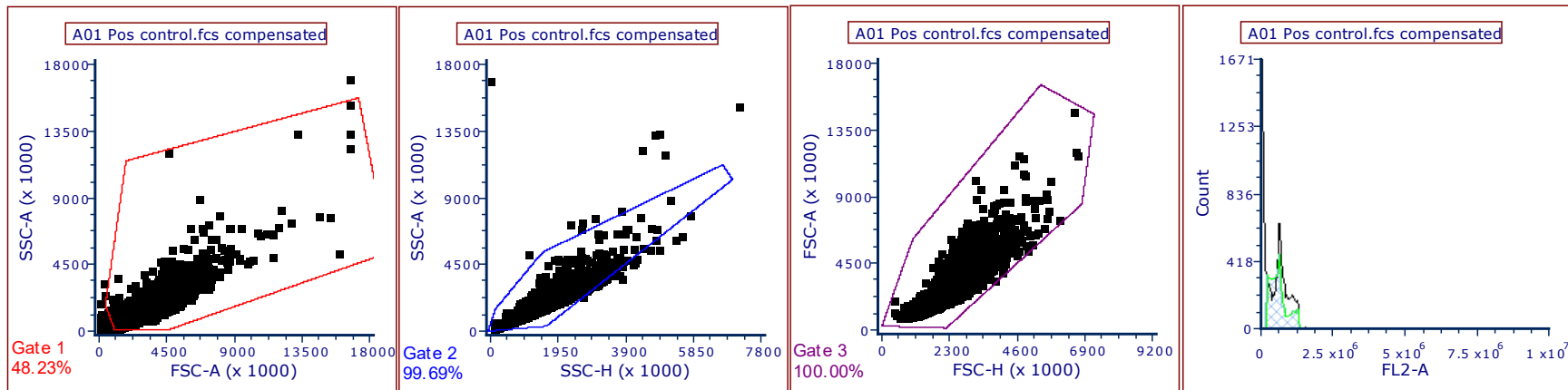
Figure 8.6 The effect of medium conditioned by HS-5 cells exposed to drugs and GW4869 on bystander TK6 cells. HS-5 cells were pre-exposed to GW4869 (5 µm) prior to exposure to chemotherapy for 24 hours. Medium conditioned by these treated HS-5 cells were used to co-culture the bystander TK6 cells for 24 hours. Data show that the conditioned medium had an effect on the cell numbers of the bystander cells.

Figure 8.7 Chemotherapy causes genomic instability in bystander TK6 cells. The data show the cell cycle of untreated bystander cells (negative) and bystander cells treated with mitoxantrone (positive control). The sets of cells had undergone atleast one cell cycle however aneuploidy was observed in the cells treated with drugs. Aneuploidy is physiologically associated with cellular stress as well as chromosome instability thus favouring cancer initiation and progression.
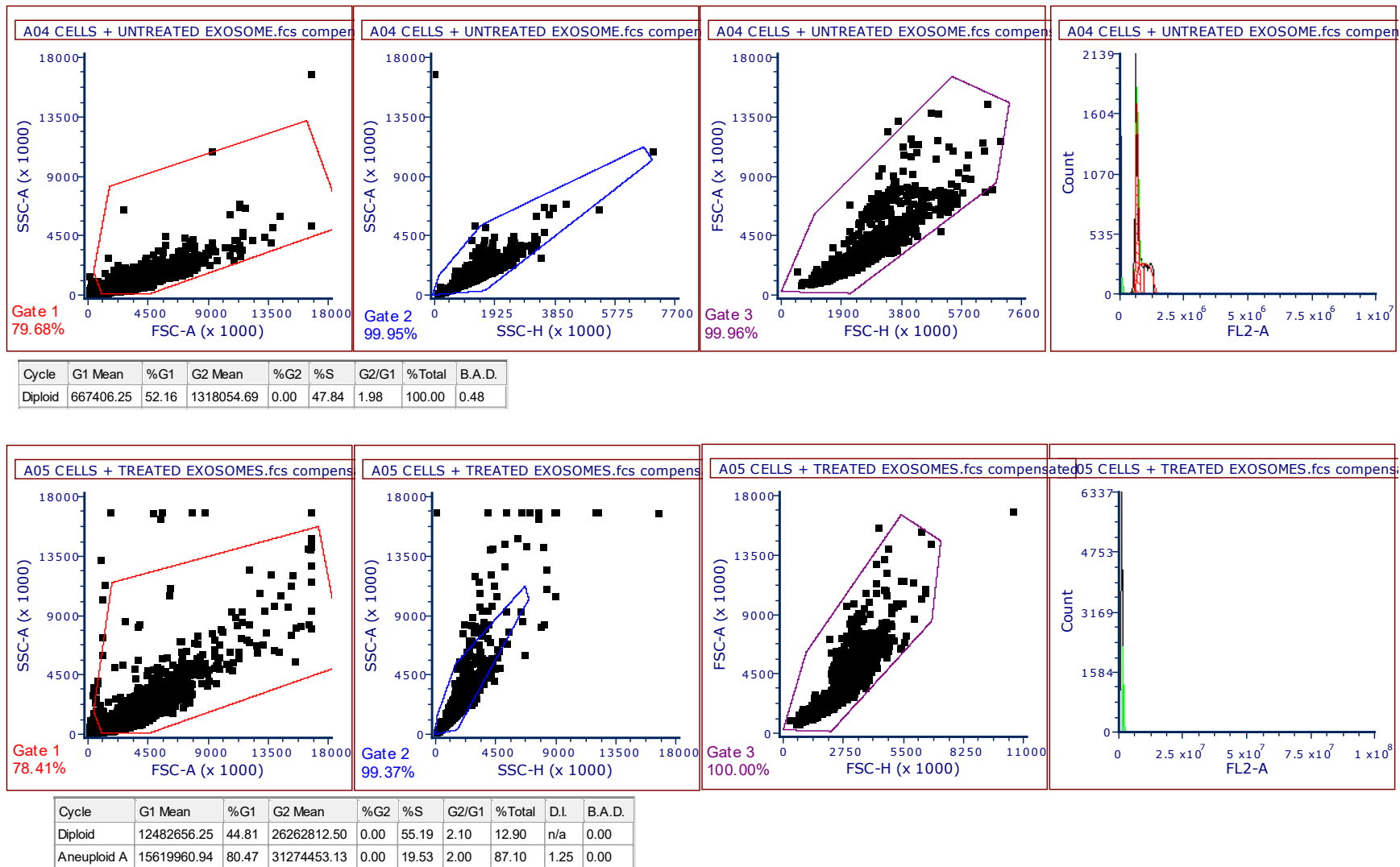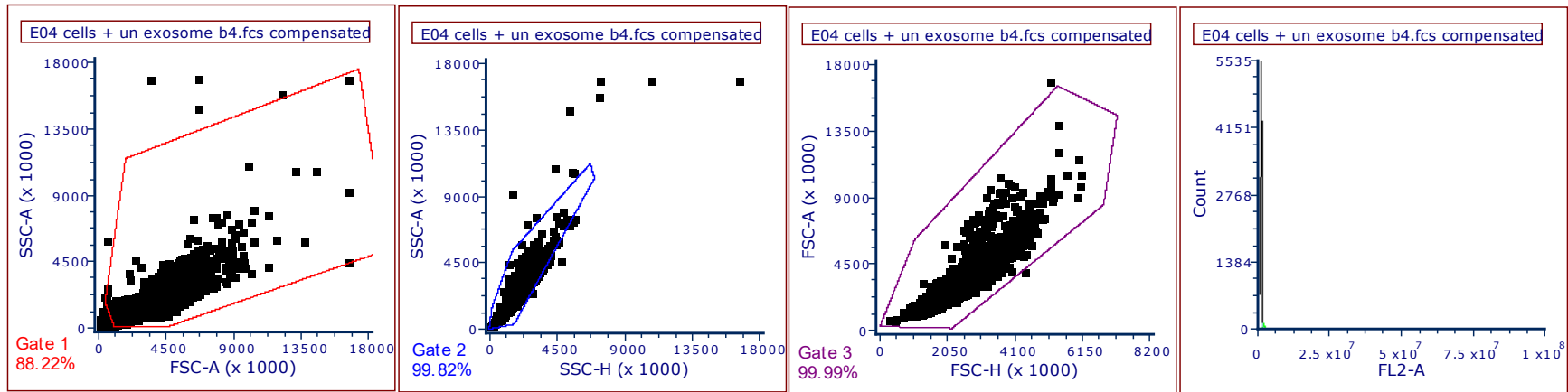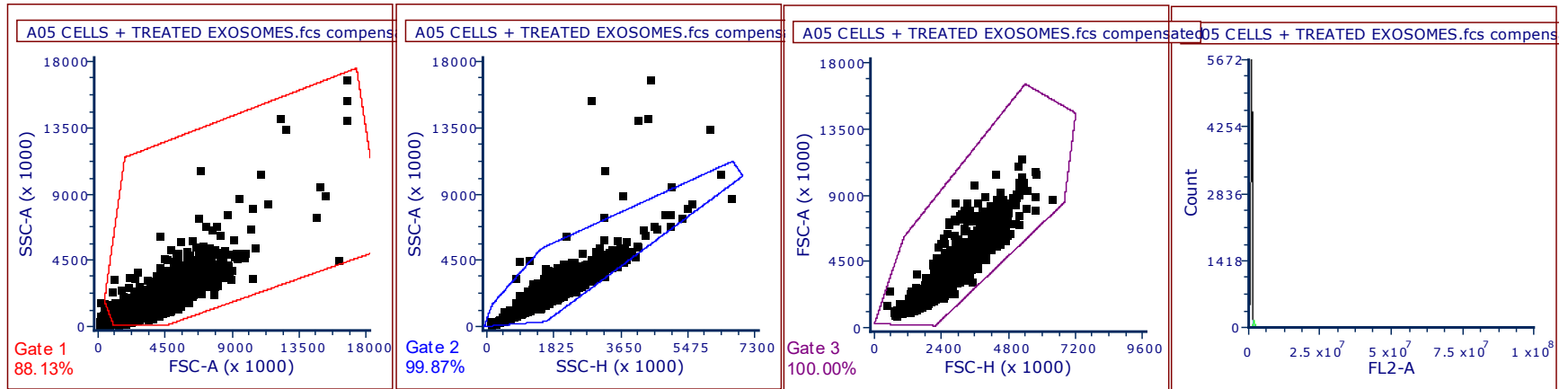
Cycle	G1 Mean	%G1	G2 Mean	%G2	%S	G2/G1	%Total	B.A.D.
Diploid	667406.25	52.16	1318054.69	0.00	47.84	1.98	100.00	0.48

Cycle	G1 Mean	%G1	G2 Mean	%G2	%S	G2/G1	%Total	D.I.	B.A.D.
Diploid	12482656.25	44.81	26262812.50	0.00	55.19	2.10	12.90	n/a	0.00
Aneuploid A	15619960.94	80.47	31274453.13	0.00	19.53	2.00	87.10	1.25	0.00

Figure 8.8 sEVs derived from drug-treated stromal cells induce aneuploidy in bystander TK6 cells. sEVs derived from untreated and treated HS-5 cells were cultured with bystander TK6 cells for 24 hours. Aneuploidy was found in the cells co-cultured with treated sEVs but not in the cells co-cultured with untreated sEVs.
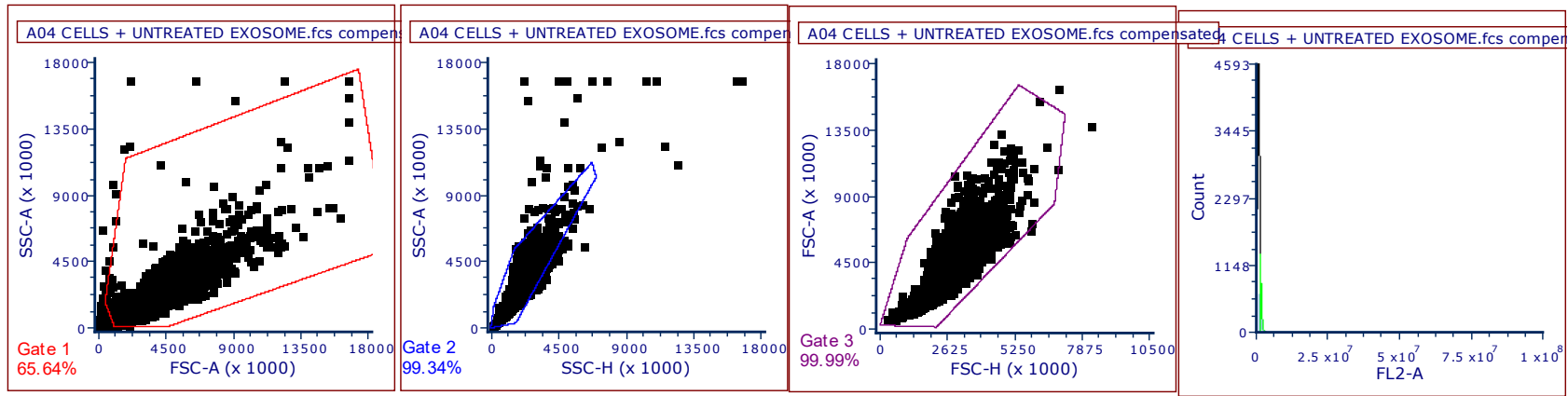
Figure 8.9 Heparin ameliorates aneuploid effect of sEVs in bystander TK6 cells. Pre-treatment of cells with heparin inhibited the development of unbalanced chromosome content (aneuploidy) in the bystander cells.

Top panel — A04 CELLS + UNTREATED EXOSOME.fcs compensated

Gate 1: 65.64%
Gate 2: 99.34%
Gate 3: 99.99%

Cycle	G1 Mean	%G1	G2 Mean	%G2	%S	G2/G1	%Total	D.I.	B.A.D.
Diploid	12501093.75	99.94	24759296.88	0.06	0.00	1.98	46.19	n/a	0.00
Aneuploid A	17186601.56	99.99	33631171.88	0.01	0.00	1.96	53.81	1.38	0.00

Bottom panel — A05 CELLS + TREATED EXOSOMES.fcs compensated

Gate 1: 65.63%
Gate 2: 99.51%
Gate 3: 99.98%
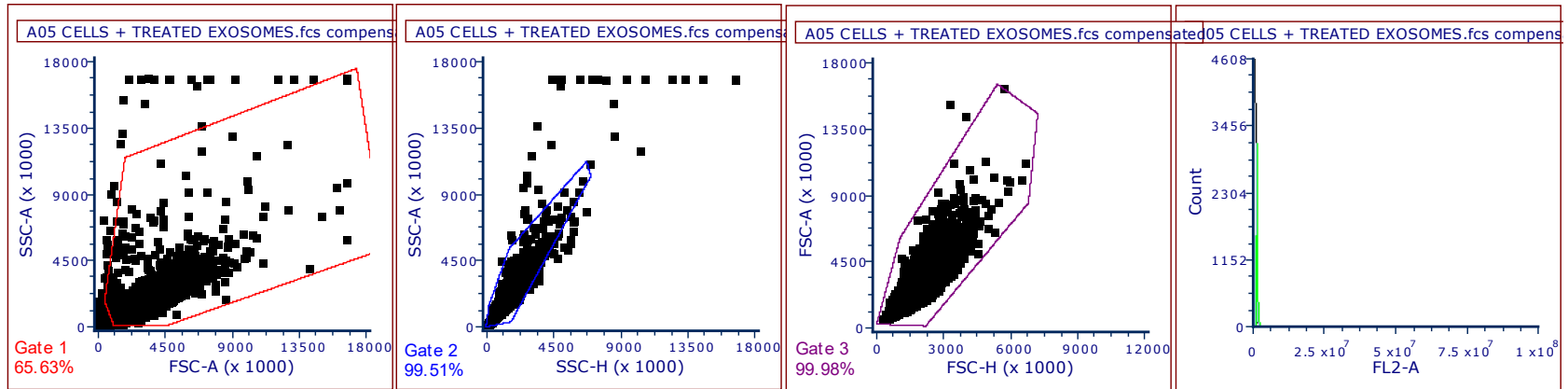
Cycle	G1 Mean	%G1	G2 Mean	%G2	%S	G2/G1	%Total	D.I.	B.A.D.
Diploid	10153789.06	98.16	23039335.94	0.00	1.84	2.27	75.37	n/a	0.00
Aneuploid A	14459257.81	100.00	28634570.31	0.00	0.00	1.98	24.63	1.42	0.00

Figure 8.10 Pre-expsoure of bystander TK6 cells to sEVs does not protect them from chemotherapy-induced aneuploidy. Chromosomal instability were found in the cells following exposure to chemotherapy despite pre-treatment with untreated and/or treated sEVs. However, more aneuploid cells were found in cells pre-treated with untreated sEVs.

329

Table 8.3 BSA Standard Preparation for Bradford Assay

Vial	Volume of diluent	Volume and source of BSA	Final BSA Concentration
A	2370 µl	30 µl of BSA stock	25 µg/ml
B	4950 µl	50 µl of stock	20 µg/ml
C	3970 µl	30 µl of stock	15 µg/ml
D	2500 µl	2500 µl of vial B solution	10 µg/ml
E	2000 µl	2000 µl of vial D solution	5 µg/ml
F	1500 µl	1500 µl of vial E dilution	2.5 µg/ml
G	5000 µl	0	0 µg/ml = PBS Blank

Table 8.4 BSA Standard Preparation for Bicinchoninic Acid Assay

Vial	Volume of diluent	Volume and source of BSA	Final BSA Concentration
A	700 µl	100 µl of BSA stock	250 µg/ml
B	400 µl	400 µl of vial A solution	125 µg/ml
C	450 µl	300 µl of vial B solution	50 µg/ml
D	400 µl	400 µl of vial C solution	25 µg/ml
E	400 µl	100 µl of vial D solution	5 µg/ml
F	400 µl	0	0 µg/ml = PBS Blank